

SOUNDNESS ASSESSMENT OF HISTORIC STRUCTURAL TIMBER  
BY THE USE OF NON-DESTRUCTIVE METHODS

A THESIS SUBMITTED TO  
THE GRADUATE SCHOOL OF NATURAL AND APPLIED SCIENCES  
OF  
MIDDLE EAST TECHNICAL UNIVERSITY

BY

AYŞENUR KANDEMİR

IN PARTIAL FULFILLMENT OF THE REQUIREMENTS  
FOR  
THE DEGREE OF DOCTOR OF PHILOSOPHY, IN RESTORATION  
IN  
ARCHITECTURE

MARCH 2010

Approval of the thesis:

**SOUNDNESS ASSESSMENT OF HISTORIC STRUCTURAL TIMBER  
BY THE USE OF NON-DESTRUCTIVE METHODS**

submitted by **AYŞENUR KANDEMİR** in partial fulfillment of the requirements  
for the degree of **Doctor of Philosophy in Architecture Department, in  
Restoration, Middle East Technical University** by,

Prof. Dr. Canan ÖZGEN  
Dean, Graduate School of **Natural and Applied Sciences**

Assoc. Prof. Dr. Güven Arif SARGIN  
Head of Department, **Architecture**

Prof. Dr. Emine N. CANER SALTİK  
Supervisor, **Architecture Dept., METU**

Asst. Prof. Dr. Ayşe TAVUKÇUOĞLU  
Co-Supervisor, **Architecture Dept., METU**

**Examining Committee Members:**

Prof. Dr. Ömür BAKIRER  
Architecture Dept., METU

Prof. Dr. Emine N. CANER SALTİK  
Supervisor, Architecture Dept., METU

Prof. Dr. Tamer TOPAL  
Geological Engineering Dept., METU

Assoc. Prof. Dr. Özgür YAMAN  
Civil Engineering Dept., METU

Asst. Prof. Dr. Sarp TUNÇOKU  
Architecture Dept., İYTE

**Date:**

March 24, 2010

**I hereby declare that all information in this document has been obtained and presented in accordance with academic rules and ethical conduct. I also declare that, as required by these rules and conduct, I have fully cited and referenced all material and results that are not original to this work.**

Name, Last Name: Ayşenur Kandemir

Signature :

## **ABSTRACT**

### **SOUNDNESS ASSESSMENT OF HISTORIC STRUCTURAL TIMBER BY THE USE OF NON-DESTRUCTIVE METHODS**

Kandemir, Ayşenur

Ph.D., Department of Architecture, Restoration

Supervisor: Prof. Dr. Emine N. Caner- Saltık

Co-Supervisor: Asst. Prof. Dr. Ayşe Tavukçuoğlu

March 2010, 228 pages

The use of non-destructive testing (NDT) methods was needed for the conservation studies of historic timber structures. The aim of this study was to develop combined use of ultrasonic pulse velocity (UPV) measurements and infrared (IR) thermography, together with visual analyses for soundness assessment of timber. An important timber structure in Ankara, Aslanhane Mosque and traditional timber dwellings, in Ayaş and İstiklal District were selected for in-situ analyses. Representative laboratory samples such as mud brick, fired brick, mud mortar, mud plaster, lime plaster, historic timbers of different species and some new timbers were used for analyses in the laboratory to develop reference data for in-situ analyses.

This study has shown that direct and indirect UPV measurements taken parallel to fiber direction were good at estimating the soundness of timber elements. UPV

measurements taken from timber samples were affected by atmospheric humidity, at which the timber was in equilibrium with or by its water content, cuts of timber and type of species.

Quantitative Infrared thermography (QIRT) was good at soundness assessment and defect inspection of timber. The study showed that, the even or heterogeneous distribution of surface temperatures, different thermal inertia characteristics, reflected by the rates of heating and cooling of materials and their ratios to sound timber were good parameters to assess the state of deterioration of timber elements, dampness problems and the compatibility of neighbouring materials with timber.

The joint use of QIRT and UPV methods combined with laboratory data has enhanced the accuracy and effectiveness of the survey.

Keywords: Historic Structural Timber, Non-Destructive Methods, Quantitative Infrared Thermography, Ultrasonic Velocity Measurements, Compatibility

## ÖZ

# TARİHİ AHŞAP TAŞIYICI YAPI ELEMANLARININ DAYANIKLILIK DURUMLARININ TAHRİBATSIZ YÖNTEMLERLE DEĞERLENDİRİLMESİ

Kandemir, Ayşenur

Doktora, Mimarlık Bölümü, Restorasyon

Tez Yöneticisi: Prof. Dr. Emine N. Caner-Saltık

Ortak Tez Yöneticisi: Y. Doç. Dr. Ayşe Tavukçuoğlu

Mart 2010, 228 sayfa

Tarihi ahşap yapıların koruma çalışmalarında tahribatsız yöntemlerin kullanılması önem taşımaktadır. Bu çalışmanın amacı, tarihi ahşap elemanların dayanıklılığını değerlendirmede ultrasonik hız ölçümleri ve kızılötesi ısı görüntüleme yöntemlerini, görsel analizlerle birlikte kullanarak geliştirmektir. Bu yöntemler Ankara Aslanhane Camisi'nde ve Ayaş ve İstiklal Mahallesi'nde bulunan geleneksel ahşap konutlarda uygulanarak değerlendirilmiştir. Tarihi ahşap yapısal elemanlarla birlikte kullanılan kerpiç, tuğla dolgu, kerpiç harç ve sıva, kireç sıva, çeşitli tarihi ahşap ve yeni ahşap malzemeler yapı üzerindeki ölçümleri değerlendirmede örnek veri oluşturmak amacıyla laboratuvarında incelenmiştir.

Bu çalışmada lif doğrultusuna paralel yönde alınan doğrudan ve dolaylı ultrasonik hız ölçümlerinin ahşabın dayanıklılığını değerlendirmede yeterli olduğu görülmüştür. Ultrasonik hız ölçümlerinin, ahşabın dengede olduğu ortamın bağıl nemine, bünyedeki su miktarına, kesim yönüne ve ahşap cinsine bağlı olarak değiştiği izlenmiştir.

Nicel kızılötesi ısı görüntülemenin (QIRT), ahşabın dayanıklılığını ve hasarını izlemekte verimli olduğu görülmüştür. Bu yöntem ahşabın bozulmuşluk derecesini, nem sorunlarını ve komşu malzemelerle uyumluluğunu belirlemede başarılı olmuştur. Değerlendirmelerde yüzey sıcaklık dağılımının tekdüze veya değişken olmasının ve malzemelerin ısınma ve soğuma hızlarının ve bu hızların sağlam ahşabinkine oranının önemli ölçütler olduğu saptanmıştır.

Nicel kızılötesi ısı görüntüleme ve ultrasonik hız ölçümleri yöntemlerinin beraber kullanımı durumunda ve laboratuvar verileriyle desteklendiğinde daha etkili sonuçlar alındığı ortaya çıkmıştır.

Anahtar Kelimeler: Tarihi Taşıyıcı Ahşap, Tahribatsız Yöntemler, Nicel Kızılötesi Isıl Görüntüleme, Ultrasonik Hız Ölçümleri, Uyumluluk

To My Son

## ACKNOWLEDGMENTS

I would like to thank my supervisor Prof. Dr. Emine Caner Saltık for valuable help, her deep knowledge about the subject matter, encouragement, sacrifices and patience. I am also thankful to my co-supervisor Asst. Prof. Dr. Ayşe Tavukçuoğlu for her courage, helpfulness, sacrifices and effort during the entire investigation. I also would like to express my thanks to Assoc. Prof. Dr. Neriman Şahin Güçhan for her help on the traditional timber structures in Anatolia.

I am also grateful to Alp Güney, assistant, Elif, Duygu, Cemre and Yunus, the project assistants of the Material Conservation Laboratory.

I would also like to thank General Manager Assistant Mr. Serhad AKCAN for his encouragement and support during the study. I am also grateful to my colleagues Emel and Serap for their tolerance.

I owe special thanks to my mother and my father for their great support, unlimited patience and encouragements not only throughout this study but also throughout all my life. I am also thankful to my elder sister Prof. Dr. Olcay Kandemir for her valuable encouragement during this long way.

Finally, my special thanks and love to my husband, Architect Giray Yücel for his valuable support, and to our son Mehmet Burak Yücel for his understanding.

## TABLE OF CONTENTS

ABSTRACT.....	iv
ÖZ.....	vi
DEDICATION.....	viii
ACKNOWLEDGMENTS.....	ix
TABLE OF CONTENTS.....	x
LIST OF TABLES.....	xiv
LIST OF FIGURES.....	xvi
LIST OF ABBREVIATIONS.....	xxiv
CHAPTER	
1. INTRODUCTION.....	1
1.1 Aim and Scope of the Study .....	1
1.2 Procedure .....	4
1.3 Content of the Thesis.....	5
2. THE USE OF TIMBER IN TRADITIONAL BUILDINGS IN ANATOLIA...6	
2.1 Studies on Traditional Buildings .....	6
2.2 Structural Features of Timber Framed Buildings in Turkey.....8	
2.2.1 Structural System of Foundations and Basement Floor.....9	
2.2.2 Masonry (Stone and mud brick) and Timber Framed Walls in the Ground Floor.....	11
2.2.3 Single Posts in the Ground Floor.....	14
2.2.4 Masonry Systems (Stone, Mud brick and Timber) in Upper Floor(s) .....	14
2.2.5 Timber Framed Walls in Upper Floor(s).....	15
2.2.6 Infill Materials .....	17
2.2.7 Plaster Materials .....	18
2.2.8 Structure of Floor and Ceiling .....	19
2.2.9 Projections .....	21

2.2.10 Structure of Roof .....	22
3. PROPERTIES OF WOOD AFFECTING ITS MECHANICAL BEHAVIOUR .....	24
3.1 Chemical and Physical Structure of Timber.....	24
3.1.1 Chemical Structure of Wood .....	24
3.1.2 Physical Structure of Wood .....	26
3.1.3 Cutting Wood .....	28
3.1.4 Effects of Chemical Components on wood properties and uses ...	29
3.2 Moisture Content in Timber.....	30
3.3 Density of Timber.....	33
3.4 Mechanical Properties of Timber.....	35
3.4.1 Factors Affecting Mechanical Properties .....	38
3.4.2 Determination of Mechanical Properties of Wood in Laboratory...	43
3.5 Durability of Timber and its Deterioration .....	44
4. NON-DESTRUCTIVE METHODS AND THEIR USE ON THE ASSESSMENT OF TIMBER ELEMENTS .....	48
4.1 Visual Examination for the Surface Assessment.....	49
4.2 Acoustical Properties of Timber and Ultrasonic Testing Method .....	50
4.2.1 Acoustical Properties of Timber .....	50
4.2.2 Ultrasonic Testing Method .....	52
4.2.2.1 Sonic Stress Wave Method .....	60
4.2.2.2 Acoustic Emission and Acousto-Ultrasonic Techniques .....	62
4.3 Thermographic Methods .....	66
4.3.1 Thermal Measurement Methods .....	66
4.3.2 Basic Concepts of Infrared Thermography .....	67
4.3.3 IRT studies of Historical Buildings .....	72
4.3.4 Thermal Properties of Timber .....	77
4.3.5 IRT Studies on the Assessment of Timber Characteristics and Defect Detection .....	82

4.4 Other Non-Destructive Methods .....	87
4.5 Pseudo Nondestructive Evaluation .....	88
4.5.1 Examination of Deterioration Depth on Timber Surfaces by Pilodyn .....	89
4.5.2 The Methods of Rebound Hammer (Penetration Method).....	90
4.5.3 Resistograph Drilling .....	91
5. MATERIAL AND METHOD .....	93
5.1 Material .....	93
5.1.1 Buildings .....	93
5.1.2 Laboratory Samples .....	99
5.2 Methods .....	100
5.2.1 Laboratory Studies .....	101
5.2.2 In-situ Studies .....	108
6. RESULTS .....	113
6.1 Laboratory Analyses of Samples by UPV and QIRT .....	113
6.1.1 Laboratory UPV Analyses .....	114
6.1.2 Laboratory QIRT Analyses .....	122
6.2 In-situ Analyses by UPV and QIRT.....	146
6.2.1 Direct and Indirect Velocity Measurements on Timber Elements .	146
6.2.2 In-situ QIRT Analyses on Timber Elements .....	153
7. DISCUSSION AND CONCLUSION .....	174
7.1 Structural Timber in Historic Buildings .....	174
7.2 Soundness Investigation of Timber by UPV Measurements .....	175
7.2.1 Establishing Reference Data by Laboratory Analyses.....	176
7.2.2 Evaluation of In-situ Measurements .....	180
7.3 Soundness Investigation by QIRT Studies .....	181
7.3.1 Establishment of Reference Data by Laboratory QIRT Analyses .	182
7.3.2 Evaluation of In-situ QIRT Measurements .....	187
7.3.3 Combined Use of QIRT and UPV for In-situ Soundness Investigations .....	192

7.4 A Proposal for Soundness Investigation of Timber .....	193
7.5 Conclusion .....	198
REFERENCES.....	202
APPENDIX .....	217
CURRICULIUM VITA.....	226

## LIST OF TABLES

### TABLES

Table 3.1 The percentage of cellulose, hemicellulose and lignin in softwoods and hardwoods.....	25
Table 3.2 Structure of softwoods and hardwoods summarized from Ridout (2001).....	27
Table 3.3 Mechanical Properties of wood and other materials in relation to specific gravity.....	36
Table 4.1 Acoustic Velocity in some Engineering Materials.....	54
Table 4.2 Thermophysical properties of some building materials).....	71
Table 4.3 Thermal properties of pine wood species studied photoacoustic and phoyothermal techniques.....	80
Table 4.4 Emissivity value for the timber species and some common building materials .....	81
Table 5.1 The description of laboratory samples examined in this study: sample code, its definition and density.....	103
Table 5.2 Neighbouring samples collected from the selected houses, Mud brick and brick infill, lime and mud plaster, repair plaster with high gypsum content.....	104
Table 6.1 Reference UPV data for the visually sound and deteriorated timber samples measured in the laboratory.....	121
Table 6.2 Rate of heating up and cooling down of the marble, fried brick, oak and pine timber.....	126
Table 6.3 Rate of cooling down of the deteriorated and sound and beech timber .....	128
Table 6.4 Rate of heating, rate of cooling and soundness ratio of timber samples .....	133

Table 6.5 Rate of heating, rate of cooling and soundness ratio of deteriorated and sound old pine and knots on the surfaces of them.....	136
Table 6.6 Rate of heating and cooling of samples their ratios to sound timber .....	140
Table 6.7 Rate of heating and cooling of samples their ratios to sound timber...	146
Table 6.8 Rate of cooling of timber beam and post and their ratios to sound timber post/beam.....	164
Table 6.9 Rate of cooling of timber post/ beam, mudbrick infill and their ratios to sound timber post/beam.....	167
Table 6.10 The thermal behavior of interior plaster layer covering the timber frame structure .....	171
Table 6.11 The rate of cooling down, RC, for the laboratory samples (fired repair-brick, fired brick and sound pines), and for the in-situ brick and mortar infill and structural timber of Ayaş House façade .....	173
Table 7.1 Rate of heating and cooling rate of timber species with different densities.....	183

## LIST OF FIGURES

### FIGURES

Figure 2.1	Timber framed wall system in traditional dwellings from Bursa-Cumalıkızık, the Street Eğrek and N:18 .....	15
Figure 2.2	A Safranbolu House with the projection with bracing element.....	22
Figure 3.1	Schematic representation of a sector of wood (A) transverse, (B) radial, (C) Tangential Surfaces.....	29
Figure 3.2	Wood Moisture Content Equilibrium Curves .....	31
Figure 3.3	The relationship of strength(y) and density(x), 1. Static Bending(MOR), 2. Axial compression, 3. Hardness .....	40
Figure 4.1	Pulse velocity versus moisture in the axial direction.....	57
Figure 4.2	Pulse velocity vs. content z direction: axial direction x and y direction: radial direction.....	57
Figure 4.3	Thermal Measurement Method .....	67
Figure 5.1.	Front views of Ayaş House and Aslanahane Mosque, front and side views of the Istiklal House .....	95
Figure 5.2	The location of Aslanhane Camii, Altındağ District, Can Sokak....	95
Figure 5.3	a) The ground floor of the Aslanhane Camii b) First floor of the Aslanhane Camii c) The section of the Mosque from the north south direction.....	96
Figure 5.4	a) Interior view from the Aslanhane Mosque showing the some timber columns supporting the roof and timber ceiling structure b) The view of west façade showing the stone masonry walls with timber lintels and bond beams .....	97
Figure 5.5	From the view of the commercial and administrative center of the Settlement, Cumhuriyet Meydanı, located in the north of <i>Ayaş Çayı</i> and the location of selected house, Hükümet Caddesi, Akpınar Sokak, No: 1, Ayaş.....	97

Figure 5.6 The Plans of settlement of Ayaş and the location of selected building, Hükümet Caddesi, Akpınar Sokak No:1 .....	98
Figure 5.7 Location of the house from İstiklal District, Kargı sok. No: 25/C Ulus .....	98
Figure 5.8 Old sound and deteriorated timber samples , New pine, beech, oak timber samples, stone and fired brick infill samples.....	101
Figure 5.9 Schematic drawing showing the indirect UPV measurements .....	105
Figure 5.10 Schematic drawing showing the direct UPV measurements.....	105
Figure 5.11 The experimental setup of sequential IR imaging at laboratory for the monitoring of sound oak timber, sound pine timber marble, fired brick samples during heating and then cooling periods.....	108
Figure 5.12 The QIRT experimental set-up at İstiklal House showing IR camera automatically-recording IR images of target area at 10s intervals during the heating and cooling periods of a day .....	112
Figure 6.1 The average EMC of all old and new timber samples during moisture absorption and desorption indicating slower desorption .....	115
Figure 6.2 EMC of old and new pine by weight measurements and surface moisture readings by protimeter .....	115
Figure 6.3 Changes in ultrasonic velocity values of old and new timber samples due to the changes in moisture content .....	116
Figure 6.4 The $UPV_{L-DIRECT}$ and $UPV_{R-DIRECT}$ measurements for the deteriorated and sound old pine samples collected from traditional houses as well as for sound new pine samples .....	117
Figure 6.5 The laboratory UPV measurements taken in indirect mode both perpendicular and parallel to fiber direction.....	119
Figure 6.6 The transit time versus distance showing the presence of the knots on the timber surfaces.....	120
Figure 6.7 Indirect UPV measurements taken from the surface of timber sample with knot; YC1-08 and SEC1-08.....	120

Figure 6.8. a) Laboratory samples oak (YM1), pine 1(EC3), pine 2(EC4), marble 1(QIMG1), marble 2(I3) and fired brick 1(FB1), fired brick 2 (FB2) b) IR image of samples at the beginning of heating period c) Differential IR image of samples at the heating period d) Differential IR image of samples at the cooling period.....	123
Figure 6.9.a The surface temperature lines versus square root of time during heating period of samples using a halogen lamp (650 Watt).....	124
Figure 6.9.b The surface temperature lines versus square root of time during cooling period of samples.....	124
Figure 6.9.c The temperature difference lines versus square root of time for oak, pine, marble and repair fired brick samples heated by the halogen lamp (650 Watt) and then monitored by the sequential IR imaging during the heating period.....	125
Figure 6.9.d) The temperature difference lines versus square root of time for oak, pine, marble and repair fired brick samples heated by the halogen lamp (650 Watt) and then monitored by the sequential IR imaging during the cooling period.....	125
Figure 6.10 a) View of timber samples: Old pine (SEC1-08, SEC2-08), new pine (EC4, YC7-08, YC6-08) deteriorated pine (FEC3), new sound beech (YK5-08) b) Their differential IR image.....	127
Figure 6.11.a The surface temperature lines versus square root of time during cooling period.....	127
Figure 6.11.b Temperature difference lines versus square root of time during cooling period.....	128
Figure 6.12 a) The view of samples before analyzed by QIRT: old pine with low density (FEC3- 0.38 g/cm <sup>3</sup> ), new oak (YM1-0,870), new beech (YK5-0.784) sound old pine (SEC1-09-0.634), deteriorated old pine (SEC2-09-0.421 g/cm <sup>3</sup> ) visually deteriorated but inner part sound pine (SEC1-08, 0.449 g/cm <sup>3</sup> ), sound new pine (YC1-08- 0.408 g/cm <sup>3</sup> ) b) IR image of sample at the beginning of heating period c) Differential IR image of samples during heating period of 814 seconds. ....	130
Figure 6.13 The surface temperature and temperature difference lines versus square root of time during heating period for the samples in Figure 6.12.a .....	131

Figure 6.14 a) IR image of samples in Figure 6.12.a at the beginning of cooling period b) Differential IR image of samples during cooling period of 756 seconds. ....	132
Figure 6.15 The surface temperature and temperature difference lines versus square root of time during cooling period for the samples in Figure 6.12.a .....	132
Figure 6.16 a The surface temperature and temperature difference lines versus square root of time during heating period compared with their knots for the samples in Figure 6.12.a .....	134
Figure 6.16.b The surface temperature and temperature difference lines versus square root of time during cooling period compared with their knots for the samples in Figure 6.12.a.....	135
Figure 6.17 a) The view of samples before QIRT analyses: mud brick infill, fired brick infill, sound old timber (SEC1-09-0.634), deteriorated old pine (SEC2-09-0.421 g/cm <sup>3</sup> ), Exterior lime plaster together with its mud layer b) IR image of samples at the beginning of heating period c) Differential IR image of samples during heating period of 642 seconds. ....	137
Figure 6.18 The surface temperature and temperature difference lines versus square root of time during heating period of the group with mud brick, fired brick, sound and deteriorated timber, exterior lime plaster together with its mud layer.....	138
Figure 6.19 a) IR image of samples in Figure 6.17.a at the beginning of cooling period b) Differential IR image of samples during cooling period of 596 seconds.....	139
Figure 6.20 a) The lines of surface temperature versus square root of time during cooling period of the group with mud brick, fired brick, sound and deteriorated timber, exterior lime plaster together with its mud layer.....	139
Figure 6.20 b) The lines of temperature difference versus square root of time during cooling period of the group with mud brick, fired brick, sound and deteriorated timber, exterior lime plaster together with its mud layer. ....	140

Figure 6.21 a) The view of samples before analyzed by QIRT: mud brick infill, thick interior repair plaster (high gypsum content) together with its mud layer, mud plaster, sound old timber (SEC1-09-0.634), exterior lime plaster together with its mud layer b) IR image of sample at the beginning of heating period c) Differential IR image of samples during heating period of 592 seconds. ....	142
Figure 6.22 The lines of surface temperature and temperature difference versus square root of time during heating period of the group with mud brick, interior lime plaster, mud plaster sound timber, and exterior lime plaster together with its mud layer. ....	143
Figure 6.23 a) IR image of samples in Figure 6.17.a at the beginning of cooling period b) Differential IR image of samples during cooling period of 670 seconds.....	144
Figure 6.24 The lines of surface temperature and temperature difference versus square root of time during cooling period of the group with mud brick, interior lime plaster, mud plaster sound timber, and exterior lime plaster together with its mud layer. ....	145
Figure 6.25 Plan of Aslanhane Mosque showing the columns investigated by UPV.....	147
Figure 6.26 The ultrasonic velocity values taken at different levels along the height of timber columns in Aslanhane Camii, K1, K2, K3, K5 and K7.....	148
Figure 6.27 Indirect UPV measurements (top) from the beam and direct UPV measurements (bottom) from the post at İstiklal House.....	151
Figure 6.28 Location of UPV measurements taken from İstiklal house, the red lines show the direct measurements and the blue ones show the indirect measurements which were taken from the timber elements.....	151
Figure 6.29 Indirect UPV measurements parallel to fiber direction. UPVL-INDIRECT (IN-SITU) = 1176 - 1337m/s for the sound timbers, UPVL-INDIRECT (IN-SITU) = 493 - 727m/s for the deteriorated timbers .....	152
Figure 6.30 The lines of transit time curve versus distance according to in-situ indirect UPV measurements from the timber structural elements..	152

- Figure 6.31 View of the west façade of the building (left); IR image taken after sunset (right) showing that stone masonry façade with its timber lintels and bond beams had damp zones. Timber elements were warmer than stone masonry, but they had damp zones due to damp cement mortar repairs.....154
- Figure 6.32 a)View of a window from the west facade of the building with timber lintel at its top b) IR image of the selected region, taken in day time c) Line temperature analysis of the timber lintel showing 5.5 °C surface temperature difference due to close relationship with wet cement neighbouring materials.....154
- Figure 6.33 The view of the pillar K2 (left) and its IR image (right) showing an even temperature distribution on its surfaces with a difference of 2 °C.....155
- Figure 6.34 a) View of the timber ceiling b)IR image of the selected region showing the damp areas at ceiling c) The line analyses graph of timber ceiling .....156
- Figure 6.35 a) View of the interiors surfaces of the east wall b) IR image of the wall at the selected region showing the damp areas sourced from the faults in roof drainage.....157
- Figure 6.36 a) View of east interior wall of Aslanhane Mosque b) IR image of east interior wall c)The graph of the line analyses on IR images from the east wall.....157
- Figure 6.37 a) The view of Pillar K1 b) Its IR image showing that during an hour of heating with the stove there existed 39.3 °C temperature difference on the surfaces along the periphery of the pillar at +1.10 m height, and cracks were also detected as the hottest traces c) Line analysis of IR images of pillar K1 taken from the surfaces facing the stove (left) and remaining at the back of the stove .....158
- Figure 6.38 The view of Pillar K2 (left) and its IR image (right) showing that there was a temperature variation of 27.8 °C which was similar to the temperature variations observed at the Pillar K1, and knots and cracks were easily detected as the coldest patches and the hottest patches/traces, respectively.....159

Figure 6.39 Partial view from the west façade of Aslanhane Camii and its IR images taken in December in daytime and at night, having the outside conditions of 1.5°C and 29%RH and -0.7°C and 31%RH, respectively. ....	159
Figure 6.40 a) View of the wall section from Ayaş House b) The surface of the wall section was heated by hair dryer then monitored by the sequential IR imaging during the cooling period, first sequential image taken at the ambient conditions of 25.1°C and 33%RH c) The differential IR image showing the temperature difference between the initial and the last IR images of the cooling period of 603 seconds.....	161
Figure 6.41 a) Partial view of the severely-deteriorated timber post (M7-Post) at İstiklal House b) The IR image of the timber taken at the ambient conditions of 25.5°C and 33%RH after heated uniformly with hair dryer for one minute c) The differential IR image showing the temperature difference between the initial and the last IR images of the cooling period of 476s.....	162
Figure 6.42 After the heating of the wall section of İstiklal House with hair dryer, and the temperature lines versus square root of time and the differential temperature lines versus square root of time for timber elements during cooling period of about 225s.....	163
Figure 6.43 Rate of cooling down of deteriorated timber elements to rate of cooling down of sound elements.....	164
Figure 6.44 After the heating of the wall section of İstiklal House with hair dryer, and the temperature lines versus square root of time and the differential temperature lines versus square root of time for mudbrick infill and timber elements (at bottom) during cooling period of about 225s .....	166
Figure 6.45 View of the interior wall at Ayaş House and the IR image of the selected region in November in daytime; showing that the timber frame structure underneath the historic plaster layers were clearly detected in IR images with a warmer and even surface temperature distribution ( $7.8^{\circ}\text{C}\pm 0.1^{\circ}\text{C}$ ).....	168
Figure 6.46 The surface temperature lines versus square root of time and temperature differences lines versus square root of time for the slightly cooling periods of daytime at the interior wall surface of Ayaş House .....	169

Figure 6.47 The surface temperature lines versus square root of time and temperature differences lines versus square root of time for the slightly heating periods of daytime at the interior wall surface of Ayaş House .....	170
Figure 6.48 Partial view from the west side of the Ayaş House and its IR image taken in November under the exposure of solar radiation when the outside temperature was 12.2°C and 42%RH, showing that the brick infill had the coldest surface temperature of 21.9°C±0.1°C, the brick mortar had the warmer surface temperature of 25.2°C±0.5°C and the timber elements had the warmest surface temperature of 32.2°C ±1.7°C. ....	172
Figure 6.49 Partial view from the north façade of the Ayas House and its IR images taken in November in daytime and at night, having the outside conditions of 13.0°C and 39%RH and 7.4°C and 62%RH, respectively. The analyses showed that the timber elements cooled down faster than the brick and mudmortar infill during the cooling period of 9977s. The differential temperature was calculated to be -6.03°C for timber elements while being -3.64°C for brick and mudmortar.....	172
Figure 6.50 At Ayas House, exterior plaster having damp zones, coldest areas with a difference of 3.2 °C below the ambient temperature.....	173
Figure 7.1 The surface temperature of different timber species with different density versus square root of time (The graph was drawn with the values of the graph given in Tanaka, (2001))......	184

## LIST OF ABBREVIATION

NDT	Non-destructive Testing
QIRT	Quantitative Infrared Thermography
IR	Infrared
IRT	Infrared Thermography
UPV	Ultrasonic Pulse Velocity
UPV <sub>L-DIRECT</sub>	Ultrasonic Pulse Velocity Longitudinal Direct
UPV <sub>L-INDIRECT</sub>	Ultrasonic Pulse Velocity Longitudinal Indirect
UPV <sub>R-DIRECT</sub>	Ultrasonic Pulse Velocity Radial Direct
UPV <sub>R-INDIRECT</sub>	Ultrasonic Pulse Velocity Radial Indirect
MoE	Modulus of Elasticity, dynes/cm <sup>2</sup> =10 <sup>-7</sup> MPa
e	Thermal Effusivity, W s <sup>-1/2</sup> m <sup>-2</sup> K <sup>-1</sup>
α	Thermal Diffusivity, m <sup>2</sup> s <sup>-1</sup>
c	Specific Heat, J kg <sup>-1</sup> K <sup>-1</sup>
k	Thermal Conductivity, Wm <sup>-1</sup> K <sup>-1</sup>
I	Thermal Inertia
T	Temperature, °C
ΔT	Temperature Difference, °C
R <sub>w</sub>	Rate of Warming Up
R <sub>c</sub>	Rate of Cooling Down
P	Density, kg/m <sup>3</sup>
ε	Emissivity
PT	Pulse Thermography
LT	Lock-in Thermography
MT	Modulated Thermography

# CHAPTER 1

## INTRODUCTION

Timber was one of the oldest construction materials. Researchers pointed out that historical wooden items and historical timber structures could be preserved in excellent conditions for thousands of years (Ridout, 2001; Tsoumis, 1991; Rug *et al.*,1991). For example, some 4000-5000 years old Egyptian excavated items were found in excellent state of preservation (Ridout, 2001). Use of timber materials and dwellings constructed with timber elements in Anatolia had gone back to ten thousand years (Acar, 2000). The earlier examples of timber dwellings in Anatolia were constructed by Hittites. Hittite dwellings constructed with mud brick masonry and timber structural elements on stone foundations were excavated in Şapinuwa Hittite site near Çorum (Güdücü, 2003). Although timber elements were totally burnt by fire, it was possible to follow the use of timber in those structures. The earliest surviving timber architecture in Anatolia was the burial chambers of The Grand Tumulus of Gordion that were built in around 700 B.C. (İdil, 1997). Although the timber elements in Grand Tumulus of Gordion look in fairly good state of preservation it is necessary to study their state of preservation by non-destructive methods and their microclimatic conditions need to be studied for their long term preservation.

Timber has been an important structural material of both monumental buildings and traditional architecture in Anatolia. It was used as important structural elements in the construction of the timber framed traditional architecture and in stone, brick and mud brick masonry systems. In the timber framed systems, structural and constructional timber elements were used as the main post, stud, lintel, beam, brace, tie beam in the wall construction, foot and wall plate, girder

and covering plate in the floor and ceiling construction, sill, frame, sash in the window and door construction, beam, post, brace, tie beam, purlin and rafter in the roof construction etc. In stone and brick masonry walls, timber was generally used as lintel and tie beam.

The survival of historical timber framed dwellings for long period of time was related to use of compatible materials and the adequacy of structure and construction technologies used in the past. The natural characteristics of older wood were another advantage for their durability. The removal of the timber elements from buildings and/or use of new materials that are non-compatible with timber would be dangerous for both durability and historical authenticity. Although durability of timber in the historical structures is directly related to its compatibility with the other materials in the structure, those conditions are not well studied and described. Studies on the compatibility and durability properties, of timber and its neighbouring materials in the historic structures are useful not only for their repair and conservation but also to for the new developments in the construction and design fields. It has to be emphasized that methods of the investigation of historic structures should not give any harm to them therefore they should be non-destructive as far as possible (Sasse and Snethlage, 1997)

Compatibility and durability conditions are usually described with some physical, mechanical and chemical parameters of timber element and its neighbouring materials (Pizzo, 2002; Akkuzugil, 1997).

Pizzo (2002) studied wood and epoxy adhesive interface compatibility comparing the values of thermal expansion coefficients of these materials. It was concluded that thermal expansion coefficient was one of the important physical parameters that should be taken into account to predict the compatibility and durability of the interface between timber and epoxy adhesive interface. Epoxies adhesives that have shown greater differences in terms of thermal expansion coefficients, had

decreasing mechanical compatibility with timber. Akkuzugil (1997) has analyzed water vapor permeability properties of materials in some traditional half timber houses in Ankara. She found that the materials touching or surrounding the wood, such as exterior and interior plasters and mud brick infill allowed the constant passage of water vapor. As a result, the risk of condensation in timber elements was prevented. In other words, equivalent air thickness (SD) of those materials was similar among each other and lower than timber. Therefore SD value was found to be an important compatibility parameter for the durability of half timber dwellings.

One of the most significant problems that were a threat to the traditional dwellings was the restorations involving wrong interventions. During those restorations, the traditional timber buildings were demolished partly or completely and rebuilt with modern techniques and materials. If not demolished, there were a lot of mistakes done during the restoration interventions that caused rapid deterioration and loss of authenticity. The repair materials were almost always not compatible with the historic materials. The timber elements of traditional timber framed buildings were often replaced with the new ones without assessment of their structural conditions. On the other hand, recent researches demonstrated that the old timber elements were stronger than the newly replaced ones (Ridout, 2001; Mouzouras, 1989; Rug *et. al.*, 1991).

It is evident that in the field of conservation science there is urgent need for the studies on the development of non-destructive testing methods for timber. And this study was planned to fulfill the primary parts of that need for historic timber structures

## **1.1 Aim and Scope of the Study**

The aim of the thesis is to evaluate the historical use of the structural timber together with its neighboring materials, to develop NDT methods on soundness of historic timber and its state of deterioration and to evaluate its compatibility and durability conditions. For those purposes, some traditional timber framed houses in Ayaş and İstiklal District in Ankara and a monument from Selçuk Period were selected as case studies. Both laboratory analyses and field surveys were planned to be carried out.

In the study, the traditional timber dwellings and a stone masonry structure were examined by using ultrasonic pulse velocity (UPV) measurements and infrared (IR) thermography methods both in-situ and in laboratory with the following objectives, namely, i) to assess the soundness of historic timber elements and to discuss the compatibility criteria for timber elements and neighboring materials in contact with them, such as mud brick, fired brick, stone infill materials, forming the overall structural system ii) to study those non-destructive methods in detail at laboratory by using representative samples iii) to evaluate those non-destructive methods on the soundness assessment of structural timber elements in historic buildings and provide some improvements on the use of those non-destructive methods for in-situ investigation of timber.

## **1.2 Procedure**

The study has started with literature survey about the use of timber structural elements in historical buildings, physical and mechanical properties of timber and available non-destructive techniques on their analyses. The study has focused on the soundness assessment of timber elements in historic structures by ultrasonic

pulse velocity (UPV) measurements and quantitative IR thermography (QIRT) supported by laboratory analyses.

First laboratory analyses with representative building materials using UPV and QIRT were done to establish a data base for the field work. Later on those non-destructive methods were conducted in traditional timber dwellings, namely İstiklal House, Ayaş House, and in a stone masonry structure in Ankara, Aslanhane Camii.

### **1.3 Content of the Thesis**

The study is composed of seven chapters. The first chapter is introduction, where the purpose and content of the study is introduced and the procedure is briefly described. In the second chapter, general information about the structural features of traditional dwellings is represented. In the third chapter, properties of timber affecting the mechanical properties are given. In the fourth chapter, general information about the non-destructive methods is introduced. The fifth chapter is allocated to material and method of the study. In the sixth chapter, results of the study are submitted. In the last chapter the results are discussed and conclusions are given.

## CHAPTER 2

### THE USE OF TIMBER IN TRADITIONAL BUILDINGS IN ANATOLIA

In this chapter, studies on traditional timber framed buildings and their structural features are introduced.

#### 2.1 Studies on Traditional Buildings

Traditional Anatolian dwellings are the documents of our architectural heritage. The studies on the classification of traditional dwellings were performed by considering the examples of standing the old buildings starting from late eighteenth century. Due to inadequacy of the knowledge of the dwellings before that time, researchers explored the written documents such as *vakfiyeler* (documents of vakıf), construction and restoration documents, *tapu tahrir defterleri* (register of deeds documents), *şer-i siciller* (register of law court) etc. for the earlier examples (Madran, 1994; Tanyeli, 1996). Arel (1982) emphasised that for the traditional dwellings the architectural analysis and historical research need to be carried out together.

The traditional dwellings were classified based on the plan types (Eldem, 1968; Aksoy, 1963; Kuban, 1982; Küçükerman, 1973), on the relationship of courtyard and building with the street (Yavuz, 2000; Asatekin, 1994), and on consideration of regional climatic and environmental differences (Aksoy, 1963; Kuban, 1966; Tanyeli, 1979; Eriç, 1979).

The traditional buildings were also examined based on their structural and constructional features. The investigation of the structural and constructional features of the historical dwellings was important not only for their classification and identification, but also for their repair and conservation. There was not enough research on the subject. However the interest on the investigation of the structural and constructional features of the dwellings have increased in recent years.

Şahin (1995) has extensively studied and documented the architectural and structural characteristics and the construction process of timber framed Ankara houses. Kaya (1996) has extensively explored structural members of Safranbolu Houses. Türkmen (1995) has studied the connections of the structural timbers in the countryside of Rize region . The wall, flooring, roof and heating systems of the traditional houses located in the East Black Sea Region were explored and traditional construction techniques were studied by Sümerkan (1990). Çobancaoğlu (1998), examined the structural systems of the traditional timber framed dwellings in Turkey in relation to their region. Kandemir (2000) studied the architectural and structural characteristics of the traditional houses in Cumalıkızık (Bursa) with the aim of preparing a guide for their preservation and rehabilitation. She has focused on the window structures and their maintenance issues and illustrated the structural details of the windows.

Akkuzugil (1997) explored the physical properties of the historical plasters of selected traditional dwellings in Ankara, which were studied earlier by Şahin (1995). Akkuzugil concluded that timber framed structures, infill materials and plasters have compatible physical properties. By this way those buildings were able to survive for some centuries.

## 2.2 Structural Features of Timber Framed Buildings in Turkey

The traditional houses were mainly constructed with timber framed construction systems. Those systems have some common characteristics with some regional differences.

Foundations and the lower parts of the outer walls in the ground floor are almost always stone masonry. On the other hand, the inner partition walls might be stone masonry or timber framed with mud brick or brick infill. Walls of upper floors are usually timber framed. In some cases, one or more walls might be of stone masonry, e.g. service walls.

Stone, timber and mud brick were the main construction materials of the traditional dwellings. The mortar of stone masonry walls with timber lintels might be mud or lime based. The infill material of the timber framed walls was generally mud brick or brick. In addition to that, the '*bağdadi*' technique was used for the construction of timber framed walls. The pieces of brick and timber were filled in timber framed wall structures and then the outer and inner surface was covered with timber laths as a feature of the '*bağdadi*' construction technique. Moreover, the stone was used as an infill material in the East black Sea Region. The walls were plastered with lime or mud plasters or they were left without plastering.

The ground floor was covered with the pressed earth in the service spaces while inhabitable spaces were covered with timber panels. Upper floors were constructed by floor girders and covered by timber panels. Ceilings were covered by timber or not covered. In some cases, '*bulgurlama*' technique was used for the floor construction especially in the Central Anatolia. *Bulgurlama* was a kind of timber floor technique that was composed of double layer floor girders which was filled by earth in between.

Structural elements of the roof were made of timber. Ridge or hip roof was the preferred form of roof. The roofs were generally covered with ‘over and under’ tiles, but there are examples that the timber was used as a roof covering material especially in the Black Sea Region.

In addition, differences related with periods and regions were observed. For example, ground floor walls were constructed in part or completely with timber framed system in the last periods of the traditional dwelling constructions. Moreover in the timber-framed systems, there are differences in the dimensions of the timber elements and dimensions of the intervals. In the East Black Sea Region there are examples of traditional houses built with timber masonry system.

The structural and constructional characteristics of the traditional houses were discussed in more detail below.

### **2.2.1 Structural System of Foundations and Basement Floor**

Generally information about the foundations was limited in the related studies. The foundations and the basement floor of Safranbolu houses were constructed with stone masonry system (Kaya, 1996). Çobancaoğlu (1998) indicated that the foundations of traditional dwellings in central Anatolia, west of Anatolia and Marmara region were rubble stone masonry. Şahin (1995) clarified that the timber beams in the stone foundation walls were used regularly at one meter intervals.

Before the construction, whatever the kind of foundations was, the excavations were done until reaching a relatively strong ground. Because of that, the depth of the foundations varied. As an example, the depth of foundations of Ankara houses is between 20 cm and 200 cm (Şahin, 1995). Çobancaoğlu (1998) indicated that the depth of foundations changed between 50 cm and 80 cm in the Central

Anatolia, 100 cm and 150 cm in the North Anatolia and 50-100 cm in the West Anatolia.

In the foundations of Ankara houses a type of andezite called as Ankara stone was commonly used. The upper section (approximately above 100 cm) of the masonry base was composed of mud brick or rubble stone. Generally the thickness of the walls varied between 60 cm and 80 cm for Ankara houses, 60 and 70 cm for the houses of Central Anatolia, 50 and 70 cm for the houses of West Anatolia (Şahin, 1995; Çobancaoğlu, 1998).

In accordance with structural characteristic of foundations, there were three types as; discontinuous, continuous and composite foundations. Discontinuous foundation was commonly used in North Western Anatolia (Beyazır, Nallıhan), North Anatolia (Bolu, Sinop, Samsun, Terme, Sürmene, Rize, Artvin)(Şahin, 1995; Çobancaoğlu, 1998). In that system, the timber posts with a cross section of 20x20 cm or thick timber logs were placed on the top of the irregular stone piers. The openings between the posts were filled with mud brick or stone walls (Şahin, 1995). Stone piers raise to 25-40 cm or 20-30 cm above the ground level (Şahin, 1995; Çobancaoğlu, 1998). In addition Çobancaoğlu (1998) explained that the posts of the foundations were directly placed on the ground in some examples and chest-nut species was used for the foundation of posts.

The continuous foundations with the form of frame delivered the loads coming from load bearing walls to the ground. This kind of foundations constructed with rubble stone masonry could be observed in some Ankara houses built at the end of 19<sup>th</sup> century (Şahin, 1995). Continuous foundations could also be observed in North Anatolia, West Anatolia and Marmara Region (Çobancaoğlu, 1998).

In the composite foundations, the foundation of external edges of the building was rubble stone masonry forming an outer frame, and the inner axis or partition walls

built of timber framed system were supported by separate main posts. That type of foundation was common in North Western and Central Anatolia (Şahin, 1995).

According to Şahin (1995), the rubble stone foundation walls were reinforced with the timber beams placing on the interior and exterior faces of the wall around at interval of one meter. She also emphasized that the timber beam was placed in the wall to provide unity of the wall and especially resin riche pine beam was used as a damp proof material due to lack of hydrosopicity perpendicular to the fiber orientation and lack of hydrosopicity in resin rich pine. The beams with a cross section of 10 cm x10 cm used in the both face of the walls were connected to each other regularly by tie beams with a cross section of 10 cm x10 cm or 5 cm x10 cm.

### **2.2.2 Masonry (Stone and mud brick) and Timber Framed Walls in the Ground Floor**

The ground floor walls of the traditional Ankara houses were made of stone (cut or rubble stone) or mud brick masonry (Şahin, 1995). Generally the masonry ground floor walls of the Safranbolu houses were constructed with rubble stone and in a few examples they were mud brick (Kaya, 1996). Rubble stones were occasionally used in the masonry wall of the traditional houses in the East Black Sea region. In addition to that, rarely brick masonry ground floor walls could be observed (Sümerkan, 1990). Çobancaoğlu (1998) revealed that the ground floor masonry walls of the traditional dwelling were made of rubble stone and mud brick in north and Central Anatolia, rubble stone in west and south Anatolia, rubble stone, cut stone and brick in Marmara Region.

Generally in rubble stone masonry wall with an irregular order, the bigger stone blocks were placed at the outer parts and small ones placed in the inner parts.

Earth based mortar made of silt, clay, and straw was used in Ankara and Safranbolu houses (Şahin, 1995; Kaya, 1996). Sümerkan (1990) indicated that mud and lime mortar was used for the construction of stone masonry walls in the East Black Sea Region. In accordance with types of stone, in Ankara houses andezite, in Safranbolu houses limestone, in the East Black Sea houses lime, tuff, andezite, basalt stones were used for the construction of ground floor masonry wall (Şahin, 1995; Kaya, 1996; Sümerkan, 1990).

The width of the stone masonry walls of the ground floor were varied in between 55 cm and 80 cm in Safranbolu, 40 cm and 60 cm, 90 cm and 100 cm (Especially in high level differences) in the east Black Sea, 60-90 cm in the Central Anatolia and the Marmara, 50 cm and 60 cm in the South Anatolia. The height of the ground floor masonry walls differed according to height of the ground floor such as 2.17 cm in the East Black Sea, 2.50-3.00 cm in the West Anatolia. Generally beams made of fir and pine timber were used regularly in each 80-1.50 cm. for the construction of masonry walls (Sümerkan, 1990; Şahin, 1995; Kaya, 1996; Çobancaoğlu, 1998).

Şahin (1995) indicated that the outer faces of the ground floor was made of cut stone masonry in the some examples of Ankara houses. The size of cut stone blocks varied in these examples being 25-30 cm in height and 50-60 cm in length.

At some traditional timber framed houses, the ground floor masonry walls were constructed with mud brick. In the mud brick masonry walls two different types of units were used. In Ankara houses the dimensions of bigger units were 24-30 cm x 24-30 cm x 10 cm (width, length, thickness) and the smaller units were 12.5-15 cm x 24-30 cm x 10 cm (Şahin, 1995). In some of the Safranbolu houses the dimensions of bigger units were 27 cm x 27 cm x 10 cm and smaller ones were 13 cm x 27 cm x 10 cm (Kaya, 1996). The width of the mud brick masonry walls

varied in between 50 cm and 80 cm in Ankara houses while varying in between 65 cm and 80 cm in Safranbolu houses (Şahin, 1995; Kaya 1996).

Şahin (1995) referred that, composite or framed masonry construction technique was used in some sections of some Ankara houses. In that technique, the vertical timber elements (studs) placed between the beams were used to support the mud brick masonry walls. As well as timber framed masonry system could be observed in Safranbolu and Marmara region (Kaya, 1996; Çobancaoğlu, 1998).

Some of the inner partition walls were constructed with timber framed system. Moreover in some of the examples built in late periods, some of the outer walls of the ground floor were constructed with timber-framed system. Timber framed walls will be discussed in more detailed below. Inner partition walls of the East Black Sea houses were built with timber plates. When timber plates were placed horizontally, they were connected each other by special profile and when they were placed vertically the timber laths were placed where the plates meet (Sümerkan, 1990).

In consideration of the connection between the masonry and timber framed section, the wall plates were set on the inner and outer edges of the masonry wall and then the floor girders were placed on top of them. Perpendicular the floor girders, other foot plates were placed for the main posts of the upper floor. For the connection of the girders and foot plate, the elements overlapped each other and sometimes fixed by nails or they were placed overlapping each other by special joints (Şahin, 1995).

### **2.2.3 Single Posts in the Ground Floor**

The single posts were used for supporting the eaves, projections and outer sofa. Their cross sections varied about 12 cm x 12 cm or 15 cm x 15 cm. they were placed on the top of the stone piers (Çobancaoğlu, 1998). Şahin (1995) explained that the cross section of single posts were 15x20 cm and 20x20 cm.

### **2.2.4 Masonry Systems (Stone, Mud brick and Timber) in Upper Floor(s)**

#### **Stone and Mud Brick Masonry Walls**

Some of the masonry walls of the houses were continued to the upper floors, as a service wall, which contained fireplaces, cupboards, niches etc. In addition, Şahin (1995) had explained that in some examples the masonry walls might continue in the mezzanines then after the first floor the timber framed section starts. Sümerkan (1990) indicated that in the East Black Sea Region, because of the special topographical conditions, the walls located in the high level of the site were constructed with stone masonry technique. The upper floor(s) masonry walls of the building were constructed with the same characteristics of the ground floor masonry walls as mentioned below.

#### **Timber Masonry Walls**

Generally the examples, which were constructed with timber masonry system, were observed in the East Black Sea Region as well as in the some of the forest areas such as Bolu, Gerede, Kızılcahamam etc. Sümerkan (1990) examined this system classified in two types as masonry system with timber plates and with logs. The dimensions of timber plates varied in between 4 cm and 6 cm in width and 20 cm and 30 cm in height. Their length was same as the length of the room.

The log masonry systems were composed of the logs with circular cross section about 25-35 cm in diameter.

### 2.2.5 Timber Framed Walls in Upper Floor(s)

The structural members of timber framed construction walls were the main posts and plates. The auxiliary members, which shape the facades in relation to infill material and the openings, were the studs, the window and door posts, window sills, door sills, tie beams and braces (Figure 2.1). They formed the main frame of the timber-framed construction.

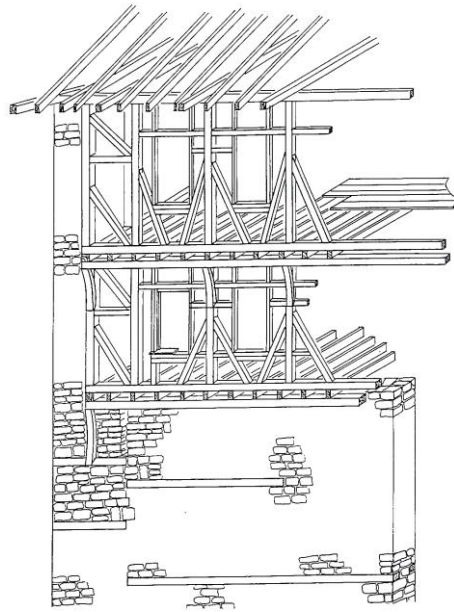


Figure 2.1 Timber framed wall system in traditional dwellings from Bursa-Cumalıkızık, the Street Eğrek and No:18 (Kandemir, 2000: 153)

Pine, chestnut, oak, poplar, cedar, willow, beech and spruce species were used for the timber framed system with differences between the regions according to vegetation of the regions.

The dimensions of the timber elements varied according to wall construction system. Dimensions of the timber elements are listed below for different regions.

**Ankara Houses** (Şahin, 1995)

Main Post: Cross section 10cm x10 cm

Stud, window and door post: Cross section 5 cm x10 cm; 40-60 cm at intervals

Foot Plate: Cross section 10 cm x10 cm, 10 cm x15 cm, 15 cm x15 cm

Wall Plate: Cross Section 10 cm x 10 cm, 10 cm x15 cm, 15 cm x15 cm

Bracing element: Cross Section 10 cm x10 cm, 5 cm x10 cm

**Safranbolu Houses** (Kaya, 1996)

Main Post: With mud brick infill, cross section 15 cm x12 cm or 14 cm x12 cm ; 70-75 cm at intervals;

With stone infill, Cross section 14 cm x11cm and 11 cm x8 cm; 30-35 cm or 20-25 cm at intervals;

Stud, window and door post: Cross section 12 cm x10 cm; 40-60 cm at intervals

Bracing element: Cross section 12 cm x9 cm

**East Black Sea Region** (Sümerkan, 1990; Türkmen, 1995; Çakır, 2000)

Main Post: With stone infill, cross section 12 cm x12 cm or 15 cm x15 cm

Stud, window and door posts: Cross section 7 cm x14 cm, 8 cm x14 cm, 5 cm x10 cm; 15-30 cm at intervals (Square formed system '*göz dolma tekniği*'); 20 cm x35 cm at intervals (Triangle shaped system '*muskalı dolma tekniği*')

**South Anatolian Region** (Çobancaoğlu, 1998)

Main Post: Cross section 12 cm x12cm or 15 cm x15 cm; 1.00-1.50 cm at intervals

**Marmara Region** (Çobancaoğlu, 1998)

Main Post: Cross section 16 cm x16 cm or 17 cm x17 cm

Wall and foot plate: Cross Section 8 cm x13 cm or 8 cm x18 cm

Generally, the construction of timber framed wall system had same characteristics. Main posts were placed at the corners of spaces. They assembled the upper and lower plates. The main posts were set on the foot plates. They were combined with the wall plate, which carried the floor girders. Studs divided the distance between the main posts regularly. The studs also were used to frame openings. The upper and lower sills for window and the upper sill for door were placed between the window and door posts. In addition the walls were divided with tie-beams with appropriate distances to place the infill material. The bracing elements supported the main posts or studs. The primary bracing elements were placed between the foot and wall plates. But secondary ones did not continued through the floor height. In the East Black Sea Region the intervals of the main posts and studs were reduced. Then the wall surfaces were divided by timber elements by forming square or triangle holes that were appropriate for stone infill (The techniques of göz dolma and muskalı dolma) (Sümerkan, 1990; Türkmen, 1995; Çakır, 2000).

### **2.2.6 Infill Materials**

Infill materials of the timber framed wall construction were brick, mud brick, stone and timber. In Ankara houses, mud brick and brick were used as infill material. The dimensions of the mud brick infill were about 24x24x10 cm, 28 cm x28 cm x10 cm, 30 cm x30 cm x10 cm, 24 cm x12.5 cm x10 cm, 30 cm x15 cm x10 cm. The dimensions of brick were about 10-11 cm x 22-23 cm x 7-8 cm, 14-15 cm x 25-26 cm x 7-8 cm, 10-20 cm x 25-39 cm x 9-10 cm (Şahin, 1995).

The infill materials of the system were mud brick, stone and timber in the Safranbolu. The dimensions of the mud brick were 27 cmx27 cmx10 cm, 27 cm x22 cm x10 cm and 27 cm x13 cm x10 cm (Kaya, 1996). Sümerkan (1990) indicated that timber, stone and mud brick was used as infill material of the

traditional houses located in the East Black Sea Region. Timber infill was about 2.5-6 cm in width and 25-35 cm in height and the length is as length of the room. Stone and stone pieces were used for the infill material of the system of '*göz dolma*' while the stone pieces were used in the system of '*muskalı dolma*'.

In accordance with the houses located in the West Anatolia region, the infill material was stone, brick, mud brick, and timber. Çobancaoğlu (1998) referred the examples of Kula, Milas, Birgi and indicated that pieces of brick, timber, mud brick was filled in between the structural elements then surface of the wall was covered by timber plates and plastered. This infill system was called technique of '*bağdadi*'. The '*bağdadi*' technique was used for the construction of dwellings also in south Anatolia.

The infill material was brick, mud brick and timber in the Marmara Region. *Bağdadi* technique could be also observed. In addition to that, the structural system was covered with the timber plates of dimensions 2-3 cm in width, 8-15 cm in height and 1.00-2.00 cm in length.

### **2.2.7 Plaster Materials**

Lime plaster with sand and lime mixture and mud plaster with clay, silt, sand and lime mixtures were commonly used for the construction of traditional timber framed dwellings (Şahin, 1995; Çobancaoğlu, 1998). Moreover, Çobancaoğlu explained that gypsum plaster was also used for the wall construction as in Çorum and Çankırı cities. Timber framed buildings with mud infill were generally plastered while those buildings with brick infill could not be plastered.

Sümerkan (1990) indicated that, the walls of the traditional houses in the Black Sea Region were: i) plastered totally with lime plaster ii) partly plastered iii) not

plastered. In addition, in some of the examples the interior façade of the wall were covered with timber plates.

### **2.2.8 Structure of Floor and Ceiling**

Timber floors were constructed by placing the floor girders on the wall plates. Then the upper surface of these girders was covered with timber panels or bricks. Generally the floor was covered with timber panels in the inhabitable spaces.

Şahin (1995) indicated that, there were two alternatives for the timber ground floor construction in the most of the Ankara houses. In the first one, timber beam placed on a stone platform. On top of this beam the floor girders were placed usually parallel to the short side. In the second type, the timbers were inserted into walls then girders were placed above them. In another alternative where the ground floor was altered, the beams on which the floor girders set are placed on top of the timber posts. In another type, the wall plates and the beam were placed on the inner and outer faces of the masonry wall. Then the girders were set and the foot plate were placed on the edges perpendicular the girders. In addition, the earth filled floor type '*bulgurlama*' could be observed in the early Ankara houses. The floor was constructed with doubled layer and the gap between the layers was filled with earth for isolation.

The technique of *bulgurlama* was used for the construction of floor in the Safranbolu houses. In the East Black Sea Region, there was a gap about 50-70 cm between the ground floor where the stable is located on and the upper floor for isolation. The gap was filled with earth or straw.

The ceilings of the floors were covered with timber panels or were not covered especially in the service spaces located in the ground floor. In the ceilings of some spaces the decoration patterns were also used.

Floor girders could be made of pine, cedar, fir or poplar and the floor and ceiling covering plates could be made of pine. The dimensions of elements of the floor and ceilings constructions are given below.

**Ankara Houses** (Şahin, 1995)

Girders: 5 cm x10 cm in cross section

Floor covering plates: 2.5-3 cm in width

**Safranbolu Houses** (Kaya,1996)

Girders: 4.10- 4.20 cm in length, 35-40 cm at intervals

**West Anatolia** (Çobancaoğlu, 1998)

Girders: 15-18 cm in diameter, 50-80 cm at intervals

Floor Covering plates: 2-3 cm in width, 18-30 cm in length

Ceilling Covering Plates: 1-1.5 cm in width

**South Anatolia** (Çobancaoğlu, 1998)

Girders: 3.50- 4.00 cm in length, 40-60 cm at intervals

**Marmara Region** (Çobancaoğlu, 1998)

Girders: 8 cm x12 cm, 8 cm x13 cm, 8 cm x18 cm in cross section, 40-70 cm at intervals

Floor covering plates: 2-5 cm in width, 15-40 cm. in height

### 2.2.9 Projections

According to their structural systems, the projections can be classified in three groups as projections with overlapping elements, projections with bracing elements and the simple projections (Şahin, 1995; Kaya, 1996; Çobancaoğlu, 1998).

The projection with overlapping elements is constructed by the timber beams overlapping each other. Şahin (1995) explained that in the earliest example the span projected by this type was about 1.50 m. This type of projection can be observed in the Ankara houses and rarely in the Safranbolu houses.

The simple type projections are occasionally can be observed as the triangular, trapezoidal and rectangular in forms in the traditional dwellings. The projections were extended about 50-60 cm in Ankara houses, 65-90 cm in Safranbolu houses, 60-70 cm in the North Anatolia houses, 40-60 cm in the Marmara houses (Şahin, 1995; Kaya, 1996; Çobancaoğlu, 1998).

The projection with bracing elements was supported by two or more bracing elements. The extending length of the projection with bracing element is about 80-130 cm in Safranbolu houses (Figure 2.2) (Kaya, 1996).

In some examples the surface of above the projections were covered with timber or plastered. Sometimes only bracing element was covered with timber laths. In some examples especially in the South Anatolia, those braces covered with laths were plastered (Çobancaoğlu, 1998).



Figure 2.2 A Safranbolu House with the projection with bracing element

### 2.2.10 Structure of Roof

Şahin (1995) defined the structure of the roof for Ankara houses. This construction system is usually used in the timber framed traditional dwellings in the other regions. Generally the roof girders are set on top of the upper storey ceiling girders to be placed the king posts. The ridge purlin is supported by the king posts. The purlins located in the different level divide the distance between the ridge purlin and the wall plate placed on the wall. Purlins are supported by the posts that are attached to each other by tie beams. Rafters are placed on top of the purlins at 40-60 cm intervals. The timber panels with 2 cm in width are covered on top of the rafters and the final covering material are placed. Generally the covering material of the roof is over and under tile. Timber also was used as a roof covering material such as in the Safranbolu and East Black Sea Region. Timber covering plates which are locally named *pedavra*, *bedevra* or *hartama* are placed in double layers to close the joints of them (Sümerkan, 1990; Kaya, 1996). Çobancaoğlu (1998) indicated that spruce and fir are used for the timber covering material. When the roof covering material is timber, the intervals of the rafters is

about 20 cm (Sümerkan, 1990). Moreover, in the South Anatolia and Central Anatolia, the roof covering material is pressed earth that is placed on the tree branches (Çobancaoğlu, 1998).

The width of the eaves varies in between 60 cm and 100 cm in Ankara houses, 50 cm and 70 cm in the East Black Sea, 80 cm and 150 cm in the West Anatolia (Şahin, 1995; Sümerkan, 1990; Çobancaoğlu, 1998).

## **CHAPTER 3**

### **PROPERTIES OF WOOD AFFECTING ITS MECHANICAL BEHAVIOUR**

In this chapter, the literature survey about chemical and physical structure of wood, its mechanical properties and factors affecting its mechanical properties are presented. Ultrasonic pulse velocity measurements, acoustical properties and their measurements and thermal properties of timber and IR Thermographic investigations will be reviewed in the next chapter in relation to non destructive analyses.

#### **3.1 Chemical and Physical Structure of Timber**

In order to understand the performance of timber species, it was helpful to appreciate the structure and composition of that material. The aim of this section was to introduce the timber material by means of examination of its chemical and physical aspects.

##### **3.1.1 Chemical Structure of Wood**

###### **Structural Polymers**

A tree is, composed of three structural polymers cellulose, hemicellulose and lignin. Cellulose forms about 40-50% of wood and is largely responsible for the strength within the cell wall. Hemicellulose, a second structural polymer, which differs somewhat between the hardwoods and softwoods, is formed from sugars

like cellulose. Hemicellulose generally forms about 20-30% of softwoods and 25-40% of hardwoods, and it is responsible for elasticity. Sugars also start the formation of a hugely complex series of molecules known as lignin. *Lignin* is the third structural component of wood. Lignin into and around cell walls gives plants the mechanical strength. Hardwoods have less lignin (20-25%) than softwoods (25-30%) (Ridout, 2001). The percentage of cellulose, hemicellulose and lignin in softwoods and hardwoods were given in Table 3.1 (Ridout, 2001).

Table 3.1 The percentage of cellulose, hemicellulose and lignin in softwoods and hardwoods (Ridout, 2001)

	<u>Softwoods</u>	<u>Hardwoods</u>
<b>Cellulose (%)</b>	40-50%	40-50%
<b>Hemicellulose (%)</b>	20-30%	25-40%
<b>Lignin (%)</b>	25-40%	20-25%

Extractives are mostly found inside the cells, and rarely in the cell walls. They consist of various aromatic compounds, which influence the color, fragrance, surface consistency, durability and pest-resistance of woods. Their percentage is about 1-3% in wood (Knut, 1999).

Starch, pectic compounds, and proteins occur in small quantities in wood. Those components are found within the storage cells and are key for the development of insects and fungi. Starch and protein are not only of great significance for the development of the larvae of many insects, but together with the solid cell wall substances are also important nutrients for wood-rotting fungi (Knut, 1999).

### **Cell Wall**

Three components mentioned above together form the wall of the cell. The basic cellulose component of a cell wall at the molecular level is usually called a microfibril. It is usually considered that the hemicellulose encrusts the cellulose

microfibrils. The three structural substances are arranged to construct the cells. Each decay organism attacks celluloses and lignin and the final results of decay will depend on the way in which the cell structure is organized. The cell wall is constructed from two or three distinct layers: the primary wall, the secondary wall, and sometimes an innermost tertiary wall or wart layer, then lumen or hollow interior of the cell (Ridout, 2001).

### **3.1.2 Physical Structure of Wood**

#### **Hardwood and Softwood**

Species of trees are divided into two classes: hardwoods, which have broad leaves; and softwoods or conifers, which have needle-like or scale-like leaves. Hardwoods shed their leaves at the end of each growing season, but most softwoods remains green throughout the year. The terms of hardwood and do not directly indicate the hardness of wood. In fact there are hardwoods which are softer than certain softwoods (American Institute of Timber Construction, 1966).

Softwood trees grow in the regions where the climate is harsh and the soil is poor in nutrients. Their ability to survive in these areas derives to a large extent from an ability to restrict water loss, by the possession of a water conducting system controlled by valves, and by narrow waxy needles that restrict vapor loss. The hardwood trees tend to favor environments where conditions are suitable for prolonged strong growth, although many are able to tolerate poor soils and harsh weather (Ridout, 2001). Some properties of softwoods and hardwoods were summarized in the Table 3.2 to point out their main differences (Ridout, 2001).

#### **Heartwood and Sapwood**

Several distinct zones are seen in the cross section of a log; the bark, a light colored zone called sapwood, an inner zone generally of darker color called

heartwood, and at the center the pith. A tree increases in diameter by adding new layers of cells from the pith outward. This new layer functions as living cells which conduct sap and store food, but eventually, as the tree increases in diameter, cells towards the center become inactive and serve only as support for the tree. The inactive inner layer is the heartwood; the outer layer containing living cells is the sapwood. There is no consistent difference between the weight and strength properties of heartwood and sapwood. Heartwood, however is more resistant to decay fungi than is sapwood, although there is a great range in the durability of heartwood from various species (American Institute of Timber Construction, 1966).

Table 3.2 Structure of softwoods and hardwoods summarized from Ridout (2001)

<b>STRUCTURE OF SOFTWOODS</b>	<b>STRUCTURE OF HARDWOODS</b>
<ul style="list-style-type: none"> <li>• Softwoods have uniform structure.</li> <li>• %90-95 of the wood consists of slender cells orientated along the axis with closed flattened or tapered ends. Those cells are known as tracheids.</li> <li>• Tracheids are the only cells that can supply most of the necessary strength to the tree while allowing water conduction.</li> <li>• Strength is supplied by seasonal thickening of the cell wall.</li> <li>• Water conduction is done with apertures in the cell walls called pits. Pits are formed from two apertures in adjacent cell walls. These apertures together form a chamber.</li> <li>• Ray cells have cellulose walls.</li> </ul>	<ul style="list-style-type: none"> <li>• Hardwoods exhibit a more complex structure.</li> <li>• Strength appears to be mainly supplied by long narrow cells with closed pointed ends called fibres. Most of the water transport is carried out in a direct fashion by elongate units known as vessels.</li> <li>• Vessels are constructed from individual cells joined end to end over a considerable distance.</li> <li>• This water transportation system is far more direct than the tracheid system of softwoods.</li> <li>• Bordered pits occur in the vessel walls.</li> <li>• Ray cells form a far greater proportion of hardwoods, amounting to 30% of the volume.</li> </ul>

### **Annual Rings**

In climates where temperature limits the growing season of a tree, each annual increment of growth usually is readily distinguishable. It is known as an annual ring and it is composed of a springwood and a summerwood band (American Institute of Timber Construction, 1966).

In many woods large thin walled cells are formed in the spring when growth is greatest, while smaller, thicker walled cells are formed later in the year. The areas of fast growth are called springwood and the areas of slower growth, summerwood. In annual rings, the inner, lighter colored area is the springwood and the outer darker layer is the summerwood. Summerwood contains more solid wood substance than springwood and therefore, is denser and stronger. The proportion of width of summerwood to width of annual ring is sometimes used as one of the visual measures of the quality and strength of wood (American Institute of Timber Construction, 1966).

### **Grain and Texture**

The terms grain and texture are used in many ways to describe the characteristics of wood. Grain often refers to the width of the annual rings. Texture usually refers to the fineness of wood structure rather than to the annual rings (American Institute of Timber Construction, 1966).

### **3.1.3 Cutting Wood**

Wood is distinguished as having been cut in one of three different directions: transverse, tangential, and radial.

Transverse cuts run at right angles to the trunk axis across the fibers. The wood surface shows the pattern of growth rings. Tangential run parallel to the trunk axis

and tangential to the growth rings. The growth rings form U-shape pattern in tangentially cut wood. Radial cuts run parallel to the trunk axis and the medullar rays. The wood shows a stripy pattern due to its growth rings when it is cut radially. The medullar rays are cut lengthwise that creates shiny bands and scaly patches called ripple marks of varying degrees of visibility. The more precise the radial cut, the more noticeable the ripple marks will be (Figure 3.1) (Knut, 1999).

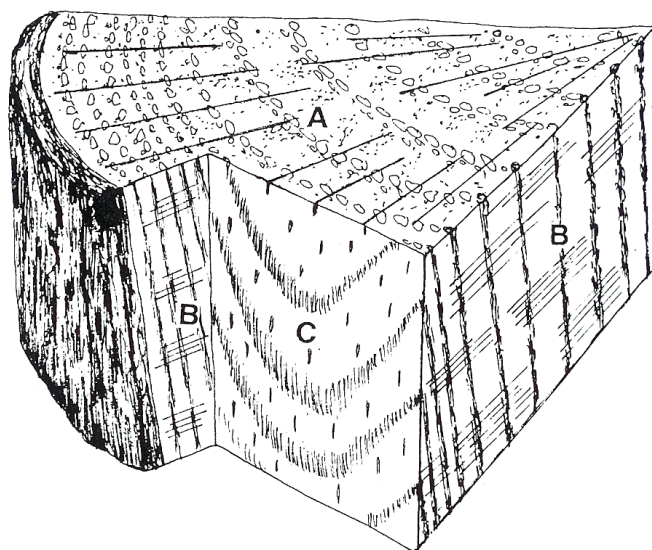


Figure 3.1 Schematic representation of a sector of wood (A) transverse, (B) radial, (C) Tangential Surfaces (Tsoumis, 1991: 6).

#### **3.1.4 Effects of Chemical Components on Wood Properties and Uses**

The contribution of the chemical components of wood to its properties is important to the concept of wood. The chemical components of wood ensure the strength. Cellulose is primarily responsible for the very high strength of wood in axial tension. Hemicelluloses and lignin bind the cells together and support the cellulosic and compressive strength (Tsoumis, 1991).

Removal of lignin and hemicelluloses drastically decreases the strength of wood in wet condition. The difference in behaviour of wood in wet and dry condition

results from the fact that in dry condition pectic substances and hemicelluloses still bond cells to one another, whereas in wet condition they are not capable of performing such a function. Thus the coherence between cells is destroyed and strength is drastically reduced or eliminated. The hygroscopicity of wood is due to its chemical composition; OH groups on cellulose chain molecules. It is also due to the presence of hydrophilic components, such as pectic substances and hemicelluloses (Tsoumis, 1991).

### **3.2 Moisture Content in Timber**

The amount of moisture in a living tree varies among species, in individual trees within the same species, in different parts of the same tree, and between heartwood and sapwood. Moisture content is the weight of the water contained in wood, expressed as a percentage of the weight of the oven dry wood. As wood loses moisture, the water in the cell cavity is evaporated first. The condition at which the water in the cell cavity has been evaporated but the cell wall is still saturated is known as fiber saturation point (American Institute of Timber Construction, 1966:4). Fiber saturation point varies between timber species but on the average it is around 30% (Tsoumis, 1991). Wood in use gives off or takes on moisture from the surroundings atmosphere with changes in temperature and relative humidity until it attains a balance relative to the atmospheric conditions. The moisture content at this point of balance is known as the equilibrium moisture content and it is shown in Figure 3.2 (American Institute of Timber Construction, 1966). Equilibrium moisture content at 100% relative humidity in normal atmospheric conditions reaches the fiber saturation point of wood.

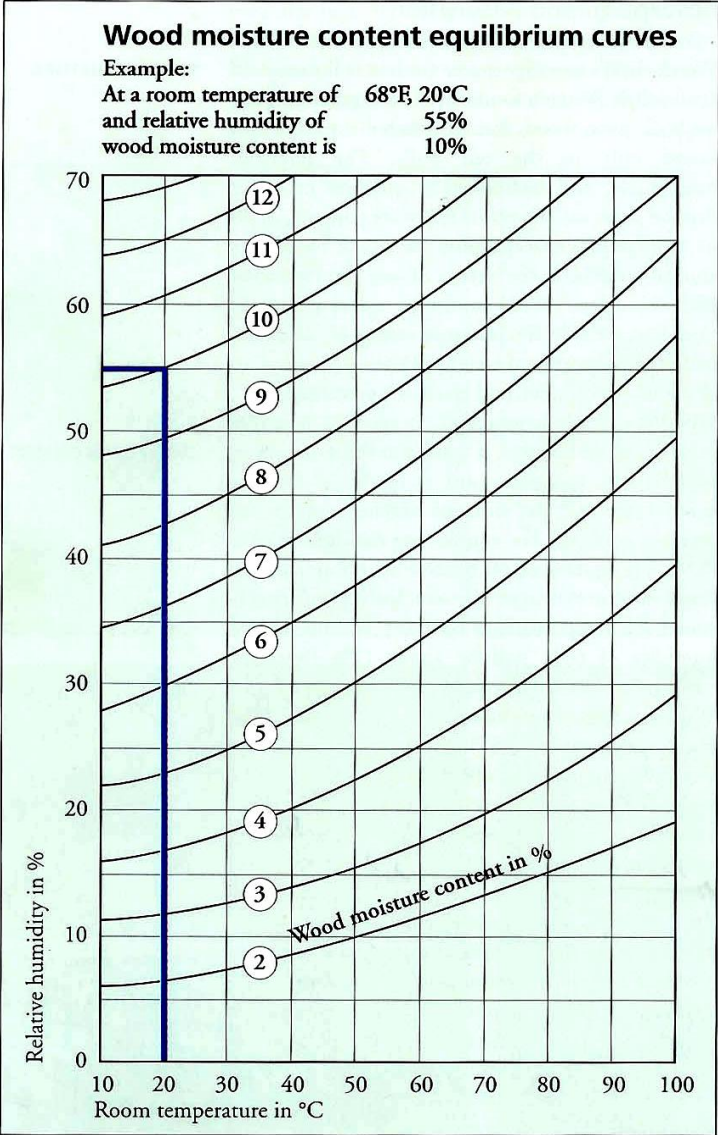


Figure 3.2 Wood Moisture Content Equilibrium Curves (Knut,1999: 20)

The quantity of moisture that is held depends on the existing atmospheric conditions as well as to the cell structure of the timber. Moisture content varies from place to place and from time to time. Depending on the meteorological data equilibrium moisture content variations of wood under shelter was estimated to be between 6-17% in Turkey, 8-23% in Greece (Tsoumis, 1991). Depending on the OH groups of the cell wall components particularly cellulose the quantity of water

vapor absorbed by a piece of timber may change. It has been demonstrated that hygroscopicity increases when wood extractives are removed. Thus timber with higher extractive content will tend to have lower equilibrium moisture (Ridout, 2001).

Water content in living trees varies from about 30% to 300%. This variation is influenced by different factors, such as tree species, position of wood in the tree and season of the year e.g., in soft woods, heartwood has lower moisture content than sapwood, in hard woods the differences are comparatively smaller (Tsoumis, 1991).

Maximum water that wood may contain depends on the space available in its mass when both cell walls and cell cavities are saturated. The maximum water content differs not only in different species but also same species between sap wood and heart wood. Maximum water content can be calculated by the equation (Tsoumis, 1991):

$$\begin{aligned}
 Y_{\max} &= 100 \left( \frac{r_w - r_o}{r_w r_o} \right) + f \\
 Y_{\max} &= 100 \left( \frac{1.50 - r_o}{1.50 r_o} \right) + f \\
 Y_{\max} &= 100 \left( \frac{1}{r_o} - 0.67 \right) + 30
 \end{aligned}
 \tag{1}$$

Where  $Y_{\max}$  is maximum moisture content (%),  $r_o$  is dry density ( $\text{g}/\text{cm}^3$ ),  $r_w$  is density of wood substance ( $1.50 \text{ g}/\text{cm}^3$ ),  $f$  is the moisture content at the fiber saturation point (30%).

Maximum water content values of a timber having basic density (bulk density) of  $0.70 \text{ g/cm}^3$  can be around 106%. An old pine having  $0.45 \text{ g/cm}^3$  can have around 185% water content in saturated condition.

Maximum moisture content is often used as an indicator of the scale of deterioration of archaeological waterlogged wood (Jensen and Gregory, 2006). When bulk density is  $0.01 \text{ g/cm}^3$  for the deteriorated timber its maximum water content may reach to about 1023% in comparison to its dry weight.

### **Determination of Moisture Content**

The moisture content of wood can be measured by a variety of methods as direct and indirect methods. Direct methods involve separation of moisture from the wood, whereas in indirect determination a property related to moisture is measured. Direct methods are (i) drying and weighing and (ii) distillation. Electric moisture meters mainly measure the moisture indirectly (Tsoumis, 1991).

Determination of moisture content also can be done by IR thermography as an indirect method. It was described in Chapter 4, Section 4.3.5

### **3.3 Density of Timber**

Density is the mass contained in a unit volume of a material, and specific gravity is the ratio of the material to the density of water. Density is measured in grams per cubic centimeter ( $\text{g/cm}^3$ ).

The density and specific gravity of wood are influenced by moisture, structure, extractives and chemical composition. Increasing moisture content increases the density of wood. While the weight of wood increases with increasing moisture content, volume increases at first, but then remains constant thereafter,

irrespective of the moisture retained. As a result apparent density becomes higher with increasing moisture content (Fig. 3.9) (Tsoumis, 1991).

The relationship of specific gravity and structure is examined on the basis of the factors that can be easily measured, such as width of growth rings and proportion of latewood. The influence of ring width is different in softwoods and in hardwoods. In softwoods, density tends to decrease with increasing ring width. In ring-porous hardwoods, density increases with increasing ring width. It is important to know that rings of the same width do not always have the same influence on density. (Tsoumis, 1991).

Higher amounts of extractives cause higher density of heartwood in comparison to sapwood, removal of extractives results in reduced density (Tsoumis, 1991).

### **Determination of Density**

Density is determined by measuring mass (weight) and volume, or by other methods. The simplest way of determining the volume is a calculation based on the direct measurement of length, width and thickness of a squared sample. For smaller blocks, and those of irregular shape the following procedure is more suitable. A beaker of water is placed on the pan or balance and counterbalanced by sand or weights. Then the test block suspended by a needle clamped in sand is lowered into the beaker and completely immersed in the water. Weights are then added to the opposite pan until equilibrium is restored, the weights in grams added to restore balance are equal to the volume of the test block in cubic centimetres (Desch, 1968). With today's technology, it is possible to calculate the volume with three-dimensional image processing to a very good approximation.

The density of wood and its variability within growth rings may be determined directly by use of instruments (densitometres) scanning transverse surfaces or their photographs on film. They record the density by measuring the absorbed

radiation ( $\beta$  or x rays) in different positions within a growth ring. Use of x ray is faster and more accurate. Sound waves have also been tried (Tsoumis, 1991).

### **3.4 Mechanical Properties of Timber**

Wood exhibits different mechanical properties in different growth direction (axial, radial, tangential). Therefore it is mechanically anisotropic. The mechanical properties of wood include its resistance to various types of loading. Different strength properties are called into play, for example, in resisting a compressive stress tending to crush a timber, a tensile stress tending to elongate it, shearing stress tending to cause one portion to slide over the remainder (Desch, 1968). Each property is discussed in the below.

#### **Strength in Tension**

This property shows considerable differences if loading is axial (parallel to grain) or transverse. Strength in axial tension is much higher (up to 50 times and more). In the transverse direction, the influence of radial or tangential loading is not consistent. Axial tensile strength of wood compares satisfactorily with metals and other materials (Table 3.3). The comparison is more favorable for wood if strength is related to density. This characteristic of wood, a light but strong material, is also expressed by the so called 'breaking length' which is the length of a theoretical ribbon of material breaking under its own weight. Breaking length is measured in kilometers, and the range for different woods is 7-30 km (softwoods 11-30 km, hardwoods 7-30 km), construction steel 5.4 km., concrete 0.2 km., PVC 4 km, etc. (Tsoumis,1991).

Axial tensile strength is greatly reduced by the presence of knots, spiral grain, or other growth abnormalities. The development of transverse tensile stresses is

carefully avoided in timber structures, because the strength of timber loaded in that manner is very small (Tsoumis, 1991).

### Strength in Compression

The strength of wood in compression is also different if loads are applied parallel or transverse to the grain. Axial compression strength is higher (up to about 15 times) and varies between 25-95 N/mm<sup>2</sup>, whereas transverse values vary between 1 and 20 N/mm<sup>2</sup>. The strength of wood in axial compression is smaller in comparison to metals, but higher in comparison to most other construction materials such as brick and stone. Stressing in transverse compression takes place, for example in railroad ties, whereas axial compression occurs in columns. The ratio of length to least dimension in width of a wooden material is important. If this ratio is smaller than 11/1 the strength, the strength of the column depends entirely on the strength of wood axial compression, if greater, the stiffness of the wood (modulus of elasticity) to resist buckling is also important (Tsoumis,1991).

Table 3.3 Mechanical Properties of wood and other materials in relation to specific gravity (Tsoumis, 1991)

Material	Specific gravity	Tensile strength	MoE
			N/mm <sup>2</sup>
Wood			
Spruce	0.44	84	9100
Oak, red	0.87	108	11650
Concrete	2.5	4	13800
Glass	2.5	50	72400
Aluminum	2.8	250	69000
Cast iron	7.0	140	82800
Steel	7.9	450	207000
PVC	1.3	60	5800
Polysterene	1	70	3450

### **Strength in Shear**

Shear may exist in longitudinal or transverse planes. Longitudinal shearing stresses are present when wooden members are stressed in bending. The strength of various woods in axial shear varies between 5 and 20 N/mm<sup>2</sup>. Strength in transverse shear acting on a cross section is 3-4 times greater than in axial shear. But this is not important in practice, since wood fails first in axial or rolling shear than in transverse shear. The highest shear stress occurs at an angle of about 45°, but the structure of wood as a whole contributes so that the planes of rupture are formed at an angle of about 60-70° in relation to the axis of the stressed member (Tsoumis, 1991).

### **Strength in Bending**

Strength in static bending is an important mechanical property, because in most structures wood is subject to bending loads. The typical case is a beam of wood bent under external forces, which act transverse to the axis. Under their action, three stresses develop; tension, compression and shear. The strength of wood in bending is usually expressed by the modulus of rupture, which shows the highest stresses in the outermost fibers of wood when the beam breaks under the influence of a load. The bending strength of wood is lower in comparison to metals, but higher than most nonmetallic materials (Tsoumis, 1991).

### **Toughness**

It refers to resistance against sudden loading. The energy absorbed by wood is higher when the load is impulsive rather than static. It has been observed that, with sudden loading, the deflection of a beam is about double in comparison to static loading (Tsoumis, 1991).

### **Elasticity**

The value of modulus of elasticity of wood varies between 2500-17000 N/mm<sup>2</sup>. Wood has a lower modulus of elasticity than other materials; however if weight is taken into consideration, wood is comparable to steel, modulus of elasticity is

different in the three growth directions. The above values apply to the axial direction, whereas transverse values are only 300-600 N/mm<sup>2</sup>. There are no differences between radial and tangential directions (Tsoumis, 1991).

### **Hardness**

It is a measure of the resistance of wood to the entrance of foreign bodies in its mass. The resistance is up to twice as high in the axial direction than sidewise, but the difference between radial and tangential surfaces is rarely important. Some woods are relatively soft (poplar, willow, pine), others have a medium hardness (pine, fir, walnut, juniper), and some are hard (yew, oak, elm, black locust, ash, beech, sycamore, hornbeam, maple, birch, olive). Tropical wood include a range from very soft (balsa) to very hard species (Tsoumis, 1991).

### **3.4.1 Factors Affecting Mechanical Properties**

The mechanical properties of wood are affected by various factors including the following; moisture, density, structure, temperature, duration of load, and defects in wood.

#### **Moisture**

It was reported by Tsoumis (1991) that moisture affected the mechanical properties when it changed below the fiber saturation point. Increase in equilibrium moisture content drastically dropped the compressive strength until the fiber saturation point was reached. After the fiber saturation point, compressive strength remained unchanged (Tsoumis 1991).

The influence of moisture content in the strength of timber was variable depending on the fiber directions. 1% change of moisture changed the strength in axial compression by 6%, bending strength (modulus of rupture) by 5%, hardness

by 2.5%-4% (more in the axial direction), modulus of elasticity by 2%, etc. Due to effect of moisture, mechanical properties were determined at a constant moisture content that was above the fiber saturation point or in air dry conditions (12%-15%) (Tsoumis,1991; Desch, *et al.*, 1996).

### **Density**

Density is the best and simplest index of the strength of wood without defects. With increasing density, strength also increases. Greater density derives from a greater proportion of cells with thick walls and small cavities and this result in greater strength of denser wood. The relationship of density and strength varies with different properties and species, but there is a linear relationship in most cases (Figure 3.3) (Tsoumis, G., 1991; Desch, *et al.*, 1996).

The effects of density on mechanical properties derive from structural differences that produce density variations. Ring width, proportion of late wood etc. affect the strength of wood (see Section 3.1). In softwoods, where latewood tends to decrease with increasing ring width, fast growing trees produce wood of lower strength. In hardwoods, wider rings are related to higher proportion of latewood and higher strength.

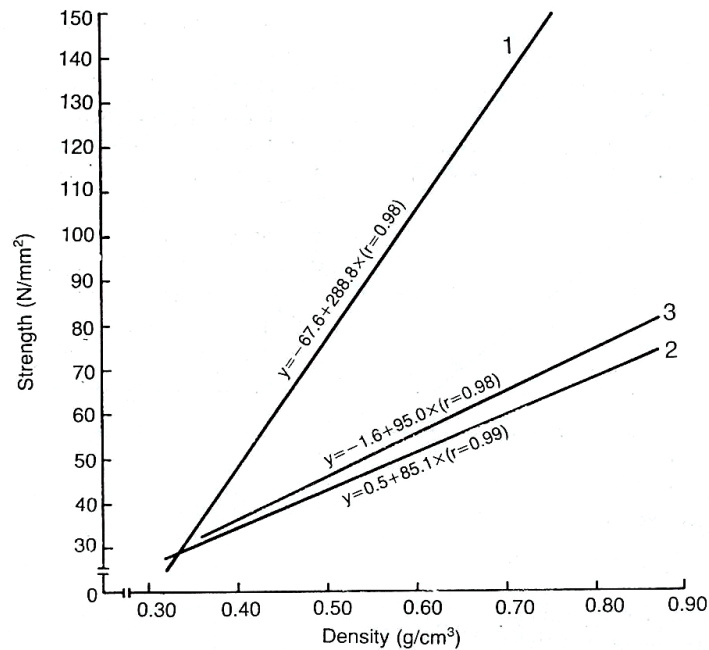


Figure 3.3 The relationship of strength(y) and density(x), 1. Static Bending(MOR), 2. Axial compression, 3. Hardness (Tsoumis,1991: 175)

### Temperature

The thermographic properties of wood will be explained in the Section 4.3.4. In general, the strength of wood is reduced with increasing temperature (Tsoumis, G.,1991; Desch, *et al.*, 1996). Long-term exposure to elevated temperatures results in a marked reduction in strength, stiffness and also toughness, the effect being greater in hardwoods than softwoods. Even exposure to cyclic changes in temperature over long periods has been shown to result in thermal degradation (Desch, *et al.*, 1996).

### Duration of Load

The duration of load has an important influence on the strength of wood. The magnitude of strength change in relation to time is influenced by the manner of loading. Under the action of a permanent load, wood exhibits the phenomenon of creep. Periodic loads result in fatigue. Permanent loading reduces the strength to 50-75% of the values obtained from static tests of short duration (Tsoumis, 1991).

In general, the behavior of wood to load duration is influenced by various factors which are related to wood species, density, moisture and the loading conditions magnitude of load, rhythm of change, etc. The resistance to fatigue increases with density. Creep increases with moisture content and temperature. (Tsoumis, 1991).

### **Defects**

Defects and decay reduce the strength of wood. The most important defects that reduce strength are knots, grain deviations, checks, tension, and compression wood.

*Knots:* A knot is an inclusion of the basal part of a branch within the stem of tree. There are two kinds of knots, depending on whether a branch was dead (dry) or alive at the time of inclusion. The knots resulting from dead branches are called encased or loose. On the other hand branches enclosed while living produce knots, such branches give rise to intergrown or tight knots. Knots may differ in shape and size. There are round, oval, and spike knots considered by shape. When considered by size, knots are classified as pin, small, medium and large. Knots affect adversely the appearance and properties of wood. Their adverse effect is due to the usually abnormal structure and higher density of their wood, local grain deviations and checks.

Depending on their type, size and location, knots may considerably reduce the strength of wood (Tsoumis, 1991). The presence of knots greatly reduces the strength of wood in axial tension while the strength in axial compression is reduced less. The strength in transverse compression on the other hand, may increase by the presence of intergrown knots. The bending strength (modulus of rupture) is considerably influenced by the position of knots. Knots found near the middle of the lower side of simple beams have the greatest adverse effect. The effect is smaller when knots are in the middle of the upper side, and very small when found between the two sides or near the ends of beam. Strength in

horizontal shear is affected little or not at all. Hardness and the resistance of wood to cleavage increase while modulus of elasticity is reduced by the presence of knots. In general, knots in the edges of wooden members have a greater adverse effect in comparison to knots of the same size located in their interior (Tsoumis, 1991).

*Grain Deviations:* The influence of grain deviations is basically due to the difference between axial and transverse strength of wood. Loading at an angle reduces strength; a greater angle results in a greater reduction. Tensile strength is affected more than compressive strength, while the reduction of bending strength is intermediate. Modulus of elasticity is also reduced by grain deviations, but the greatest effect is shown in toughness. It has been observed in beech that a 5° deviation reduces strength 10%, and a 10° deviation up to 50%. The effect of grain deviation to horizontal shear is minimal (Tsoumis, 1991).

*Checks:* Checks are formed due to differential shrinkage and swelling of knots, because their density is higher, they usually contain compression or tension, and their fiber orientation is different in comparison to those of the adjacent wood. The influence of checks depends on their size, direction, and the manner of loading. Axial tensile strength is unaffected or very little affected when checks have the same direction. The effect of checks on compressive strength is small, comparatively smaller in transverse than axial compression, but the reduction of strength in horizontal shear is considerable. The resistance of cleavage is greatly reduced when checks are present (Tsoumis, 1991).

### **3.4.2 Determination of Mechanical Properties of Wood in Laboratory**

In the assessment of the strength properties of timber small specimens (without defects) or actual structural timbers are used. There is no internationally accepted method of sampling. The American standard procedure (ASTM D143) provides sampling guide to study properties of wood. According to American Standard specimens are 5 cm x 5 cm or 2.5 cm x 2.5 cm in diameters for smaller trees. However sample size depends on property variations and is determined by statistical considerations. According to British Standard (BS378, BS 5820) the test samples must be conditioned to  $20 \pm 3$  °C and  $65 \pm 2$  percent relative humidity, and tested within the same temperature and humidity ranges.

Sampling must be performed in a methodological manner to obtain best results. Specimens from the historical timber structures should be removed without damaging the integrity of the structural member. The core samples can be put back immediately after the tests (Rug *et al.*, 1991).

#### **Strength Tests:**

Standard destructive compression, shear, tensile, and static bending strength tests are carried out in the laboratory so that the load bearing capacity of various size small specimens or test specimens of actual structural size can be determined (Sinclair, 1987; Desch, 1996).

Tests for the determination of the mechanical properties of wood are carried out with special testing machines that allow loading of a specimen with a measured load applied gradually or suddenly. Toughness is determined by tests intended to break the specimen with one stroke of a hammer. Hardness is measured by load needed to insert a steel ball with a known diameter (Tsoumis, 1991).

Few of the available strength testing methods are appropriate for in situ assessment of structural elements. The most reliable data can be obtained by a direct examination of the building itself (Lindstrom *et al.*, 1988). In the next section, the non-destructive methods for assessment of the strength of the timber will be summarized and in addition, recent developments will be discussed.

### **3.5 Durability of Timber and its Deterioration**

Deterioration of wood is closely related to the action of exterior factors rather than to the effect of time. In this section natural durability of timber and its deterioration by several decay factors will be summarized with more emphasis on decay by insects and fungi.

The resistance of wood to deterioration mechanisms that may cause degradation is called its durability (Tsoumis, 1991). According to European Standard (EN 350-1), the natural durability of wood is defined as the inherent resistance of wood to the attacks by wood destroying organisms (Acker *et al.*, 2003). The inherent resistance of wood is derived from its natural characteristics. For instance some of its extractives enhance its resistance against the destroying organisms. Ridout (2001) emphasized that the older wood had more extractives than the younger. As an example, some phenolic compounds which are found in heartwood of Scots pine are highly toxic to fungi. They are responsible for the durability of pine heartwood. The durability of softwood is largely dependent on the amount of heartwood present. The young and fast growing pine would have a low heartwood percentage and low durability. Whereas historic softwoods that were grown for long enough time would have a significant volume of heartwood and significant durability.

Wood deterioration mechanisms can be summarized as thermal degradation, light catalyzed oxidation, hydrolysis, physical degradation by wetting and drying conditions, and attack by wood destroying organisms (Stamm, 1970).

Wood is subject to thermal breakdown without undergoing burn. The first sign of thermal degradation is the loss of some water from the wood substance itself. Thermal degradation affects the three major components of wood. Hemicellulose is the most subject to thermal degradation followed by cellulose then lignin. Thermal degradation of wood is considerably more severe in the presence of moisture than its absence (Stamm, 1970). Hydrolysis is an acid or acid salt catalyzed reaction with water to produce lower polymers and various sugar. The cellulose and hemicellulose of wood are affected by hydrolysis. When wood is in contact water with long periods of time, the natural acidity of wood (pH 4 to 5 where is 7 is neutral) cause hydrolysis of the hemicellulose at ambient temperature (Stamm, 1970). Under the sunlight or ultraviolet, wood is weathered. The surface tends to brown when the wood is dry, and grey when exposed to moisture cycling conditions. That reaction is called light catalyzed oxidation that affects the lignin, extractives and some hemicellulose. Wood is also physically degraded as a result of stress gradients by changing the moisture gradients. When the free water is lost, the dimension of wood is not changed. Contraction and shrinkage occur when the bound water which is held within the cell walls is lost (Stamm, 1970).

### **Damage Caused by Fungi**

There are two main kinds of fungi as stain and decay fungi. Stain fungi cause discoloration of wood. They usually attack softwoods (pine, spruce, etc), and seldom hardwoods (poplar, beech, oak, ash, tropical species). It is generally believed that there is no strength reduction of practical importance by stain fungi. Decay fungi constitute the most important factor that affects the durability of wood (Ridout, 2001; Tsoumis, 1991).

Decay fungi consume cell walls since those organisms require nitrogen available mostly in the form of participated proteins in the cell wall structure (Ridout, 2001). In general there is more available nitrogen within the outer part of sapwood. On the other hand, usable nitrogen levels are very low in the heartwoods of traditional building timbers and heartwood of many timbers contain extractives that are poisons to fungi. (Desch, 1996). Ridout (1991) emphasized that older wood had more extractives than younger. Therefore old timber in the traditional buildings has greater natural durability and resistance to fungi attack than any modern replacement of timber.

Different species of fungi differ in moisture requirements. However in general, wood must contain at least 20% moisture for an attack to start. Conditions become favorable for continuous fungal activity when moisture increases toward the fiber saturation point (35%-50%). Very high moisture content is also restraining factor for most fungi because of lack of oxygen (Desch, 1996; Tsoumis, 1991). Optimal temperatures range from 20 °C to 25 °C for the survival of fungi (Tsoumis, 1991).

Two main types of fungi as brown and white rot and a third one being soft rot are recognized. Brown rot fungi consume mainly carbohydrates available in cellulose and hemicelluloses. White rot fungi may decompose both carbohydrate and lignin. Brown rots are more often present in softwoods while white rots are present in hardwoods (Tsoumis, 1991).

Fungal attack results in changes of colour, structure, chemical composition and properties of wood. Tsoumis (1991) has summarised those changes. The colour almost always changes and become lighter with white rot and darker with brown rot. The density of wood decreases, according to stage of attack by fungi. The reduction of weight is used as a quantitative criterion to determine the degree attack in research studies. The hygroscopicity of wood changes by fungi attack and wood absorbs water faster. Wood also absorbs more moisture from the

atmosphere at high relative humidity and less moisture at low relative humidity conditions depending on the extend of fungi attack.

The mechanical properties of wood change by fungi attack. The degree of degradation depends on wood species, species of fungus, duration and continuation of attack. The thermal and acoustical properties of wood are also affected by fungi attack because of their relationship with wood density.

### **Damage Caused by Insects**

Like fungi, insects attack the wood of living trees, timber and products. Insects tunnel in timber, if the tunnels are numerous; they may reduce the strength of timber. Some insects only attack living trees or newly felled logs, some only seasoned wood, and others only the sapwood of certain species. According to Desch (1996), insects select the parts of the timber to attack. Therefore in some cases insect damage may be limited.

The environmental conditions that affect the development and activity of insects are the same as for the case of fungi (i.e. temperature, moisture, and air). Some insects are adaptable to a wide variation of temperature and moisture while others can not tolerate a very high temperature or moisture. In general the insects are favoured by higher temperatures and in contrast to fungi, lower moisture contents of wood (Tsoumis, 1991). Ridout (2001) emphasized the critical value of moisture content for some insects 12% and for a few many insects 8%.

European Standard EN 335-1 is useful guide to classify the hazards for timber and describe the biological decay potential of building timbers (Ridout, 2001).

## **CHAPTER 4**

### **NON-DESTRUCTIVE METHODS AND THEIR USE ON THE ASSESSMENT OF TIMBER ELEMENTS**

Non-destructive evaluation of materials is the science of determining the physical and mechanical properties of a piece of material without altering its end-use capabilities (Ross *et al.*, 1993). In the analysis of the historical buildings non-destructive analyses are of prime importance to assist first aid repairs or major surgery or record the chronology of the buildings erection and alterations. Fidler (1980) summarized the uses of non-destructive technology for the analysis of historical buildings as follows; evaluation of the total structural performance, evaluation of the building envelope, analysis of the properties of individual building materials, such as moisture content, strength, stiffness, detection of concealed architectural detailing and minor structural elements, analysis of the chronology of the built form could be studied by using non-destructive evaluation methods.

In this chapter the non-destructive methods of visual examination, ultrasonic velocity measurements and Infrared (IR) thermography were described and the studies on their use in historical buildings were summarised. Finally some other non-destructive and pseudo non-destructive methods that were applied to the analyses of historic structures were also summarised.

#### **4.1 Visual Examination for the Surface Assessment**

The simpler and the oldest non-destructive method was the visual examination. Today visual examinations are the first step of observation in practice. The visual inspection methods cover wide a range of applications. It helps to the decision of where to apply other non-destructive tests. Visual inspection indicates colour change, surface degradation by appearance of cracks and fibers due to thermal degradation and light catalysed oxidation etc., deformations and surface degradation by wetting and drying, the insects holes and presence fungi fruit bodies, mycelid growths etc (Stamm, 1970; Bray and McBride, 1992). A non-destructive inspector should always be alert for visible signs of degradation that may draw attention to the several problems otherwise escape detection.

Visual inspection records are also useful in providing historical data for the problems of the buildings. Visual inspection methods include examinations by eye, photography, telescope, borescope, perioscope, optical projector, previous photography, radiographs, videotape methods etc (Bray and McBride, 1992).

Where the wood structure is exposed to view, visual examination of the members is easy, but this is usually not the case. In most cases all or at least a substantial portion of the wood framing is concealed with the interior finishes. Visual inspection may be inadequate in the most cases. But a careful visual examination of the building can often give considerable guidance as to where the structural members may be troublesome (Lindstrom *et al.*, 1988). Such as a level survey of the floors can determine where the greatest deflections are present. Sometimes large deflections are simply the result of heavy sustained loads but a deflection may also occur as a result of the loss of member support strength. Locations with water stains are prime candidates for inspection.

Visual observations alone are not enough to decide on the repair, reinforcement or replacement of the items studied. As a result, visual inspection is necessary to identify the probable trouble areas that should be studied by other non-destructive methods.

## **4.2 Acoustical Properties of Timber and Ultrasonic Testing Method**

Ultrasonic, sonic stress wave, acoustic emission and acousto-ultrasonic methods are the most widely studied non-destructive evaluation techniques for wood. Their signal features, like propagation time, velocity measurements, amplitude, attenuation, frequency etc. have been correlated to wood characteristics such as strength, modulus of elasticity, homogeneity and density. In addition, they have been used for detection of decay and biodeterioration etc.

In this section, acoustical properties of timber and ultrasonic testing method were examined in more detail.

### **4.2.1 Acoustical Properties of Timber**

When sound waves produced by another source reach wood, part of the acoustical energy is reflected and part enters its mass. Wood vibrates, and the original sound is intensified or subjected to partial or total absorption.

#### **Absorption of Sound**

Acoustical energy may be absorbed (at least partially), due to repeated refraction and reflection of sound waves. In this manner, friction of the molecules, which make up the mass of wood, transforms the acoustical energy of the sound wave to

thermal energy. The ability of wood to absorb sound is measured by the coefficient of sound absorption, which is an expression of the proportion of the absorbed sound. Wood has an advantage in comparison to the other materials, due to its porous structure, but has a relatively low coefficient of absorption less than 10 %. The coefficient is affected by wood density and other factors, such as modulus of elasticity, moisture content, temperature, intensity and frequency of sound, and condition of the surface of wood. Woods with lower density and modulus of elasticity, and higher moisture content and temperature, absorb more sound. Absorption is greater with lower frequency sounds, and it is lower in lacquered wood (Tsoumis, 1991).

### **Speed of Sound**

The speed of sound in the mass wood varies, depending on the direction (axial, transverse) and the species of wood. In the axial direction it is about 3500-5000 m/s. Transversely the speed is lower, because modulus of elasticity, which affects the speed of sound, is lower in that direction. Speed is theoretically calculated from the relationship (Sandoz, 1994; Ross, R. *et al.*, 1993; Bray and McBride, 1992).

$$MOE = \frac{V^2 \rho (1 + \sigma)(1 - 2\sigma)}{(1 - \sigma)} \quad (1)$$

If  $\sigma$  (Poisson's ratio) can be disregarded,

$$MOE = V^2 \rho \quad (2)$$

MOE= Modulus of Elasticity (Pa)

$\sigma$  = Poisson's Ratio

V = Velocity (m/s)

$\rho$  = Density (kg/m<sup>3</sup>)

Therefore the speed of sound depends on the elasticity of wood and the quantity of vibrating substance (Tsoumis, 1991).

Axial and transverse speed, in a specimen of wood, differs because their respective modulus of elasticity are different; in transverse direction modulus of elasticity is considerably lower and, therefore transverse speed is less. Moisture reduces the speed of sound because with increasing moisture, modulus of elasticity decreases and density increases. Speed is also reduced with increasing temperature, because higher temperatures produce lower density due to thermal expansion of wood (Tsoumis, 1991).

#### **4.2.2 Ultrasonic Testing Method**

##### **Basic Concepts**

Ultrasonic waves are simply waves having frequency higher than the hearing range of the normal human ear, which is considered to be 20,000 cycles per second (Hz). Most practical ultrasonic flaw detection is accomplished with frequencies from 200 kHz to 20 MHz. 50 MHz is usually used in material property investigations (Bray and McBride, 1992).

Ultrasonic inspection is performed by using electronically controlled pulses introduced into a material from an outer surface. The ultrasonic energy then travels within the material, finally reaching again an outer boundary. Material condition is diagnosed from the characteristics of the received ultrasonic energy. The ultrasonic technique has rapid testing capabilities and portable instrumentation is available for field tests. Conversely some of the disadvantages are that there may be difficulty in coupling energy to rough surfaces.

Ultrasonic wave propagation requires the presence of a medium such as a fluid or solid. Wave propagation is the vibration or periodic displacement of successive elements of the medium. These low energy vibrations can travel long distances in many liquid and solid materials. Higher ultrasonic frequencies, tend to attenuate in gases (Bray and McBride, 1992).

The speed of the wave propagation,  $V$ , usually is expressed in meters per second, and the excitation frequency ( $f$ ) in hertz. The wavelength ( $\lambda$ ) is the least distance in the propagation medium between identical particle displacements, and is given by  $\lambda = V / f$  (Bray and McBride, 1992). Thickness of the sample material, which the ultrasonic wave travels, should be greater than those  $\lambda$  values.

The major types of ultrasonic waves are longitudinal, transverse (shear), and surface. Most of the wave types are named according to relationships of particle motions to the direction of propagation of the ultrasonic beam. Longitudinal waves can propagate in solids, liquids and gases and are the most utilized wave mode for non-destructive testing materials. Transverse wave inspection is generally limited to solids (Bray and McBride, 1992).

The ultrasonic pulse velocity (UPV) method relies on the measurements of arrival times, path lengths through the specimen (Meola, *et al.*, 2005). This method also was called P-wave measurements. Wave propagation properties are directly related to the elastic properties of the medium and relative size of the object (Schafer, 2000; Halebe *et al.*, 1997; Sandoz, 1996; Ross and Pellerin, 1993; Bray and McBride, 1992; Kim, 1989; Sinclair and Farshad, 1987; Bucur, 1983). Table 4.1 lists the velocities and densities of some materials are listed.

Ultrasonic measurements can be performed in three modes being direct, semi-direct and indirect transmission modes. In the direct mode, transmitter and receiver are placed at the opposite surfaces of the tested element. In the semi-

direct method, transducers are located at a 90° angle, while in the indirect mode transmitter and receiver are arranged on the same surface of tested element. In the indirect mode, transmitter is placed on the point then, the position of receiver is changed along a specific line of points on the surface of material (Meola, *et al.* 2005; Kahraman, 2002).

Table 4.1 Acoustic Velocity in some Engineering Materials (Bray and McBride, 1992)

<b>Material</b>	<b>Density g/cm<sup>3</sup></b>	<b>Longitudinal Velocity m/s</b>	<b>Shear Velocity m/s</b>
Copper	8.9	4700	2260
Iron, cast	7.2	3500-5600	2200-3200
Lead	11.4	2160	700
Steel	7.7	5900	3230
Tin	7.3	3320	1670
Polyethylene	0.90	1950	540
Teflon	2.2	1350	-
Concrete (28 days)	2.4	4500	3750
Wood			
Spruce		5628-6308	
Parallel to grain			
Pine		3490-5535	
Parallel to grain			
Sweet gum		4826-6200	
Parallel to grain			
Pine		5080	
Parallel to grain			
Pine			
perpendicular to grain			
0°		1930	
26°		1702	
90°		2286	

Kahraman, 2002 studied with various rock samples in the laboratory to investigate the relationship between indirect and direct P-wave velocity measurements. Direct transmission measurement seemed to be the ideal way of measurements. However that was not practical on the building due to lack of availability of access. Meola, *et al.* (2005) indicated that indirect velocity measurement was the least sensitive arrangement for velocity calculations. In fact the indirect velocity values were

lower than the direct velocity values. Kahraman (2002), investigated that the indirect velocity values of rock samples were 0.57 times lower than that of direct velocity values.

Differences in the acoustic impedance of air and of solid material caused the reflection of the most of the ultrasonic energy at the surface of the solid rather than its propagation in it. Therefore, a coupling liquid or direct transducer contact was required to provide good contact and to get the ultrasonic energy into solid materials (Bray and McBride, 1992; Meola *et al.*, 2005).

### **Ultrasonic Testing for Soundness Assessment of Timber**

Ultrasonic techniques were used to assess the basic properties of materials and their degradation such as detecting cracks, voids, any other abrupt discontinuity or lack of homogeneity in metallic, non-metallic and composite materials (Bray and McBride, 1992).

Christaras (1999), estimated the weathering depth at the surface of the material by indirect UPV measurements. The depth of weathering could be calculated from the graph of transit time as a function of the distance between the centers of transducers. When the travelling speed of waves was constant, the slope of the graph should be constant for sound material. The changes on the slope showed the difference in pulse velocity and weathering thickness (Meola, *et al.* 2005; Christaras, 1999). Kahraman *et al.*, 2008 showed the relation between the pulse velocity and fracture depth. According to them, pulse velocity decreased with the increases of fracture depth.

The irregular structure of timber presented some difficulties in inspecting it with ultrasound due to the property variations naturally occurring in the growth and production process. For example moisture variations in the growth period affected the composition of the material, and density was affected in the drying process.

Speed of sound in various woods was shown in Table 4.1. Speeds for pine and the douglas fir parallel to the grain typically range from 3490 to 5535 m/s. Perpendicular to the grain the speeds were much lower, generally less than 2200 m/s. Typical frequencies used for studies in wood were in the 10 to 250 kHz range (Bray and McBride, 1992). Beal (2002) indicated that for solid wood, typical ultrasonic velocities were 1000-2000 m/s across the grain and 5000-6000 m/s along the grain. Radial velocities were about 50% greater than tangential.

Ultrasonic properties of wood have been investigated for over 30 years (Schafer, 2000). According to McCuen *et al.* (1988), non-destructive ultrasonic testing was a more accurate alternative for assessing the strength of timber than the visual inspection. Ultrasonic measurements were affective in determining the stiffness and strength of wood members by identifying the presence of defects such as knots and decay (Breeze *et al.*, 1971; Wilcox, 1988; Halabe *et al.*, 1994; Sandoz, 1996; Schafer, 2000). Those defects could be either visible on the surface of the wood or hidden beneath the surface. The technique involved the ultrasonic pulse transmission through a wood specimen and analyzing the received signal in time domain to determine material properties of wood. Experimental results have shown significant differences between the velocities of ultrasonic signals in sound areas and in areas with knots, decays and other localized defects (Breeze, *et al.*, 1971; Wilcox, 1988; Schmoldt, *et al.*, 1994).

Time of flight could also be used to estimate the modulus of elasticity (Halebe *et al.*, 1997; Sandoz, 1996; Ross and Pellerin, 1993; Bray and McBride, 1992; Kim, 1989; Sinclair and Farshad, 1987; Bucur, 1983). Many researches have shown that frequency domain signal amplitude and wave attenuation measurements, when used in conjunction with time domain velocity measurements, could be much more accurate and reliable than simply using velocity measurements in predicting the condition of wood (Olivito, 1993; Halaba *et al.*, 1994; Perez *et al.*, 1994).

Physical properties of wood such as mechanical strength, elasticity and electric conductivity, were strongly dependent on the amount of water content. Pulse velocity in the axial direction decreased with the increasing moisture (Figure 4.1). Decrease in the pulse velocity with the increasing moisture in the radial directions was lower than those in the axial direction (Figure 4.2) (Olivito, 1996).

Olivito's (1996) experimental results showed that the wave form amplitude decreased considerably with decreasing moisture content in the radial directions and became stable at 30 percent humidity. In the axial direction pulse attenuation remained almost constant. Therefore amplitude measurements were stable in axial direction being independent of moisture content and were good indicator of timber soundness.

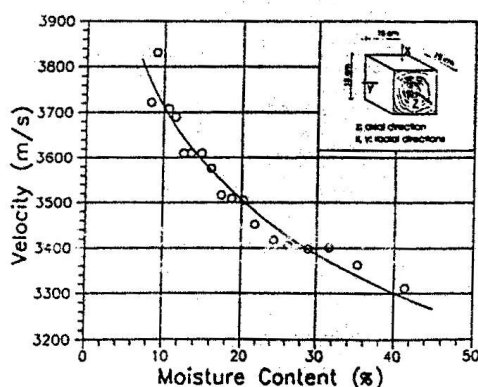


Figure 4.1 Pulse velocity versus moisture in the axial direction (Olivito, 1996: 515)

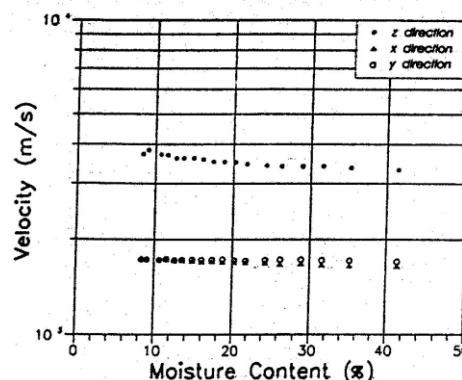


Figure 4.2 Pulse velocity vs. content content-z direction: axial direction x and y direction: Radial Direction (Olivito, 1996: 516)

Sakai *et al.* (1990) in their study, examined the ultrasonic propagation around fiber saturation point of timber. They measured the velocity and attenuation while varying the moisture content, expecting that those values might change drastically at *fiber saturation point*. Ultrasonic velocity drastically changed at the moisture content of 20-50% depending on the species and it was quite natural to associate it

with the fiber saturation point of timber, e.g. in dry pine at 10% moisture content, ultrasonic velocity was around 4900 m/s, at 20% moisture content it dropped down to 4150 m/s and stayed around that value by further increase in moisture content (Sakai *et al.*, 1990). Ultrasonic measurements thus provided an accurate way to determine the fiber saturation point. The study of Sakai *et al.* (1990) showed that the velocity was very sensitive to the amount of the absorbed water, while the attenuation showed whether there was free water or not. They indicated that the amplitude measurements were less accurate than the velocity measurements to determine the fiber saturation point.

Defects and decay reduced the strength of wood. The most important defects that reduced strength were knots, grain deviations, checks etc. Attacks by fungi, insects, and other factors, which cause deterioration of wood, also had adverse effect (Ridout, 2001; Tsoumis, 1991). The presence of knot was recognized with an increase in velocity while the decreasing the overall mechanical strength of timber in depth that might be due to the changes in fiber orientation and cracks surrounding the knot. Due to the grain deviation/different fiber orientation and fraction formed as a result of differential shrinkage, the presence of knot greatly reduced the strength of timber in longitudinal direction (Tsoumis, 1991).

Minamisawa *et al.* (1990), also emphasized that ultrasonic velocity measurements proved to be very effective in determining moisture content of wood. Some researchers designed the neural network to classify ultrasonic signals in terms of species of wood (Jordan *et al.*, 1998). Jordan *et al.* (1998) illustrated the ultrasonic velocity values for several species of timber e.g. oak having 3800-4700 m/s, pine having 4200- 4800 m/s.

Ultrasonic testing was used in characterizing the material properties of timber piles above and in water (McCuen *et al.*, 1988). McCuen *et al.* (1988) have developed guidelines that could be used to define the spacing between test points

for bridge timber piles. Another study emphasized on the importance of developing portable ultrasonic timber property monitoring device. A portable ultrasonic field instrument was designed and developed for the assessment of the condition of members in wooden bridges (Klinkhachorn *et al.*, 1998).

Ultrasonic devices were being applied to detect timber decay in historical buildings. Perez *et al.* (1994), made some laboratory tests with small wood samples to evaluate the ultrasonic application in the detection and evaluation of wood damages produced by insect attack. They have used ultrasonic velocity propagation method, with the device connected to an oscilloscope. They conclude that frequency analyses of ultrasonic signals gave more information about decayed parts of the wooden elements.

### **Imaging techniques for Ultrasonic Measurements**

Ultrasonic imaging enhanced the usefulness and reliability of ultrasonic testing. A variety of techniques might be used to image the anomaly and furnish more information. Much better imaging could be accomplished by using the phase as well as the amplitude of ultrasonic reflections and transmissions. Two basic methods of using the amplitude and phase of ultrasonic signals in imaging systems were holography and tomography (Bray and McBride, 1992).

Kanda *et al.* (1998) proposed an ultrasonic time of flight computed tomography system for visualizing the internal structure of historic relics such as the wooden pillars of shrines. They have realized a non-destructive and portable measuring system. In that study, ultrasonic wave properties were evaluated on computed tomography. In another research, a tomographic device was used for the non-destructive testing of trees. That method allowed the non-destructive inspection of standing trees for cracks, cavities and rot (Rust, 2001).

Valuzzi *et al.* (2002), made a research program for the structural rehabilitation of Arsenale of Venice. Their research was aimed at providing an adequate diagnosis of the actual construction consistency, state of conservation and structural behaviour, through the characterization of the single materials and structural elements, as well as the whole historical building. They used lightly destructive and non-destructive techniques (Dynamic measurements, sonic and tomographic inspections), which were employed on the whole walls and the stone columns. The application of tomography on stone columns and walls showed the most affected areas by humidity and used for the detection of the different material properties.

Berndt *et al.* (1999), established ultrasonic imaging techniques utilizing multiple sound paths that had potential improvements in the ultrasonic non-destructive evaluation of wood. That study tried to correlate known wood mechanical properties with parameters of ultrasonic wave propagation. The focus of that research was on the imaging of reflected energy and travel time, and the connection of them to the wood anatomy, using southern pine.

#### **4.2.2.1 Sonic Stress Wave Method**

The sonic stress wave approach was similar to the non-destructive ultrasonic stress wave evaluation except that it was applied at lower frequencies. Sonic stress wave was one of the most popular non-destructive methods used for wood. Stress waves were generated either through an impact or by a forced vibration. The sonic stress wave method itself was usually employed in two different ways using either the speed of sound or the vibration spectrum. Speed of sound measurement which was often used to express the dynamic modulus of elasticity was very popular with wood products. Speed of sound was converted to modulus of elasticity easily (Bodig, 2001).

According to Bodig (2001), in spite of its simplicity, using modulus of elasticity as a non-destructive evaluation parameter had several shortcomings. Usually only the fastest sound wave was measured and the fastest sound wave traveled in the highest quality portion of wood and bypassed weaker areas such as juvenile wood, knots, low density layers, etc. Computation of modulus of elasticity required the knowledge of mass density and currently it could not be determined non-destructively. Bodig (2001) also concluded that using the stress wave spectrum could overcome many of those shortcomings. Stress wave spectrum provided representation of the overall material conditions and characteristics. A large number of independent variables such as maximum energy, dominant frequency, attenuation etc. could be selected from a single frequency spectrum.

Machek *et al.* (2001) used vibration method to assess wood decay. That study assessed the changes in elastic behaviour and mass loss of different hardwood and softwood species exposed to decay in laboratory soil bed tests. Elastic moduli were determined using conventional static methods as well as a dynamic method based on flexural vibration. The results obtained from their study showed a high correlation between dynamic and static bending measurements for all the timber species tested at different stages of fungal decay. Furthermore, the non destructive modulus of elasticity assessment proved to be a good tool for the early detection of wood decay (Machek *et al.*, 2001).

Similar results were obtained from another research performed by Halabe *et al.* (1995) for green as well as dry southern pine. The result of research showed that the relationship between dry static bending modulus of elasticity versus green stress wave velocity, the corresponding green modulus of elasticity could directly be used to predict the dry static bending modulus of elasticity. Ultrasonic pulse wave velocity did not give good correlation with static bending modulus of elasticity. Due to higher attenuation, ultrasonic travel distances were small. The

stress wave impact technique on the other hand, used low frequency waves which could travel larger distances, thus providing an average of the material property of a specimen over its entire length. Halabe *et.al* (1995) emphasized that, the low frequency and long wavelength stress waves interacted with the entire cross-section in contrast to short wavelength ultrasonic pulse wave.

#### **4.2.2.2 Acoustic Emission and Acousto-Ultrasonic Techniques**

Among the non-destructive methods, acoustic emission and acousto-ultrasonic applications for wood are relatively new and are still being improved. Since the properties of wood, unlike those other materials, vary with respect to species, growth rate, grain angle, and other factors, acoustic emission and acousto-ultrasonic responses are more variable in wood than in other materials and problems occur with signal processing (Kawamoto *et al.*, 2002). According to Kawamoto *et al.* (2002), more fundamental research was required to identify wood properties that affected wave propagation and attenuation, such as density, defects and moisture content.

#### **Acoustic Emission Technique**

Acoustic emission technique, sometimes called stress wave emission technique, involves the transient mechanical vibrations generated by the rapid release of energy from localized sources within materials. Stress or some other stimulus is required to release or generate emissions (Bray and McBride, 1992). The mechanism of acoustic emission is the same, whether it is microcrack in a material or an earthquake. It is a release of elastic energy into acoustic emission waves by the formation of a crack in a solid (Kawamoto *et al.*, 2002). In general,

acoustic emission monitoring systems are passive devices. They simply listen to the sounds generated by crack initiation or growth, through chemical action such as corrosion or other microdynamical events. Acoustic emission techniques can be used to monitor behaviour of materials. In brief, acoustic emission can be used to monitor changing material conditions in real time and to determine the location of these emission centers as well. But since the size of defects such as cracks can not be determined, it is often necessary to assess the emission centers with some other nondestructive method such as radiography or ultrasonic (Bray and McBride, 1992).

Emission techniques are highly sensitive to crack growth, and locations of growing cracks can be determined. However, stabilized cracks and other defects cannot be detected with emission techniques. The size of cracks and other defects can not be determined (Bray and McBride, 1992).

The amount of acoustic emission wave attenuation depends on the properties of the material. Attenuation is greater in porous materials (such as wood) and viscoelastic materials than in metallic materials. For wood, the wave velocities are 4000-5000 m/s for longitudinal, 1500-2000 m/s for radial, and 1000-1500 m/s for tangential directions. Consequently radial and tangential attenuation is larger than longitudinal attenuation. Therefore, conventional acoustic emission source location techniques cannot easily be used for wood. Thus acoustic emission source location, the most identifiable and beneficial factor of the acoustic emission technique for homogenous materials, is difficult to be used on wood (Kawamoto *et al.*, 2002).

In future, possible acoustic emission investigations for wood products could be classified into five fields: Monitoring and control of drying, prediction of deterioration, estimation of strength properties, fracture analysis, and machining control (Kawamoto *et al.*, 2002).

Robbins *et al.*(1991), performed a series of experiments to detect termite activities in wood using acoustic emission monitoring. The results obtained with a computer controlled measuring system indicated that termite activities in the wood generated a significant amount of acoustic emissions with the frequency components extending to above 100 kHz. They concluded that acoustic emission events could be used to indicate the presence of termite activities in the wood. Acoustic emissions from termite activities could easily be detected using suitable sensors.

### **Acousto-Ultrasonic Techniques**

The term acousto-ultrasonics (AU) was formed by NASA Lewis Research Center to describe the practical non-destructive evaluation technique that utilized two piezoelectric sensors attached to the same surface of an object being evaluated. One of the transducers was excited using an ultrasonic pulser, and the other transducer was used as a sensor in a fashion typical of that used for acoustic emission (AE) monitoring, hence the term acousto-ultrasonics implying the combination of ultrasonic excitation and AE monitoring (Bray and McBride, 1992).

AU used stress waves to detect and evaluate diffuse defects, damage and variations in mechanical properties of materials. Whereas ultrasonic methods could be used to assess large voids or other discontinuities, AU techniques could be used to assess subtle flaws and associated strength variations in wood and wood based composite materials. The AU method has combined aspects of AE signal analysis with ultrasonic characterization methods (Kawamoto *et al.*, 2002). In other words, AU technique used ultrasonic waves to generate simulated stress waves in a material and then analyse the waves with acoustic emission methodology. AU differed from the usual ultrasonic methods primarily in the

nature of the received signal. Instead of attempting to have well defined wave propagation paths, as in flaw detection, the AU approach required that the received signal be the result of multiple interactions with the material microstructure. This meant that complex composites such as wood could be analysed even though the propagation paths could not be predicted (Lemaster *et al.*, 1994).

Lemaster *et al.* (1994), performed a study to determine the feasibility of using AU to detect biodeterioration in utility poles. Their study showed that AU was able to detect 50 mm. holes or larger in 300 mm. diameter poles when a reference signal was used. Anthony *et al.* (1994) used to AU in their research for quality assurance of finger-jointed lumber.

Bienarcki *et al.* (1993) showed in their study that AU could be applied to the assessment of elastic properties of wood. They stated that the effect of anisotropy and natural variability of wood were the major limiting factors for any non destructive acoustic evaluation technique applied to wood products.

Beal *et al.* (2002), compared the effect of decay on different AU signal features and normal vibrations in wood, such as growth ring angle, knots, and moisture gradient. The analysis was based on measurements of velocity, attenuation shape and frequency content of the received signals. All of the studied signal features were correlated with the degree of decay, however they were also affected by natural characteristics of wood.

## **4.3 Thermographic Methods**

### **4.3.1 Thermal Measurement Methods**

Thermal inspection contains all inspection methods that use heat sensing devices or substances for measuring the resulting temperatures and/or thermal gradients of a test object when it is heated or cooled. Thermal measurements have wide use for process control, process inspection, field inspections, and monitoring of thermal conditions while in service (Bray and McBride, 1992).

The ability to detect an atypical temperature or temperature difference depends on detector sensitivity. The ability of the operator to recognize a defect depends on the manner in which the data are displayed and recorded, personal knowledge of normal temperature differentials and those expected from anomalies, and on the data analysis techniques (Bray and McBride, 1992).

Measurements for thermal inspection divided in two categories:

1. Thermometry: The measurement of temperature
2. Thermography: Mapping of contours of equal temperature over a surface.

Sensing devices or substances can further be categorized as contact or noncontact. Contact sensors or substances are those that are applied to and touch the surface of the test object. Noncontact methods rely on remote sensing of infrared radiation. Figure 4.3 summarizes some of the basic contact and noncontact devices or materials used to obtain thermometric and thermographic information (Bray and McBride, 1992).

Noncontact thermal inspection methods detect infrared radiation emanating from the test object. Although IR detectors have been in existence since Herschel discovered the phenomenon in 1800, it was not until after World War 2 that they were widely used in non-destructive testing. Before mid 1960s, IR use was largely restricted to checking heat emitting objects with IR transducers and IR film cameras. In the middle to late 1960s, high speed scanning cameras and microscopes became available. Infrared measuring equipment is available in many forms. From simple photographic film cameras to complex thermal imaging cameras, from microscopes for observing very small objects to cameras with a relatively large field of view with focusing distances extending to infinity (Bray and McBride, 1992).

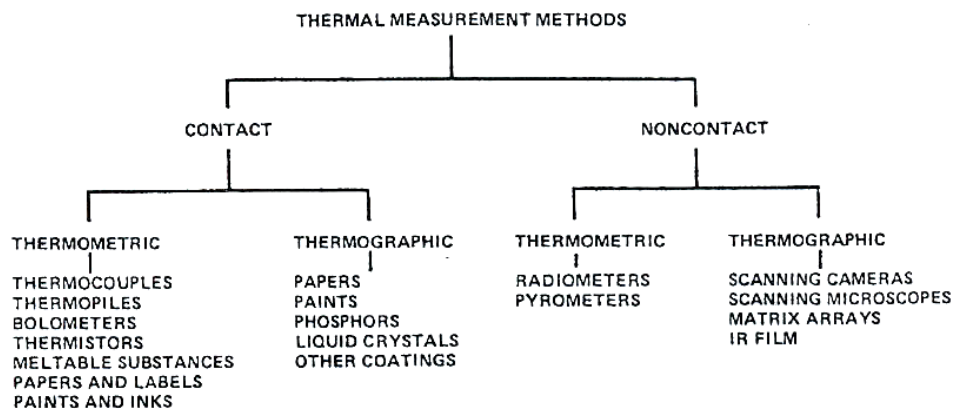


Figure 4.3 Thermal Measurement Method (Bray and McBride, 1992: 635).

### 4.3.2 Basic Concepts of Infrared Thermography

Thermography for NDT is a term for a variety of techniques used to visualize the temperature distribution at the surface of objects to assess the structure or behaviour of what is under the surface. The name implies the distribution by the

‘suffix graphy’ and surface temperature by ‘prefix thermo’ (Maldague, 2001; Bucur, 2003). for the assessment of the structure or behaviour. Generally thermography is used to indicate a non contact and non destructive method showing information about the thermal properties of a sample (Bucur, 2003).

The human naked eye can only detect visible light waves or visible radiation of the electromagnetic spectrum (0.39-0.77µm). The infrared radiation is not visible. It falls between the wavelengths of 2-15 µm that is between the visible and microwave parts of the electromagnetic spectrum. Near IR waves (0.7-25 µm) are close the visible light, far IR waves (25-1000 µm) are closer to microwave region (Balaras, 2002; Ocana 2004). Infrared thermography (IRT) technique turns the emission pattern of an object into a visible image (Ocana 2004). All objects radiate energy that is transported in the form of electromagnetic waves. Thermographic cameras measure the infrared radiation emitted by an object. Infact they do not measure the temperature but radiation of materials (Ocana,2004). However it is possible to get the temperature. The quantity of energy leaving a surface as radiant heat is given by,

$$q = \sigma \epsilon T^4 \tag{3}$$

where q is the radiated energy per unit area (W/m<sup>2</sup>), σ the Stefan-Boltzmann constant (5.67051 x 10<sup>-8</sup> W/m<sup>2</sup> K), ε the emissivity of the surface (0 < ε < 1) and the T is the absolute temperature (K) (Balaras, 2002; Ocana,2004; Maldague, 2008).

Maldague, (2008) summarises the main principle of the IRT with a basic relationship: ‘The fundamental equation of IRT relates the irradiance N<sub>cam</sub> (i.e., spectral radiant power incident on a surface per unit area) received by an infrared camera to the radiance emitted from the surface under consideration N<sub>sur</sub>, at a

given temperature T, neglecting the atmosphere contribution (the case for most NDT applications):

$$N_{cam} \approx \varepsilon N_{sur} + (1 - \varepsilon) N_{env} \quad (4)$$

where  $\varepsilon$  is emissivity which is a surface property that describes its ability to emit energy. It is a unit less quantity and spans from 0 to 1 ( $\varepsilon = 1$  for a blackbody).  $N_{env}$  is the radiance emitted by the surrounding environment considered as a blackbody.' The current IRT cameras link  $N_{sur}$  to T, allowing the retrieval of the surface temperature with some assumptions.

During Infrared Thermographic investigation, the physical properties of investigated materials need to be considered for the best possible results. Since they are closely related to the radiance emitted from the surface under consideration. Those properties are thermal properties; conductivity, diffusivity, effusivity, specific heat, spectral properties; emissivity, absorption, reflection, transmission, other properties- characteristics, porosity, volumetric mass, physiological water content. Thermophysical properties of some material were given in Table 4.2.

Diffusivity is the heat transfer inside the material. The parameter that measures the rate of heat diffusion in the sample is thermal diffusivity (Leon *et al.*, 2000). The higher its value, the quicker the heat exchange in the material that comes from the heat source (Barreira, 2007). Thermal diffusivity of a material is the related materials properties by the following equation (Avdelidis, 2004):

$$\alpha = \frac{k}{\rho c} \quad (5)$$

where  $\alpha$  is the thermal diffusivity ( $\text{m}^2\text{s}^{-1}$ ),  $k$  is the thermal conductivity, ( $\text{Wm}^{-1}\text{K}^{-1}$ ),  $\rho$  is the density ( $\text{kg/m}^3$ ),  $c$  is the specific heat capacity ( $\text{J/kg K}$ ).

Thermal effusivity expresses the material's capacity to absorb and store heat. This parameter is proportional to the thermal impedance for heat exchange of the sample. Its knowledge is important for process of surface heating or cooling (Leon *et al.*, 2000). The higher its value, the greater the heat storage capacity and the longer it takes to reach the thermal equilibrium (Barreira, 2007). On the other hand, materials with low effusivity will increase the temperature rapidly. The thermal effusivity is a parameter reflecting the thermal inertia characteristics of material.  $e$  is the thermal effusivity ( $\text{W s}^{-1/2}\text{m}^{-2}\text{K}^{-1}$ ) of a material is related to its properties by the following equation (Avdelidis, 2004):

$$e = \sqrt{k\rho c} \tag{6a}$$

$$e = \sqrt{\alpha \rho c} \tag{6b}$$

$$e = \frac{k}{\sqrt{\alpha}} \tag{6c}$$

### **Effect of Moisture on the Thermal Properties of Material**

When the investigated materials has some moisture on it, its the density, specific heat capacity and thermal conductivity are affected in such away that temperature changes are much slower in a moist area (Grinzato, *et al.*, 2002). It can be understood from the following equation (Avdelidis and Moropoulou, 2004):

$$Q = mc\Delta T \tag{7}$$

Where Q is the absorbed energy (J), m is the mass (kg), c is the specific heat capacity ( $\text{kg}^{-1}$ ),  $\Delta T$  is the change in temperature (K).

Another consideration when an infrared thermographic survey is performed is the thermal effusivity values of materials with low effusivity values will increase the temperature rapidly (Avdelidis and Moropoulou, 2004). The following equation explains this situation.

$$T = \frac{Q}{e\sqrt{\pi t}} \quad (8)$$

Where Q is the input energy (J), and e is the effusivity ( $\text{Ws}^{1/2}\text{m}^{-2}\text{K}^{-1}$ )

Table 4.2 Thermophysical properties of some building materials (Source: Holman, 1981)

Material	Temperature	Thermal conductivity k ( $\text{Wm}^{-1}\text{C}^{-1}$ )	Density $\rho$ ( $\text{kgm}^{-3}$ )	Specific Heat C ( $\text{kJ kg}^{-1} \text{ }^\circ\text{C}^{-1}$ )	Thermal dlffusivity $\alpha$ ( $\times 10^{-7} \text{ m}^2/\text{s}$ )
Building Brick	20	0.69	1600	0.84	5.2
Cement Portland		0.29	1500		
Plaster, Gypsum	20	0.48	1440	0.84	4.0
Granite		1.73-3.98	2640	0.82	8-18
Limestone	100-300	1.26-1.33	2500	0.90	5.6-5.9
Marble		2.07-2.94	2500-2700	0.80	10-13.6
Sandstone	40	1.83	2160-2300	0.71	11.2-11.9
Wood (across the grain)					
Fir	23	0.11	420	2.72	0.96
Maple or oak	30	0.166	540	2.4	1.28
Yellow pine	23	0.147	640	2.8	0.82
White pine	30	0.112	430		

### 4.3.3 IRT studies of Historical Buildings

#### Passive and Active Thermography

Thermography provides a map of surface temperature distribution that allows the examination of materials properties and their defects. If the inspection is performed with heat flux that is generated by natural boundary conditions, it is called passive IR thermography because of the high thermal inertia value of material (Grinzato *et al.*, 2002). In passive thermography, a potential problem is indicated by irregular temperature profiles (Maldague, 2001). In active infrared thermography, the sample is heated by an external controlled heat source and its surface temperature is monitored as a function of time through changes of emitted infrared radiation. The specific thermal properties of the material under test influence transport of heat thus causing surface temperature to change with respect to areas with different thermal properties. This allows recognizing the subsurface anomalies (Maldague, 1994). Depending on the heat source, active thermography is referred to pulsed thermography (PT) or lock-in-thermography (LT).

In PT, an heating pulse from a laser, flash lamp or microwave heating source deposits heat on the sample surface in a short time. Following this pulse, the surface temperature increases linearly as  $t^{1/2}$  due to the combined effects of direct heating and thermal diffusion ( $t$  is the time variable). Consequently, thermal diffusion from the surface changes the temperature near the defect region after a thermal transit time approximately equal to  $z^2/\alpha$ , where  $z$  is the defect depth and  $\alpha$  is the thermal diffusivity (Maldague, 1998) ( $\alpha = k/\rho C_p$  with  $k$  the thermal conductivity,  $C_p$  the specific heat, and  $\rho$  the mass density). Analyses with PT can be performed in transmission and reflection modes. In the transmission mode, the IR camera is placed on the opposite to the heating source. In real applications, in most cases opposite sides of the material is not accessible. Therefore the reflection

mode is applied. In reflection mode both IR camera and heating source is on the same side (Meola *et al.*, 2005).

The lock-in technique uses thermal waves and collects a series images and compares their temperatures computing amplitude and phase angle of wave pattern at each point. So an amplitude image or a phase image is the resulting image (Meola *et al.*, 2005). Wu and Busse (1998), used LT technique for the coatings related to the measurement of thickness and detection of deteriorated areas. They also used LT for detection of hidden subsurface features such as subsurface knot under veneer in veneered wood.

Darabi (2000) explained the LT technique in his study as ‘In LT, a sine-shaped periodical heat flux at a given frequency  $\omega$  stimulates the sample surface. Following periodical heat injection, the surface temperature in stationary regime is recorded and time-delayed thermal waves due to defects can then be monitored. The phase image in LT is relatively independent of emitted thermal power and thus the SNR (signal-to-noise ratio) is improved with respect to PT while uniform heating sources are not mandatory. Using the phase image, LT allows to detect defects at depths up to about twice the thermal diffusion length ( $\mu$ ) given by:’

$$\mu = \sqrt{\frac{2k}{\omega\rho C_p}} = \sqrt{\frac{2\alpha}{\omega}} \quad (9)$$

(k the thermal conductivity, Cp the specific heat, and  $\rho$  the mass density)

Meola *et al.* (2004) used the term of modulated thermography (MT) as lock-in thermography. A phase angle value may be related to a specific characteristic (density, porosity, hardness, etc.) of the material in the MT or LT technique. Thus,

MT can be used for characterization of many materials either metallic, or plastics, composites, etc.

Maldaque *et al.* (2002), explained the fundamental theory of pulsed phase thermography (PPT) which combines the pulsed acquisition procedure of the 'pulsed thermography' (PT), with the phase/frequency concepts of lock-in thermography.

Both active and passive thermography can be used in the historic structures depending on the problems to be investigated. Titman summarises the cases that induced temperature difference in the historic structures so that the conditions for the examination of different materials and deterioration problems in the structure are established (Titman 2001).

Those conditions that are necessary for thermographical testing of structures. They were as follows:

- a) Heat or cold source within a structure may enable its location. It will lead the changes in surface temperature and may enable its location.
- b) If there is a stable thermal gradients through and element of a structure and if there is not significant variations of thermal conductivity of the element, in other words if the element compositions is uniform, its surface temperature will also be uniform. If there is local damage within the element that will lead to variations in conductivity which are indicated by surface temperature variations.
- c) In the absence of (a) and (b) application of hot or cold source to a surface will cause the surface to heat up (or cool down) at varying rates and to differing ultimate surface temperatures depending on the thermal resistance of the element. Hence sub surface material anomalies or defects can be investigated. Dangers of induced heat in historic structures should be taken into consideration before its application (Titman, 2001).

Modern IRT cameras detect surface temperature variations both qualitatively and quantitatively. In quantitative measurements various parameters need to be entered into the software for accurate measurements, typically ambient temperature, humidity, distance from the target, emissivity (Titman, 2001).

IR thermography is used for monitoring the buildings in qualitative or quantitative way (Grinzato, 2002). IR thermography is applied to historic structures for several purposes such as discovery of the hidden structures, the state of finishing e.g. surface paint, the moisture content, detection of building defects, investigation of any structural cracks etc. (Grinzato *et al.*, 1998, Titman, 2001; Grinzato *et al.*, 2002; Bressan, *et al.*, 2002; Giovanni *et al.*, 2002, Avdelidis *et al.*, 2003; Avdelidis and Moropoulou, 2004; Tavukçuoğlu, *et al.*, 2005; Tavukçuoğlu, *et al.*, 2007; Tavukçuoğlu, *et al.*, 2008). Using a quantitative processing of sequential IR imaging, it is possible to identify and to understand the features of different kinds of defects (Grinzato *et al.*, 1998).

According to Grinzato (2002), the inspection of historical buildings is an important application area for thermography, because of its optical and imaging nature. The knowledge on the monument can be improved by locating the hidden structures, openings and the wall layers below the plasters. Recently some efforts have been devoted to drawing up standard procedures for Thermographic investigations. The most critical point is the choice of the right weather and time for the test. The building's orientation, use, materials, dimensions etc. affect the thermal investigations. It is important to take the situations into consideration where infrared imaging may not be appropriate. High winds, for example can reduce the effectiveness of outdoor thermographic surveys due to the surface temperature shear effects. Likewise, rain may lead to surface cooling, thus masking thermal effects from below the surface (Avdelidis *et al.*, 2003).

Thermography is very useful for the monitoring of the moisture on the building surface and the microclimatic condition. Identification of thermal bridges where the low surface temperature may allow the water vapour to condense on the surface is important for historical buildings (Bressan *et al.*, 2002). The presence of moisture in porous materials that arises as a result of the capillary movement or water sorption causes signs of deterioration. The presence of water in porous materials affects their density, specific heat capacity and thermal conductivity so temperature changes are much slower in moist areas (Avdelidis and Moropoulou 2004; Grinzato, 2002). Water detection in porous materials such as stones by means of infrared imaging is therefore possible (Avdelidis *et al.*, 2003). Thermography is also used for detecting the defects in the structure such as cracks. A crack depth can be estimated by thermography assessing if it is only across the coating, across the thickness of the wall material or across the whole thickness of the masonry (Bressan *et al.*, 2002).

Thermal imaging can prove highly cost effective in view of its speed and the general lack of access requirements compared with other methods. Titman (2001) indicates that in experienced hands, thermography offers a powerful non-destructive technique applicable to a multitude of situations.

Tavukçuoğlu, *et al.*, (2007), used the single IR images to understand the moisture distribution on roof and parapet surfaces of the historical building. QIRT analyses were used to examination of thermal performance of an historical Turkish bath (hamam) and its materials by Tavukçuoğlu *et al.* (2008). They have analyzed in the laboratory, the thermophysical properties of historic brick, brick mortar and plasters in terms of density ( $\rho$ ), porosity ( $\phi$ ), specific heat ( $c$ ), thermal effusivity ( $e$ ), thermal conductivity ( $k$ ) and thermal diffusivity ( $\alpha$ ). They explored thermal failures in the structure, such as heat loss, thermal bridges, air leakages and condensation problems by the joint interpretation of the microclimatic and quantitative IR thermography analyses and their comparisons with the laboratory

data. The reasons of thermal failures and their locations at the domes were explained by joint analysis of heat transfer calculations and QIRT analyses.

#### **4.3.4 Thermal Properties of Timber**

Timber as constructional and structural element may deteriorate in time due to several factors of decay in buildings. Therefore the information on the initial strength of timbers and evaluation of reduction in their strength are very important. In that context, detection of deteriorated locations, observations on the state of deterioration, specifying the positions to evaluate the strength need to be investigated in timber elements. The methods for those purposes must be reliable and practical, possible to inspect a wide area and non destructive. IR thermography is such a method of investigation.

In this section, thermal properties of timber are summarized, since those thermal properties of timber are important in thermographic investigations. The major thermal properties of timber affecting thermographic investigations are expansion and contraction aspects, specific heat, thermal conductivity, thermal insulating capacity, the thermal diffusivity and thermal effusivity (Tanaka, 2001).

#### **Expansion and Contraction of Wood**

When wood is heated, its dimensions increase, when cooled, they decrease. That phenomenon is called thermal expansion and contraction. Expansion is measured by the coefficient of thermal expansion, which refers to oven-dry wood, and measures the elongation of unit length when its temperature increases by 1°C. Due to wood structure, the coefficient of thermal expansion is different in different direction of growth. It is much smaller in the axial (longitudinal) direction than transversely to growth rings, and smaller in radial than tangential direction. The relationship between expansion and temperature is nearly linear in

all three growth directions. The relationship of expansion and density is linear, but the influence of density is very small in the axial direction (Tsoumis, 1991).

### **Thermal Conductivity**

Thermal conductivity is expressed by the coefficient of thermal conductivity. This is a measure of the quantity of heat in calories, which will flow during a unit of time(s) through a body of 1 cm thickness and a surface area of 1 cm<sup>2</sup> when a difference of 1 °C is maintained between the two surfaces.

Wood is low in thermal conductivity because its structure is porous. Thermal conductivity is influenced by various factors, such as wood structure, density, moisture, temperature, extractives and defects (checks, knots, grain). Axial thermal conductivity is about twice higher in comparison to the transverse (radial, tangential) direction. Coefficient of thermal conductivity of different woods, at a temperature of 20°C, was calculated on the average, as follows:

Axial        0.191- 0.284 kcal.m/h.°C

Radial       0. 104- 0.151 kcal.m/h.°C

Tangential 0.090- 0.140 kcal.m/h.°C

Between the radial and tangential direction important differences do not exist. Thermal conductivity increases with wood density, moisture content, and temperature. The relationship is linear. In general, wood with moisture contents higher than 40% has an approximately 1/3 higher conductivity than dry wood. Thermal conductivity is also affected by extractives; woods with high extractive content (dark coloured) have a higher conductivity (Tsoumis, 1991).

### **Thermal Insulating Capacity**

The meaning of thermal insulating capacity is opposite to that of the thermal conductivity. Wood possesses a greater insulating capacity in the transverse direction. This is an advantageous property, considering common usages of wood (e.g. in the construction of doors and windows partitions, etc.).

Low density woods are the better insulators. Wood is a better insulator at lower temperatures (the effect is small). In general, wood is better in comparison to other materials from a thermal insulating point of view. Its thermal conductivity is lower than metals, marble, glass, concrete, etc. (Tsoumis, 1991).

### **Specific Heat**

Specific heat of a body is the quantity of heat needed to increase the temperature of its unit mass by 1 °C. Specific heat is measured in cal / g °C or kcal / kg °C. The specific heat of wood is higher in comparison to metals and other common materials. Specific heat is not considerably affected by species and density of wood, but increases when its temperature and moisture content increase (Tsoumis, 1991).

### **Thermal Diffusivity and Thermal Effusivity of Timber**

Thermal diffusivity is a measure of the rate of change of the temperature of a material, when the temperature of its surroundings changes. Wood has a much lower diffusivity. Diffusivity is lower in wood of lower moisture content and higher density (Tsoumis, 1991).

Thermal diffusivity measurements and thermal effusivity calculations were done by Leon *et al.* (2000) for the pine wood species with photoacoustic and photothermal techniques at 20 °C room temperature and 10 % moisture content. Thermal diffusivity values were measured and thermal conductivity and thermal effusivity were calculated from the equations in section 4.4.2 and summarized below, where  $\alpha$  is thermal diffusivity and  $e$  is the thermal effusivity. Thermal diffusivity and thermal effusivity values of pine species were variable in tangential, radial and axial directions. Sample data from their studies are shown in Table 4.3

$$\alpha = \frac{k}{\rho c} \quad \text{and} \quad e = \sqrt{k\rho c} \quad (5, 6a)$$

Table 4.3 Thermal properties of pine wood species studied photoacoustic and phoyothermal techniques (Leon *et al.* 2000)

Pine Species flow	Density $\rho$ ( $\times 10^3 \text{ kg/cm}^3$ )	Thermal diffusivity $\alpha$ ( $\times 10^{-7}$ $\text{m}^2/\text{s}$ )	Heat Capacity $pc$ ( $\times 10^6 \text{ J/m}^3 \text{ K}$ )	Thermal conductivity $k$ ( $\times 10^{-1}$ $\text{W}/(\text{mK})$ )	Thermal Effusivity $e$ ( $\text{Ws}^{1/2}/(\text{m}^2 \text{ K})$ )
Maximinoi Moore					
Tangential	0.58	1.03 $\pm$ 0.10	0.88 $\pm$ 0.04	0.91 $\pm$ 0.10	282 $\pm$ 20
Radial	0.58	1.24 $\pm$ 0.12	0.93 $\pm$ 0.05	1.15 $\pm$ 0.13	327 $\pm$ 23
Axial	0.58	2.00 $\pm$ 0.18	0.90 $\pm$ 0.04	1.80 $d$ $\pm$ 0.20	402 $\pm$ 28
Leiophylla Schl. Et Cham.					
Tangential	0.44	1.03 $\pm$ 0.10	0.72 $\pm$ 0.04	0.74 $\pm$ 0.08	231 $\pm$ 16
Radial	0.44	1.62 $\pm$ 0.16	0.70 $\pm$ 0.04	1.13 $\pm$ 0.13	282 $\pm$ 20
Axial	0.44	2.30 $\pm$ 0.20	0.68 $\pm$ 0.03	1.56 $\pm$ 0.17	326 $\pm$ 23
Teocote Schl. Et Cham					
Tangential	0.69	0.93 $\pm$ 0.09	0.99 $\pm$ 0.05	0.92 $\pm$ 0.10	302 $\pm$ 21
Radial	0.69	1.23 $\pm$ 0.12	1.09 $\pm$ 0.05	1.34 $\pm$ 0.15	382 $\pm$ 27
Axial	0.69	1.95 $\pm$ 0.19	1.04 $\pm$ 0.05	2.03 $\pm$ 0.22	459 $\pm$ 32

The Table 4.3 showed that thermal diffusivity is highest in the axial direction followed by radial and tangential direction for all timber species. In general thermal diffusivity values of timber decreased with increase in its density. On the other hand, thermal effusivity of timber increased with increase in its density. Specific heat was not considerably affected by species and density of wood. It was also seen that, thermal conductivity changed with the direction of wood, it was highest in axial direction followed by radial and tangential direction (Leon, et.al, 2000). In the fiber direction, dry wood conducted heat 2.5 times faster than in transverse direction (Tanaka, 2000).

The degree of dampness affected the thermal conductivity in such a way that in the fiber direction the wet wood conducted heat only 1.5 times faster than in transverse direction, as the presence of water equalized the differences (Tanaka,

2000). The moisture content have resulted in decrease in diffusivity however, its influence on diffusivity was lower when compared with thermal conductivity (Tanaka, 2000).

### **Emissivity of Timber**

Emissivity is expressed as a ratio of the radiation emitted by the surface of a material to the radiation emitted by a blackbody, under the same parameters of temperature, direction and spectral band. It is a correction parameter in variable radiation emissions from different materials allowing for accurate temperature measurement. Every material has a different emissivity which is expressed on a unitless scale of 0 to 1, 0 being perfectly reflective (perfect mirror) and 1 being perfectly absorbent (perfect blackbody). Emissivity values are not constant even for individual materials and change based on temperature, direction and spectral band (Spencer *et al.*, 2008). Emissivity values of some materials are given in Table 4.4

Table 4.4 Emissivity value for the timber species and some common building materials

Material	Description	Temperature (C°)	Emissivity (Ref.)
Brick	Common	17	0.86-0.81(FLIR,2006)
Gypsum		20	0.8-0.9(FLIR,2006)
Lime		-	0.3-04 (Colwell,1983)
Paint	Oil based	100	0.92-0.96(Colwell,1983)
Pine	Planed	70	0.81-0.89(FLIR,2006)
Oak	Planed	70	0.88(FLIR,2006)
Cedar	Planed	21	0.665(FLIR,2006)
Tree			0.5-0.7(Colwell,1983)
Plank		20	0.8-0.9(Colwell,1983)
Wood			0.95(Colwell,1983)
Granite			0.90(Colwell,1983)
Marble	Gray-polished	20	0.93(Colwell,1983)
Concrete			0.92(Colwell,1983)
Glass	polished	20	0.94(Colwell,1983)

#### **4.3.5 IRT Studies on the Assessment of Timber Characteristics and Defect Detection**

The application field of IR thermography to non-destructive testing of wood has been very large. It was used to examine the defects in trees (Catena and Catena, 2000), to examine various characteristics of timber such as knots, the slope of the grain, density, moisture content distribution, ruptures, defects and delaminations in wood-based composites. (Masuda and Takahashi, 2000; Steele *et al.*, 2000; Murata and Sadoh, 1994; Tanaka, 1994, Tanaka and Divos 2000, Naito *et al.*, 2000). The use of IR thermography on the study of timber characteristics and detection of defects in timber were mostly done by studying the heating and cooling characteristics of timber. They were briefly summarized below.

Tanaka (2000) indicated that the surface temperature was a function of the wood density. He has found a linear relationship between the density and surface temperature, when the cooling time was over 20 minutes. As a result, rate of cooling of timber species also seemed to be closely related to their density.

Tanaka (2000) has studied the detection of knots by IR thermography. He explained that a coniferous knot that had higher density than the wood material around and decayed wood on the surface that had lower density than the intact part) could be detected by thermography. Deciduous knots were also detectable, even if there was no difference in density. Since the fiber direction differed in knots that resulted in the difference in heat diffusivity.

Tanaka (2000) used the daily temperature change as thermal gradient and examined a large column (diameter 70 cm.) made from *hinoki*. High temperature difference (1.3 °C) was measured between the knot and the wood material around. The diameter of knot was 5 cm. Tanaka found that the surface temperature

depended on density. He concluded that detection of defects on surface like decay or knot was possible by thermography simply by using the daily temperature change.

The theoretical consideration of heat transition in wood was verified successfully by the experiments like the effect on surface temperature and the heat conductivity in different anatomical orientation of timber. In the Tanaka's research two outdoor tests were carried out, to evaluate the best time of the daily natural air temperature change as heat transient. More than 0.7 °C temperature differences were found between intact and decayed wood surfaces. Similar temperature differences were found between the knot and around the knot. He concluded that that relative simple method could be a useful tool in the evaluation of old wooden structures.

As thermal conductivity properties of timber were found to be related to its extractives content, timber with high extractive content (dark coloured) was expected to have higher conductivity (Tsoumis, 1991). According to Ridout (2001), older wood had more extractives than younger. He concluded that products made from the wood of younger trees would be less resistant to decay than those made from older trees. More extractives resulted in higher conductivity as in older wood. So higher temperature (or lower temperature) did not always indicated that the wood has some problems.

According to Ridout (2001), at high relative humidity conditions high moisture meter readings in an old timber structure may be taken at 1 cm depth in comparison to new timber. In contrast, at 10 cm depth, old timber had lower moisture content than the new one. So, when detection of moisture problems were performed with thermography, higher equilibrium moisture content at the surface of old timber with respect to the newer ones should be taken in to account. Differences in equilibrium moisture content at high relative humidity conditions

might be due to the age of timber and not due to the dampness problems. As the differences in equilibrium moisture content result in temperature change in old and newer timber, they could be detected in historic structures during passive and active IR thermographic measurements.

Indirect evaluation of moisture content and its distribution in wood was studied by Cielo *et al.* (1988) and Bernatowicz, (1994) with photothermal parameters. The photothermal parameters related to moisture content were thermal conductivity, thermal diffusivity, thermal effusivity, wood specific heat and wood density. The specific heat of wood was between 0.25-0.35 cal/gK for wood densities ranging from 300-900 kg/m<sup>3</sup> (Bucur, 2003). Measurements of the thermo physical properties were performed on the front or back surfaces of wood panel samples. Veneer wood samples were heated at the front and back surface temperature was recorded with an infrared detector. The thermal diffusivity in the longitudinal direction was twice that in the radial and tangential directions. The front surface temperature measurements needed shorter observation times than back surface temperature measurements. They have noted an increase in thermal effusivity and conductivity with the increase in moisture content. Cielo *et al.* (1988) noted that surface temperature measurements were more sensitive to timber moisture content than thermal diffusivity measurements. They have found that at low moisture contents, evaporating cooling had small effect on temperature rise during heating of the surface. At high moisture contents, corresponding to the presence of free water, the effect of the rising temperature with external heating is predominant, probably because of the losses due to surface evaporation. As a result thermal diffusivity and differential temperature decreased with increasing water content in timber, although previously Tsoumis (1991) has assumed the contrary.

Ludwig *et al.* (2004), have examined the effect of moisture content on temperature change of timber samples and its detection by IRT in more detail. During their work, only one end of the timber beam was soaked in water and

uneven wetting produced a high variety of moisture content. They used active IRT using the heat source (incandescence lamp with 250 W power) to make a correlation between the temperature difference and water content of the pine samples. They found that the active approach was better in comparison to passive one to show the correlation existing between the increase of temperature ( $\Delta T$ ) and the water content. The method for the measuring the water content consisted of the comparison of temperature increase in the different areas after the application of heating. The water diffusing in the wood fibres caused increase in the specific heat of the material, thermal conductivity and density. In the case of constant heating ( $Q$ ) flux applied to the surface of the material, the differential temperature which is the difference between the surface temperature ( $T$ ) and the initial temperature ( $T_0$ ) was shown by the equation below.

$$T - T_0 = \frac{2Q\sqrt{t}}{e\sqrt{\pi}} \quad (10)$$

Increase in effusivity by the presence of excess water in timber, resulted decrease in temperature difference during a heating period. Ludwig et al. have emphasized that at critical moisture content for wood preservation (from 12% to 25%) the values of evaporation flux were very low (less than  $10^{-5}$  kg/m<sup>2</sup>s). Therefore the cooling evaporation produced very low signal (0.5 °C) that could be masked by other thermal effects. The evaporating flux could be detected in damp wood by IRT at values higher than  $2 \times 10^{-5}$  kg/m<sup>2</sup>s. This threshold corresponded to the cooling of about 2-3 °C, being dependent on the thermal characteristics of the material. That active approach well suited for the detection of damp wood being particularly sensitive in the case of high water content. The sensitivity of IRT analyses was lower than that of the traditional techniques (gravimetric test, electrical conductivity) to detect the water content. However IRT allowed to localize the areas with different content (e.g. 50%-150% water content) in a fast and absolutely non-destructive way (Ludwig *et al.*, 2004). That was well

explained in the graph that they have drawn the temperature increase versus water content of the oak beam.

Naito *et al.* (2000), used to finite element method to demonstrate the transient temperature on the wood surface. The temperature distribution as a function of heating and slope of the grain deduced with the finite element method and the real experimental image were similar each other. They showed that the slope of the grain could be measured with an infrared camera.

Koch *et al.* (1998) described the experimental device to study the density variations mapping of the annual rings. Density imaging was obtained with coherent far-infrared pulses which were generated and detected by small photoconductive dipole antennae gated by ultra short laser pulses in the near infrared. They have concluded that the false colour image of density variation in transverse sections of wood give a better understanding of the anatomical structure of wood.

The propagation of thermal waves in specimens under stress gave the opportunity to study wood rupture phenomena by non-contact IR thermography. Okumura *et al.* (1996), studied the behaviour of three species of wood under static unconfined compression. With samples under longitudinal compression, a rapid increase in temperature from 19.6 °C to 22 °C along the fracture plane was observed. The temperature increase in specimens under radial and tangential compression was between 20 °C and 21.2 °C. In both cases the highest temperature demonstrated the fracture line. The most important increase in the temperature was observed in samples under compression in the longitudinal direction.

Naito *et al.* (1998), studied the temperature distribution in yellow cedar specimens with a 5 mm diameter hole drilled in the compressed zone under static bending test. At very low loading level, the temperature increased 0.6 °C under the loading point and the presence of the hole was not observed. The hole could be

visible by increasing the loading. The rise in local temperature in the hole was similar to that in the fractured zone of Okumura's (1996) study.

For the investigation of defects in wood composites, the lock-in thermography method was suggested (Wu and Busse, 1995). Wu and Busse (1995), demonstrated the feasibility of this technique by using a sample composed of several veneer laminae of different thickness, glued on a chipboard or on a solid wood block of different tree species. The phase images were taken at 0.03 Hz. They studied the detection of the holes that were opened with different diameters under the surface, the detection of knots present on solid wood blocks covered with veneer sheets, detection of the species of the solid wood (maple and oak) blocks glued under the plywood composed of different veneer sheets. As a result of their studies, holes with a diameter greater than 4 mm were detected. The detection of knots was possible until 2 mm underneath the surface layer. The differences between the thermal properties of maple and oak could be observed for all thicknesses of plywood composed of different laminae.

#### **4.4 Other Non-Destructive Methods**

Electrical properties were used as non-destructive parameters to find out the relationship between moisture content and electrical resistance of wood. Electrical resistance was also used in the detection of decay with in-situ examinations (Bodig, 2001).

*Gamma radiation* was a useful tool for quantifying decay. It was also employed with a trace element for quantifying distribution of preservatives in wood. One of the limitations of that method was the regulation associated with the use of a radioactive source (Bodig, 2001).

Penetrating Radar method was found to be at its initial formative stage with wood products. The method has promised to be able to detect and quantify degradation at inaccessible locations (Bodig, 2001).

X-ray method was mostly used in laboratory environment or in production lines due to the bulky nature of the x ray source and the measuring equipment (Bodig, 2001).

#### **4.5 Pseudo Nondestructive Evaluation**

Pseudo nondestructive methods were often used in conjunction with visual observations. Those methods were sounding with a hammer to listen to hollow sound in poles, the use of a knife for scraping of a degraded surface to determine the depth of degradation, core sampling by drilling to examine the depth of degradation, use of the pilodyn to estimate of deterioration depth, use of the rebound hammer to estimate strength of timber elements and use of resistograph drilling to determine the soundness of timber.

Three of those methods namely the use of pilodyn, rebound hammer and resistograph drilling were briefly explained below since their use was more abundant.

#### 4.5.1 Examination of Deterioration Depth on Timber Surfaces by Pilodyn

The pilodyn was originally developed as a means of detecting the soft rot decay in the telegraph poles in service but has been used for a number of other applications such as assessment of the structural timbers (Clarke *et al.* 1985; Mouzouras *et al.*, 1990).

The instrument operated by a pin of known diameter into the wood by means of spring of known energy. The instrument was held perpendicular to the wood surface and the spring was released by depressing the firing cap. The depth of penetration of the pin was read of from a scale (millimeters) on the instrument. After each test the pin could be removed from the wood and the instrument used repeatedly. The assumption was made that the greater the deterioration of the wood the greater the depth of penetration of the pin (Clarke *et al.*, 1985).

Clarke *et al.* (1985) emphasized that, moisture content, particularly sound wood, and the direction of sampling (i.e. radial, tangential, longitudinal) could have marked influence on the depth of pin penetration. Moreover the total energy required to fracture wood was a result of the interaction of the various wood properties determining its strength characteristics. Clarke *et al.* (1985) used the pilodyn for the assessing the condition of waterlogged wooden objects. They used the spring rates at 2 Joules and 6 Joules. They concluded that, if penetration greatest than 40 mm was obtained, particularly with a 2J Pilodyn, then the depth of deteriorated material could be considered extensive, conversely, if there was little penetration (10 mm. or less) using 6J, 12J, 18J instruments, then deterioration might be assumed to be minimal.

Mouzouras *et al.* (1990) performed a study to assess the deterioration of timbers of the ships using the data obtained with pilodyn instrument. They used a pilodyn

instrument with a spring load of 2J and a needle of 2mm in diameter and 40mm in length. Their results showed that relatively sound timbers had needle penetration values ranging between 10 and 16mm while maximum penetration of 40 mm was measured only for some examples. They concluded that there was little decay of timbers.

#### **4.5.2 The Methods of Rebound Hammer (Penetration Method)**

The technique of the penetration test consisted in the penetration of a steel pin into wood with repeated and constant energy blows transmitted by a rebound hammer. That test, based on the penetration measurement layer after layer, made it possible to distinguish between different degrees of decay in each layer as a function of number of blows necessary for 1 cm penetration (Ronca *et al.*, 1998).

This technique gave more information than that was given by the penetration of a semispherically ended rod or steel balls, because those methods only gave indications about the superficial layer conditions. Also the pilodyn technique gave information about the average strength of superficial layers of about 4 cm depth without providing any detailed data. The evaluation of the decay of successive layers of wood was particularly important because the extent of the decay might be quite different from one layer to the next (Giuriani *et al.*, 1993).

Giuriani *et al.* (1993), proposed and adopted this technique for investigation of the wood truss, arch of the roof vault at Loggia Monument (a 16th. century building in Italy). The decayed areas of one significant arch were indicated. Three different degrees of degradation were adopted. The first one corresponded to a very decayed situation (the blow number for 1 cm. penetration was less than 2), the second indicated a better situation (the blow number for 1 cm. penetration was less than 6). Non decayed wood required more than 10 blows for every centimeter

of penetration. They tested their method by correlation between penetration test result and a standard three point flexural test. They reported a good correlation between the flexural strength and penetration test results.

Another study about mechanical characterization of wooden structures was reported by Ronca *et al.* (1998). They showed that the fundamental penetration test parameter, which was the average of the number of blows for each centimeter penetration, was greatly influenced by the moisture content and the penetration direction with regard to the fiber direction. Where the moisture content was high (30%) the difference between the radial and the tangential penetration results was approximately 5-6%, it could reach 20% for low water contents. They underlined that the radial penetration was the one that could be performed easily and reliably.

#### **4.5.3 Resistograph Drilling**

The drill resistance method has been well known in the wood industry since about 20 years. That method could be applied for the maintenance of old buildings or woodwork especially for the detection of rot. The basic principle of the drill resistance method was to measure the drilling torque while a rotating drill bit was fed at constant rate into the wood. The drill resistance was recorded during the test cycle in a computer memory or on a chart recorder and could be represented as a curve showing the drill resistance as a function of drilling depth, called a 'dendrogram' (Helms *et al.*, 1994).

Helms *et al.* (1994) have developed an instrument for detection of damage on construction timbers and trees. The instrument used a thin flexible steel wire which was 400 mm long and 1.5 mm in diameter. They evaluated the results in a qualifying way. Qualifying way means that the relations of absolute value of the

amplitude level itself was evaluated. Decay in the annual rings of a tree was examined that way (Helms *et al.*, 1994).

Rinn (1994) examined the applications of the resistograph drilling method. He indicated that resistograph drilling machines was a reliable tool for wood analysis in scientific and practical applications. He added that another important area of application was to preserve old wooden buildings in Europe, especially in Germany. Ceiling beams, rafters and finger joints had to be inspected before renovation or reconstruction of old buildings was planned and carried out.

## **CHAPTER 5**

### **MATERIAL AND METHOD**

In this chapter, historical buildings that were used as case studies, sampling for the development of standard measurements in the laboratory and description of the non-destructive measurements with ultrasonic pulse velocity measurements and IR thermography were presented. The steps of the measurements and the instruments were outlined in the methods.

#### **5.1 Material**

Pilot studies were performed in three historic buildings. Their brief history and architectural characteristics were summarized and representative laboratory samples were described below. Laboratory samples were used to establish the reference data on non-destructive measurements.

##### **5.1.1 Buildings**

The studies were conducted on a mosque constructed in 13<sup>th</sup> century, Aslanhane Camisi, 19<sup>th</sup> century traditional timber dwellings, Ayaş House and Istiklal House in Ankara (Figure 5.1). Aslanhane Camisi, belonging to Selçuk Period was constructed in 1289-1290 according to its inscription panel (Öney, 1990). It is one of the most important mosques belonging to Selçuk Period located on the south of the Citadel Ankara (Figure 5.2). Aslanhane Camisi, was a stone masonry structure

while its roof and timber ceiling structure were supported by twenty-four wooden columns (Figures 5.3 and 5.4). The structure was still functioning and its interior was heated with a stove, burning coal and/or firewood in winter.

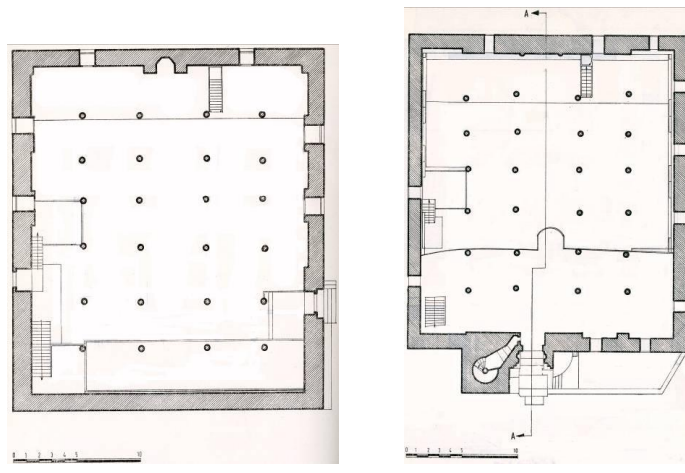
Ayaş House is located in Ayaş Township at the north-west of Ankara. Its main façade is placed on a square, Cumhuriyet Meydanı which is the commercial and administrative center of the township (see Figure 5.5 and 5.6). The other selected traditional timber dwelling is in the historic district İstiklal (Yahudi) Mahallesi, in Ulus, that is the centre of old Ankara. İstiklal Mahallesi was known as Jewish district in the Ottoman Period. Figure 5.7 showed the location of İstiklal House. Both of the houses were composed of a mud brick masonry at the ground floor and timber frame structure at the upper level(s). The mud brick masonry was supported by timber bond beams while the timber frame upper structure consisted of timber studs, joists, lintels and bracings together with mud brick and fired brick infill. The houses under examination were not inhabited and were partially damaged, such as most glazing of the windows were broken and the exterior and interior plaster layers were considerably lost due to the lack of maintenance. Therefore, their interiors and boundary surfaces were exposed to the outside climatic conditions. Those houses were selected because they were among the most typical examples of the traditional timber dwellings in Ankara region. Since they were not inhabited and partially deteriorated, the timber structure elements were possible to be studied.



Figure 5.1. Front views of Ayaş House (at the top left) and Aslanhane Mosque (at the top right), front and side views of the Istiklal House (at the bottom)

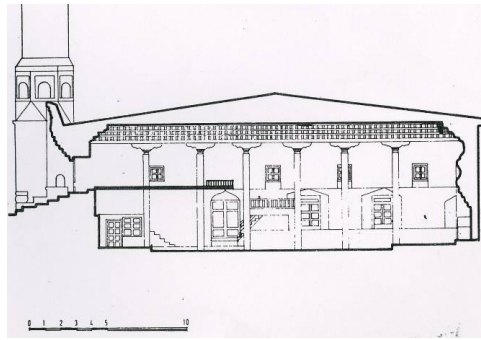


Figure 5.2 The location of Aslanhane Camisi, Altındağ District, Can Sokak, Ankara



a)

b)



c)

Figure 5.3 a) The ground floor of the Aslanhane Camisi b) First floor of the Aslanhane Camisi c) The section of the Mosque from the north south direction (Öney, 1990 ,1971)

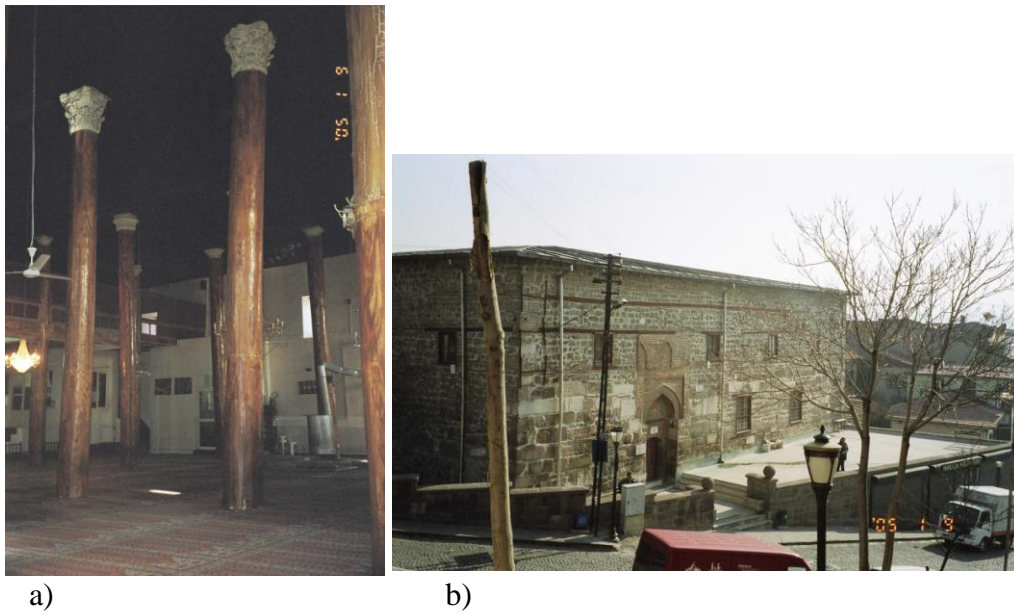


Figure 5.4 a) Interior view from the Aslanhane Mosque showing the some timber columns supporting the roof and timber ceiling structure b) The view of west façade showing the stone masonry walls with timber lintels and bond beams



Figure 5.5 From the view of the commercial and administrative center of the Settlement, Cumhuriyet Meydanı, located in the north of *Ayaş Çayı* and the location of selected house, Hükümet Caddesi, Akpınar Sokak, No: 1, *Ayaş*

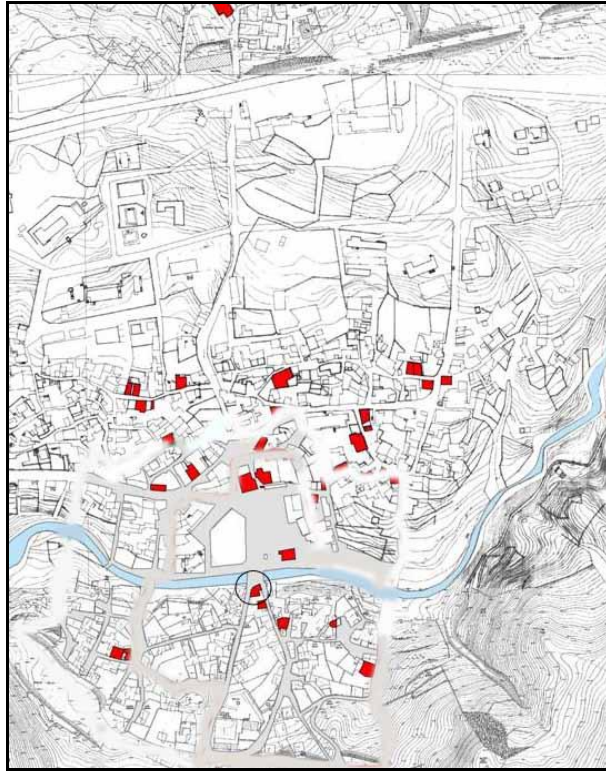


Figure 5.6 The Plans of settlement of Ayaş and the location of selected building, Hükümet Caddesi, Akpınar Sokak No: 1 (Güçhan, et.al. 2006)



Figure 5.7 Location of the house from İstiklal District, Kargı sok. No: 25/C Ulus, Ankara

### 5.1.2 Laboratory Samples

The historic timber samples as well as historic brick, mud brick and plaster samples were collected from those structures for the laboratory analyses to obtain data for better interpretation of in-situ measurements (Figure 5.8, Tables 5.1 and 5.2).

The samples collected for laboratory studies are as follows:

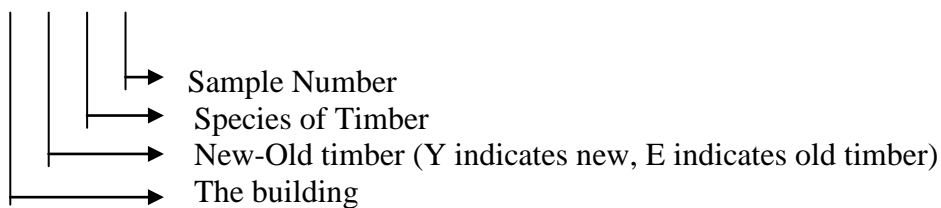
- i ) Sound Timbers: Some of the sound timber samples were the “new timbers” newly prepared for the laboratory analyses and some of them were the “old timbers” collected from historic houses. The different timber species which were the sound ones and cut in different directions such as radial, tangential and longitudinal cuts has served as standard samples.
- ii) Deteriorated Timbers: Timber samples that had various types of deterioration, such as color change at their surfaces, cracks, knots and insect galleries at different directions in the volume of the samples were selected.
- iii) Stone, mud brick, fired brick and plaster samples: The historic neighbouring materials being in contact with the structural timber, such as historic brick, mud brick and plaster samples were collected from historic structures for the laboratory analyses to obtain data for better interpretation of in-situ measurements.

Laboratory analyses were performed on those three groups of samples for the following aims:

- To have experience on reliability, efficiency and precision of each NDT method, UPV measurements and IR thermography, on timber specimens and historic neighboring materials.
- To establish a reference data base for the field work with those NDT methods.

Labeling of the samples was arranged as follows: the first letter if present, gave the building that the sample was taken from, for instance A for Ayaş House. The next letter indicated whether it was an old timber or a new one, E and Y respectively. The last letter was for the timber type, C for pine, K for beech, M oak, I for linden, G for horn-beam, O for olive, W for willow, P for poplar, N for walnut. The number at the end was the sample number for different samples of same type.

P E X 1



## 5.2 Methods

The in-situ examination of sound and deteriorated timbers was done by QIRT and UPV measurements together with supplementary visual decay analyses. Those in-situ investigations of NDT were supported by laboratory NDT analyses of the samples collected from the site. Laboratory analyses of historic and new timber samples as well as historic brick, mud brick and plaster samples were analyzed to obtain data for better interpretation of in-situ measurements. Laboratory analyses and in-situ studies were described below.



Figure 5.8 Old sound and deteriorated timber samples, new pine, beech, oak timber samples, stone and fired brick infill samples

### 5.2.1 Laboratory Studies

Laboratory studies were performed on the samples by UPV measurements and IR thermography.

#### Ultrasonic Pulse Velocity (UPV) Measurements

It was necessary to understand how the moisture content and type of timber and its defects affected ultrasonic pulse velocity measurements. Therefore, the fifteen

old and new timber samples consisting of some pine, linden, horn-beam, poplar, walnut, olive and willow samples were examined. The timber samples were put at fixed RH conditions that were formed in glass desiccators by using the proper saturated salt solutions. Their equilibrium moisture content (EMC) and ultrasonic velocity measurements were done at 56%, 75% and 90% RH conditions during the periods of moisture absorption and desorption. EMC was determined by recording the increase and decrease in weight. A *Protimeter Surveymaster SM* was used to get data about the moisture content at the surfaces. Ultrasonic velocity measurements of laboratory samples were taken in the direct transmission mode when the samples were in equilibrium with the 56%, 75% and 90% RH conditions by using the portable *PUNDIT Plus CNS Farnell* Instrument with 220 kHz transducers. Measurements parallel and perpendicular to fiber direction were taken. Coupling gel was used to ensure the good contact between the timber surface and transducers.

The soundness of timber was examined by using ultrasonic testing in direct and indirect transmission modes. The UPV measurements were taken from the deteriorated and sound historical timber (pine), sound new timber (pine, oak, beech), fired brick, mud brick and stone (marble) samples for comparisons. The presence of defects, such as knots, cracks and insect holes were examined. Those measurements were carried out using the same portable equipment, with 220 kHz transducers. The plastic film (*Parafilm 'M'*) was preferred as a coupling material. Other coupling agents were not preferred due to their staining problems.

In the indirect method, the probes were located at the same surface, the transducer was kept at a fixed point, while the receiver was moved on the points marked along a line. The points were marked at 15 mm intervals. From each point, fifteen readings of transit time were recorded and the distance between the centers of transducer and receiver was noted (Figure 5.9). Diagrams were drawn by plotting the transit time versus distance. The change on the slope of the regression lines

would show the change in UPV at the deeper parts of the material depending on the presence of defects (Christaras, 1999).

The direct UPV measurements ( $UPV_{DIRECT}$ ) were performed by the arrangement of transducer and receiver at the opposite sides of the surfaces. Fifteen readings of transit time were recorded for three points at each timber surface and the distance between the transducer and receiver was noted. The UPV measurements were taken from longitudinal, radial and tangent to fiber directions of timber samples due to the effect of cutting direction of timber on UPV values. (Figure 5.10).

Table 5.1 The description of laboratory samples examined in this study: sample code, its definition and density

Sample Code	Sample Definition	Density ( $\rho$ ) g cm <sup>-3</sup>
SEC1-08	Deteriorated old pine -from Safranbolu traditional house- Species A	0.449
SEC2-08	Deteriorated old pine from Safranbolu traditional house - Species A	0.440
SEC1-09	Sound old pine A - from Safranbolu traditional house - Species A	0.634
SEC2-09	Deteriorated old pine - from Safranbolu traditional house	0.421
YC1-08	Sound new pine - Species D	0.408
YC7-08	Sound new pine - Species C	0.557
YC6-08	Sound new pine - Species C	0.502
FEC3-08	Deteriorated old pine - from Safranbolu traditional house- Species B	0.378
EC4-08	New pine	0.532
YK5-08	Sound new beech	0.784
YM1-08	Sound new oak	0.870
FB1	New fired brick	1.543
FB2	New fired brick	1.551
I3	Marble	2.612
QIMG1	Marble	2.767

Table 5.2 Neighbouring samples collected from the selected houses, Mud brick and brick infill, lime and mud plaster, repair plaster with high gypsum content

Sample Code	Description	Photos
IMB-1	Mud brick infill taken from exterior wall of the İstiklal House.	
AB-1	Brick infill taken from exterior wall of the Ayaş House	
ILPI-1	Exterior lime plaster together with its mud layer taken from İstiklal House	
IMPI-1	Exterior mud plaster taken from İstiklal House	
ARPI-1	Thick interior repair plaster (high gypsum content) together with its mud layer from Ayaş House	

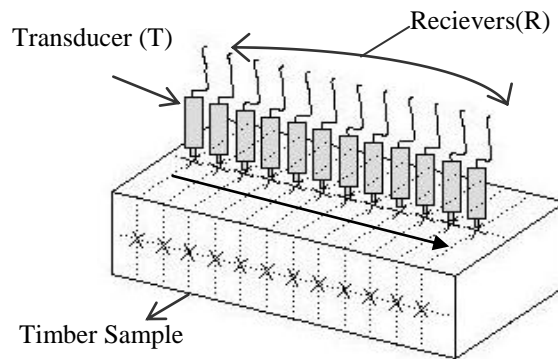


Figure 5.9 Schematic drawing showing the indirect UPV measurements

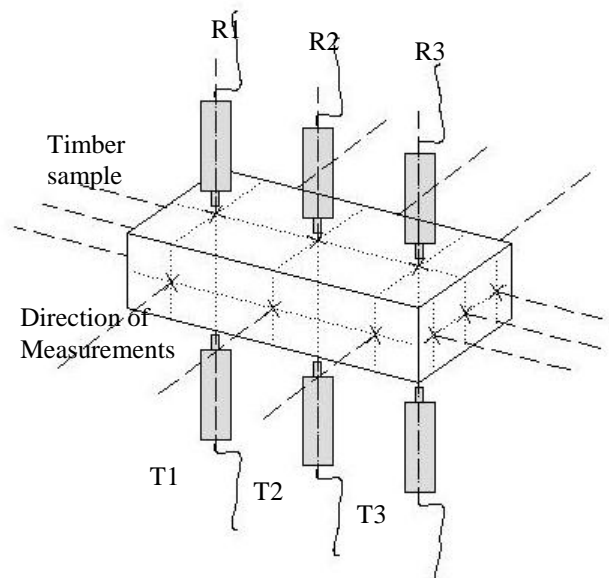


Figure 5.10 Schematic drawing showing the direct UPV measurements

The spacing between the transducers indirect and direct transmission measurements was important. Halabe (1997) suggested the placement of transducers with a center-to-center distance of 30 cm in the indirect transmission mode. In this study, the spacing of transducers in direct transmission mode was in the range of 4 cm to 20 cm, depending on the size of timber specimens. The spacing between the transducers in indirect transmission mode was in the range of

1.5 cm to 17 cm depending on the dimensions of timber samples and their surface conditions.

A special care was given to apply an adequate pressure by the hand of the operator while holding the transducers on timber surfaces in order to obtain consistent readings (Biernacki and Beal, 1993).

The soundness of timber elements could be estimated by using UPV measurements e.g. estimation of the modulus of elasticity (Ross, R.et.al., 1993; Sandoz,J.,1996). The direct longitudinal velocity measurements of the timber samples were used for the calculation of modulus of elasticity (MoE) by the following equation (Sandoz, 1994; Ross, R.et.al., 1993; Bray, 1992).

$$MoE = \frac{V^2 \rho (1 + \sigma)(1 - 2\sigma)}{(1 - \sigma)} \quad (1)$$

If  $\sigma$  (poisson's ratio) was disregarded,

$$MoE = V^2 \rho \quad (2)$$

MoE= Modulus of Elasticity (Pa)

$\sigma$  = Poisson's Ratio

V = Velocity (m/s)

P = Density ( $\text{kg/m}^3$ )

## **QIRT Studies in the Laboratory**

Deteriorated and sound historical timber, new timber, fired brick, mud brick, mud mortar and plaster samples were examined by quantitative IR thermography (QIRT) in the laboratory.

In the laboratory the IRT studies were done by using “*FLIR ThermaCAM E65*” and “*AGEMA Model 550*” thermographic equipments. IR images were then analysed by using the softwares of “*ThermoCAM Reporter 2000*” and “*ThermoCAM Researcher Professional*”. Climatic data were obtained by use of an environmental meter, *Kestrel 3000* and ‘*HOBOWare Pro*’ dataloggers. The distance between the IR camera and the samples was measured by the ‘*BOSCH DLE 150 laser meter*’.

Thermal gradients between the inside and outside as well as artificial heating produced by halogen lamps with maximum outputs of 650 Watts and 1000 Watts (2 x 500 Watts) were used for the laboratory samples. The sequential IR imaging was performed by taking infrared images successively at 2-10 seconds intervals for a period 5-10 minutes during the heating and cooling period. The experimental set up for taking successive IR images was shown in Figure 5.11.

The thermal monitoring of timber samples was done to determine the rates of warming up ( $R_W$ ) and/or cooling down ( $R_C$ ) in relation to their soundness and moisture content. The linear regression for each sampling area was achieved by plotting the surface temperature changes as a function of square root of time. The thermal behavior of those materials was evaluated together with their UPV values for the deterioration assessment of timber samples. For that purpose, the relationship between the fast or slow warming up/cooling down of timber surfaces and their UPV values, taken at perpendicular-to-fiber and parallel-to-fiber directions, were investigated.

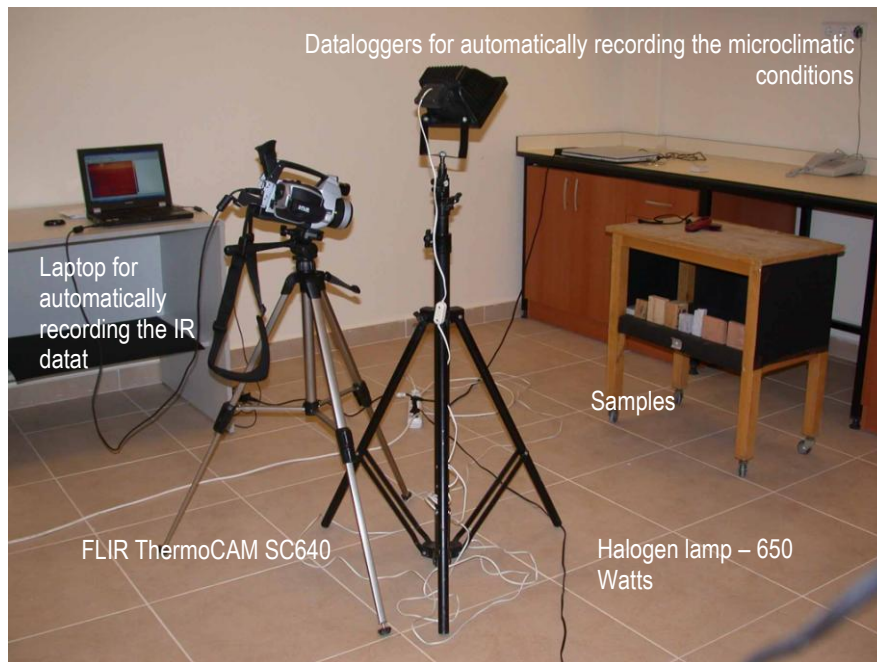


Figure 5.11 The experimental setup of sequential IR imaging at laboratory for the monitoring of sound oak timber, sound pine timber marble, fired brick samples during heating and then cooling periods.

### 5.2.2 In-situ Studies

In-situ studies were done at Aslanhane Camisi, İstiklal House and Ayaş House by UPV measurements and QIRT.

#### Ultrasonic Pulse Velocity Measurements

Ultrasonic Pulse velocity measurements were taken in Aslanhane Camisi, İstiklal House and Ayaş House by a portable “*PUNDIT Plus CNS Farnell*” instrument. At Aslanhane Camisi, timber columns were examined with 54 kHz transducers by taking transit time readings in direct transmission mode (cross section). Each column was examined in east–west and north–south cross directions by taking measurements at different levels with 30 cm intervals. For accurate

measurements, ultrasound couplant gel was used to provide good contact between the timber surfaces and transducers. All measurements were taken perpendicular-to-fiber direction and five readings for each point were recorded to get reliable data. The column diameters were taken as the distance travelled by the ultrasonic wave. The diameter of each column decreased with height. During the survey, the RH and ambient temperature data were taken by the use of an environmental meter, “*Kestrel 3000*”. The moisture content of the timber columns were measured by means of a protimeter, “*Surveymaster SM*”.

At İstiklal House, direct and indirect UPV measurements were taken on the timber posts and beams by using 220 kHz transducers. For accurate measurements, plastic stickers (*TACK IT*) were used to provide good contact between the timber surfaces and transducers. Ten readings of transit time were taken at each point.

At the site, the spacing of the transducers in the direct transmission mode were in the range of 5-50 cm depending on the dimensions of the timber elements while in indirect mode, the spacing were in the range of 1.5-25 cm. In the indirect mode the readings were over range above the 25 cm for the timber elements at site.

In Ayaş House, it was tried to take UPV measurements, from the timber elements and plastered wall surfaces. The outside noisy environment especially the traffic affected the measurements. Therefore reliable UPV measurements could not be taken in that structure.

### **In-situ Infrared Thermography**

In-situ IRT studies were done by single and sequential IR images at Aslanhane Camisi, İstiklal House and Ayaş House.

At Aslanhane Camisi, an “AGEMA, model 550” thermovision camera was used to produce thermal maps for the interior and exterior surfaces of the walls, timber columns, timber ceiling and the floor. The camera was given inputs on ambient temperature, relative humidity, distance to target area, and a relevant emissivity of target surfaces to achieve accurate surface temperature data. Target surfaces mainly consisted of stone masonry walls, oil painted timber pillars, unpainted timber ceiling, plastered and oil painted walls. The climatic data were obtained by use of an environmental meter, “Kestrel 3000”. The IR images were then analysed by using the softwares “IRwin 5.1” and “ThermoCAM Reporter 2000”. The IR images of the subject areas were taken in segments together with their photographs. During the survey, the distance between camera and target area was calculated from the measured plan and section drawings for each IR image. The IR images were taken twice a day, once in the morning and once at night.

At İstiklal House, the IRT studies were done by using the “ThermoCAM SC640” thermographic equipment. The sequential IR images were taken from the south-east exterior façade of the building in series, at every two seconds for a period of 5-10 minutes (Figure 5.12). The IR images were then analysed by using the softwares of “ThermoCAM Reporter 2000” and “ThermoCAM Researcher Professional”. The climatic data were obtained by use of an environmental meter, “Kestrel 3000” and “HOBOWare Pro” dataloggers. The distance between the IR camera and the target surfaces was measured by the ‘BOSCH DLE 150 laser meter’. Daily temperature gradients and artificial heating by hair dryer with 1000 Watts were used for the analyses of building surfaces during heating and cooling periods.

At Ayaş House, “FLIR ThermaCAM E65” thermographic equipment was used for the single and sequential IR imaging from the interior and exterior building surfaces. The IR images were taken in series at two to ten seconds intervals in daytime and at night for a period of 5-10 minutes. The sequential images were

taken during the heating up and cooling down period of daytime due to the daily temperature gradients. The IR images were then analysed by using the softwares of “*ThermoCAM Reporter 2000*” and “*ThermoCAM Researcher Professional*”. The Climatic data were obtained by use of an environmental meter, “*Kestrel 3000*”. The distance between the IR camera and the target surfaces was measured by the “*BOSCH DLE 150 laser meter*”.

The thermal properties of timber and its traditional neighbouring materials were studied quantitatively by determining the rate of cooling and heating of those materials and their ratios to the sound timber one in order to discuss the soundness, degree of decay and compatibility of those materials, based on the relationship of effusivity (thermal inertia) with thermophysical properties of materials that were given Sections 4.3.2-4.3.4. Temperature versus time graphs of QIRT were studied previously (Tanaka and Divos, 2000). In this study, the temperature versus square root of time expressing the rate of heating and cooling was used. Those relationships of rate of heating and cooling were expressed as ratios to sound timber one as well. Those relationships were expressed below.

$$R_w = \frac{T}{\sqrt{t}} \quad \text{and} \quad R_c = \frac{T}{\sqrt{t}} \quad (3)$$

$$e \approx \frac{1}{R_w} \quad \text{and} \quad e \approx \frac{1}{R_c} \quad (4)$$

$$\text{Comparative Ratio: } \frac{R_{W-MATERIAL}}{R_{W-SOUND-TIMBER}} \quad \text{and} \quad \text{Comparative Ratio: } \frac{R_{C-MATERIAL}}{R_{C-SOUND-TIMBER}} \quad (5)$$

$R_w$  = Rate of warming up ( $^{\circ}\text{C}/\sqrt{\text{s}}$ )

$R_c$  = Rate of cooling down ( $^{\circ}\text{C}/\sqrt{\text{s}}$ )

$e$  = Effusivity

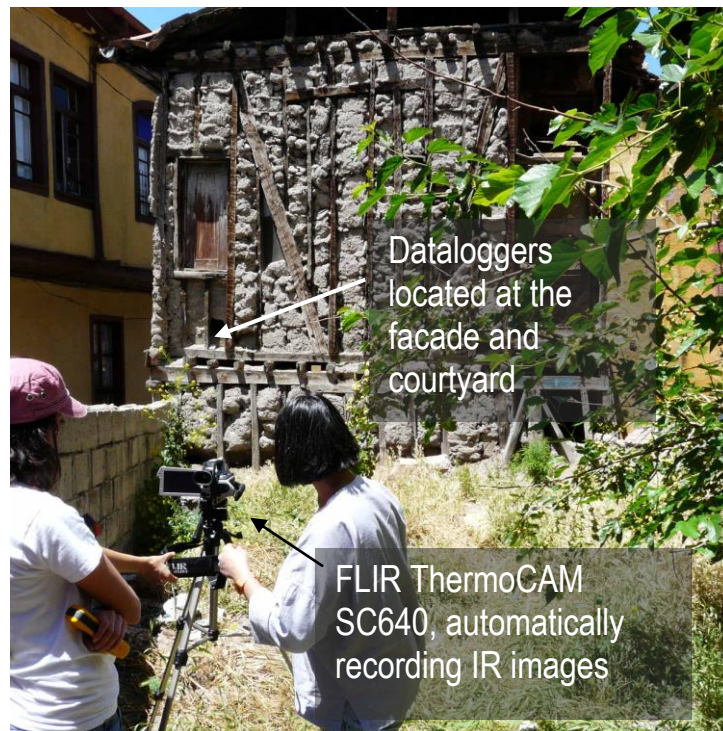


Figure 5.12 The QIRT experimental set-up at İstiklal House showing IR camera automatically-recording IR images of target area at 10s intervals during the heating and cooling periods of a day

## **CHAPTER 6**

### **RESULTS**

Laboratory analyses and in situ measurements were performed to assess the soundness of structural timber elements. The non-destructive methods of ultrasonic velocity measurements and IR thermography were studied in detail for their joint use to assess the soundness of timber.

The laboratory analyses were planned to build up reference data and to define their use on the correct interpretation of in-situ measurements of timber in historic structures. In-situ measurements were performed to define healthy boundary conditions for timber in relation to its compatible neighbouring materials and incompatible ones.

#### **6.1 Laboratory Analyses of Samples by UPV and QIRT**

The comparative data were developed in the laboratory in order to make correct interpretations of in-situ measurements both for UPV and QIRT analyses to assess the soundness of timber and its compatibility with the neighboring materials.

### **6.1.1 Laboratory UPV Analyses**

Laboratory UPV analyses were carried out on sound and deteriorated timber samples to establish reference data to assess the effect of moisture content and degree of deterioration on the measurements in relation to soundness of timber.

#### **The Equilibrium Moisture Content Affecting Ultrasonic Pulse Velocity**

“In laboratory analyses, moisture absorption and desorption of timber samples were examined at 56%, 75% and 90% RH conditions that were established in large glass desiccators. Timber samples kept at constant RH conditions established their equilibrium moisture content (EMC) which was measured by their weights. The EMC of timber samples changed in the range of 8.9 % to 18.6% at those RH values studied. The average EMC values for all samples during the moisture absorption and desorption were given in Figure 6.1. Both old and new timber samples gave out moisture more slowly than they took it in, e.g. during desorption at 56% RH, the samples kept 2.3% more moisture than the amount during absorption at the same RH (Figure 6.2). It was seen that the moisture absorption was more rapid than moisture desorption for timber elements. The protimeter readings done at the surface of the laboratory samples gave similar EMC readings to weight measurements. However, old pine samples kept more moisture at their surfaces than the new ones (Figure 6.2). Those data showed the importance of the microclimatic conditions on the moisture content of the timber elements in the structure” (Kandemir *et al.*, 2007).

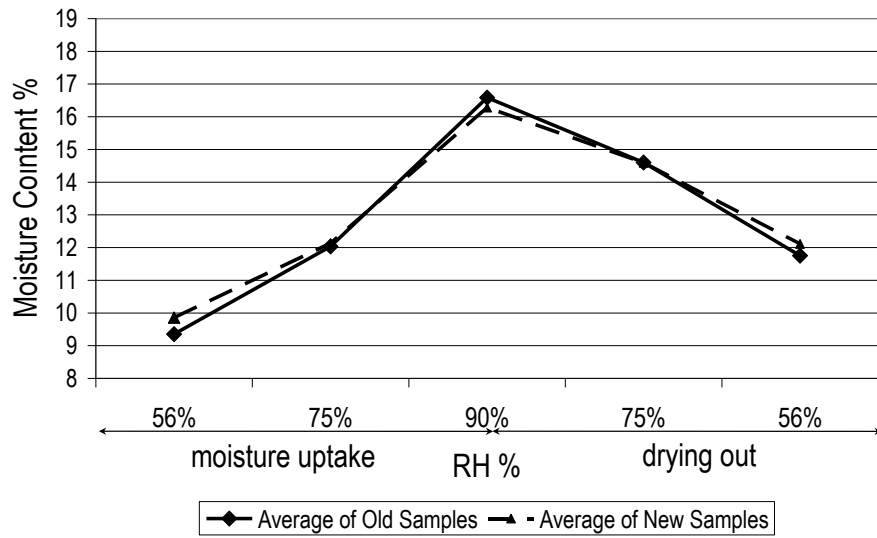


Figure 6.1 The average EMC of all old and new timber samples during moisture absorption and desorption indicating slower desorption (Kandemir *et al.*, 2007).

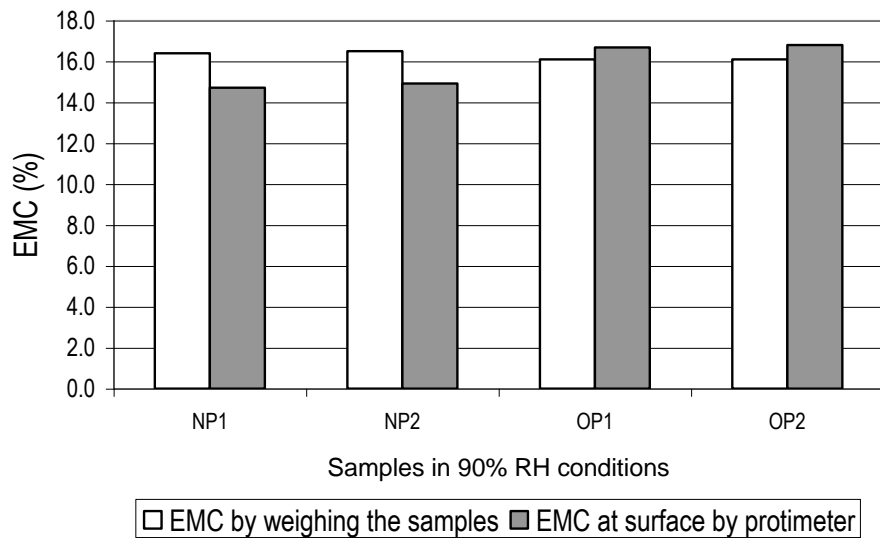


Figure 6.2 EMC of old and new pine by weight measurements and surface moisture readings by protimeter (Kandemir *et al.*, 2007).

“Ultrasonic velocity measurements done on the laboratory samples clearly reflected the changes in moisture content at different RH conditions. During the changes in RH from 56% to 90%, the variation in average ultrasonic velocity values in direct transmission mode was found to be in the range of 586 m/s to 1040 m/s in perpendicular-to-fiber direction while it was in the range of 2062 m/s to 3482 m/s in parallel-to-fiber direction (Figure 6.3). It was clearly observed in Figure 6.3 that ultrasonic velocity values increased at lower moisture conditions. Ultrasonic velocity values at low RH conditions revealed the physico-mechanical properties of the surfaces better than at high RH conditions. It was seen that the knowledge on microclimatic conditions was an important input to interpret the ultrasonic velocity values” (Kandemir *et al.*, 2007).

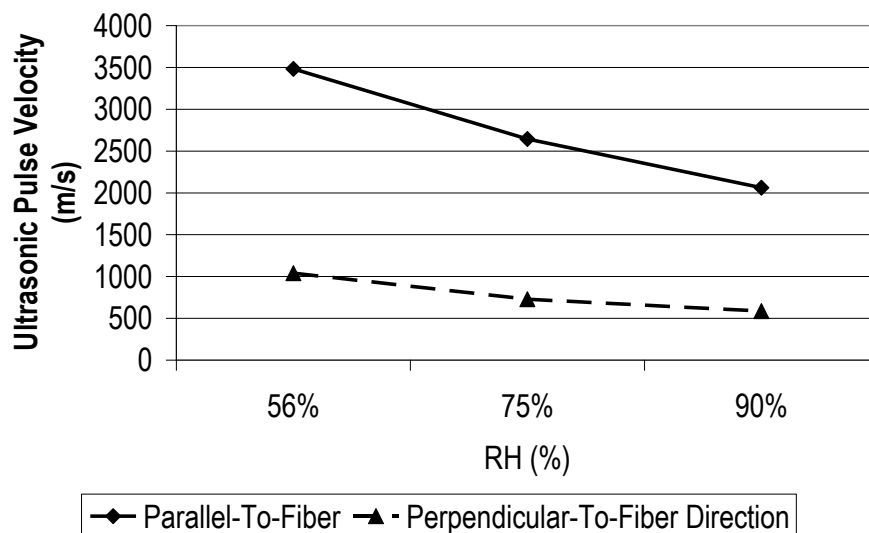


Figure 6.3 Changes in ultrasonic velocity values of old and new timber samples due to the changes in moisture content (Kandemir *et al.*, 2007)

### Direct and Indirect Velocity Measurements on the Timber Samples

Here the results of UPV measurement were summarized for the timber samples listed in Table 5.1. The ultrasonic pulse velocity longitudinal direct ( $UPV_{L-DIRECT}$ ) and ultrasonic pulse velocity radial direct ( $UPV_{R-DIRECT}$ ) measurements for the deteriorated and sound old pine samples collected from traditional houses as well as for new pine samples showed that all samples had sufficient physicommechanical

properties due to the  $UPV_{R-DIRECT}$  values around 1000m/s and the  $UPV_{L-DIRECT}$  values around 3500 m/s. The  $UPV_{DIRECT}$  values of sound old pine samples proved their inherently good physicommechanical properties, even better than the sound new pine samples. The old pine samples having radial cracks and insect holes at outer rings were determined to still keep their inherent strength in its core. The sound new pine samples had similar  $UPV_{DIRECT}$  values with the sound old pines. The presence of knots was determined to reduce the soundness of timber with a certain decrease in UPV in longitudinal and radial direction (Figure 6.4, Table 6.1).

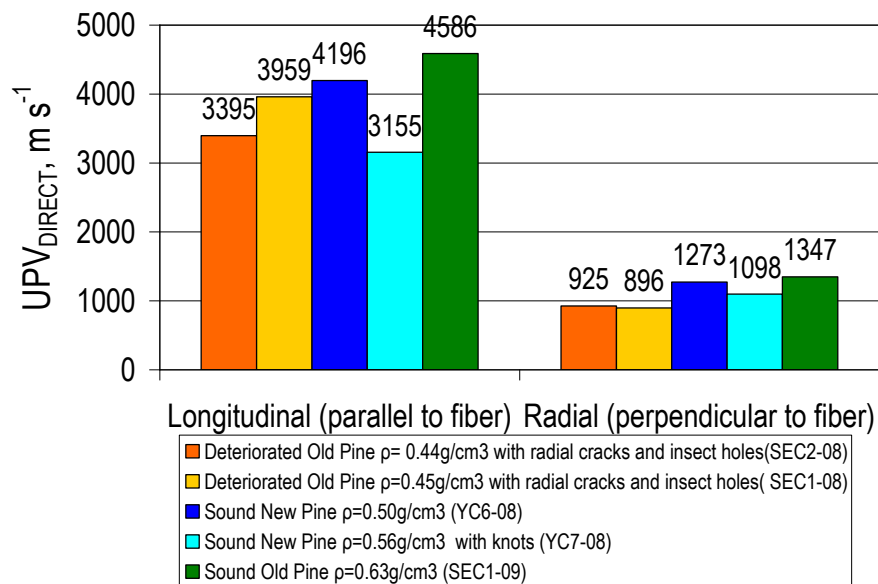


Figure 6.4 The  $UPV_{L-DIRECT}$  and  $UPV_{R-DIRECT}$  measurements for the deteriorated and sound old pine samples collected from traditional houses and sound new pine samples

According to the graph stated on the Figure 6.4, old and new pine samples were found to be sound due to the direct UPV values in perpendicular to the fiber direction being close to the 1000 m/s (Beall, 2002). The old pine samples that seemed to be deteriorated in visual observations were determined to be sound with their UPV values being similar to the sound old pine ones. The sound old

pine exhibited its inherent good mechanical properties. The sound new pines had similar physico-mechanical properties with the old ones. The deteriorated old pines having radial cracks and insect holes were found to be still sound proved by their radial UPV values close to 1000 m/s and longitudinal UPV values around 3500 m/s.

According to the direct UPV measurements, the deteriorated old pine sample was determined to be still sound since the direct UPV measurements parallel to fiber and perpendicular to fiber directions within acceptable ranges as indicated in literature (Beall, 2002; Bray, 1992). The old timber that suffered from insect attack was observed to have deterioration only at its outer rings. The outer rings/parts of the old pine were observed to be severely deteriorated and the direct UPV measurements taken tangent to fiber direction signaled the decrease in soundness at the outer rings. However, the soundness of the timber was found to be still enough due to the healthy/sound inner part of the sample. The UPV measurements taken at both parallel and perpendicular to fiber directions clearly indicated the soundness of the timber elements.

The UPV measurements taken in indirect mode both perpendicular and parallel to fiber directions exhibited strong relationship to density and mechanical properties of timber elements. The deteriorated old pine and new pine were found to have almost the same soundness while the new one slightly more sound than the old one. The sound old pine had the best physico-mechanical properties. That result was in agreement with the density of timber samples (Figure 6.5). In relation to their direct velocity measurements in longitudinal and radial directions and MoE values, indirect longitudinal velocity of sound pine range varied in the range of 1278 m/s and 1439 m/s, while the indirect radial velocity of sound pine varying in the range of 1063-1087 m/s.

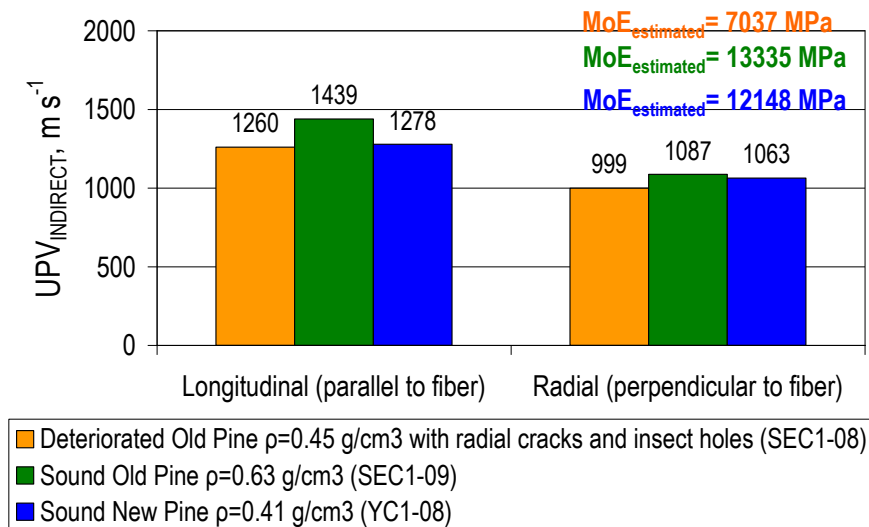


Figure 6.5 The laboratory UPV measurements taken in indirect mode both perpendicular and parallel to fiber direction.

The changes in UPV by defects and decay were examined in sound and deteriorated timber samples that had cracks and knots (Figure 6.6 and 6.7, Table 6.1). In Figure 6.6, the graph shows the transit time values versus distance for two timber samples with knots. Their slope of linear regression increased due to the location of defect composed of knot with surrounding cracks. Sharp increase in transit time signaling the decrease in UPV showed the deterioration such as crack, fiberization, knot etc. The increase in transit time of old deteriorated pine (SEC1-08) showed the presence of deep crack(s) through the knot. The presence of that knot at old timber (SEC1-08) considerable reduced the strength of timber in longitudinal direction (Figures 6.6 and 6.7).

Considering all UPV data, it must be noted that indirect measurements were systematically lower than the direct measurements (Figures 6.4 and 6.5).

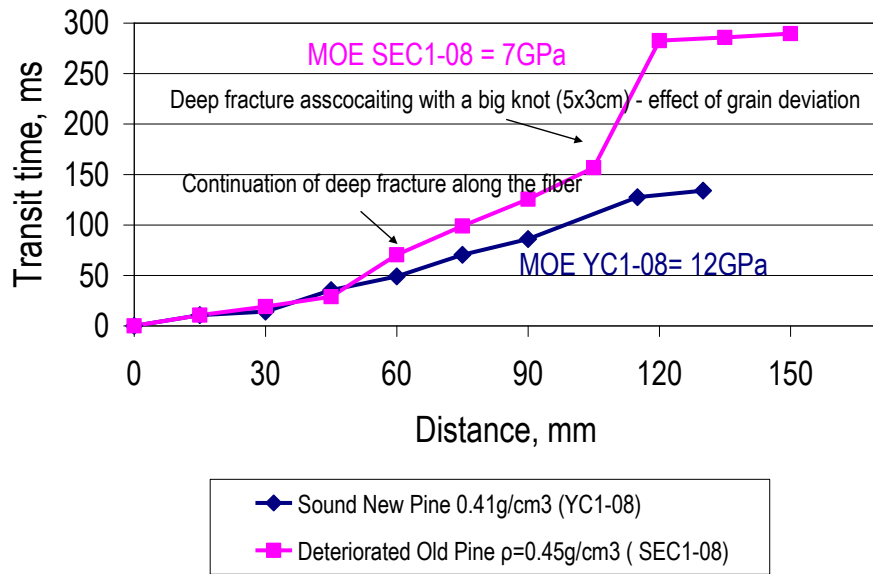


Figure 6.6 The transit time versus distance showing the presence of the knots on the timber surfaces.



Figure 6.7 Indirect UPV measurements taken from the surface of timber sample with knot; YC1-08 (left) and SEC1-08 (right)

Table 6.1 Reference UPV data for the visually sound and deteriorated timber samples measured in the laboratory.

Sample Code	Sample Definition	$\rho$ g cm <sup>-3</sup>	UPV <sub>R</sub> - DIRECT m s <sup>-1</sup>	UPV <sub>L</sub> - DIRECT m s <sup>-1</sup>	MoE (Estimated) GPa
SEC1-08	Deteriorated old pine from traditional house - Species A	0.449	896	3959	7.0
SEC2-08	Deteriorated old pine from traditional house - Species A	0.440	925	3395	5.0
SEC1-09	Sound old pine A - from traditional house - Species A	0.634	1347	4586	13.3
SEC2-09	Severly deteriorated old pine - from traditional house - Species A	0.421	NA (Not Available)	NA	NA
YC1-08	Sound new pine - Species D	0.408	812	5457	12.2
YC7-08	Sound new pine - Species C	0.557	1098	3155	5.5
YC6-08	Sound new pine - Species C	0.502	1273	4196	8.8
EC3-08	Deteriorated old pine - Species B soft	0.378	589	2352	2.1
EC4-08	New Pine timber Species E	0.532	1397	2225	2.6
YK5-08	Sound new beech	0.784	1256	3017	7.1
YM1-08	Sound new oak	0.870	1600	4426	17.0

## 6.1.2 Laboratory QIRT Analyses

### **Thermal Behavior of Timber, Fired Brick and Marble**

Thermal behavior was studied by the sequential IR imaging of several timber samples together with the neighbouring historic brick, mud mortar and stone samples during the heating and cooling periods. Temperature versus square root of time was drawn for each sample and they were compared.

Oak timber (YM1-08) and old pine (EC3-08), new pine (EC4-08), marble 1 (QIMG1), marble 2 (I3), repair fired brick 1 (FB1) and repair fired brick 2 (FB2) were heated by the halogen lamp (650 Watt) and then monitored by the sequential IR imaging during the heating and cooling periods. At the beginning the timber samples were warmer than the fired brick samples. Marble samples were the coldest ones (Figures 6.8.a,b). On the other hand, differential IR image of heating period has shown that the rate of heating was higher for timber in comparison to fired brick. Heating of the marble samples were the slowest (Figure 6.8.c). The differential IR image of the cooling period has shown that cooling was faster for timber in comparison to fired brick. Cooling of marble samples was slowest (Figure 6.8.d). Quantitative analyses of differential IR images were shown in Figures 6.9.a,b. In those lines, the rate of heating and cooling of the samples could be followed easily by the R value belonging to each sample. Rate of heating and cooling of each sample were compared with the rate of sound timber sample (Table 6.2). It was seen that rate of heating was highest for sound timber sample (RW-Oak=0.1191 RW-Pine=0.1424), followed by the fired brick sample (RW-Fired brick=0.1024), marble having slowest rate (RW-Marble=0.0674). The same trend was found at the cooling lines, rate of cooling was highest for timber followed by fired brick samples. When those rates were compared with the rate of sound timber in terms of ratios, found by dividing the rate of each sample with the rate of sound timber one, it was better seen that heating and cooling rates of timber samples were closer to the fired brick than to marble (Table 6.2).

Comparison of the rates have clearly indicated the differences in thermal behavior of samples, e.g. the oak sample with the density of 0.87g/cm<sup>3</sup>, had slightly slower heating and cooling rate than the pine sample with the density of 0.53g/cm<sup>3</sup> (See Figures 6.9.a,b and Table 6.2). Those temperature differences could also be followed in differential IR images. The QIRT analysis seemed to be sensitive enough to differentiate the timber species.

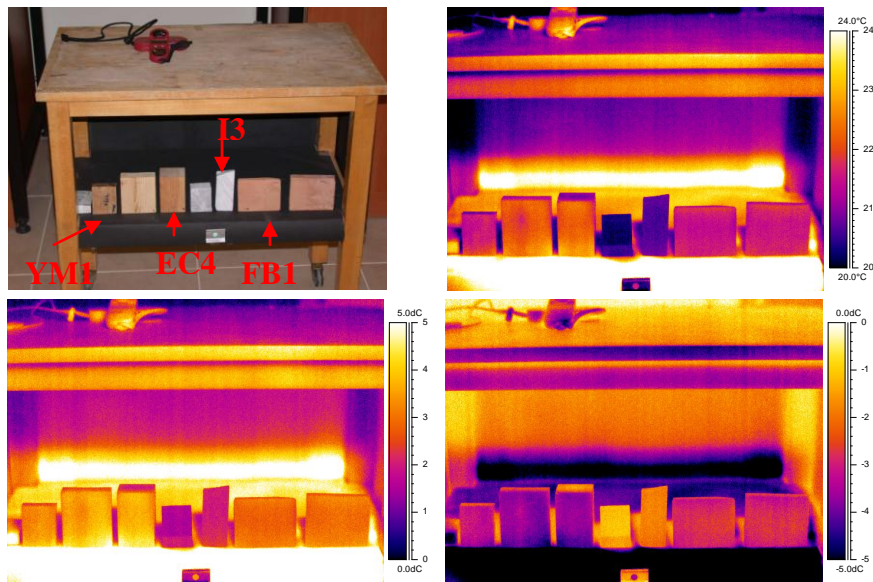


Figure 6.8 a) Laboratory samples oak (YM1), pine 1(EC3), pine 2(EC4), marble 1(QIMG1), marble 2(I3) and fired brick 1(FB1), fired brick 2 (FB2) b) IR image of samples at the beginning of heating period c) Differential IR image of samples at the heating period d) Differential IR image of samples at the cooling period.

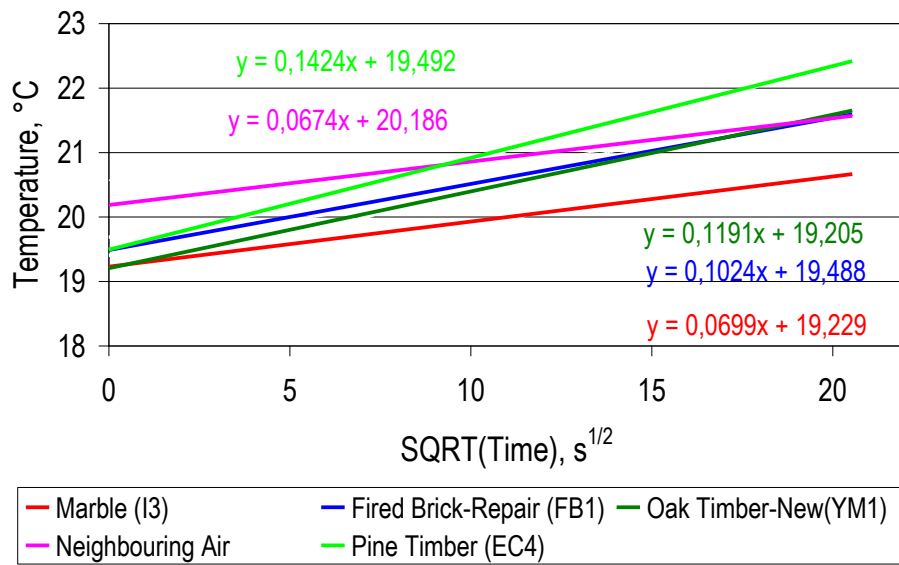


Figure 6.9.a The surface temperature lines versus square root of time during heating period of samples using a halogen lamp (650 Watt)

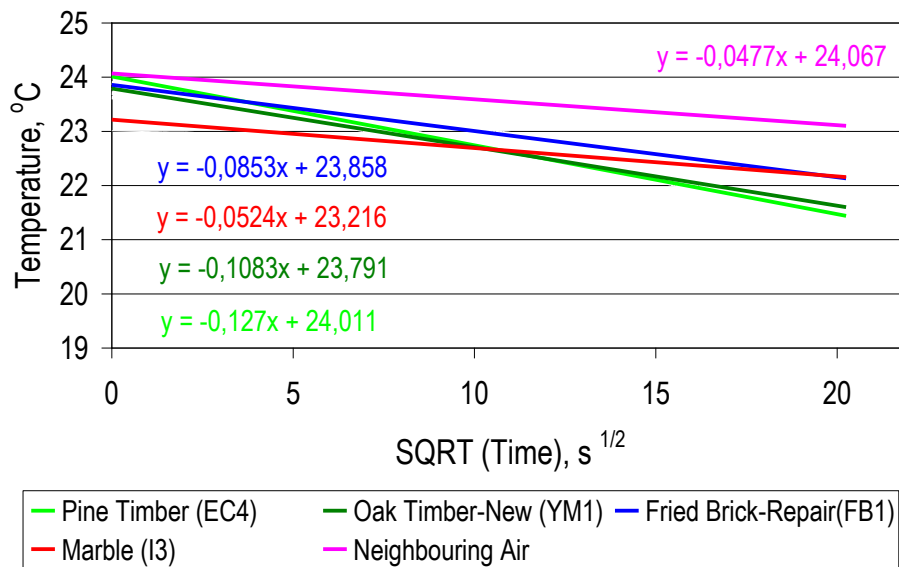


Figure 6.9.b The surface temperature lines versus square root of time during cooling period of samples

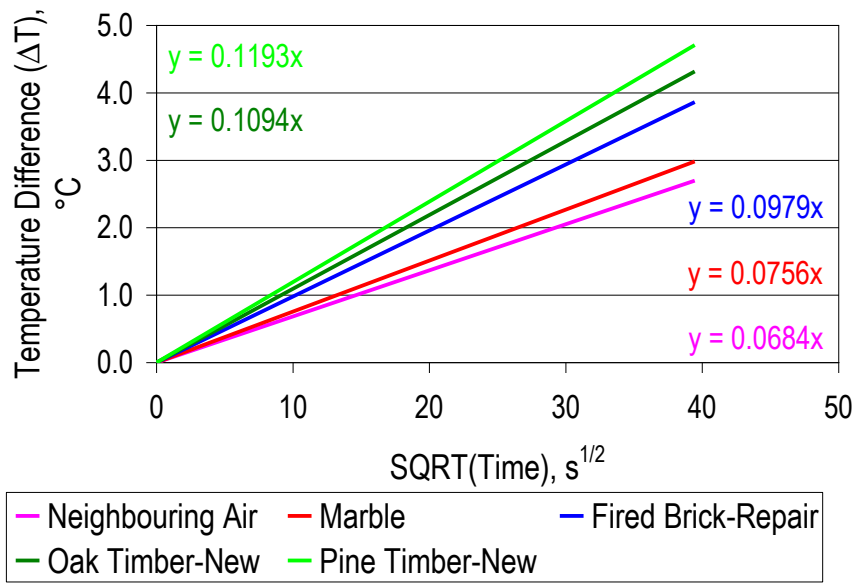


Figure 6.9.c The temperature difference lines versus square root of time for oak, pine, marble and repair fired brick samples heated by the halogen lamp (650 Watt) and then monitored by the sequential IR imaging during the heating period

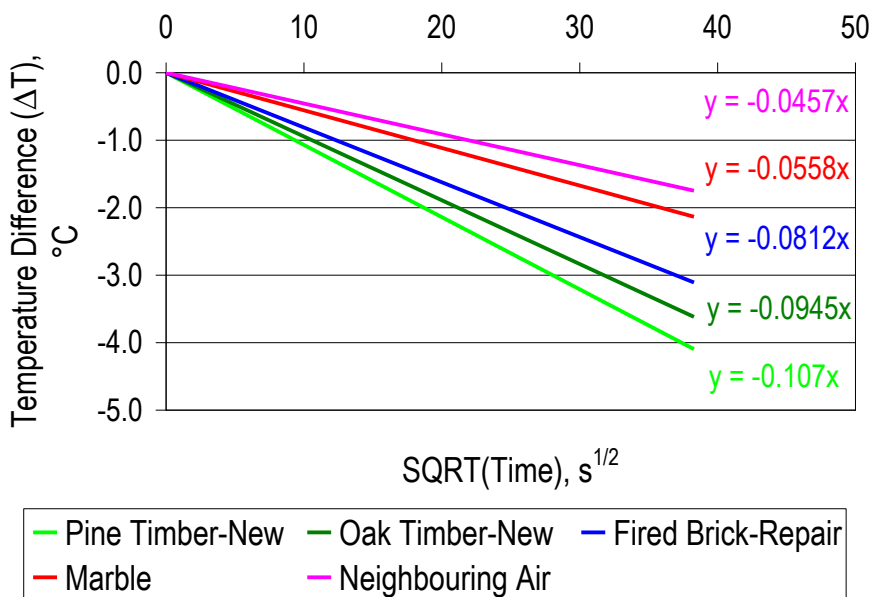


Figure 6.9.d) The temperature difference lines versus square root of time for oak, pine, marble and repair fired brick samples heated by the halogen lamp (650 Watt) and then monitored by the sequential IR imaging during the cooling period

Table 6.2 Rate of heating up and cooling down of the marble, fried brick, oak and pine timber

Definition	R <sub>w</sub> - Rate of heating up T/√s	$\frac{R_{w-material}}{R_{w-TIMBER}}$	R <sub>C</sub> - Rate of cooling down T/√s	$\frac{R_{C-material}}{R_{C-TIMBER}}$
Neighbouring Air	0.0674	0.4733	-0.0477	0.3756
Marble	0.0699	0.4909	-0.0524	0.4126
Fried Brick-repair	0.1024	0.7191	-0.0853	0.6717
Oak Timber-New	0.1191	0.8364	-0.1083	0.8528
Pine Timber	0.1424	1.0000	-0.1270	1.0000

### Comparison of the Sound and Deteriorated Timber for Their Thermal Properties

Several timber samples, indicated in Table 6.1, being visually deteriorated old pines (SEC1-08, SEC2-08, FEC3), sound new beech (YK5-08), sound new pine (YC7-08, YC6-08, EC4-08), previously kept at 20.5°C and 20.5%RH laboratory conditions, were examined by the sequential IR imaging during the cooling period of 507 seconds in outdoor conditions (Figure 6.10.a). The boundary conditions were 7.9°C±0.1°C and 40.6%RH±0.7%. The differential IR image produced from the last and 1st IR image was shown in Figure 6.10.b. The lines showing surface temperature versus square root of time and temperature difference versus square root of time have shown that the deteriorated pine sample cooled down faster than the sound one, while the sound beech sample, having the highest density, exhibited the slowest cooling rate (Figures 6.11.a,b). The values of rate of cooling and their comparison with sound pine were indicated in Table 6.3. It was seen that rate of cooling was highest for deteriorated timber sample (EC3-08-<sub>RC</sub> - deteriorated pine= 0.1518). The cooling rate of beech was the slowest (YK5<sub>RC</sub> - new beech= 0.0891). Cooling rate of deteriorated pine was considerably higher than the sound one, RC deteriorated pine/ RC sound pine = 1.6980 (Table 6.3).

Those results proved that the QIRT allowed to differentiate the sound and deteriorated timber as well as different timber species. Those results have also indicated the difference in their thermal behavior.

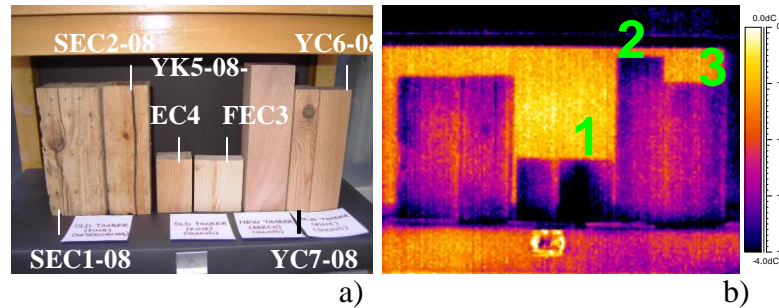


Figure 6.10 a) View of timber samples: Old pine (SEC1-08, SEC2-08), new pine (EC4, YC7-08, YC6-08) deteriorated pine (FEC3), new sound beech (YK5-08) b) Their differential IR image.

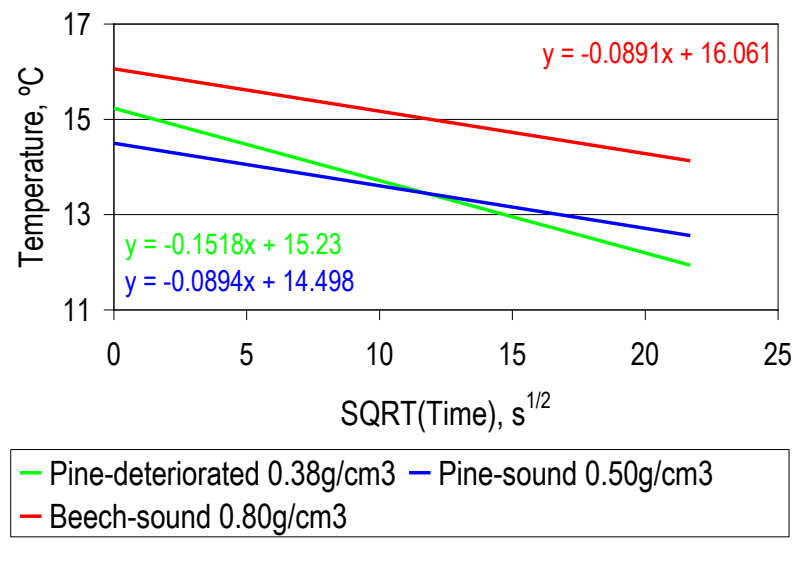
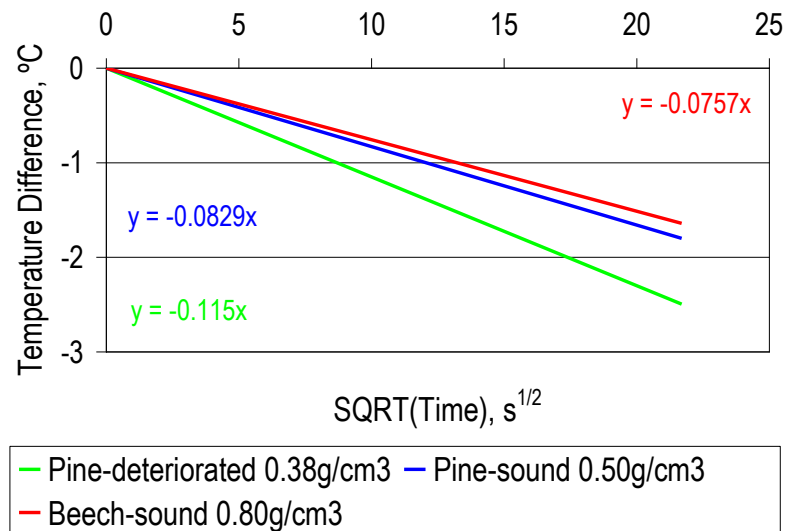


Figure 6.11 a) The surface temperature lines versus square root of time during cooling period



b)

Figure 6.11 b) Temperature difference lines versus square root of time during cooling period.

The deteriorated pine sample cooled down faster than the sound pine. The deteriorated and sound pine timbers could be clearly distinguished from each other due to the lower thermal inertia characteristics of the deteriorated one having warmer initial temperature and faster rate of cooling down (Table 6.3).

Table 6.3 Rate of cooling down of the deteriorated pine, sound pine and sound beech

Definition	RC - Rate of cooling down $T/\sqrt{s}$	$\frac{R_{C.material}}{R_{C-SOUND PINE}}$
Deteriorated Pine (EC3-0.38 g/cm <sup>3</sup> )	0.1518	1.6980
New Beech (YK5- $\rho=0.80$ g/cm <sup>3</sup> )	0.0891	0.9966
Sound Pine (YC6-08- $\rho=0.50$ g/cm <sup>3</sup> )	0.0894	1.0000

Another group of timber samples, whose UPV measurements and densities were previously determined and indicated in Table 6.1, being pine (EC3- 0.38 g/cm<sup>3</sup>), new oak (YM1-0.870 g/cm<sup>3</sup>), new beech (YK5-0.784 g/cm<sup>3</sup>) sound old pine (SEC1-09-0.634 g/cm<sup>3</sup>), deteriorated old pine (SEC2-09-0.421 g/cm<sup>3</sup>) visually deteriorated but inner part sound pine (SEC1-08- 0.440 g/cm<sup>3</sup>), sound new pine (YC1-08- 0.408 g/cm<sup>3</sup>), were examined by the sequential IR imaging (Figure 6.12.a) during the heating period of 814 seconds with halogen lamps (2x500 Watt) and cooling period of 756 seconds. The boundary conditions were 23.09°C±0.06°C and 48.93%RH±0.13%. The lines indicating surface temperature versus square root of time during heating and cooling have shown that the both rate of heating and rate of cooling depended on state of deterioration of timber as well as its density for most samples (Figures 12-14). The timbers with lower density had higher rate of heating and cooling (EC3-08, SEC2-09) indicating their lower thermal inertia. However, for the new pine, although its density was lower than the old deteriorated pine, its rate of heating and cooling was slower than the old deteriorated pine. It has indicated that, surface soundness of new pine with low density (YC1-08), was much better than the deteriorated old pine surface that had a sound core (SEC1-08) (Figures 6.13, 6.15 and Table 6.4). QIRT analysis was good at seeing the degree of decay of old pines of similar type (SEC1-09, SEC1-08, and SEC2-09). The severely deteriorated one SEC2-09 had the highest rate of heating and cooling and its density was lowest. The sound old pine had the lowest rate of heating and cooling and had considerable high density indicating its higher thermal inertia.

Among those samples, there was a deteriorated old pine sample (EC3-08) of different species having lower density. Its quite high rate of heating and cooling indicated its low thermal inertia and considerable deteriorated state.

It was seen that heating and cooling lines drawn by using temperature versus square root of time were more representative of different samples at beginning of

the heating and cooling periods in laboratory conditions, e.g. at the first 100-200 seconds. That aspect needed to be considered at field measurements.

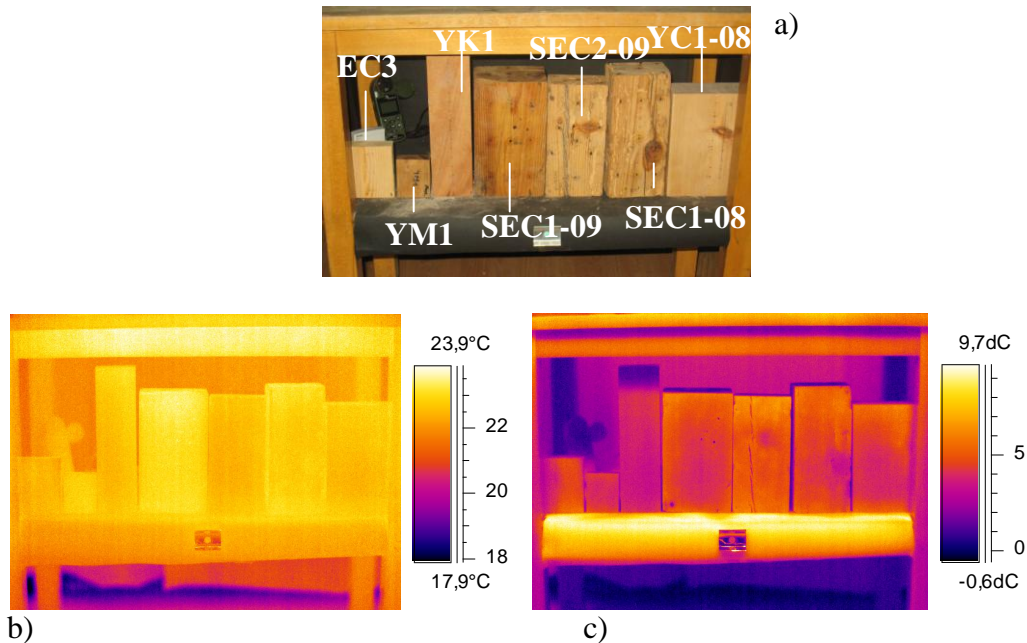


Figure 6.12 a) The view of samples before analyzed by QIRT: old pine with low density (FEC3- 0.38 g/cm<sup>3</sup>), new oak (YM1-0,870), new beech (YK5-0.784) sound old pine (SEC1-09-0.634), deteriorated old pine (SEC2-09-0.421 g/cm<sup>3</sup>) visually deteriorated but inner part sound pine (SEC1-08, 0.449 g/cm<sup>3</sup>), sound new pine (YC1-08- 0.408 g/cm<sup>3</sup>) b) IR image of sample at the beginning of heating period c) Differential IR image of samples during heating period of 814 seconds.

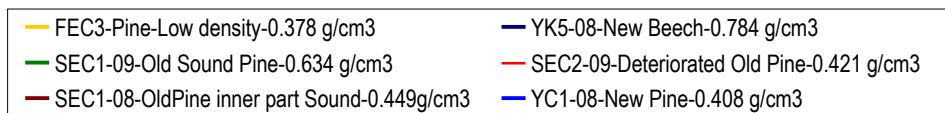
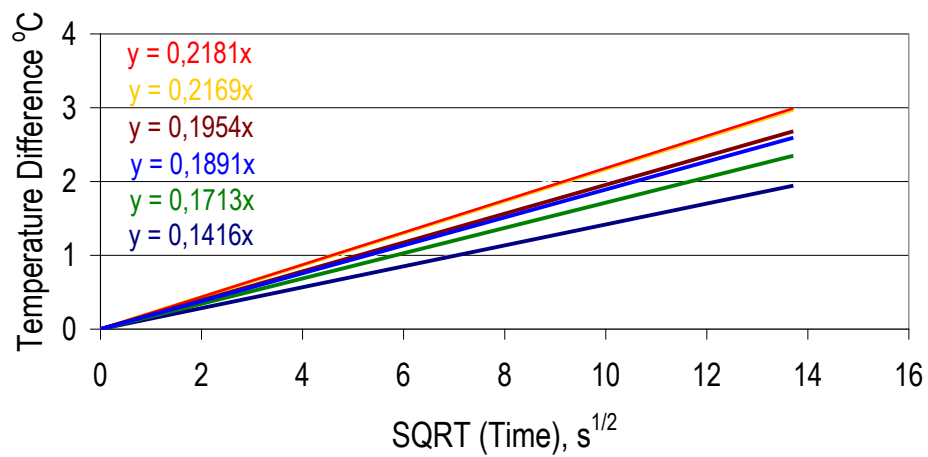
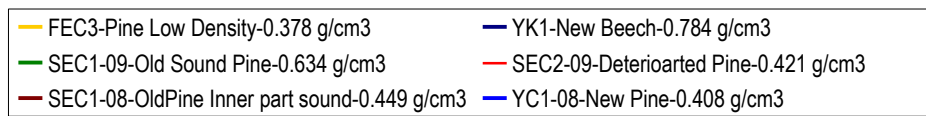
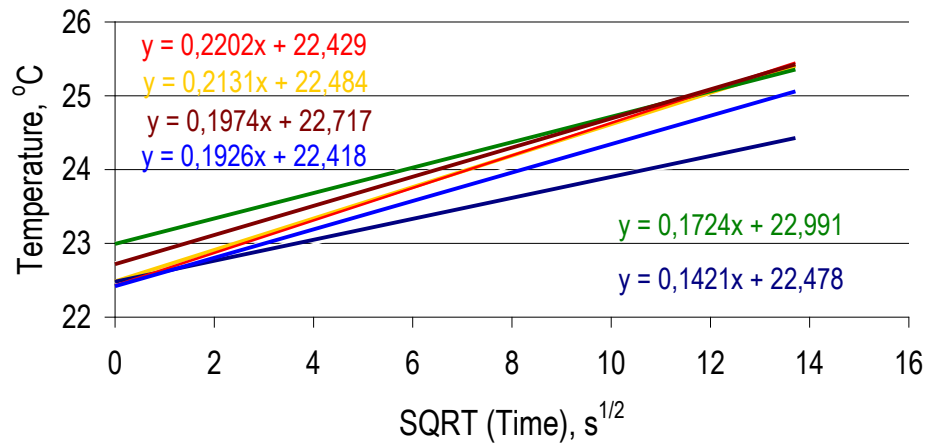


Figure 6.13 The surface temperature and temperature difference lines versus square root of time during heating period for the samples in Figure 6.12.a

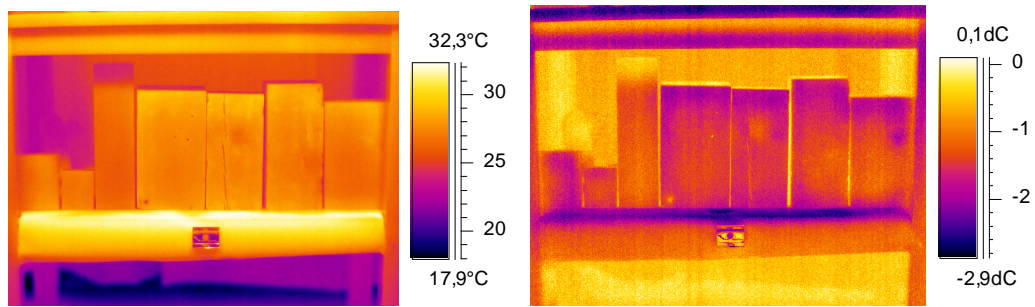


Figure 6.14 a) IR image of samples in Figure 6.12.a at the beginning of cooling period b) Differential IR image of samples during cooling period of 756 seconds.

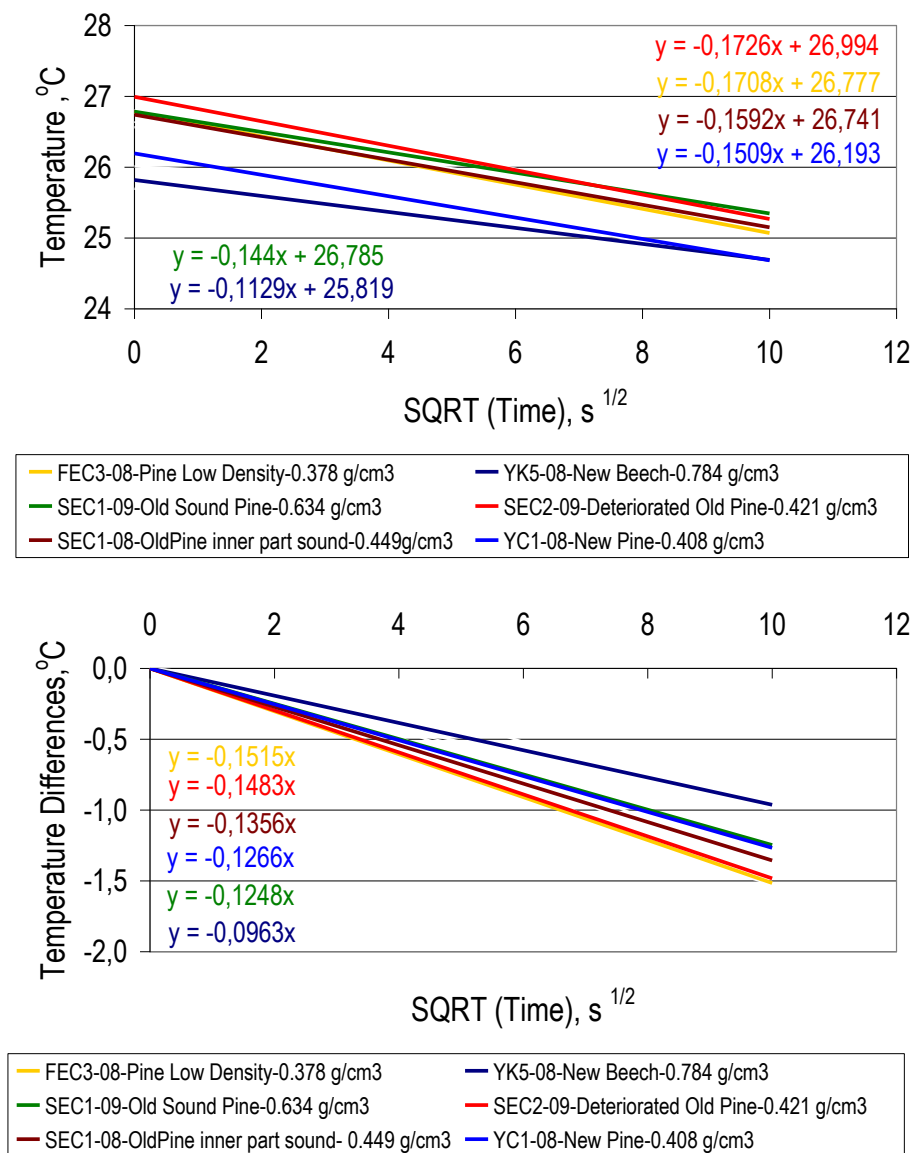


Figure 6.15 The surface temperature and temperature difference lines versus square root of time during cooling period for the samples in Figure 6.12.a

Table 6.4 Rate of heating, rate of cooling and soundness ratio of timber samples

Definition	Rate of heating up- $R_W$	Rate of cooling down- $R_C$	$^*R_W$	$^*R_C$
			$\frac{R_W}{R_{W-old\ sound}}$	$\frac{R_C}{R_{C-old\ sound}}$
SEC2-09-Severely Deteriorated Old Pine ( $\rho=0.421\text{g/cm}^3$ MOE=NA)	0.2202	-0.1726	1.2773	1.1987
FEC3-08-Old Pine low density- ( $\rho=0.378\text{g/cm}^3$ MOE=2.091GPa)	0.2131	-0.1708	1.2361	1.1861
SEC1-08 Old pine-inner part sound ( $\rho=0.449\text{g/cm}^3$ MOE=7.037GPa)	0.1974	-0.1592	1.1450	1.1056
YC1-08-New Pine- ( $\rho=0.408\text{g/cm}^3$ MOE=12.148GPa)	0.1926	-0.1509	1.1172	1.0479
SEC1-09-Sound Old Pine ( $\rho=0.634\text{g/cm}^3$ MOE=13.335GPa)	0.1724	-0.1440	1	1
YK5-08-New Beech ( $\rho=0.784\text{g/cm}^3$ MOE=7.137GPa)	0.1421	-0.1129	0.8242	0.7840

\* Heating and cooling ratios of samples with reference to a selected sound timber sample were used calculated to express the soundness of samples.

During the heating and cooling periods, knots on the timber samples shown in Figure 6.12.a, were also examined with respect to the rate of heating up and cooling down. Due to higher density of the knots, they had slower rate of heating and cooling in comparison to timber surfaces next to the knots. (Figure 6.16.a,b). QIRT analyses have shown that the surfaces of the deteriorated old pine warmed up and cooled down 1.44 (0.2202/ 0.1528) and 1.71 (-0.1726/-0.1012) times faster than the knot surfaces respectively (see Table 6.5). The knot on the deteriorated pine had the slower rate of heating and cooling than its deteriorated surroundings. However the knots were far more sound than the timber parts next to them. Therefore, the soundness of timber with QIRT analyses should be done on the timber surfaces without knots.

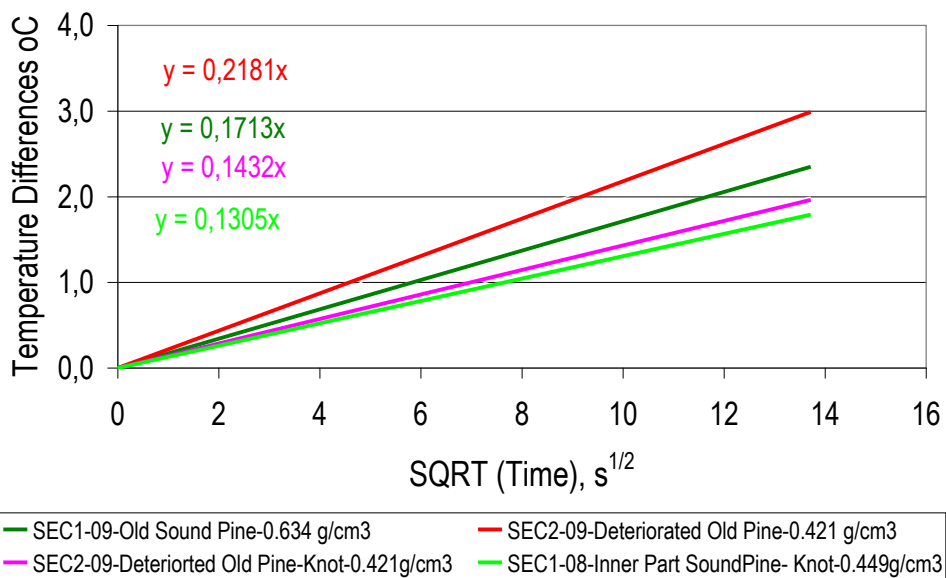
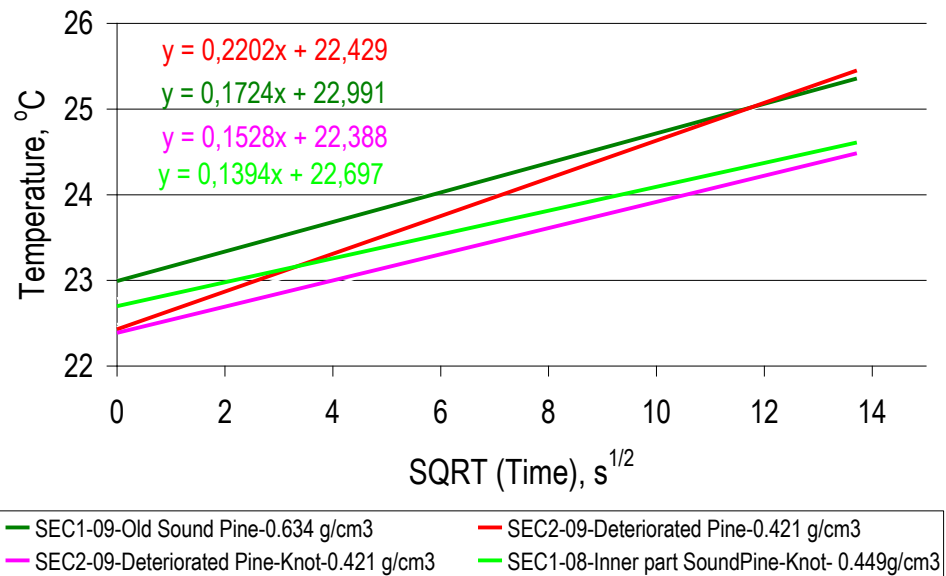


Figure 6.16.a The surface temperature and temperature difference lines versus square root of time during heating period compared with their knots for the samples in Figure 6.12.a.

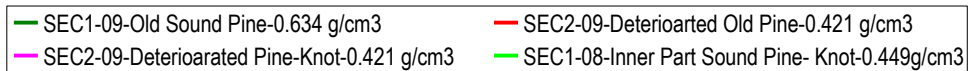
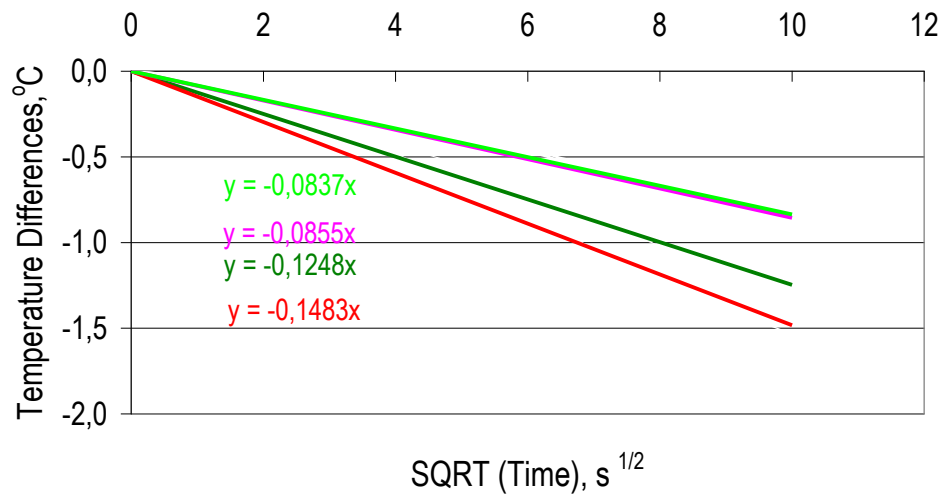
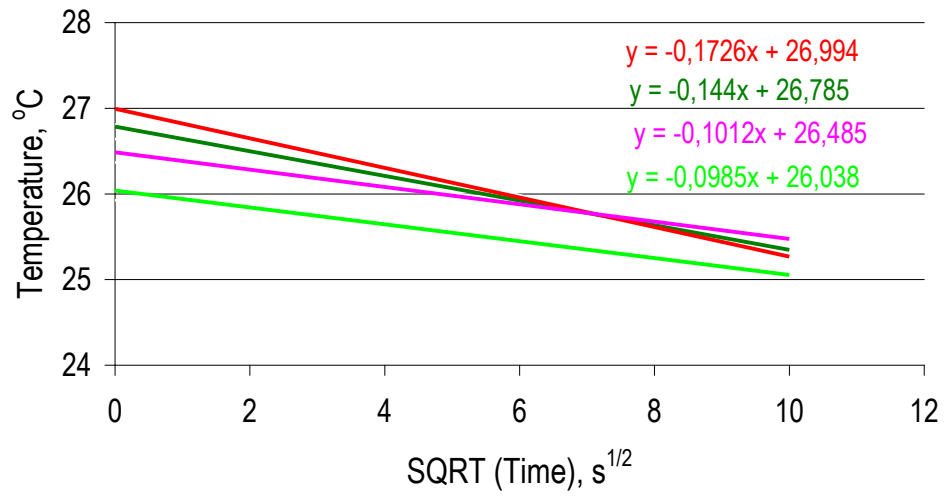


Figure 6.16.b The surface temperature and temperature difference lines versus square root of time during cooling period compared with their knots for the samples in Figure 6.12.a.

Table 6.5 Rate of heating, rate of cooling and soundness ratio of deteriorated pine, sound old pine and their knots

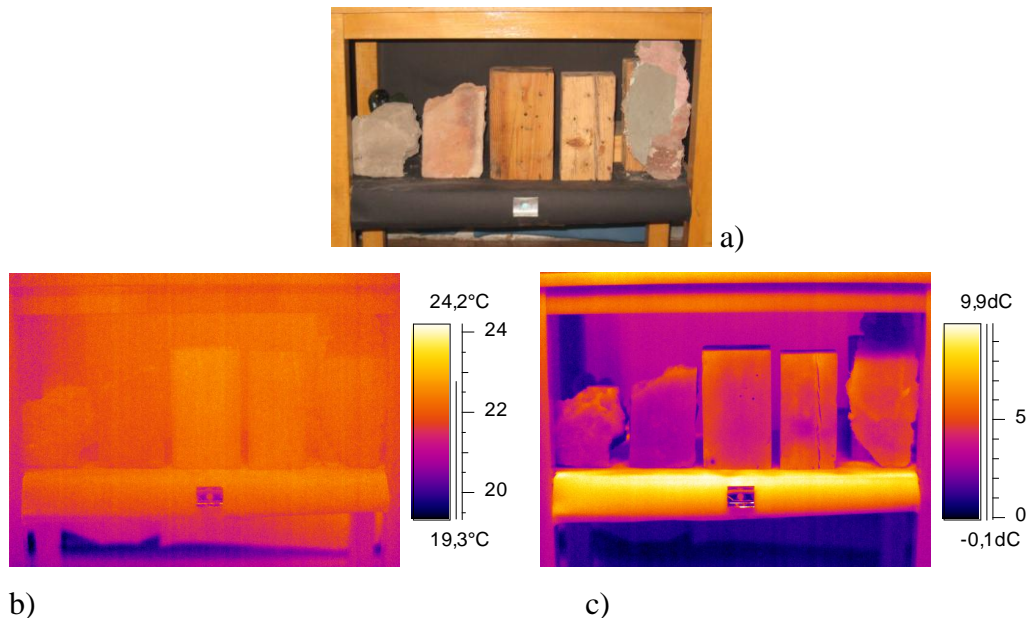
<b>Definition</b>	Rate of heating up- $R_W$	Rate of cooling down- $R_C$	$\frac{*R_W}{R_W\text{-sound old pine}}$	$\frac{*R_C}{R_C\text{-sound old pine}}$
SEC2-09-Severely Deteriorated Old Pine ( $\rho=0.421\text{g/cm}^3$ MOE=NA)	0.2202	-0.1726	1.2772	1.1986
SEC2-09-Severely Deteriorated Old Pine- <b>Knot</b> ( $\rho=0.421\text{g/cm}^3$ MOE=NA)	0.1528	-0.1012	0.8863	0.7028
SEC1-08 Old pine-inner part sound- <b>Knot</b> ( $\rho=0.449\text{g/cm}^3$ MOE=7.037GPa)	0.1394	-0.0985	0.8085	0.6840
SEC1-09-Sound Old Pine ( $\rho=0.634\text{g/cm}^3$ MOE=13.335GPa)	0.1724	-0.1440	1	1
* Heating and cooling ratios of samples with reference to a selected sound timber sample were used calculated to express the soundness of samples.				

### **Thermal Properties of Timber and Its Neighboring Materials Used in the Traditional Houses**

Thermal properties of timber and its neighboring materials in timber framed houses were studied in the laboratory by using representative samples from a historic structure. The samples were sound and deteriorated pine timber (SEC1-09, SEC2-09), mud brick infill, fired brick and exterior lime plaster together with its mud plaster layer, interior lime plaster and mud plaster (Figures 6.17.a, 6.24.a). QIRT images of those samples were analyzed in groups as described below during the heating and cooling periods. The rate of cooling and heating of samples were studied in detail by plotting the lines of temperature versus square root of time and comparing their slopes.

*The group consisting of mud brick, fired brick, sound and deteriorated timber, exterior lime plaster together with its mud layer.*

The group of samples, being mud brick, fired brick, sound old pine (SEC1-09-0.634 g/cm<sup>3</sup>), deteriorated old pine (SEC2-09-0.421 g/cm<sup>3</sup>), exterior lime plaster with thick mud layer, were examined by the sequential IR imaging (Figure 6.17.a) during the heating period of 642 seconds with halogen lamps (2x500 Watt) and cooling period of 596 seconds. The boundary conditions were 22.95°C±0.03°C and 47.57% ±0.13% RH. The data obtained was used to compare the rate of heating and cooling of samples that were related to their thermal inertia (Figures 6.18-6.20). It was seen that fired brick had the slowest rate of heating and cooling. The rates have increased in the samples in the following order: mud brick, exterior lime plaster together with its mud layer, sound timber and deteriorated timber. The sound timber and lime plaster had quite similar rate of heating and cooling. That was clearly seen in Table 6.6 where the rates of heating and cooling were compared with sound timber as a ratio. Deteriorated timber had the fastest rate of heating and cooling.



b) Figure 6.17 a) The view of samples before QIRT analyses: mud brick infill, fired brick infill, sound old timber (SEC1-09-0.634), deteriorated old pine (SEC2-09-0.421 g/cm<sup>3</sup>), exterior lime plaster together with its mud layer b) IR image of samples at the beginning of heating period c) Differential IR image of samples during heating period of 642 seconds.

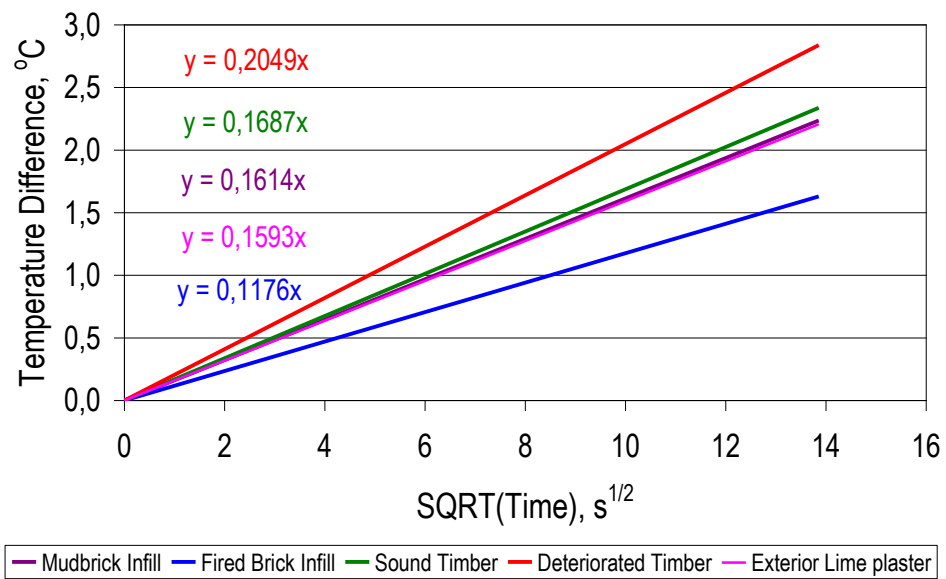
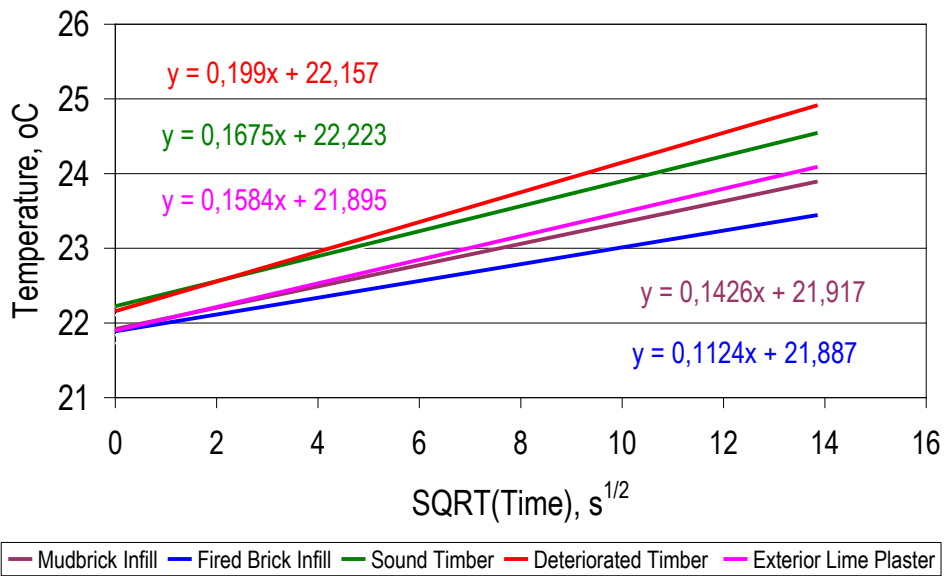


Figure 6.18 The surface temperature and temperature difference lines versus square root of time during heating period of the group consisting of mud brick, fired brick, sound and deteriorated timbers, exterior lime plaster together with its mud layer.

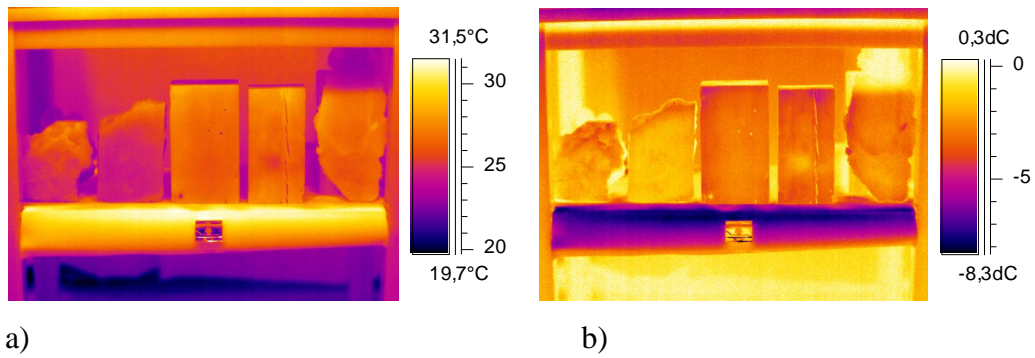


Figure 6.19 a) IR image of samples in Figure 6.17.a at the beginning of cooling period b) Differential IR image of samples during cooling period of 596 seconds.

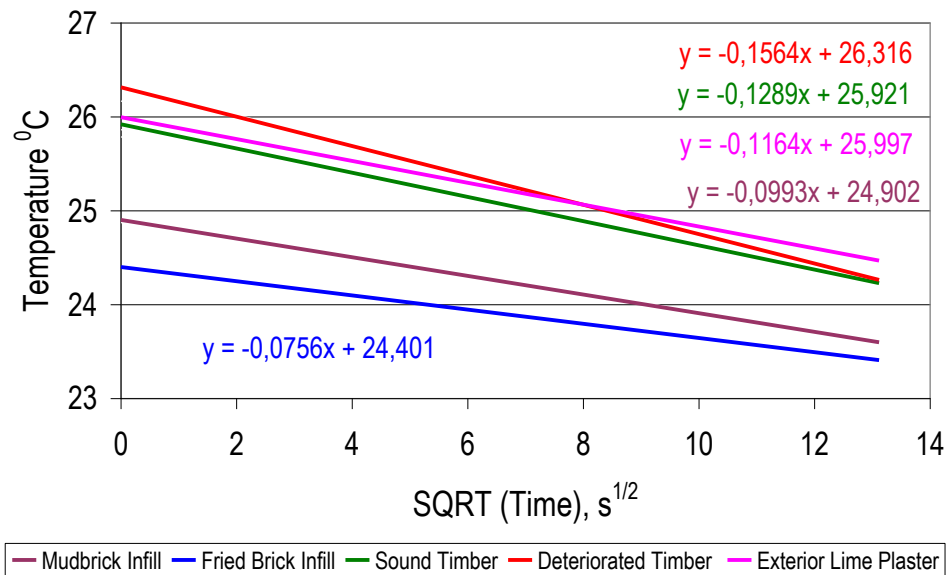


Figure 6.20 a) The lines of surface temperature versus square root of time during cooling period of the group consisting of mud brick, fired brick, sound and deteriorated timbers, exterior lime plaster together with its mud layer

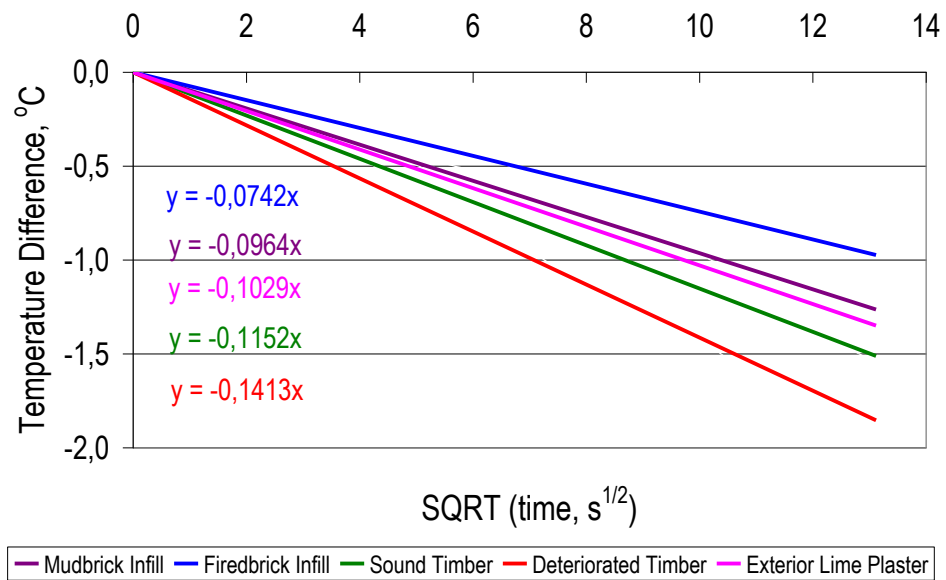


Figure 6.20 b) The lines of temperature difference versus square root of time during cooling period of the group consisting of mud brick, fired brick, sound and deteriorated timbers, exterior lime plaster together with its mud layer.

Table 6.6 Rate of heating and cooling of samples their ratios to sound timber

Definition	$R_w$ - Rate of heating up $T/\sqrt{s}$	$\frac{R_w\text{-material}}{R\text{-WTIMBER}}$	$R_c$ - Rate of cooling down $T/\sqrt{s}$	$\frac{R_c\text{-material}}{R\text{-CTIMBER}}$
Mudbrick Infill	0.1426	0.8513	-0.0993	0.7704
Fried Brick Infill	0.1124	0.6710	-0.0756	0.5865
Deteriorated Timber	0.1990	1.1881	-0.1564	1.2133
Exterior Lime Plaster	0.1584	0.9457	-0.1164	0.9030
Sound Timber	0.1675	1.0000	-0.1289	1.0000

*The group consisting of mud brick, thick interior repair plaster (high gypsum content) together with its mud layer, mud plaster, sound timber, and exterior lime plaster together with its mud layer.*

Another group of samples, being mud brick, thick interior repair plaster (high gypsum content) together with its mud layer, mud plaster, sound old pine (SEC1-09;  $\rho=0.634 \text{ g/cm}^3$ ), exterior lime plaster with thick mud layer, were examined by the sequential IR imaging (Figure 6.21.a) during the heating period of 592 seconds with halogen lamps (2x500 Watt) and cooling period of 670 seconds. The boundary conditions were  $22.93^\circ\text{C}\pm 0.06^\circ\text{C}$  and  $48.67\%\text{RH}\pm 0.07\%$ . It was seen that thick interior repair plaster (high gypsum content) together with its mud layer had the slowest rate of heating and cooling. Exterior lime plaster with thick mud layer and exterior mud plaster warmed up and cooled down together with the sound old pine, exterior mud plaster having almost the same heating and cooling rate with the sound old pine (Figures 6.22-6.24). QIRT analyses have shown that the surfaces of the mud mortar warmed up and cooled down 0.82 and 0.86 times slower than the sound old pine surfaces respectively (see Table 6.7). Heating and cooling rate ratios of neighbouring materials; lime, mud plaster and mud brick infill in comparison to sound pine were found to be in the range of 0.98-0.82 in laboratory conditions (see tables 6.6,6.7). However, heating and cooling rate ratios of fired brick materials to sound pine were in the range of 0.71- 0.58 in the laboratory (see Tables 6.5, 6.6). On the other hand, heating and cooling rate ratio of the thick interior repair plaster (high gypsum content) together with its mud layer was in the range of 0.66-0.54 (Table 6.7).

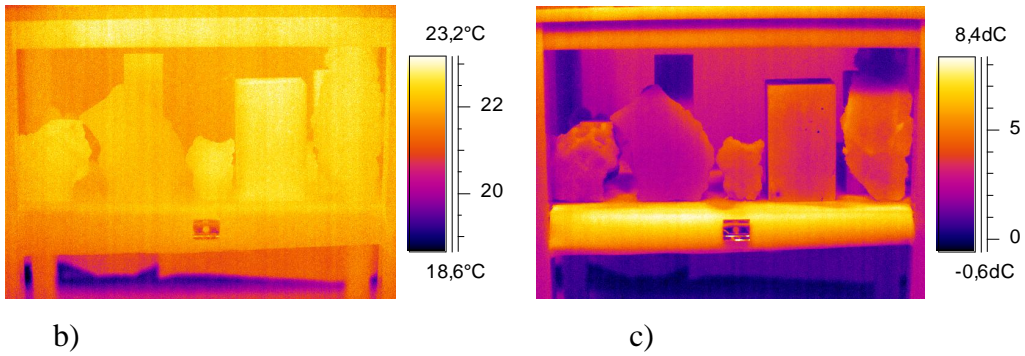


Figure 6.21 a) The view of samples before analyzed by QIRT: mud brick infill, thick interior repair plaster (high gypsum content) together with its mud layer, mud plaster, sound old timber (SEC1-09-0.634), exterior lime plaster together with its mud layer b) IR image of sample at the beginning of heating period c) Differential IR image of samples during heating period of 592 seconds.

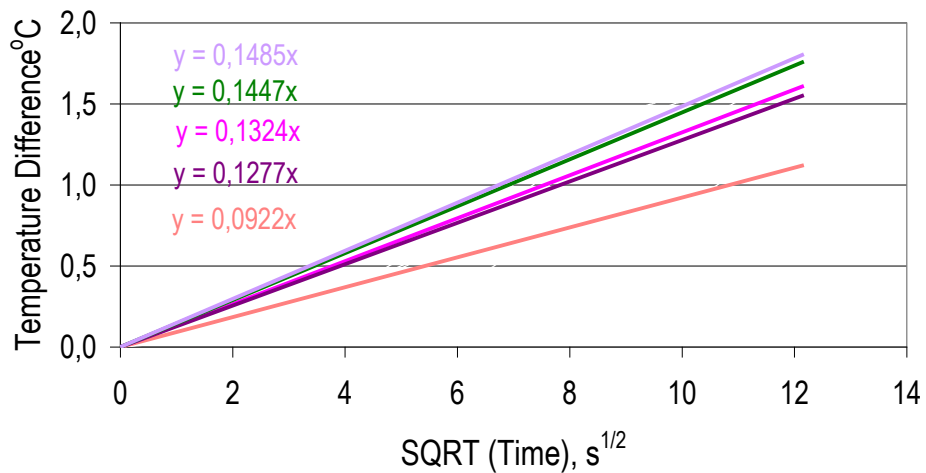
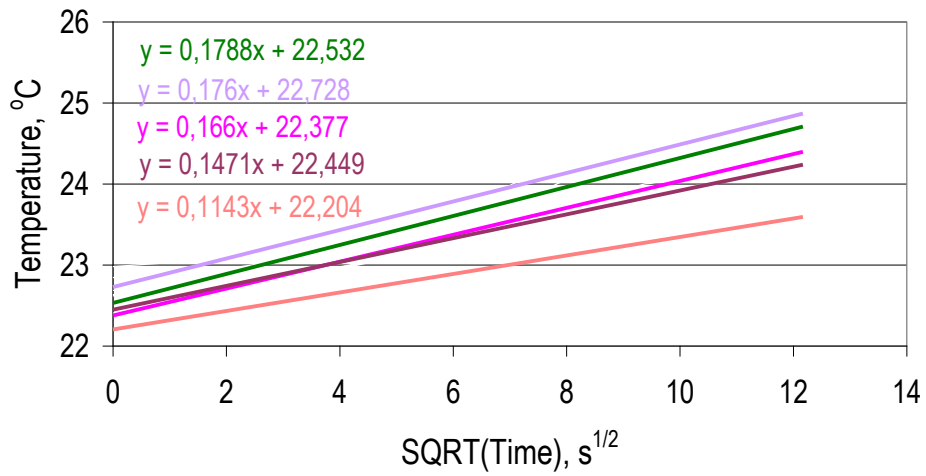


Figure 6.22 The lines of surface temperature and temperature difference versus square root of time during heating period of the group consisting of mud brick, interior lime plaster, mud plaster sound timber, and exterior lime plaster together with its mud layer.

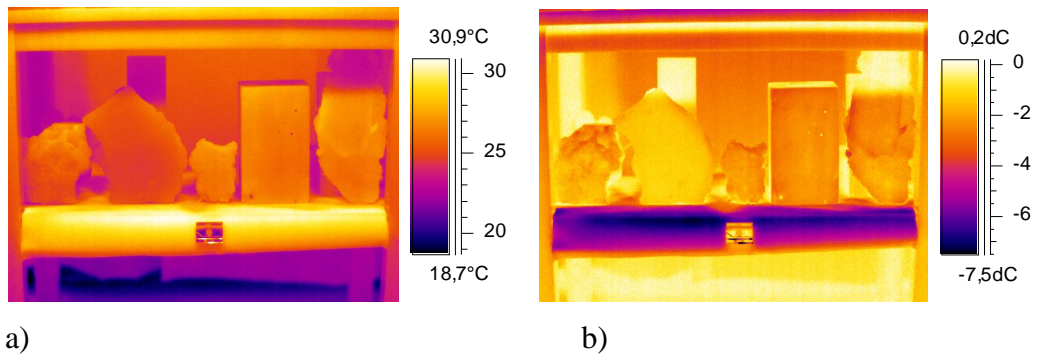


Figure 6.23 a) IR image of samples in Figure 6.17.a at the beginning of cooling period b) Differential IR image of samples during cooling period of 670 seconds.

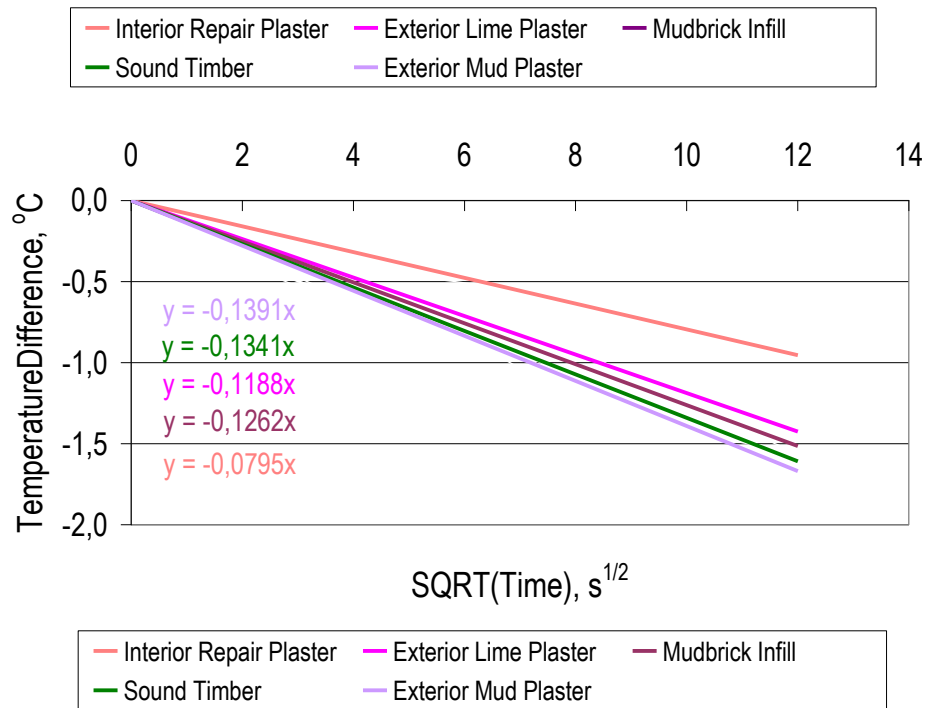
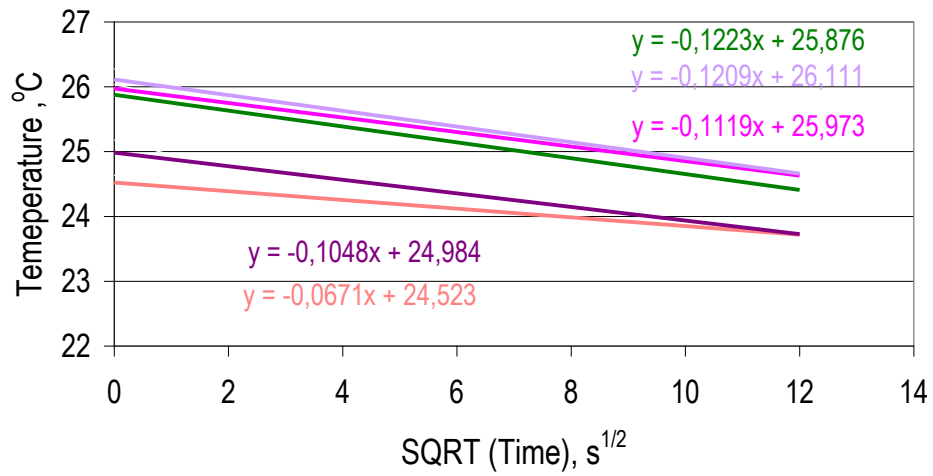


Figure 6.24 The lines of surface temperature and temperature difference versus square root of time during cooling period of the group consisting of mud brick, interior lime plaster, mud plaster sound timber, and exterior lime plaster together with its mud layer.

Table 6.7 Rate of heating and cooling of samples their ratios to sound timber

Definition	R <sub>C</sub> - Rate of heating up T/√s	$\frac{R_{C-material}}{R_{CTIMBER}}$	R <sub>C</sub> - Rate of cooling down T/√s	$\frac{R_{C-material}}{R_{CTIMBER}}$
Mudbrick Infill	0.1471	0.8227	-0.1048	0.8569
Interior Repair Plaster	0.1143	0.6393	-0.0671	0.5487
Exterior Mud Plaster	0.1760	0.9843	-0.1209	0.9886
Exterior Plaster	0.1660	0.9284	-0.1119	0.9150
Sound Timber	0.1788	1.0000	-0.1223	1.0000

## 6.2 In-situ Analyses by UPV and QIRT

QIRT analyses together with another non-destructive method namely UPV were used for the soundness assessment of the timber and its relationship with its neighbouring materials.

### 6.2.1 Direct and Indirect Velocity Measurements on Timber Elements

“In Aslanhane Camii, measurements were done in the direct transmission mode passing through the cross section of the timber columns, using with 54 kHz transducers to produce ultrasonic velocity data of the timber columns, K1, K2, K3, K5, and K7 (Figure 6.25). Each column was examined in east–west and north–south cross sections, directions and taking measurements at five different levels along the height of the columns with 30 cm intervals” (Kandemir *et al.*, 2007) .

“The diameter of each column decreased with height representing the whole tree. During the survey, the boundary conditions were  $14.73^{\circ}\text{C}\pm 1.00^{\circ}\text{C}$  and  $25.50\%\text{RH}\pm 0.70$  in ground floor. The timber columns were dry according to protimeter readings” (Kandemir *et al.*, 2007).

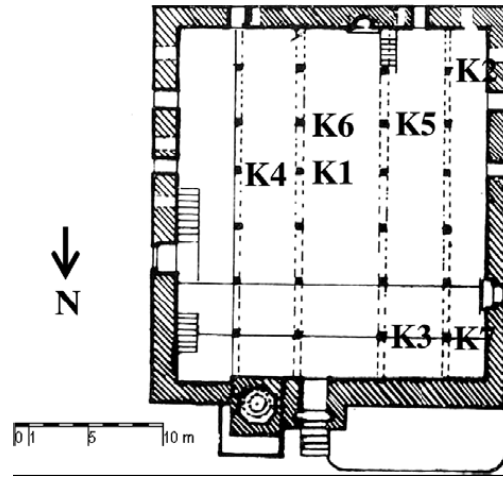
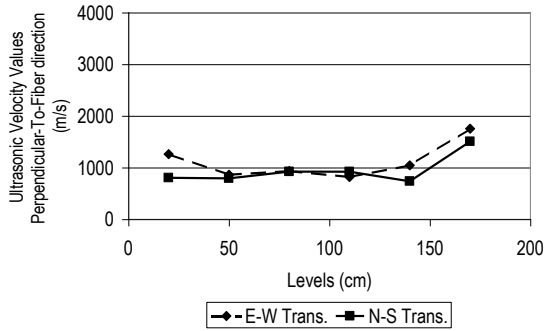


Figure 6.25 Plan of Aslanhane Mosque showing the columns investigated by UPV (Vakıflar Genel Müdürlüğü, 1983)

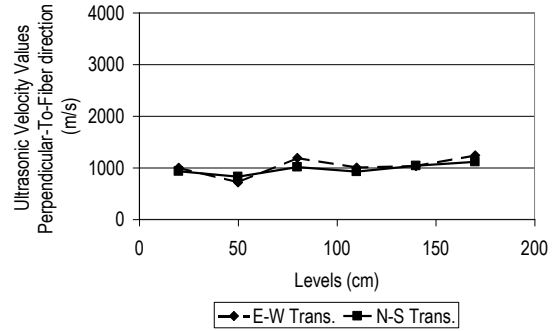
“The ultrasonic velocity values taken from the timber columns were in the range of 706 to 1753 m/s in perpendicular-to-fiber direction (Figure 6.26). Ultrasonic velocities were lower at the upper parts of the columns. That might be due to the characteristics of the relatively younger upper part of the tree trunk (see Figure 6.26, the column K7). Inconsistency of the ultrasonic velocity values of the column K3 must be due to the previous repairs on that column which were visible” (Kandemir *et al.*, 2007).

“The average ultrasonic velocities of sound laboratory timber samples perpendicular-to-fiber direction were 1040 m/s at 56% RH (Figure 6.3). In literature, the ultrasonic velocity values for sound timber were given in the range of 1000 to 2000 m/s (Beal,2002; Bray,1992). Considering those data and data

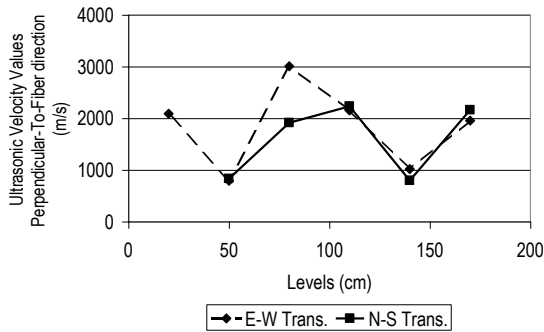
obtained in laboratory, it was concluded that timber columns were sound” (Kandemir *et al.*, 2007).



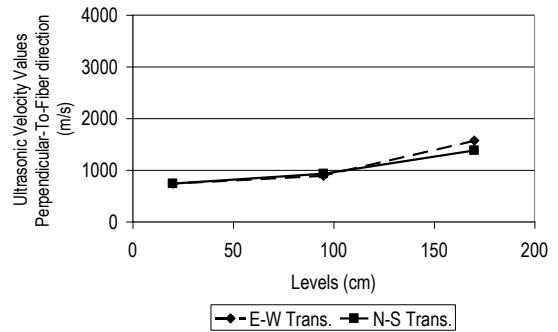
**Timber Pillar K1**



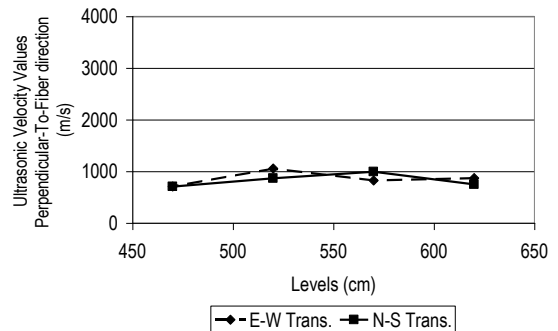
**Timber Pillar K2**



**Timber Pillar K3**



**Timber Pillar K5**



**Timber Pillar K7**

Figure 6.26 The ultrasonic velocity values taken at different levels along the height of timber columns in Aslanhane Camii, K1, K2, K3, K5 and K7 (Kandemir *et al.*, 2007).

In İstiklal House, indirect and direct UPV measurements were taken on the timber elements such as posts and beams by using 220 kHz transducers. In Figure 6.27, it can be seen how direct and indirect UPV measurements were taken. M1, M2, M3, M4 and M5 were indirect measurements on the timber beams. M6, M7 measurements were indirect measurements on the post. M7-b, M8, M9, M10 were the direct measurements on the post passing through the cross section (Figure 6.28). The points of indirect and direct measurements were indicated in blue and red colours respectively in Figure 6.28.

Indirect UPV measurements from some timber posts and beams were given in Figure 6.29. It was observed that indirect ultrasonic velocities of timber elements ( $UPVL_{-INDIRECT}$ ) were in the range of 1176 to 1337 m/s in parallel to fiber direction that was in the longitudinal direction. The structural timber elements, M1, M2 M3, M4 and M6 were sound although some of them visually looked deteriorated. Those values were in acceptable ranges for the sound timber when compared with the reference data obtained in laboratory (see section 6.1.1). In the laboratory studies the indirect ultrasonic velocity values for sound old pine was found to be about 1439 m/s and the modulus of elasticity (MOE) was calculated to be about 13335 MPa. Comparisons with the laboratory data indicated that, timber elements were sound. Partial deteriorations on some parts of timber posts and beams were detected by their decreased ultrasonic velocity values. Deteriorated states of those parts were also observed visually. Those results were also supported with some in-situ  $UPVR_{-DIRECT}$  measurements taken wherever cross arrangements for the transducers could be made. UPV direct measurements perpendicular the fiber direction taken from the M2-beam and M6-post were about 1400- 1660m/s. In literature, the ultrasonic velocity values for sound timber taken perpendicular the fiber direction were given in the range of 1000 to 2000 m/s (Beal, 2002; Bray,1992). It was found that some of the timber elements (M7-post, M5-beam) were deteriorated according to their lower UPV values when

compared with the laboratory results ( $UPV_{L-INDIRECT}$ ). Those indirect velocity values were in the range of 493 m/s to 727 m/s in parallel to fiber direction.

In Figure 6.30 the graph shows the transit time curve versus distance for a number of timber elements. Their slopes have differed due to their state of deterioration. Sharp increase in transit time showed the deterioration such as crack, fiberization, knot etc. The increase in transit time of M2-beam after point 7 showed the presence of deep crack(s) through the knot. M7-post was observed fairly deteriorated. Indirect measurements and direct UPV measurements taken on site from M7-post were in good relationship. The direct measurements taken from M7-post were not available due to its severely deteriorated condition and sharp increase in transit time showed the presence of deeper crack. The M4-beam and M5-beam were observed to be partially deteriorated due to the decrease in indirect velocity measurements parallel to the fiber direction from 1911 m/s to 1047 m/s in deteriorated parts. The sharp increase in transit time signaled the deteriorated part (see Figure 6.30). Higher indirect UPV measurements were obtained at first readings when the transducers were closer to each other when compared with the indirect velocities obtained from reference samples at laboratory. This could be probably due to the surface deposits on historic timber surfaces. When the transducers were far apart, the transit time readings represented the deeper parts of timber elements and those values were comparable with the indirect velocities of laboratory sound timber samples.



Figure 6.27 Indirect UPV measurements (left) from the beam and direct UPV measurements (right) from the post at İstiklal House.

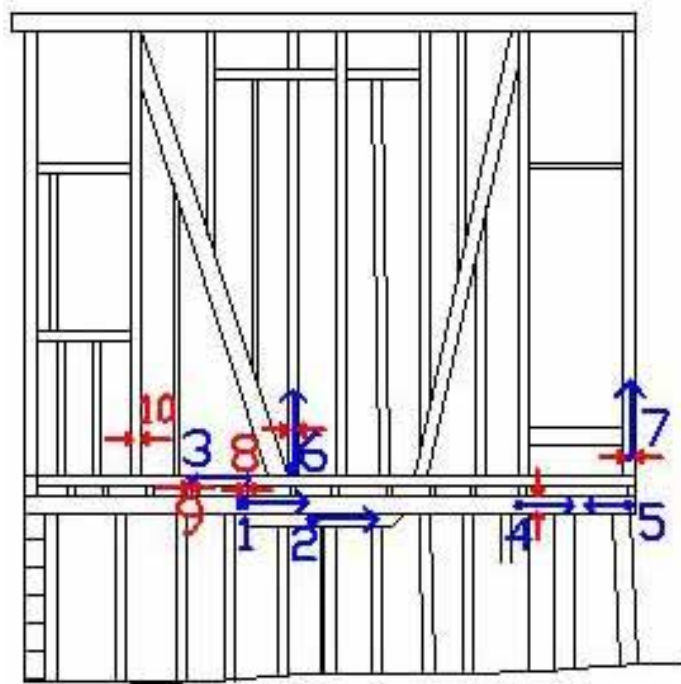


Figure 6.28 Location of UPV measurements taken from İstiklal house, the red lines show the direct measurements and the blue ones show the indirect measurements which were taken from the timber elements.

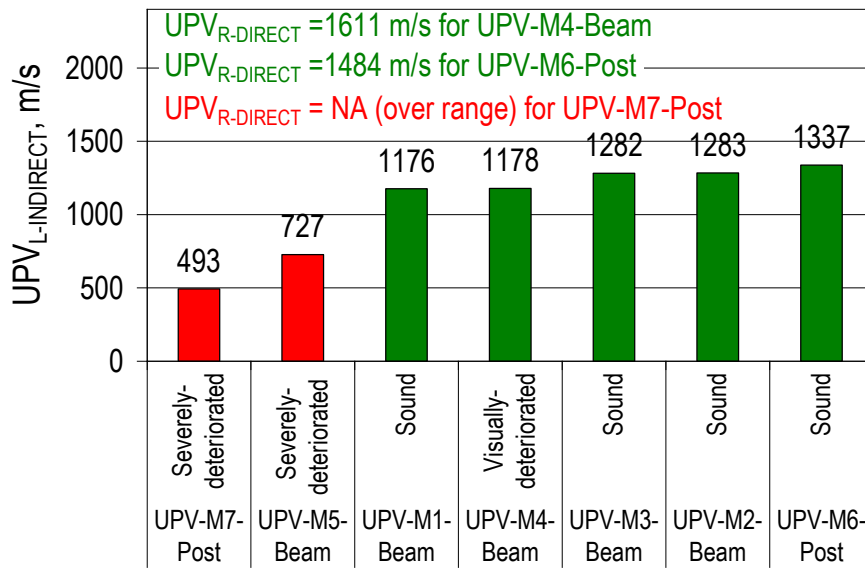


Figure 6.29 Indirect UPV measurements parallel to fiber direction. UPV<sub>L-INDIRECT</sub> (IN-SITU) = 1176 - 1337m/s for the sound timbers, UPV<sub>L-INDIRECT</sub> (IN-SITU) = 493 - 727m/s for the deteriorated timbers.

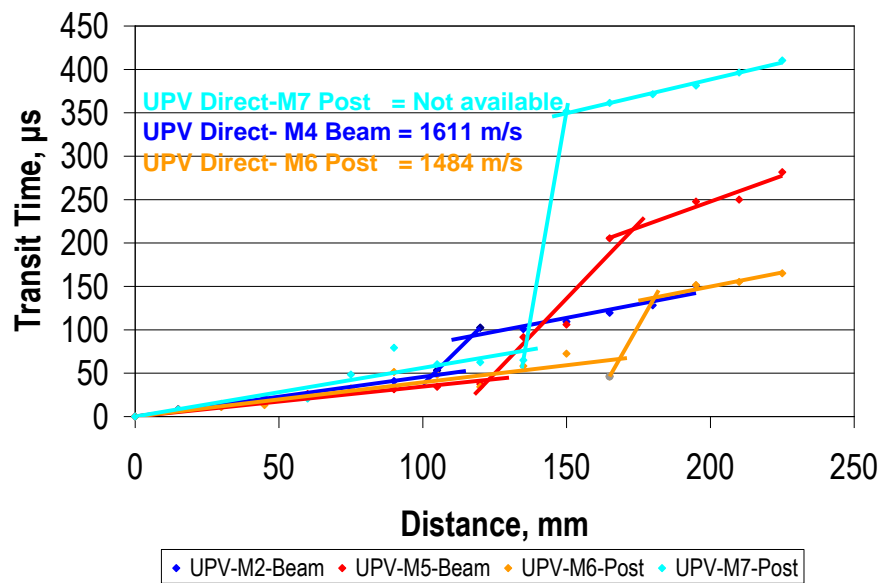


Figure 6.30 The lines of transit time versus distance showing in-situ indirect UPV measurements from the timber structural elements

Third historic structure to be investigated by UPV measurements was Ayaş House. It was experienced that in-situ UPV measurements, taken from the timber elements and plastered wall surfaces were badly-affected from the outside noisy environment especially the traffic. Therefore reliable measurements could not be taken in that structure.

### **6.2.2 In-situ QIRT Analyses on Timber Elements**

In-situ QIRT analyses were performed in three historic structures namely Aslanhane Camii, Istiklal House and Ayaş House. Results of those analyses were described below.

“The IR images were taken from the interior and exterior surfaces of the walls, the timber ceiling, floors and timber pillars of Aslanhane Camii twice a day, once in the morning and once at night in winter. Target surfaces mainly consisted of stone masonry walls, oil painted timber pillars, unpainted timber ceiling, plastered and oil painted walls” (Kandemir *et al.*, 2007).

In the IR images shown in Figures 6.31 and 6.32, stone masonry façade with its timber lintels and bond beams were observed with its damp zones. The boundary conditions for those images were 1.5 °C and 29% RH. “In the IR images, timber elements were found to be warmer than the stone masonry nearby. Damp areas indicated the cement mortars introduced in the masonry during recent repairs. It was seen that the timber elements were affected from those damp areas produced by cement mortars. The temperature variations on the surface of timber lintel in Figure 6.32 was found to be reaching 5.5°C showing the considerable moisture content variations in timber. It indicated that the timbers suffered from the dampness problems” (Kandemir *et al.*, 2007).



Figure 6.31 “View of the west façade of the building (left); IR image taken after sunset (right) showing that stone masonry façade with its timber lintels and bond beams had damp zones. Timber elements were warmer than stone masonry, but they had damp zones due to damp cement mortar repairs” (Kandemir *et al.*, 2007)

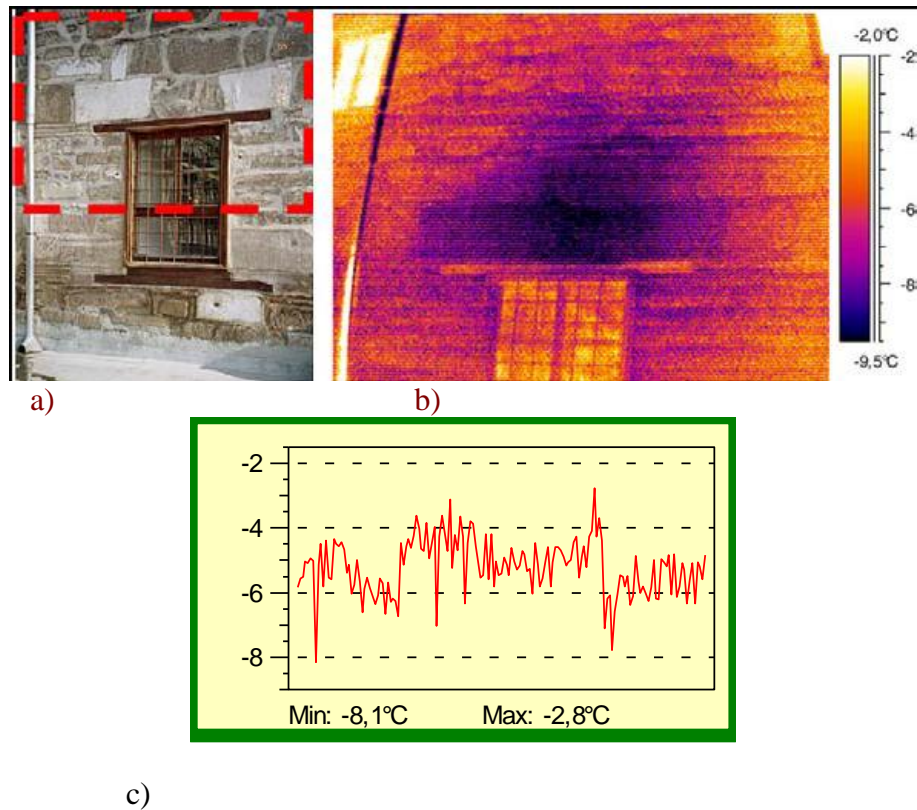


Figure 6.32 a)View of a window from the west facade of the building with timber lintel at its top b) IR image of the selected region, taken in day time c) Line temperature analysis of the timber lintel showing 5.5 °C surface temperature difference due to close relationship with wet cement neighbouring materials (Kandemir *et al.*, 2007)

“IR images were also taken from the timber columns to evaluate their conditions. Those images were analyzed together with UPV measurements from the columns. During the site survey, boundary conditions were  $14.5^{\circ}\text{C}\pm 0.1$  and 29%RH. The consistent ultrasonic velocity values for the column K2 with an average of 1000 m/s was also supported by its infrared images with an even temperature distribution with a difference of  $2^{\circ}\text{C}$ ” (Figure 6.33) (Kandemir *et al.*, 2007).

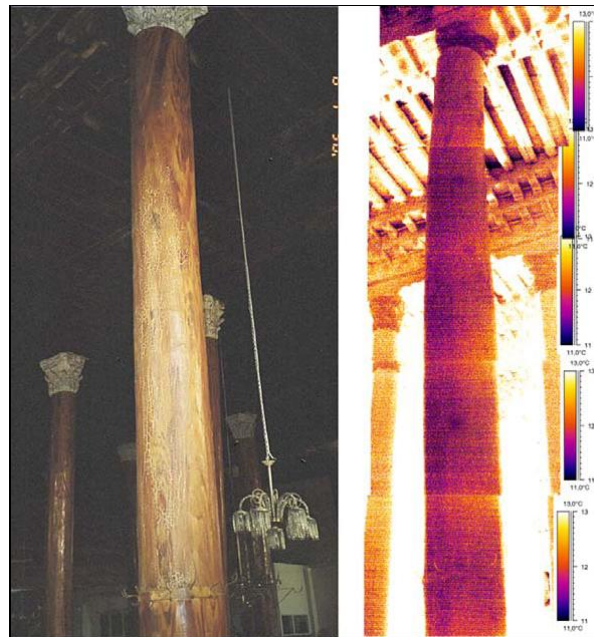


Figure 6.33 The view of the pillar K2 (left) and its IR image (right) showing an even temperature distribution on its surfaces with a difference of  $2^{\circ}\text{C}$  (Kandemir *et al.*, 2007).

“The timber elements at the ceiling exhibited temperature differences in IR images (Figure 6.34). Their boundary conditions were  $13.7^{\circ}\text{C}$  and 28 % RH. The images were processed to show the temperature distribution on timber elements. They exhibited around  $3^{\circ}\text{C}$  differences in temperature. The ones in further contact with the roof structure were about  $2^{\circ}\text{C}$  cooler than the ones closer inside. The slightly cooler timber elements did not necessarily indicate higher moisture content than the others. On the other hand, the coolest patch in the middle of IR image with  $4^{\circ}\text{C}$  difference showed a damp zone. It indicated a rain penetration

problem that had to be eliminated. The damp zones at the eaves level were also detected at the east wall of the building showing the existence of roof drainage faults. The timber lintels and bond beams in stone masonry were suffering from damp conditions at upper parts of the building due to roof drainage faults” (Figure 6.35) (Kandemir *et al.*, 2007).

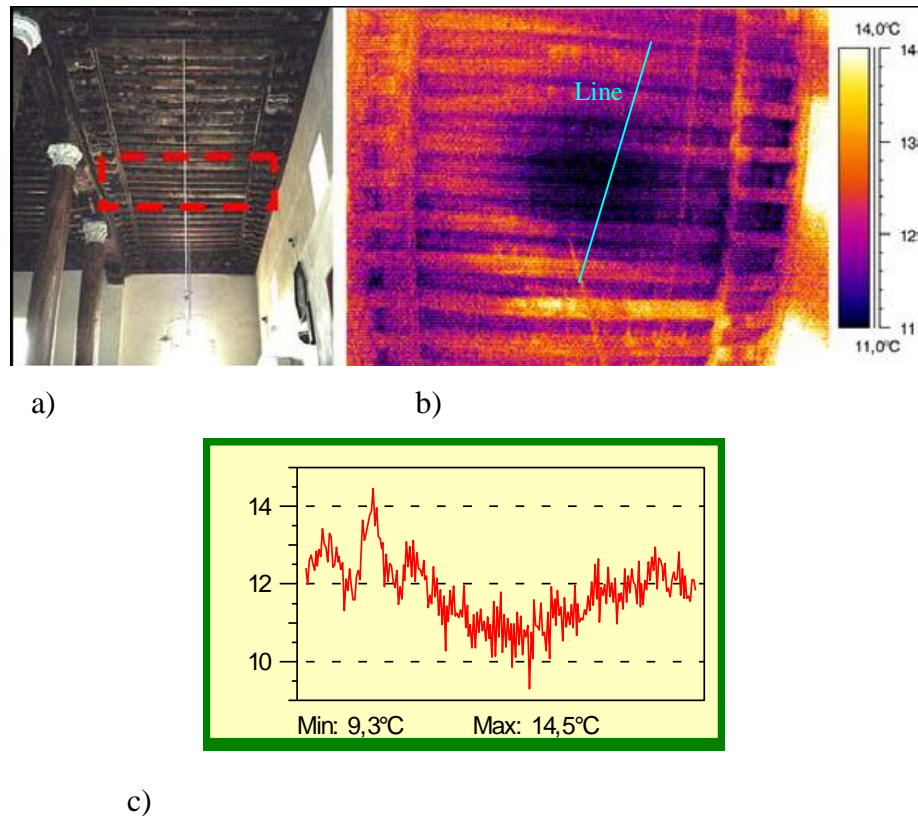


Figure 6.34 a) View of the timber ceiling b)IR image of the selected region showing the damp areas at ceiling c) The line analyses graph of timber ceiling

“Single IR image taken from the oil painted east wall of the Aslanhane Mosque showed that the surface temperature of the wall differed from 10.8 °C to 15.6 °C along with its height. The low temperatures in the lower parts were due to the entrapped moisture sourced from the recent incompatible repairs in those parts undertaken with the cement-based plaster and oil-based paints” (Figure 6.36) (Kandemir *et al.*, 2007).

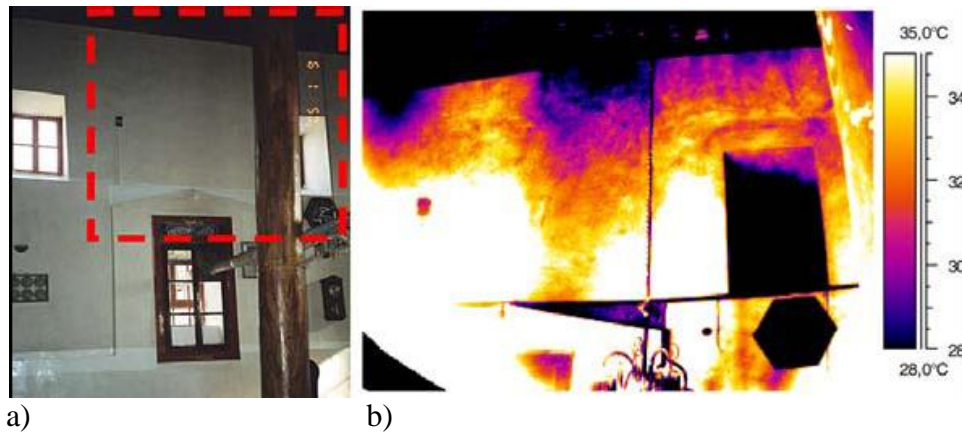


Figure 6.35 a) View of the interiors surfaces of the east wall b) IR image of the wall at the selected region showing the damp areas sourced from the faults in roof drainage.

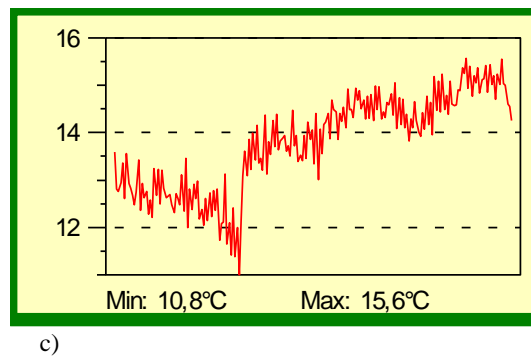
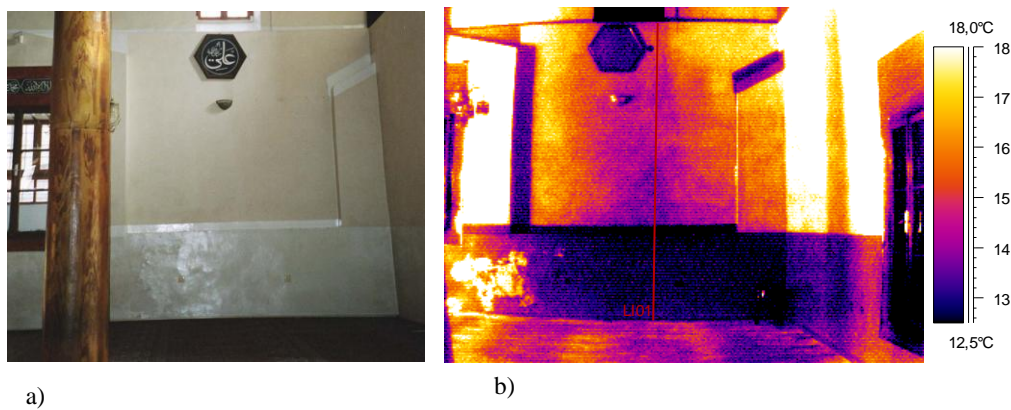


Figure 6.36 a) View of east interior wall of Aslanhane Mosque b) IR image of east interior wall c) The graph of the line analyses on IR images from the east wall

“Some IR images were taken while the stove was in function in winter. At the column K1, which was the closest one to the stove, the line analysis along its

periphery at +1.10 m height showed that there existed 39.3 °C temperature difference on its surfaces during an hour of heating with the stove (Figure 6.37). The crack was detected as the hottest traces. A similar temperature variation of 27.8 °C was also detected at column K2, which was far away from the stove (Figure 6.38). At the lower levels where timber columns were exposed to the stove heating, cracks were visually observed and they were detected as the hottest traces in IR images (Figures 6.39 and 6.40). The faults on timber surfaces, such as knots as the coldest patches and cracks as the hottest patches or traces, were easily detected by IRT (Figure 6.38). Timber pillars close to the stove must have suffered from extreme thermal expansion and contraction movements for several times” (Kandemir *et al.*, 2007).

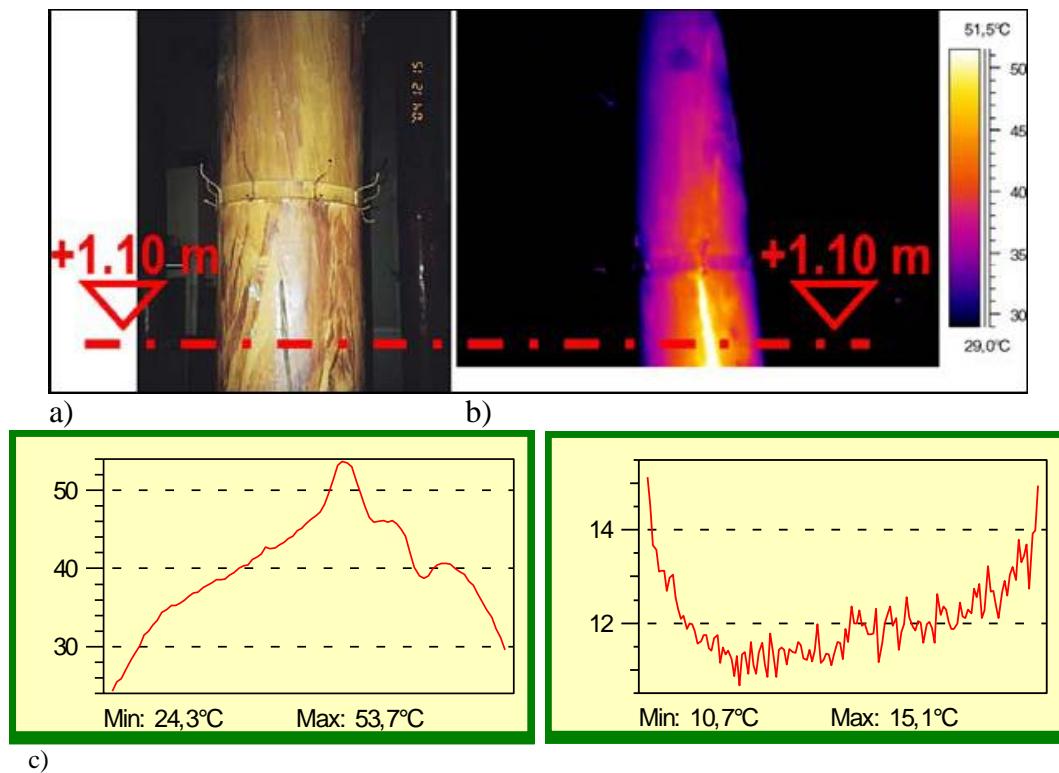


Figure 6.37 a) The view of Pillar K1 b) Its IR image showing that during an hour of heating with the stove there existed 39.3 °C temperature difference on the surfaces along the periphery of the pillar at +1.10 m height, and cracks were also detected as the hottest traces c) Line analysis of IR images of pillar K1 taken from the surfaces facing the stove (left) and at the back of the stove.



Figure 6.38 The view of Pillar K2 (left) and its IR image (right) showing that there was a temperature variation of  $27.8^{\circ}\text{C}$  which was similar to the temperature variations observed at the Pillar K1, and knots and cracks were easily detected as the coldest patches and the hottest patches/traces, respectively (Kandemir *et al.*, 2007).

In Aslanhane Mosque, IR images were also taken from the west façade in day time and at night. The differential analyses of day and night IR images showed that the timber elements cooled down faster than the stone masonry in the cooling period of 34983 seconds (Figure 6.39). The differential temperature was calculated to be  $-6.97^{\circ}\text{C}$  for timber elements while being  $-3.87^{\circ}\text{C}$  for stone masonry.

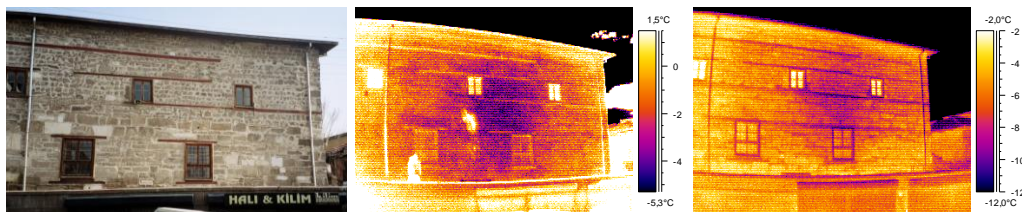


Figure 6.39 Partial view from the west façade of Aslanhane Camii and its IR images taken in December in daytime and at night, having the outside conditions of  $1.5^{\circ}\text{C}$  and 29%RH and  $-0.7^{\circ}\text{C}$  and 31%RH, respectively.

Sequential IR analyses were done in timber elements and mud brick of İstiklal house. The comparison of differential IR images and QIRT analyses were done in several parts of the structure. The surfaces with knots, severely deteriorated, partially deteriorated and sound areas were analyzed both by differential IR images and by drawing their cooling lines as temperature versus square root of time. Cooling lines were also obtained for the mud brick in the same area and compared with timber ones. The rates of cooling for timber surfaces and mud brick infill were compared and the ratios of cooling rates with respect to sound timber were also compared.

The surface of the wall section was heated by hair dryer then monitored by the sequential IR imaging during the cooling period of 603 seconds at the ambient conditions of 25.1°C and 33%RH (Figure 6.40.a,b,c). Differential IR image of sound post and sound mud brick infill showed even temperature distribution. However deteriorated ones showed heterogeneous temperature distribution (Figure 6.40.c). Differential IR image has also showed that deteriorated timber post cooled down faster than the sound one indicated by its colder temperature.

The sequential IR images of severely-deteriorated timber post (M7-Post) were taken at the ambient conditions of 25.5°C and 33%RH after been heated uniformly with hair dryer for one minute. The differential IR image showed the temperature difference between the initial and the last IR images of the cooling period of 476 seconds (Figure 6.41.a,b,c). Almost same ambient conditions with the previous sequential IR imaging in the structure, enabled their combined analyses (Figure 6.40.c, Figure 6.41.c) In the differential IR images, the partial deterioration of the timber elements was discovered. In Figure 6.41, severely deteriorated part of the post could be easily detected.

The results of QIRT analyses were shown in Figures 6.44-6.46 Table 6.8 and 6.9. It was seen that the deteriorated timber cooled down faster than the sound timber

while the cooling down rate was the fastest for the severely-deteriorated timber. Analyses of the surfaces with knots showed that knot surfaces cooled down slowly in comparison to the other parts of the timber surfaces (Figure 6.42).

QIRT analyses have shown that the surfaces of deteriorated timber post/beam cooled down 1.55 times faster than the sound old post/beam surfaces. (see Table 6.8 and Figure 6.43 ). Cooling rate ratio of severely deteriorated post in comparison to sound post/beam was found to be 2.48 (see tables 6.8 and Figure 6.43). However, cooling rate ratio of knot surface to sound post/beam surface without knot was 0.76 (see Table 6.8). That must have been due to the higher specific gravity of knot area.

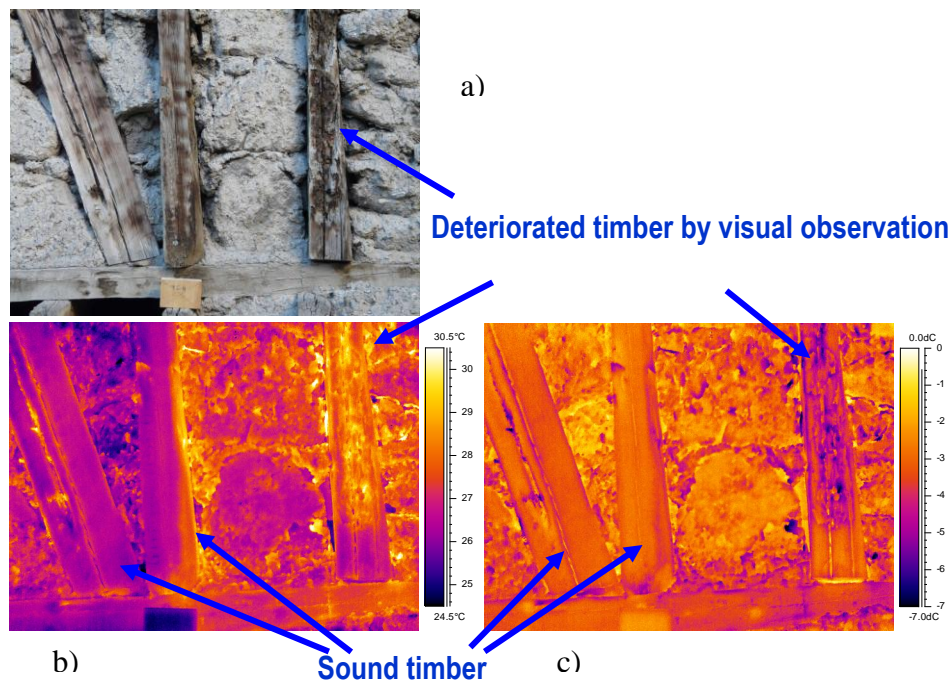


Figure 6.40 a) View of the wall section from Ayaş House b) The surface of the wall section was heated by hair dryer then monitored by the sequential IR imaging during the cooling period, first sequential image taken at the ambient conditions of 25.1°C and 33%RH c) The differential IR image showing the temperature difference between the initial and the last IR images of the cooling period of 603 seconds.

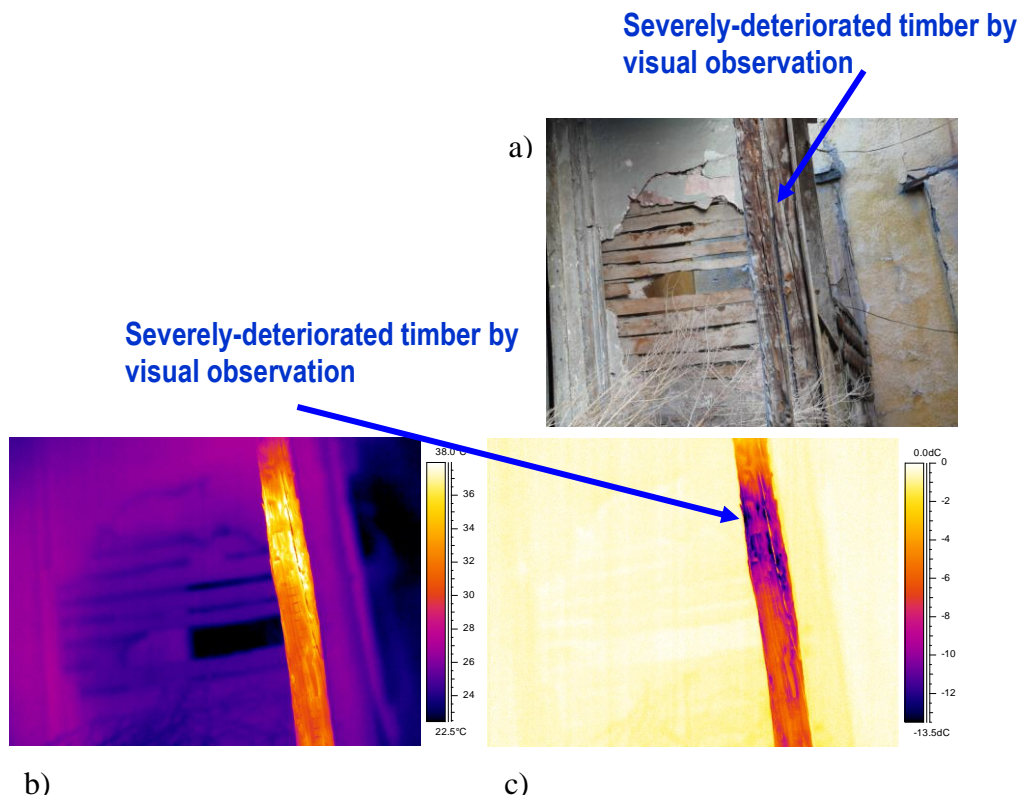


Figure 6.41 a) Partial view of the severely-deteriorated timber post (M7-Post) at Istiklal House b) The IR image of the timber taken at the ambient conditions of 25.5°C and 33%RH after heated uniformly with hair dryer for one minute c) The differential IR image showing the temperature difference between the initial and the last IR images of the cooling period of 476s.

The cooling rate ratio of knot surfaces to sound pine was found to be 0.70 at laboratory analyses (Table 6.5). That result was similar to in-situ value which was 0.76. The surface of deteriorated timber has cooled down in the range of 1.21-1.70 times faster than the sound timber surface in laboratory conditions (see Table 6.4 and 6.6). However in-situ cooling rate ratio of deteriorated post surfaces to sound ones was in the range of 1.55-2.48 (Table 6.8). That result showed that deteriorated timber elements of İstiklal house were more deteriorated than the deteriorated laboratory samples.

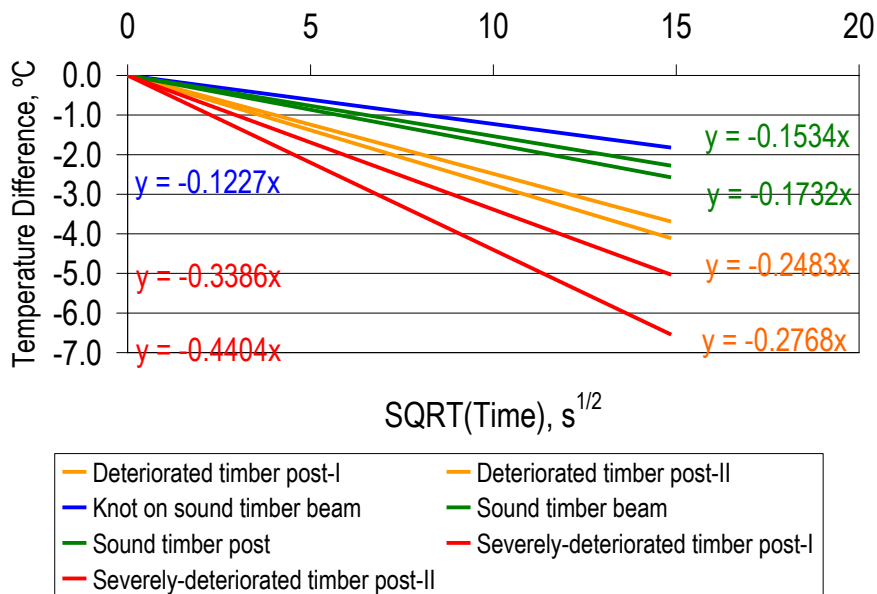
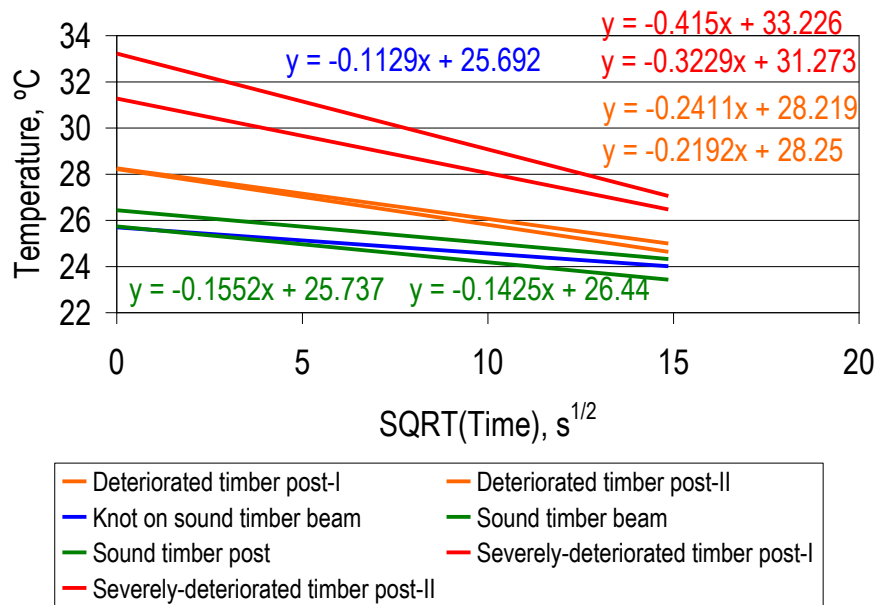


Figure 6.42 After the heating of the wall section of İstiklal House with hair dryer, and the temperature lines versus square root of time and the differential temperature lines versus square root of time for timber elements during cooling period of about 225s

Table 6.8 Rate of cooling of timber beam and posts and their ratios to sound timber beam and posts

Definition	$R_C$	$R_{C-DET}$
		$R_{C-SOUND}$
IN-SITU		
Knot on the beam	-0.1129	0.7585
Deteriorated timber post by visual observation	-0.2302	1.5462
Severely-deteriorated timber post by visual observation	-0.3690	2.4787
Sound timber beam/post	-0.1486	1

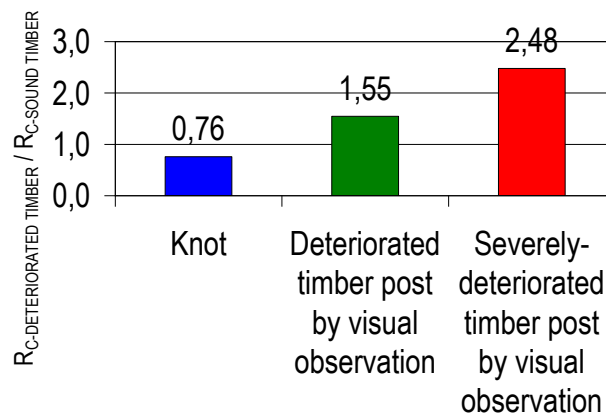


Figure 6.43 Rate of cooling down of deteriorated timber elements to rate of cooling down of sound elements.

QIRT analyses showed that sound timber elements and mud brick infill were cooled down at almost the same rate (Figure 6.42).

In Figure 6.40.a the results of QIRT analyses on surfaces of the deteriorated timber posts, sound timber posts, deteriorated mud brick infill, and mud brick infill with scale were shown. The sound mud brick (MoistureContent,  $\Theta = 12.5\%$

$\pm 0.3$ ) presented similar rate of cooling down with the sound timber ( $\Theta = 8.5 \pm 0.7$ ) at the same boundary conditions of 25.5°C and 33%RH after homogeneous heating up process with hair drier. That signaled that sound timber and neighbouring mud brick infill had similar cooling down properties while deteriorated timber presented noticeably faster cooling down than sound and deteriorated mud brick (Figure 6.44). The cooling rate ratio of sound mud brick infill to sound beam was 0.94 (see table 6.9). In the laboratory, the cooling rate ratio of sound mud brick infill to sound pine samples was 0.86. At laboratory, for the exterior mud plaster, that ratio was 0.99. For the exterior lime plaster the ratio was 0.91 (see Table 6.7). Those in-situ and laboratory results were compatible with each other. The differences in rate ratios between the in-situ mud brick infill and laboratory mud brick infill indicated that laboratory mud brick infill sample was more sound than the visually sound mud brick infill in İstiklal house.

At timber framed traditional Ayaş House differential IR images were taken from the interior wall surfaces and main façades. QIRT analyses were done for daily heating and cooling periods of structure.

In the single IR image of Ayaş House from an interior wall surface, the timber frame structure hidden behind the historic plaster layers was easily detected with warmer and evenly-distributed surface temperatures in the range of  $7.8^{\circ}\text{C} \pm 0.1^{\circ}\text{C}$  pattern (Figure 6.45). The width of timber elements could also be clearly observed.

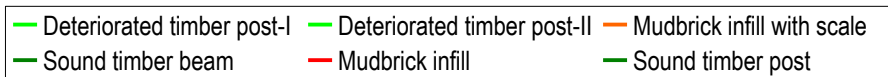
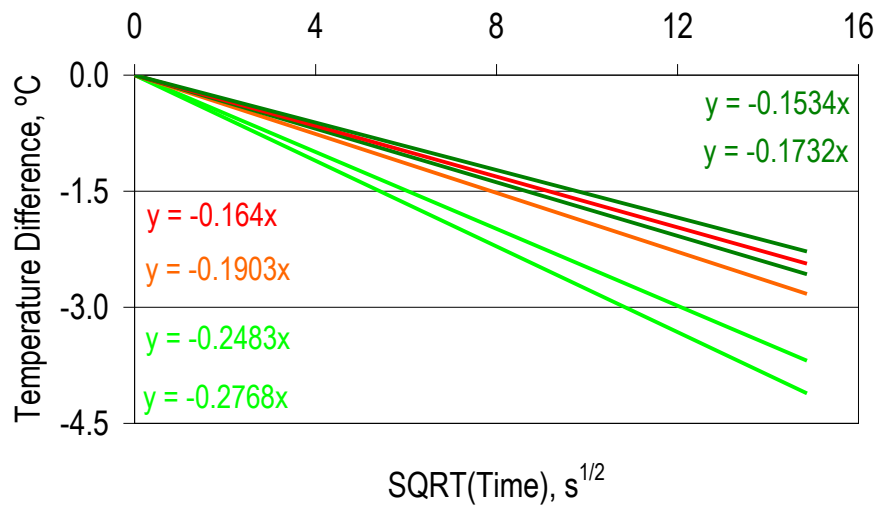
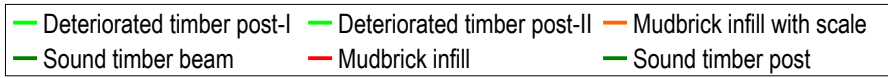
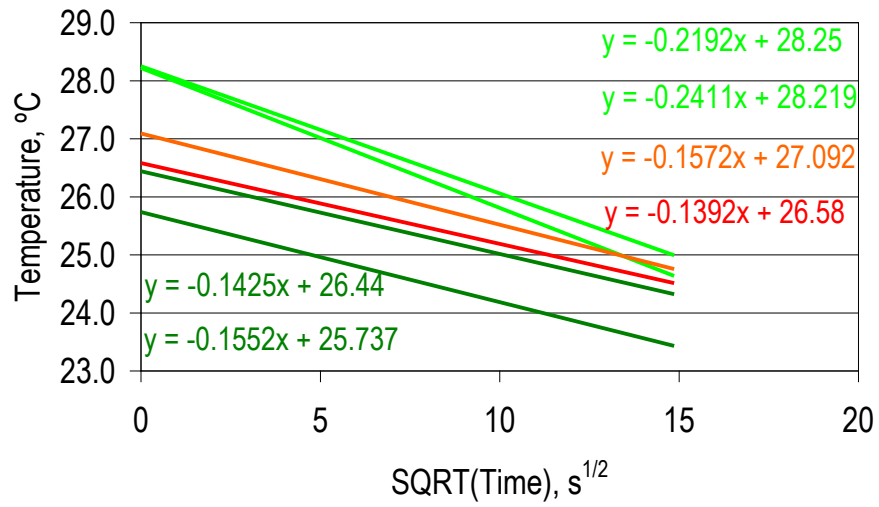


Figure 6.44 After the heating of the wall section of İstiklal House with hair dryer, and the temperature lines versus square root of time and the differential temperature lines versus square root of time for mudbrick infill and timber elements (at bottom) during cooling period of about 225s

Table 6.9 Rate of cooling of timber post/ beam, mudbrick infill and their ratios to sound timber post/beam

Definition	$R_C$ - Rate of cooling down $T/\sqrt{s}$	$\frac{R_C}{R_{C\text{-Sound Timber}}}$
IN-SITU		
Sound mudbrick	-0.1392	0.9350
Mudbrick with scale	-0.1572	1.0577
Deteriorated timber post	-0.2302	1.5460
Sound timber beam/post	-0.1489	1

In the differential IR image of the same area, the analysis of surface temperature versus time during the slightly cooling and slightly heating periods in daytime showed that the plaster surfaces covering timber and infill surfaces presented similar cooling-down and heating up rates, in other words, they responded in the same way the exposed ambient conditions (Figures 6.46, 6.47). The constant and similar rate of heating on wall surfaces indicated that there was no evaporative cooling on wall surfaces during the progressive heating of daytime, while the surface temperatures were slightly below the ambient temperature. This meant that, the wall area examined was almost dry and in equilibrium with the exposed humidity condition of 49%RH. The in-situ moisture content measurements taken from the plaster covering timber surfaces proved that its moisture content was in the range of 7.9%±1.1%, which was the characteristic wood moisture content at 40%±5%RH (Knut, 1999).

Plaster surfaces, behind which timber and mud brick infill were placed, showed similar rates of cooling down indicating similar behavior of plaster layer on timber or mud brick infill to the environmental changes of temperature and humidity (Table 6.10).

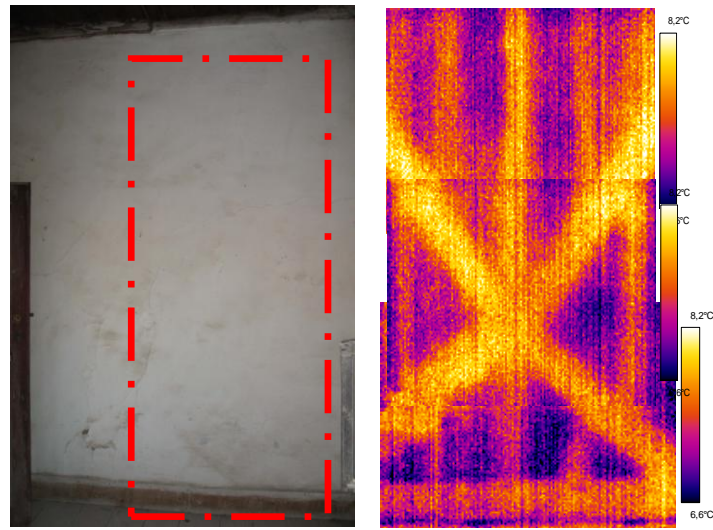


Figure 6.45 View of the interior wall at Ayaş House and the IR image of the selected region in November in daytime; showing that the timber frame structure underneath the historic plaster layers were clearly detected in IR images with a warmer and even surface temperature distribution ( $7.8^{\circ}\text{C}\pm 0.1^{\circ}\text{C}$ ).

The thermal behavior of the exposed timber and infill materials, when they were not covered with protective historic plasters, was different than that of plaster-covered ones.

Single IR analyses of facades in Ayaş House were done during the heating up period of the exposed building surfaces in daytime (under the exposure of solar radiation) (Figure 6.48). The timber elements, brick and mud mortar infill of the wall structure could be individually observed at single IR images due to their different optical and thermo-physical properties. The timber elements had the warmest surfaces while the mud mortar infill was warmer than the fired-brick infill (Figure 6.48). Those timber elements with surface temperatures in the range of  $32.2^{\circ}\text{C} \pm 1.7^{\circ}\text{C}$ , had the quite heterogeneous surface temperature distribution while the plaster surfaces covering timber had even distribution at the interiors (Figure 6.45). That behavior signaled a probable weathered state of exposed timber elements or heterogeneous exposure of facades to sun.

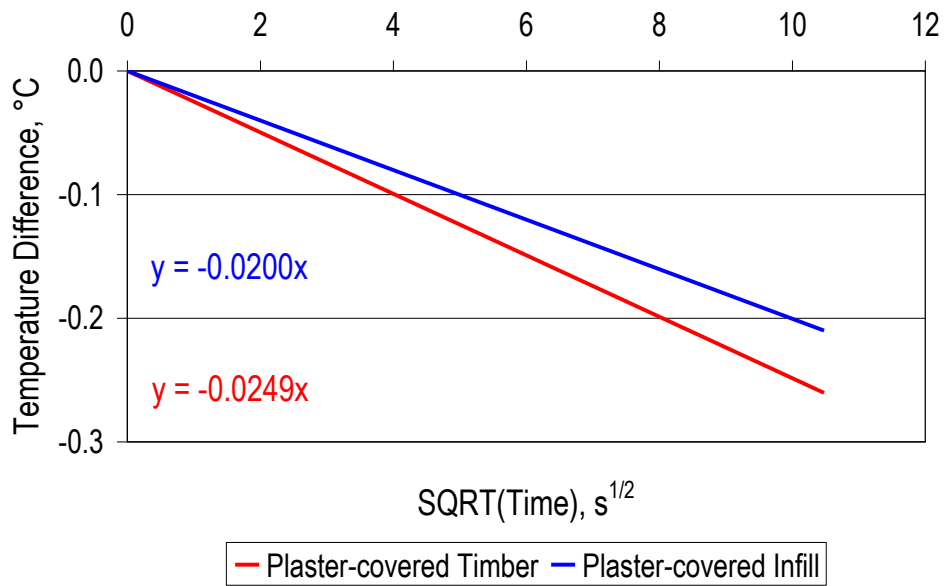
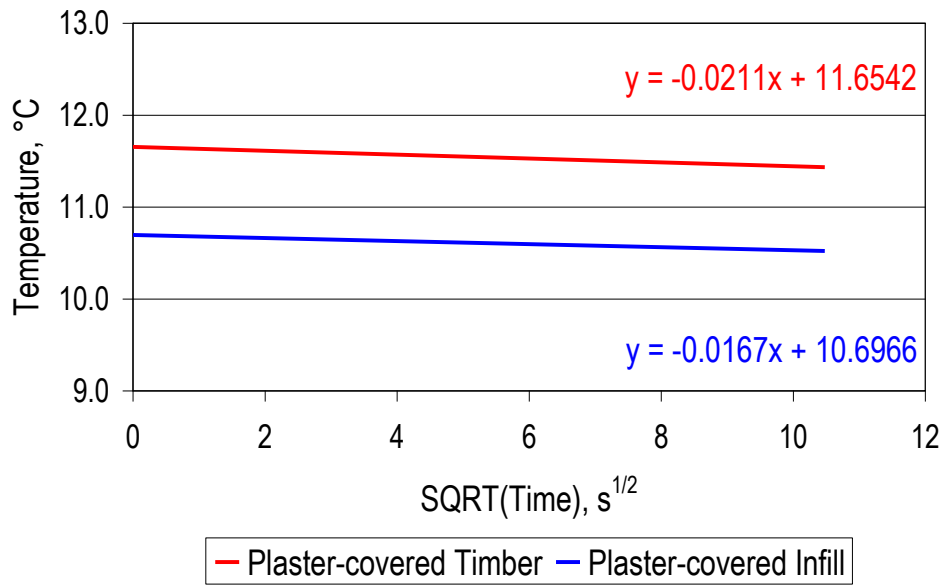


Figure 6.46 The surface temperature lines versus square root of time and temperature differences lines versus square root of time for the slightly cooling periods of daytime at the interior wall surface of Ayaş House.

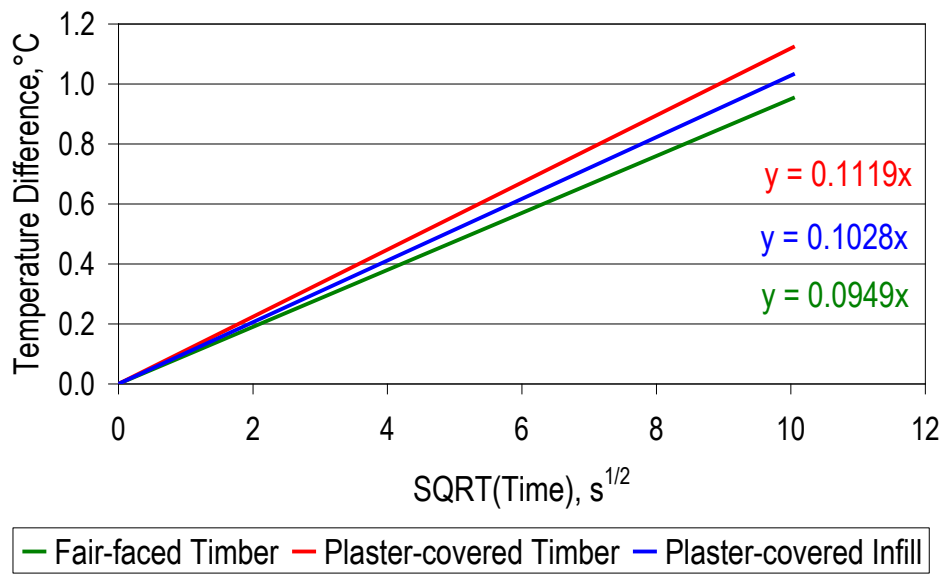
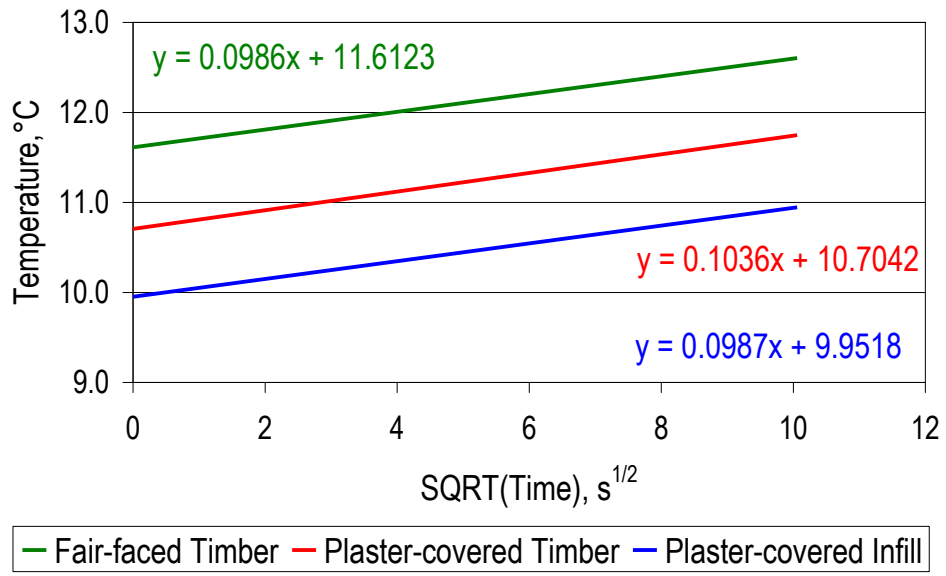


Figure 6.47 The surface temperature lines versus square root of time and temperature differences lines versus square root of time for the slightly heating periods of daytime at the interior wall surface of Ayaş House.

Table 6.10 The thermal behavior of interior plaster layer covering the timber frame structure

Definition	$R_W$ - Rate of heating up $\Delta T/\sqrt{s}$	$R_{W-PL.COV}$ ————— $R_{W-TIMBER}$
IN-SITU		
Plaster-cov. timber	0.1036	<b>1.050</b>
Plaster-cov. infill	0.0987	<b>1.001</b>
Fair-faced timber	0.0986	1

Differential IR analyses during the cooling period of night has shown that the exposed timber elements cooled down faster than the exposed brick and mud mortar infill being 1.65 times faster (Figure 6.49, Table 6.11). That should be due to their different thermal inertia characteristics and moisture content as well as their state of deterioration.

The timber and infill surfaces kept behind the protective historic plaster layers showed similar cooling rate behavior because of protective action of plaster layer (Figure 6.47).

Those in-situ results were compared with previous laboratory results (Table 6.11). It was seen that the ratio of cooling rate for fired brick with reference to sound timber was the same in laboratory samples. Laboratory samples were considered to be quite sound since they were compared with a sound timber sample. On the other hand, that comparison could not be made for the materials of Ayaş House façade. Structural timber elements of the Ayaş House façade were found to have similar cooling rate behavior. If the cooling rate of structural timber at the façade was taken as reference, brick and mud mortar of the façade could be found to be sound. However that conclusion could not be made, since the soundness ratio was not derived with reference to a sound timber at the same conditions (Table 6.11).

Single IR image taken from another Ayaş House has shown an advanced dampness problem and signaled the danger for the structural timber elements behind the cement plaster (Figure 6.50).

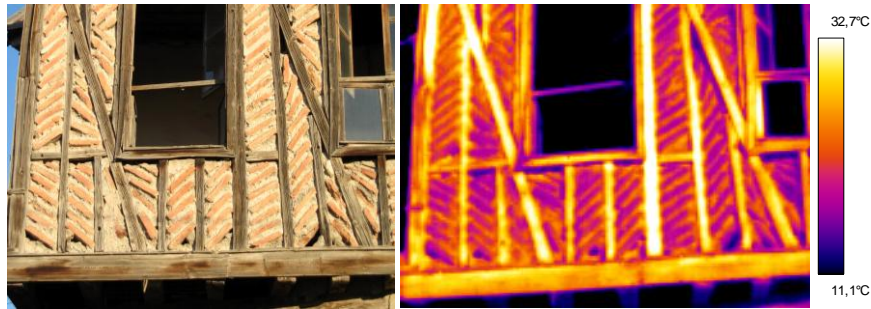


Figure 6.48 Partial view from the west side of the Ayaş House (at the left) and its IR image (at the right) taken in November under the exposure of solar radiation when the outside temperature was 12.2°C and 42%RH, showing that the brick infill had the coldest surface temperature of 21.9°C±0.1°C, the brick mortar had the warmer surface temperature of 25.2°C±0.5°C and the timber elements had the warmest surface temperature of 32.2°C ±1.7°C.

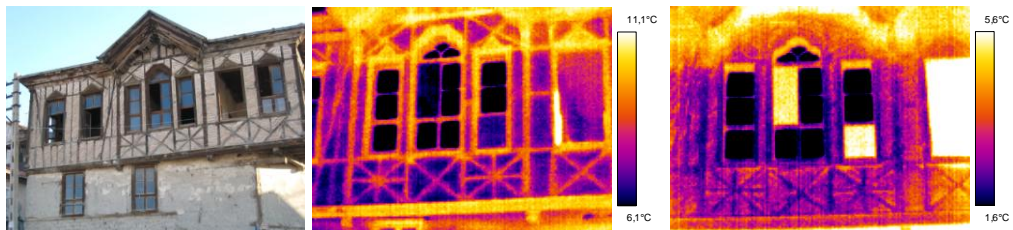


Figure 6.49 Partial view from the north façade of the Ayaş House and its IR images taken in November in daytime and at night, having the outside conditions of 13.0°C and 39%RH and 7.4°C and 62%RH, respectively. The analyses showed that the timber elements cooled down faster than the brick and mudmortar infill during the cooling period of 9977s. The differential temperature was calculated to be -6.03°C for timber elements while being -3.64°C for brick and mudmortar.

Table 6.11 The rate of cooling down, RC, for the laboratory samples (fired repair-brick, fired brick and sound pines), and for the in-situ brick and mortar infill and structural timber of Ayaş House façade.

Definition	RC - Rate of cooling down $\Delta T/\sqrt{s}$	$R_{C-BRICK}$
		$\frac{-}{R_{c-TIMBER}}$
LABORATORY		
Fired brick-repair (see Table 6.2)	-0.0853	0.6717
Sound Pine (ref) (see Table 6.2)	-0.1270	1
Fired brick (see Table 6.6)	-0.0756	0.5865
Sound pine (see Table 6.6)	-0.1289	1
IN-SITU		
Brick+mortar infill	-0.0364	0.6037
Structural timber on the façade	-0.0603	1

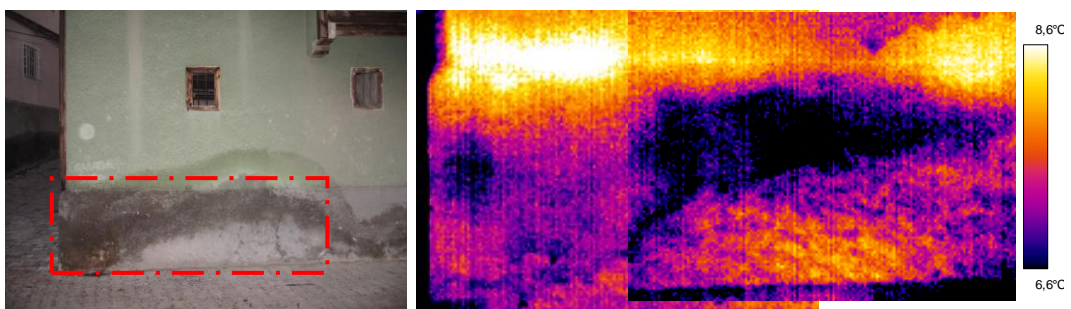


Figure 6.50 At Ayaş House, exterior plaster having damp zones, coldest areas with a difference of 3.2 °C below the ambient temperature.

## CHAPTER 7

### DISCUSSION AND CONCLUSION

Experimental results were discussed in the following headlines covering the related studies in literature survey: structural timber in historic buildings, soundness investigation of timber by UPV measurements, soundness investigation by QIRT studies, a proposal for soundness investigation of timber. Finally conclusions were made.

#### 7.1 Structural Timber in Historic Buildings

Timber was used as an important structural and construction element in the historical buildings in Anatolia. In Chapter 2, the types of traditional buildings where the timber was used as structural element were described. In timber framed traditional architecture, timber was used for the main structural elements of the wall construction. Timber was also used as single columns, lintel and tie beams in stone and brick masonry systems of historic structures. In timber framed structures as well as in most of historic masonry buildings, floors, ceilings and roofs were mostly constructed with timber structural elements. Timber was also the main material for window and door construction.

In those buildings, timber was in touch with other building materials. In timber framed houses infill materials were namely mud brick and brick. In addition to that, the *'bağdadi'* technique was used for the construction of timber framed walls. Moreover, the stone was used as an infill material in the East Black Sea

Region. In masonry structures, timber was in touch with stone, mud brick, or brick. The walls were mostly plastered with mud and lime plasters. They were sometimes left without plaster.

In timber framed historic structures, the floors in the ground floor was covered with the pressed earth in the service spaces while the inhabitable spaces were covered with timber panels. Upper floors were constructed by floor girders and covered by timber panels. In some cases, '*bulgurlama*' technique was used for the floor construction especially in the Middle Anatolia. '*Bulgurlama*' was a kind of timber floor technique that was composed of double layer floor girders which was filled with earth in between. Ceilings were usually covered with timber panels or not covered, leaving the timber beams in exposed state.

Structural elements of the roof were made of timber. Ridge or hip roof was the preferred form of roof. The roofs were generally covered with 'over and under' tiles, but there were examples that the timber was used as a roof covering material especially in the Black Sea Region.

The soundness of timber was very much related with its compatibility properties of those neighbouring materials with timber. Therefore, in this study, traditional building materials that were in touch with timber such as mud brick, brick, mud mortar and plaster, lime plaster were also examined together with timber during UPV and QIRT studies.

## **7.2 Soundness Investigation of Timber by UPV Measurements**

In order to use UPV measurements on the soundness investigations of timber it was necessary to study the conditions that affect the UPV measurements. In this study, those major conditions that affect the UPV measurements such as,

equilibrium moisture content, fiber direction, type of timber and its density, degree of deterioration and defects as knots were examined in laboratory conditions and in-situ.

### **7.2.1 Establishing Reference Data by Laboratory Analyses**

Laboratory analyses were carried out on sound and deteriorated timber samples to establish reference data to assess the influence of moisture content, fiber direction, type of timber and its density, degree of deterioration and defects as knots in relation to soundness of timber.

#### *Effect of Moisture Content*

Increase in equilibrium moisture content of timber up to fiber saturation point, where the cell walls were saturated, was known to cause drastic decrease in UPV values. UPV stayed rather constant at higher water contents when cell cavities of timber started to be filled with water and continued to increase up to complete saturation (Sections 3.2 and 4.2.2) (Sakai *et al.*,1990). Laboratory analyses of this study have confirmed their results. It was seen that, during the changes in RH from 56% to 90%, direct ultrasonic velocity values were found to be in the range of 586 m/s to 1040 m/s in perpendicular-to-fiber direction while it was in the range of 2062 m/s to 3482 m/s in parallel-to-fiber direction (Figure 6.3). In addition, the analyses on the rate of moisture absorption and desorption have shown that, desorption was slower than absorption in timber (Figure 6.1). Both old and new timber samples gave out moisture more slowly than they took it in. That must be due to the attraction of water molecules by the hydroxyls of timber's chemical constituents mainly cellulose by forming strong hydrogen bonds. Apparently, their release needed more energy than required to evaporate water from a free surface (Tsoumis, 1991).

It was concluded that the moisture absorption was more rapid than moisture desorption for timber elements. The protimeter readings done at the surface of the laboratory samples gave similar EMC readings to weight measurements. However, old pine samples kept more moisture at their surfaces than the new ones (Figure 6.2). That finding was in agreement with some studies in literature (Ridout, 2001). Those data showed the importance of the microclimatic conditions on the moisture content of the timber elements in the structure as well as timber's age.

Ultrasonic velocity values at low RH conditions revealed higher velocities than at high RH conditions. Therefore, the knowledge on microclimatic conditions was an important input to interpret the ultrasonic velocity values.

#### *Effect of Fiber Direction on UPV and Modulus of Elasticity (MoE)*

Effect of fiber direction on UPV values during direct measurements and their comparison with the indirect measurements in axial and radial directions were studied in varieties of timber species.

Since timber was anisotropic, UPV measurements have reflected the differences in physico-mechanical properties of timber in relation to fiber direction. As seen in Table 6.1 and Figure 6.4, direct UPV values parallel to fiber direction were found to be considerably higher than the ones perpendicular to fiber direction, e.g. in sound old pine being 4586 m/s and 1347 m/s respectively. In general, indirect measurements were much lower than the direct ones. For the sound old and new timber samples, the indirect velocities in parallel to fiber direction were found to be lower than the direct velocities in the same fiber direction with the ratios in the range of 0.23 and 0.42 (with an average ratio of 0.32). For example, in the sound old pine indirect UPV parallel to fiber direction was 1440 m/s whereas the direct one was 4586 m/s (Figures 6.4-6.5). Kahraman (2002), investigated whether there was a relationship between the indirect and direct

velocity measurements in stone samples. He has found that the indirect velocity values of rock samples were 0.57 times lower than that of direct velocity values. The direct UPV values at parallel to fiber direction seemed to be the ideal way of measurements, since their values were higher. However, those types of measurements were not always practical on the historic building due to lack of access. An improvement in indirect measurements was suggested by Sandoz, (2005) by inserting the probes with some angle to timber in such a way that direct measurements position parallel to fiber could somehow be obtained.

On the other hand, this study has found that the indirect measurements of UPV parallel to fiber direction done in the laboratory gave good results to predict the soundness of timber. This conclusion was based on comparison with the direct measurements (Figure 6.5). In addition, indirect UPV measurements taken in radial direction were lower than indirect UPV measurements taken in parallel to fiber direction (Figure 6.5).

In this study, direct UPV values parallel to fiber direction and densities were used for calculating the MoE of laboratory timber samples. The equation described in Section 5.2.1 was used in the calculations. The results were shown in Table 6.1 and Figure 6.5. MoE values of dry sound old pine with the density of  $0.63 \text{ g/cm}^3$  was found to be about 13335 MPa, dry sound new pine having the density of  $0.41 \text{ g/cm}^3$  being 12148 MPa, dry deteriorated old pine having the density of  $0.45 \text{ g/cm}^3$  being 7037 MPa. In the literature, the MoE values of pine species having varying densities of  $0.35\text{-}0.59 \text{ g/cm}^3$  were found to be in the range of 8500-13700 MPa (Green *et al.*, 1999). Aydın *et al.* (2007) studied the mechanical properties of some perfect timber species which were commonly used in Turkey. They have studied MoE values through measurements of compression test. According to their results, MoE of pine with the density of  $0.365 \text{ g/cm}^3$  and 13.5 % moisture content was found to be about 12750 MPa, hornbeam having the density  $0.532 \text{ g/cm}^3$  and 15.5 % moisture content being 15260 MPa. It could be concluded that

MoE values calculated in this study and those studies in literature showed that calculated MoE values were good indicators of soundness for timber.

Sakai *et al.* (1990) studied the MoE of timber species in dry, moist, wet and saturated states. They have found that MoE of timber species have decreased with the increase in moisture content till fiber saturation point. After the fiber saturation point, the MoE have increased with increasing the moisture content. The increase in MoE with increase in water content above the fiber saturation point was due to free water storage in the vacant space inside the cells.

#### *Effect of Type of Timber and its Density*

Some researches illustrated the ultrasonic velocity values for several species of timber (Jordan *et al.*, 1998). In this study, UPV values of different species either old or new were found to be quite variable and overlapping each other e.g. the UPV of oak being around 4400 m/s, pine being around 3150-4200 m/s. However, density of timber was directly related to its UPV value. Therefore, when it came to the soundness assessment of timber, it was much better to consider density and UPV values together in the laboratory and compare that data with the same type of timber species (Table 6.1).

#### *Effect of Defects as Knots*

During direct and indirect UPV measurements, defects such as cracks in sound and deteriorated timber were recognized with increase in transit time and decrease in velocity. Knots have usually cracks around them. Those cracks around the knots were also detected by decreasing UPV. On the other hand, the presence of knots was recognized with an increase in velocity in new timber as well as in old one during indirect UPV measurements parallel to fiber direction (Figures 6.6 and 6.7). However the knots have decreased the overall soundness of timber in depth which might be due to the changes in fiber orientation and cracks surrounding the knot. The presence of knot considerably reduced the soundness of timber in

longitudinal direction as proved by decreasing MoE values in old and new pine (Figures 6.6, Table 6.1). The new pine with knots had considerably lower MoE in comparison to new pine without knots, the values being 5544 MPa and 8838 MPa respectively (Figure 6.4).

### **7.2.2 Evaluation of In-situ Measurements**

Most of the time, only in-situ indirect UPV measurements could be taken in historic buildings due to lack of access. Good contact of transducers with the timber surface was necessary for healthy ultrasonic measurements as well as comparisons with the laboratory data.

In-situ indirect UPV measurements of this study, has assured the soundness of timber elements in some parts and extensive deterioration in other parts. They were used as reference areas in QIRT measurements (Figure 6.29).

It was observed that indirect ultrasonic velocities of timber beams and posts were in the range of 1337 to 1176 m/s in parallel to fiber direction, that was in the longitudinal direction. In the laboratory studies the indirect ultrasonic velocity values for sound old pine was found to be about 1439 m/s and the modulus of elasticity (MOE) was calculated to be about 13335 MPa. Comparisons with the laboratory data indicated that, timber elements were sound (see section 6.1.1). Partial deteriorations on some parts of timber posts and beams were detected by their decreased ultrasonic velocity values. Those results were also supported with some in-situ UPVR-DIRECT measurements wherever cross arrangements for the transducers could be made. UPV direct measurements perpendicular to the fiber direction were about 1660-1400 m/s, in agreement with values given in literature (Beal,2002; Bray,1992).

The lines of transit time versus distance in a number of timber elements showed sharp increase in transit time with the crack, fiberization, knot etc. Some posts were found to be fairly deteriorated and some partially deteriorated (Figure 6.30).

Direct UPV measurements were taken from the timber posts of Aslanhane Mosque in perpendicular to the fiber direction. They were in the range of 706 to 1753 m/s. Those values were in range of sound timber in the literature and in agreement with the laboratory measurements (Beal, 2002; Bray,1992) (Figures 6.3 and 6.26).

### **7.3 Soundness Investigation by QIRT Studies**

In order to use QIRT for the soundness investigations of timber, it was necessary to develop good methods and reference data in the laboratory for several issues: i) thermal properties of different timber species by QIRT ii) discussion of compatibility in terms of thermal properties of timber and its neighbouring materials iii) detection of deterioration and defects in timber.

Those methods and standard data developed in this study were used during the in-situ measurements for i) the detection of dampness problems in timber and its historic structure ii) detection of deteriorated and sound timber iii) for detecting compatibility of neighbouring materials with timber.

Finally, combined use of QIRT and UPV was discussed for in-situ soundness investigations.

### **7.3.1 Establishment of Reference Data by Laboratory QIRT Analyses**

In this study, it was found that thermal properties of timber and its neighbouring materials were best followed by their rate of heating and cooling during passive and active QIRT analyses, using visual analyses and single IR images as starting points.

Rate of heating and cooling of timber samples that looked severely deteriorated, deteriorated and sound by visual observation as well as the neighbouring historic brick, mudmortar and stone samples were followed in sequential IR imaging by means of differential temperature curves as a function of time. Rate of heating and cooling of each sample were compared with the rate of sound timber sample whose soundness was verified by other tests. Since those rates were inverse propositional with the effusivity (thermal inertia) of the samples, by using those values, it was possible to discuss thermal properties of those materials in relation to each other, as well as their state of deterioration and development of dampness problems in the structure (Tanaka, 2000) (Section 4.3.5).

#### *i) Thermal Properties of Different Timber Species by QIRT*

The best conditions to follow the rate of heating and cooling of different timber species were obtained with active thermography, using a heat source that was sufficient to produce a thermal gradient without harming the materials.

The lines showing surface temperature versus square root of time has demonstrated the different dry sound timber species such as oak, pine and beech. For dry sound timbers, the differences in their rate of heating and cooling were mainly due to the differences in their density (Figures 6.13 and 6.15, Table 6.4).

It was seen that rate of cooling was the highest for the lowest density timber and the lowest for the highest density one. That was a good indication for the inverse relationship between the rate of heating and cooling in relation to density of timber. That was why different species of timber could be detected by their rates of heating and cooling in QIRT analyses (Chapter 6, Figures 6.13, 6.15, Table 6.4).

Old pine with low density had highest rate of heating and cooling and lowest thermal inertia. Pine with higher density had lower rate of heating and cooling and higher thermal inertia. Beech having the highest density had lowest rate of heating and cooling and highest thermal inertia (Table 7.1). The same results were obtained by Tanaka (2000) for Japanese timber species with different densities. His results on temperature, cooling time and density were compiled in this study to obtain the rates of cooling in Figure 7.1.

Table 7.1 Heating and cooling rate of timber species with different densities.

SAMPLE	Rate of heating up- $R_w$	Rate of cooling down- $R_C$
FEC3-08-Old Pine low density- ( $\rho=0.378\text{g/cm}^3$ MOE=2.091GPa)	0.2131	-0.1708
YC1-08-New Pine- ( $\rho=0.408\text{g/cm}^3$ MOE=12.148GPa)	0.1926	-0.1509
SEC1-09-Sound Old Pine ( $\rho=0.634\text{g/cm}^3$ MOE=13.335GPa)	0.1724	-0.1440
YK5-08-New Beech ( $\rho=0.784\text{g/cm}^3$ MOE=7.137GPa)	0.1421	-0.1129

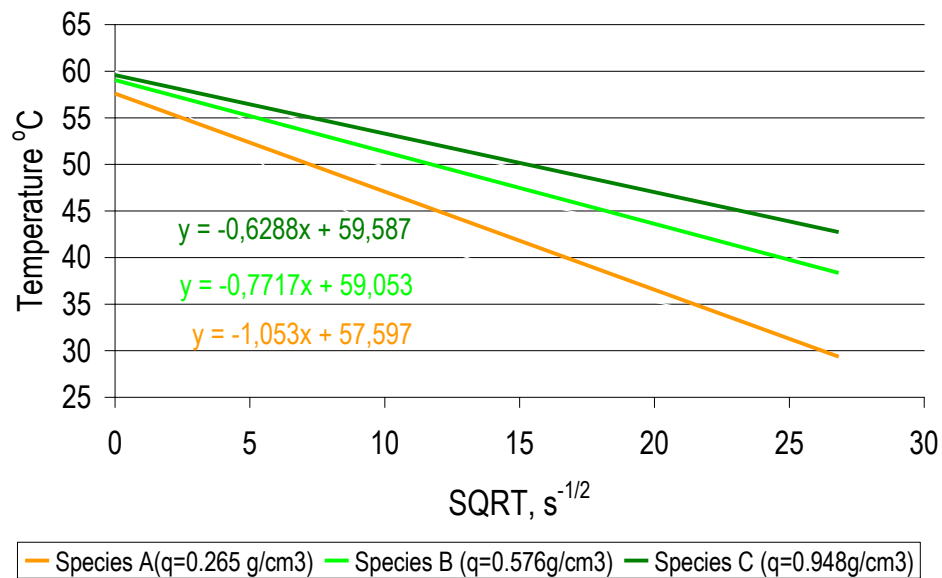


Figure 7.1 The surface temperature of different timber species with different density versus square root of time (The graph was drawn with the values of the graph given in Tanaka, (2001))

*ii) Discussion of Compatibility in terms of Thermal Properties of Timber and its Neighbouring Materials*

Thermal properties of neighbouring materials and structural timber representing the traditional structures were examined in the laboratory and in-situ with QIRT. Samples of neighbouring materials for structural timber consisted of mud brick infill, fired brick infill, mud mortar, interior gypsum plaster, exterior mud plaster, exterior lime plaster. The rate of heating and cooling of those samples were used to see their compatibility ranges and discover the incompatible situations.

Compatibility directly influenced the durability of timber that was defined by some physical, mechanical and chemical parameters. Pizzo (2002) studied wood and epoxy adhesive interface compatibility comparing the values of thermal expansion coefficients of those materials. It was concluded that it was one of the important physical parameters that should be taken into account to predict the compatibility and durability of the interface. Akkuzugil (1997) has analyzed water

vapor permeability properties of materials in some traditional half timber houses in Ankara. She found that the materials touching or surrounding the wood, such as exterior and interior plasters and mud brick infill allowed the constant passage of water vapor. As a result, the risk of condensation in timber elements was prevented. In other words, equivalent air thickness (SD) of those materials was similar among each other and lower than timber. Therefore SD value expressing the water vapor permeability was an important compatibility parameter for the durability of half timber dwellings.

In this study, it was seen that exterior lime plaster on the thick mud plaster layer and exterior mud plaster alone warmed up and cooled down together with the sound old pine, having almost the same heating and cooling rate with the sound old pine (Figures 6.18-6.24). On the other hand, the thick interior repair plaster (high gypsum content) together with its mud layer had the quite slow rate of heating and cooling. Compatibility relationship of those materials could be well demonstrated by the ratios of their rate of heating and cooling to the sound timber, as shown in Tables 6.6 and 6.7. Surfaces of the mud brick warmed up and cooled down 0.82 and 0.86 times slower than the sound old pine surfaces respectively (see Table 6.7), for the exterior mud plaster, that ratio was 0.99, for the exterior lime plaster the ratio was 0.91. Heating and cooling rate ratios of neighbouring materials; lime plaster, mud plaster, mud mortar and mud brick infill in comparison to sound pine were found to be in the range of 0.99-0.82 (see tables 6.6,6.7). However, heating and cooling rate ratios of fired brick materials to sound pine were in the range of 0.71- 0.58 (see Tables 6.2, 6.6). On the other hand, heating and cooling rate ratio of the thick interior repair plaster (high gypsum content) together with its mud layer was in the range of 0.66-0.54 (Table 6.7). Heating and cooling rate ratios in the range of 0.80-1.20 could be considered good compatibility conditions for timber in terms of thermal properties. As the ratios get lower or higher than that range, incompatibility might be considered.

### *iii) Detection of Deterioration and Defects in Timber by QIRT*

The results of this study have proved that the QIRT allowed to differentiate the sound and deteriorated timber and indicated that some difference existed in their thermal properties. Comparisons were made with samples of deteriorated pine, sound pine and sound beech.

It was seen that cooling rate of deteriorated pine was considerably higher than the sound one, RC deteriorated pine/ RC sound pine = 1.6980 (Table 6.3). The cooling rate of sound beech was the slowest (YK5<sub>RC</sub> -new beech= 0.0891). It was highest for deteriorated pine sample (EC3-08-<sub>RC</sub> -deteriorated pine= 0.1518). The deteriorated and sound pine timbers could be clearly distinguished from each other due to the lower thermal inertia characteristics of the deteriorated one - warmer initial temperature and faster rate of cooling down (Table 6.3).

When the timber deteriorated, its density dropped and its rate of heating and cooling increased. By that way, deteriorated timber could be detected in structures through QIRT analyses. (Chapter 6, Figure 6.11.a-b, Table 6.3).

QIRT analysis was good at seeing the degree of decay of old pines of similar type (SEC1-09, SEC1-08, and SEC2-09). The severely deteriorated one SEC2-09 had the highest rate of heating and cooling and its density was lowest. The sound old pine had the lowest rate of heating and cooling and had considerable high density indicating its higher thermal inertia (Section 4.3.4, Tables 4.3 and 6.4, Figures 6.13, 6.15).

The heating and cooling lines drawn by using temperature versus square root of time were more representative of different samples at beginning of the heating and cooling periods obtained by active IR thermography in laboratory conditions, e.g.

at the first 100-200 seconds. That aspect needed to be considered at field measurements.

As a result, heating and cooling rate ratios of visually deteriorated pine with sound interior in comparison to sound pine were found to be 1.15 and 1.11 respectively (Table 6.4). Heating and cooling rate ratios of severely deteriorated timber to sound pine were measured twice and found to be in the range of 1.19-1.28 and 1.20-1.21 (see Tables 6.5, 6.6). It was seen that the heating and cooling rate ratios have increased due to decrease in density of deteriorated pine species. In another laboratory analysis, the ratio of very deteriorated pine to sound one was 1.69 (see Table 6.3).

Coming to defects as knots, QIRT analyses have shown that the surfaces of the deteriorated old pine warmed up and cooled down 1.44 (0.2202/ 0.1528) and 1.71 (-0.1726/-0.1012) times faster than the knot surfaces respectively (see Table 6.5). The knot on the deteriorated pine had the slower rate of heating and cooling than its deteriorated surroundings. The knot in the sound pine had slower rate of heating and cooling than the knot in the deteriorated pine. Meaning that the knot in the deteriorated pine could be expected to be deteriorated up to some extent (Table 6.5). Those results showed that the soundness of timber with QIRT analyses should be done on the timber surfaces without knots to have better idea of the degree of decay.

### **7.3.2 Evaluation of In-situ QIRT Measurements**

The IR images of timber surfaces have reflected the changes in their thermal characteristics due to the type, age and state of deterioration of timber, microclimatic conditions, existence of incompatible neighbouring materials, etc (Tsoumis, 1991; Ridout,2001; Tanaka,2000; Ludwig, 2004). In this study, in-situ

IR analyses were discussed for the following headlines: i) the detection of dampness problems in timber and its historic structure ii) detection of deteriorated and sound timber iii) detecting compatibility of neighbouring materials with timber.

*i) Detection of Dampness Problems in Timber and Its Historic Structure*

Aslanhane Camii was examined for its damp zones by taking several single IR images in passive mode and by differential IR images. Target surfaces mainly consisted of stone masonry walls, oil painted timber pillars, unpainted timber ceiling, plastered and oil painted walls.

At the timber ceiling of Aslanhane Camii, timber elements exhibited temperature differences in IR images (Figure 6.34). The images were processed to show the temperature distribution on timber elements. They exhibited around 3 °C differences in temperature. The ones in further contact with the roof structure were about 2 °C cooler than the ones closer inside. The coolest patch in the middle of IR image with 4 °C difference indicated a damp zone possibly due to the rain penetration problem (Figure 6.34). The damp zones at the eaves level were also detected at the east wall of the building showing the existence of roof drainage faults. The timber lintels and bond beams in stone masonry were suffering from damp conditions at upper parts of the building due to roof drainage faults (Figure 6.35). The colder areas with temperature differences higher than 3 °C showed the presence of damp areas (Kandemir *et al.*, 2007).

In the stone masonry façade with its timber lintels and bond beams, some damp zones were observed near the cement mortars (Figures 6.31 and 6.32). The temperature variations on the surface of timber lintel in Figure 6.32 was found to be reaching 5.5°C showing the considerable moisture content variations in timber.

It indicated that the timbers suffered from the dampness problems (Kandemir *et al.*, 2007).

The differential analyses of day and night IR images showed that the timber elements cooled down faster than the stone masonry (Figure 6.39). The differential temperature was calculated to be  $-6.97^{\circ}\text{C}$  for timber elements while being  $-3.87^{\circ}\text{C}$  for stone masonry.

Single IR image taken from the oil painted east wall of the Aslanhane Mosque showed that the surface temperature of the wall differed from  $10.8^{\circ}\text{C}$  to  $15.6^{\circ}\text{C}$  along with its height. The low temperatures in the lower parts were due to the entrapped moisture sourced from the recent incompatible repairs in those parts undertaken with the cement-based plaster and oil-based paints (Figure 6.36) (Kandemir *et al.*, 2007).

#### *ii) Detection of Deteriorated and Sound Timber*

Analyses of different timber elements of İstiklal house were done by QIRT. Differential IR image of sound post and sound mud brick infill showed even temperature distribution. However deteriorated ones showed heterogeneous temperature distribution (Figure 6.40.c). It was seen that the deteriorated timber cooled down faster than the sound timber while the cooling down rate was the fastest for the severely-deteriorated timber. Analyses of the surfaces with knots showed that knot surfaces cooled down slowly in comparison to the other parts of the timber surfaces (Figures 6.42-6.46, Table 6.8). Cooling rate ratios of deteriorated timber, severely deteriorated post and a knot in comparison to sound post/beam were found to be 1.55, 2.48 and 0.76 respectively. That meant that thermal inertia of deteriorated timber decreased due to decrease in density and increase in porosity.

When compared with the laboratory analyses, the cooling rate ratio of knot surfaces in sound pine was 0.70 in laboratory samples (Table 6.5), whereas it was 0.76 for in-situ knot in İstiklal House. The surface of deteriorated timber in laboratory conditions has cooled down in the range of 1.21-1.70 times faster than the sound timber surface (see table 6.4 and 6.6). However in-situ cooling rate ratio of deteriorated post/beam surfaces to sound ones was in the range of 1.55-2.48 (Table 6.8). That result showed that deteriorated timber elements of İstiklal house were more deteriorated than the deteriorated laboratory samples.

It was possible to detect the cracks as the hottest traces and knots as the coldest patches in single IR images of columns in Aslanhane Mosque (Figures 6.37-40). It was concluded that degree of deterioration of timber elements as well as defects such as knots and cracks could be evaluated by studying with single IR images and sequential ones.

### *iii) Detecting Compatibility of Neighbouring Materials with Timber*

Compatibility of neighbouring materials with timber elements were studied in İstiklal House and Ayaş House.

The QIRT analyses on surfaces of the deteriorated timber posts, sound timber posts, mud brick infill with scale and mud brick infill were done in İstiklal House (Figure 6.44, Table 6.9). The sound mud brick presented similar rate of cooling down with the sound timber indicating that timber elements and neighbouring mud brick infill had similar thermal inertia characteristics and they were compatible with each other.

The deteriorated timber presented noticeably faster heating up and cooling down than sound timber and deteriorated mudbrick. The cooling rate ratio of sound mudbrick infill to sound beam was 0.94 (see table 6.9). In the laboratory the

cooling rate ratio of sound mud brick infill to sound pine samples was 0.86. At laboratory for the exterior mud plaster this ratio was 0.99, for the exterior lime plaster the ratio was 0.91 (see Table 6.7). Those in-situ and laboratory results were consistent with each other.

In Ayaş House, an analysis of plastered wall surface covering timber elements and mud brick infill was done (Figure 6.45). Since it was possible to detect the timber elements and mud brick infill behind the plaster, plaster surface covering timber elements and plaster surface covering mud brick infill could be analyzed. Their heating up and cooling down rates during the daytime were similar which indicated that they responded similarly to the exposed ambient conditions (Figures 6.48, 6.49, Table 6.10).

The in-situ moisture content measurements taken from the plaster-covered timber surfaces proved that the moisture content was in the range of  $7.9\% \pm 1.1\%$ , which was the characteristic wood moisture content at  $40\% \pm 5\%RH$  (Knut,1999). Those results exhibited the soundness of timber frame elements in the wall section and the healthy boundary conditions achieved through protective historical plasters.

Differential IR analyses during the cooling period of night has shown that the exposed timber elements in Ayaş House cooled down faster than the exposed fired brick and mudmortar infill with a 1.65 times faster cooling rate (Figure 6.49, Table 6.11). That should be due to their different thermal inertia characteristics as well as their state of deterioration.

At Aslanhane Mosque, similar to the case of Ayaş House, the exposed timber elements have cooled down faster than the exposed stone masonry (Figure 6.41). Here, the exposed structural timber elements were warmer than the stone masonry nearby during daytime. However, wall had damp zones due to the cement mortars introduced during recent repairs. This meant that the structural timber elements

were suffering from unhealthy boundary conditions. Timber elements exposed to the outside atmospheric weathering cycles, had dampness problems which would accelerate their decay.

### **7.3.3 Combined Use of QIRT and UPV for In-situ Soundness Investigations**

More reliable non-destructive investigations could be done if UPV measurements and IR Thermographic survey were used together to support each other.

UPV measurements of timber were directly proportional to physico-mechanical properties of timber and its state of deterioration. However there were quite of number of parameters that affect those measurements. The cuts of timber, its type, atmospheric humidity at which the timber was in equilibrium or its water content should be considered during those measurements. In addition, UPV measurements could only be done at reachable and touchable surfaces of timber elements whereas IR thermography could be done at all surfaces.

Some representative samples of historic building materials, as well as the repair ones, taken from the building under investigation and several old and new timber samples were investigated in the laboratory for better UPV and QIRT interpretations and their combined use for wider QIRT analyses of the structure (Sections 6.1.1, 6.1.2, 6.2.1, 6.2.2).

Although limited UPV measurements could be taken from timber elements, they provided valuable data on the soundness of timber. Those parameters affecting the UPV measurements could be well taken into consideration. Those UPV measurements would be very useful for QIRT analyses for wider investigation of the structural timber in the monuments.

UPV direct measurements perpendicular to the fiber direction taken from the M2-beam and M6-post were about 1660-1400 m/s. Their indirect ultrasonic velocities (UPVL-INDIRECT) of M2-beam and M6-post were 1283 m/s and 1337 m/s. According to those results M2-beam and M6-post were sound. M7-post was found to be severely deteriorated because of its low indirect velocity value (493 m/s) where no direct velocity measurements could be taken. UPV values of sound M6-post and severely deteriorated M7-post were accepted as reference values for in-situ values of sound and deteriorated timber. In QIRT analyses their rate of heating and cooling and their ratios were used as reference in the examination of other areas. Decisions on the soundness of timber by QIRT analyses, using rate of heating and cooling, and their ratios to sound timber, were based on those data.

In single IR images even temperature distribution was a sign of soundness in some cases and uneven distribution of temperature was signaled dampness problems as well as deterioration. That type of information needed to be supported by UPV measurements, e.g. the timber columns in Aslanhane Mosque had even temperature distribution with a difference of 2 °C and the consistent ultrasonic velocity values perpendicular to fiber direction, being about 1000 m/s revealed the soundness of timber column (Figure 6.33).

#### **7.4 A Proposal for Soundness Investigation of Timber**

Soundness investigation of timber is proposed has several steps indicated below.

##### *Visual Examination as a First Step of Soundness Investigation*

The study should start with visual analyses. Location and distribution of the decay areas observed visually have to be pointed out as well as the healthy parts of the building and its timber elements: Damp areas, areas on timber elements that have colour change, insect holes, fungi growth, deformations should be noted on the

drawings, sketches or photographs as well as the healthy areas of timber and its neighboring materials. After the evaluation of visual analyses, selection of parts to be investigated with UPV and QIRT should be done. QIRT analyses should be supported by UPV measurements.

Some representative samples of building materials taken from the building under investigation and several old and new timber samples may be collected for laboratory investigations for UPV and QIRT.

#### *Selection of the Areas to be Studied by UPV*

##### *i) The Places Where Measurements can be Taken*

UPV measurements can only be done in restricted areas where we can reach and where the free surfaces exist for direct cross sectional measurements and indirect measurements. All those areas are important since they serve as in-situ standard data (comparison data) for QIRT measurements.

##### *ii) Determination of Cuts and Grain Direction in Timber*

Since the UPV values are variable in longitudinal, tangential and radial directions, expected UPV values would be in relation to those directions e.g. higher values in axial directions, smaller in tangential directions. Direction of the measurements in relation to timber structure should be well noted (See Chapter 3, Section 3.1.3)

##### *iii) State of Dampness in the Investigation Area*

Visual investigations may point out the damp zones however one needs to check whether the area is dry, wet or soaked with water. If possible, protimeter reading can be taken to verify the damp zones. On the other hand, microclimatic conditions of the timber elements need to be known if possible with a thermohygrograph since equilibrium moisture content of timber is closely related with environmental relative humidity and UPV measurements decrease at higher

equilibrium moisture content and stay quite constant in damp conditions above the fiber saturation point (Sections 4.2.2, 4.3.5, 6.1.1 and 6.2)

*iv) How to Take Direct and Indirect Measurements of UPV*

Where the cross sections are reachable direct measurements are preferred. If it is not possible, indirect measurements should be taken. It must be remembered that indirect UPV measurements are lower than the direct ones. The coupling is needed to provide good connection with the probes and timber surface and to acquire accurate transit time readings. Those measurements should be taken with specialists having enough experience of UPV data acquisition.

*v) Comparison of the UPV Values Taken on Site with Sound Area Measurements of Timber and with Laboratory Measurements as well as Their Comparison with Values Available in Literature*

Those comparisons are needed for the interpretation of data on the degree of soundness.

*vi) Diagnosis*

It is necessary to decide whether the measurements are sufficient to show the soundness of timber or some more data are needed. It may also be necessary to make QIRT investigations to decide on the soundness of timber in a wide area and unreachable points in the building.

*Selection of the Areas to be Studied by QIRT*

Since wood is a biological product that have certain physical and structural characteristics that are closely related to its thermal properties, its QRT investigations should be done by taking into consideration all those properties. On the other hand, QIRT measurements need to be done with certain calibrations to obtain reliable results. Therefore, QIRT investigations of timber should be done by reviewing the aspects related to timber and QIRT setup, hardware and

microclimatic parameters. In addition, there is need for laboratory measurements of timber samples that will be useful for the interpretations of in-situ data. It is advised that the reference samples, representing the decay problems and sound situation, can be useful during the in-situ measurements for the comparisons. In case of using reference samples, they should be left on site for a certain period of time before the study of IR imaging.

*i) The Places Where Measurements can be Taken*

The QIRT survey should start from the part of the structure where the soundness of its timber elements can be assessed by UPV measurements. The key concern is to determine the thermal inertia characteristics of timber elements where the UPV measurements are taken. The sound timber is the reference/control sample for the QIRT analyses on site. Its soundness should be proved by UPV measurements. During the in-situ sequential imaging, the control sample should be involved in the field of IR view together with the other timber elements under study at the same boundary conditions. The thermal response of the sound timber sample under the exposed conditions is the reference/control data for soundness assessment of other timber elements. The warming up and cooling down rates of each timber element/sample is compared with the rates of the sound timber. The differences in those rates are due to the changes in physico-mechanical and thermophysical properties of timber elements depending on its state of deterioration. The increase in warming up and cooling down rates when compared with the rates of sound timber give the hints on the state of deterioration of timber elements.

As the next step, the sequential IR imaging can be conducted on the other parts of timber structure that are not possible to access for ultrasonic testing. Here, the knowledge gained on in-situ thermal response characteristics of sound and deteriorated timber would serve as comparison data to analyze other regions.

*ii) Determination of Cuts and Fiber Direction in Timber*

It is necessary to record the direction of fibers for the timber elements under examination by QIRT since thermal conductivity coefficients and the thermal inertia characteristics vary with fiber direction. Therefore, it is advised to compare the warming up/cooling down rates of timber elements cut in the same direction. (See Chapter 4, Section 4.3.4)

*iii) State of Dampness in the Investigation Area*

The presence of moisture in timber elements and their boundary conditions need to be known in order to interpret the in-situ IR data for soundness assessment. IR scanning of the structural timber frame is useful to locate the damp zones and their distribution in the structure. A special care should be given to the presence of moisture in the examined area during the QIRT survey. If possible protimeter reading can be taken to verify the damp zones. The microclimatic monitoring is also needed to estimate the equilibrium moisture content in timber in relation to the ambient relative humidity as well as wet and waterlogged zones. (Sections 4.3.4 and 4.3.5).

*iv) The Use of Single and Sequential Images by IR Thermography / Use of QIRT*

Single IR imaging of the whole structure is useful to point out the damp and deteriorated zones as a start. The soundness assessment of timber requires detailed QIRT analyses. The thermal monitoring of timber surfaces during the exposure conditions of heating and cooling is useful to find out the thermal inertia characteristics of timber elements in relation to their state of deterioration. The heat source on site may be sunlight, if it directly heats the surfaces of timber frame structure during the day. In absence of direct exposure to sun, some additional heating devices, such as hair drier or lamp, can be used for evenly-heating the surfaces. During the sequential imaging, since the width of timber elements are small in size, such as 15cm in width, it is better to focus on target area, by reducing the distance between the camera and the target area and/or by

using longwave sensitive camera with high resolution in order to increase the number of pixels and enhance the accuracy in data acquisition.

*v) Comparison of QIRT Analyses Done on Site and in Laboratory Including Sound and Deteriorated Areas of Timber*

The ratios of warming up and cooling down rates for timber elements with respect to sound timber should be calculated during in-situ and laboratory analyses of samples. Those ratios of in-situ areas and laboratory samples are used as comparison data to decide on state of deterioration of timber elements in the structure under survey.

*vi) Preparation to Diagnostic QIRT Analyses*

Laboratory samples for UPV analyses can serve as laboratory samples for IR imaging. It is better to start with single IR imaging at the site after doing some preliminary IRT calibrations. Laboratory samples need to be selected to provide comparative data of IRT to distinguish variations of wood species within a structure and their neighbouring materials. Background on physical and chemical characteristics affecting thermal conductivity and thermal inertia of timber is needed. Information on surface and subsurface abnormalities within timber elements and wall systems is useful.

## **7.5 Conclusion**

Timber has been commonly used as structural material in historic masonry structures and traditional timber framed houses. Therefore, soundness assessment of structural timber elements on site, by using nondestructive testing methods was very important in conservation studies of those structures.

In this study, two non-destructive methods, UPV measurements and IR thermography with QIRT analyses were studied in detail for soundness assessment of structural timber.

There were quite a number of parameters that affected UPV measurements of timber. The atmospheric humidity at which the timber was in equilibrium or its water content, cuts of timber, its type, should be considered during those measurements. In addition, UPV measurements could only be done at reachable and touchable surfaces of timber elements whereas IR thermography could be done at all surfaces.

The UPV values of timber decreased with the increase in moisture content up the fiber saturation point and it stayed almost constant in wet and waterlogged states. On the other hand, the old timber samples kept more moisture at their surfaces when compared with new ones while both were under the same environmental conditions. However the core of old timber samples was drier.

Since timber was anisotropic, UPV measurements have reflected the differences in physicomechanical properties of timber in relation to fiber direction. Direct UPV values parallel to fiber direction were found to be considerably higher than the ones perpendicular to fiber direction. The indirect ultrasonic velocities were found to be lower than the direct velocities with the ratio of 0.32 in average in comparison to the measurements taken in parallel to fiber direction.

This study revealed that direct UPV measurements taken parallel to fiber direction were good at estimating the state of deterioration of structural timber elements. However it was difficult, sometimes not possible, to examine all timber elements in-situ by direct ultrasonic testing. In that case, in-situ indirect ultrasonic testing mode parallel to fiber direction could be used to estimate the soundness of timber elements. Indirect UPV measurements taken in radial direction were lower than

indirect UPV measurements taken in parallel to fiber direction. Those lower UPV measurements were more difficult to be used for soundness investigations in historic structures.

MoE values, estimated from direct UPV values parallel to fiber direction and densities by calculations, were good indicators for soundness of timber. However they were of restricted use since direct in-situ measurements were rarely possible.

The QIRT was good at soundness assessment and defect inspection of timber. The study showed that, the even or heterogeneous distribution of surface temperatures, different thermal inertia characteristics reflected by the rate of heating and rate of cooling of materials and their ratios to sound timber were good parameters to express the state of deterioration of timber elements as well as the compatibility of neighbouring materials with timber.

The interpretation of single IR images had difficulties due to the different heating and cooling characteristics of timber elements in relation to its anisotropic nature and influence of environmental conditions and neighbouring materials. Therefore, thermal characteristics of timber elements needed to be studied by QIRT both in laboratory and in-situ.

The reference data obtained in laboratory helped us to better understand the thermal behavior of timber in relation to its state of deterioration and environmental conditions. The comparison of the reference data with the in-situ data was necessary for the correct interpretation of the results.

The use of QIRT to produce knowledge on the heating and/or cooling rate characteristics of timber elements, their comparison with sound timber and expressing them as their ratio to sound timber provided valuable data for soundness investigations to express the state of decay of timber as well as state of

compatibility of the neighboring building materials with timber. It was found that traditional neighbouring materials such as mud brick infill, fired brick infill, mud mortar and mud plaster, lime plaster had compatible thermophysical properties with timber. Those compatibility relationships with new repair materials should be maintained for long term health of historic structure.

The joint use of QIRT and UPV methods combined with laboratory analyses has enhanced the accuracy and effectiveness of the survey and facilitated to take decisions on the state of deterioration of timber, to evaluate healthy boundary conditions with the neighbouring materials of timber and build up the urgent and long-term conservation programs.

Both QIRT and UPV methods need to be improved for better in-situ measurements as well as for the calculation of some thermophysical parameters and strength parameters of timber and its neighbouring materials. It was thought that direct measurements of UPV on timber elements could be taken by inserting the transducers with an angle to the surface so that measurements parallel to the fiber direction could be achieved. Semi destructive ways should be found for that. Future studies could be performed on the in-situ measurements and software to calculate some more physical and mechanical parameters of timber by QIRT measurements.

All those results should be evaluated together with the historical background of the structure.

## REFERENCES

- Acar, E. 1996. Anadolu'da Tarih öncesi Çağlardan Tunç Çağı Sonuna Kadar Konut ve Yerleşme, Tarihten Günümüze Anadolu'da Konut ve Yerleşme. Habitat II, Sey, Y. (Ed), Türkiye Ekonomik ve Toplumsal Tarih Vakfı, İstanbul, p.380-394
- Acker, J.V., Stevens, M., Carey, J., Sierra-Alveraz, R., Miltz, H., Le Bayon, I., Kleist, G., Peek, R., D. 2003. Biological Durability of Wood in Relation to Enduse. Holz als Roh-und Werkstoff, n.61, p.35-45
- Akın, N. 1996. Osmanlı Döneminde Anadolu Konutuyla Balkan Konutu Arasındaki Ortaklıklar. Tarihten Günümüze Anadolu'da Konut ve Yerleşme. Habitat II, Sey, Y. (Ed), Türkiye Ekonomik ve Toplumsal Tarih Vakfı, İstanbul p.269-277
- Akkuzugil, E. 1997. A Study on Historical Plasters. Unpublished MSc Thesis, METU, Department of Architecture, Supervisor: Saranlı, T.
- Akok, M. 1951. Çorum un Eski Evleri, Arkitect, n.9-10, p.171
- Akok, M. 1950. Trabzon'un Eski Evleri, Arkitect, n. 5-8, p.103
- Aksoy, E. 1963. Orta Mekan: Türk Sivil Mimarisinde Kuruşuş Prensibi, Mimarlık ve Sanat, n.7-8, p.39
- Akyazı, M.A. 1998. Proposal for the Repair and Conservation of Haraçoğlu Konak in Bursa. Unpublished M.Sc Thesis, Middle East Technical University, Department of Architecture, Supervisor: Güçhan, Ş.N.
- Altınsay, G., Hersek C., Kayademir, Morçöl, Özkaya, Paytar, Şahin, Tuncer. 1988. İstiklal Mahallesi, Orta Doğu Teknik Üniversitesi, Ankara
- Arel, A. 1982. Osmanlı Konut Geleneğinde Tarihsel Sorunlar. Ege Üniversitesi Güzel Sanatlar Fakültesi, İzmir
- Asatekin, G. 1994. Anadolu'daki Geleneksel Konut Mimartisinin Biçimlenmesinde Aile Konut Karşılıklı İlişkilerinin Rolü, Kent, Planlama, Politika, Sanat, p.65-87

American Institute of Timber Construction. 1966. Timber Construction Manual. John Wiley and Sons Inc., First Edition, Washington, D.C.

Anon Ultrasonic Testing Inspection. 1968. U.S. Dept. of Transportation, p.1-10

Avdelidis, N.P., Moropoulou, A., Theoulakis, P. 2003. Detection of Water Deposits and Movement in Porous Materials by Infrared Imaging, *Infrared Physics&Technology*, n. 44, p.183-190

Avdelidis, N.P., Moropoulou A. 2004. Applications of Infrared Thermography for the Investigation of Historic Structures, *Journal of Cultural Heritage*, v.5, p.119–127

Aydın, S., Yardımcı, M.Y., Ramyar, K. 2007. Mechanical Properties of Four Timber Species Commonly used in Turkey, *Turkish J. Eng. Env. Sci.* n.31, p.19-27

Baldassino N., Piazza M., Zanon P. 1996. In situ Evaluation of Mechanical Properties of timber Structural Elements, *Proc. 10<sup>th</sup> International Symposium on non destructive Testing of wood*, Lossanna, 26-28 Agosto, p.369-378

Bammer, A. 1996. Çadır ile Anadolu Evi İlişkileri. Tarihten Günümüze Anadolu'da Konut ve Yerleşme. *Habitat II*, Sey, Y. (Ed), *Turkiye Ekonomik ve Toplumsal Tarih Vakfı*, İstanbul, p.234-247

Baysal, N.K. 1994. Use of Contemporary Materials and Technologies in Restoration Applications of Traditional Buildings. Unpublished Master Thesis, *Dokuz Eylül Üniversitesi*, Supervisor: Meriç, R.

Bektaş, C. 1996. Türk Evi. *Yapı Kredi Yayınları*, Beyoğlu, İstanbul

Beall, F.C. 2002. Overview of the use of Ultrasonic Technologies in research on Wood Properties, *Wood Science and Technology*, n.36, p.197-212

Beery, B.Y. 1938. The Development of the Bracket Support in Turkish Domestic Architecture. *Ars Islamica* 5, Michigan

Berndt, H., Schniewind, A.,P., Johnson, G.,C. 1999. High-Resolution Ultrasonic Imaging of Wood, *Wood Science and Technology*, n.33, p.185-198

Bernatowicz G. 1994. Determination of Moisture Distribution and Check Formation by means of Thermography, *Ann Warsaw Agric Univ for Wood Technology*, n.45, p.65-69

- Biernacki, J.M. and Beall, F.C. 1993. Development of an Acousto-Ultrasonic Scanning System for Nondestructive Evaluation of Wood and Wood Laminates, *Wood and Fiber Science*, v.25, n.3, p.289-297
- Bodig, J. 2001. The Process of Nondestructive Evaluation Research for Wood and Wood Composites, *Proceedings of the 12<sup>th</sup> International Symposium on Non Destructive testing of Wood University of Western Hungary, Sopron*, 13-15 September 2000, v.6, n.03
- Booker, R., Haslett, T.N. 2001. Acoustic emission Study of Within-ring Internal Checking in Radiata Pine- *Wood NDT 2000, Proceedings of the 12<sup>th</sup> International Symposium on Non Destructive testing of Wood University of Western Hungary, Sopron*, 13-15 September 2000, v.6, n.03
- Bray, D.E and McBride, D. 1992. *Nondestructive Testing Techniques*. John Wiley&Sons, Inc., Canada
- Breeze, J.E., Nilberg, R.H. 1971, Predicting by Sonic Measurements The Strength of Logs and Poles having Internal Decay, *Forest Products Journal*, v.21, n.5, p.39-43
- Bressan, C., Grinzato, E., Marinetti, S., Bison, P, G., Bonacina, C. 2002. Monitoring of the Scrovegni Chapel by IR Thermography: Giotto at Infrared, *Infrared Physics&Technology*, v.43, p.165-169
- BS EN 335-1:1992. Hazard Classes of Wood and Wood-Based Products Against Biological Attack, Classification of Hazard Classes.
- Bucur, V. 2003. *Non-destructive Characterization and Imaging of Wood*. Springer-Verlag Berlin Heidelberg, Germany
- Bucur, V. 1985. *Acoustics of Wood*. CRC Press, Boca Raton
- Bucur, V. 1983. An Ultrasonic Method for Measuring the Elastic Constants of Wood Increment Cores Bored from Living Trees, *Ultrasonics*, n.21, May, p.116-126
- Carlomagno, G.M., Meola, C. 2002. Comparison Between Thermographic Techniques for Frescoes, *NDT, NDT&E International*, n.35, p.559-565
- Catena G., Catena A. 2000. Thermography for the Evaluation of Cavities and Pathological tissues in trees, *Agric Ricerca*, v.1855, p.47-64

Cestari, C.B., Lombardi, C., Gubetti, E., Pignatelli, O. 2002. Arsenal Project-the Timber of Tesone '111': Technological Characteristics, Dating and Assessment of thermo-hygrometric Behavior for Restored Functionally Proposal, *Journal of Cultural Heritage*, v.3, p.53-57

Christaras, B. 1999. Effectiveness of In-situ P-wave Measurements in Monuments, in: *Proceedings of the 9th Eurocare Euromarble EU496 Workshop*, 8-10 October, 1998, Munich.

Cielo, P., Krapez J.C., Lamontagne, M. 1988. Lumber Moisture Evaluation by a Reflective Cavity Photothermal Technique. *Rev. Phys. Appl.*, v.23, p.1565-1576

Clarke, R.W. and Squirrel, J.P. 1985. The Pilodyn- An Instrument for Assessing the Condition of Waterlogged Wooden Objects, *Studies in Conservation*, v. 30, p.177-183

Colwell, R.N. ed. 1983. *Manual of Remote Sensing*. Vols.1 and 2, 2<sup>nd</sup> edition, American Society for Photogrammetry and Remote Sensing, Falls Church, VA

Çakır, S. 2000. Geleneksel Karadeniz Ahşap Konut Yapım Yönteminin Çağdaş Teknoloji Açısından Değerlendirilmesi. Unpublished PHD Thesis, Mimar Sinan Üniversitesi, Supervisor: Ökten, S.

Çakıroğlu, N. 1952. *Kayseri Evleri*. Pulhan Matbaası, İstanbul

Çobancaoğlu, T. 1998. Türkiye'de Ahşap Ev'in Bölgelere göre Yapısal Olarak İncelenmesi ve Restorasyonlarında Yöntem Önerileri. Unpublished PHD Thesis, Mimar Sinan Üniversitesi, Supervisor: Aşkun, İ.Y.

Darabi, A. 2000. Detection and Estimation of Defect Depth in Infrared Thermography Using Artificial Neural Networks and Fuzzy Logic. Département de Génie électrique et de Génie Informatique Faculté Des Sciences Et De Génie Université Laval Québec, Unpublished PHD Thesis, Département de Génie Électrique Et De Génie Informatique, Faculté Des Sciences Et de Génie Université Laval, Québec, Canada

Davis, G. 1997. The Performance of adhesive Systems for Structural Timbers, *Int. J. Adhesion Adhesives*, v.17, n.3, p.247-255

Desch, H.E. 1968. *Timber Its Structure and Properties*, Fifth Edition, St.Martin's Press, New York

Desch, H.E., Dinwoodie, J., M. 1996. *Timber, Structure, Properties, Conversion and Use*, Food Products Press, New York

- Dickens, J.R., Bray, D.E., Bender, D. 1997. Beam Profiles in Wood from Critically Refracted Longitudinal Wave Probes, *Materials and Evaluation*, v.55, n.6, p.721-725
- Edlund, M.L., Nilsson, T. 1998. Testing Durability of Wood, *Materials and Structures*, v.31, November 1998, p.641-647
- Eldem, S.H. 1968. Türk Evi Plan Tipleri. İ.T.Ü. Mimarlık Fakültesi, İstanbul
- Erdem, M. 1979. Adıyaman da Kerpiç bir Ev, *ODTÜ Mimarlık Fakültesi Dergisi*, v.5, n.1.
- Eriç, M. 1979. Geleneksel Türk Mimarisinde Malzeme Seçim ve Kullanımı, *Yapı*, n.33, 3, p.42-45
- Eser, L. 1955. Kütahya Evleri. Pulhan Matbaası, İstanbul
- Evren, M. 1959. Türk Evinde Çıkma. İstanbul Teknik Üniversitesi, Mimarlık Fakültesi, Fakülteler Matbaası, İstanbul
- Fidler, J. 1980. Non-Destructive Surveying Techniques for the Analysis of Historical Buildings, *Association for Studies in the Conservation of Historic Buildings*, v.5
- FLIR Systems. 2006. User's Manual ThermaCAM Researcher Professional Edition. Version 2.8 SR-3.
- Freas, A. 1982. Evaluation Maintenance and Upgrading of Wood Structures: A guide and Commentary. American Society of Civil Engineers, New York
- Giuriani, E. and Gubana, A. 1993, A Penetration Test to Evaluate Wood Decay and its Application to the Loggia Monument, *Materials and Structures*, v.26, p.8-14
- Güçhan, Şahin, N., Bilgin, G., Çelik G., Efe İ. and Kılınç, A., Master Course Rest 507 DESIGN IN RESTORATION III, Survey, Analysis and Preservation of Historic Towns & Areas, 2006 Fall Semester , METU, Faculty of Architecture
- Güdücü, G., 2003, Archaeometrical Investigation of Mud Plasters on Hittite Buildings in Şapinuwa-Çorum, Unpublished Msc. Thesis, METU, Supervisor: Saltık, E.C., Demici, Ş.

Green, D.W., Winandy, J.E., Kretschmann, D.E. 1999. Mechanical Properties of Wood, Wood Handbook : Wood as an Engineering Material. Madison, WI , USDA Forest Service, Forest Products Laboratory, General Technical Report FPL, Chapter 04

Grinzato, E., Bison, P.G., Marinetti, S. 2002. Monitoring of Ancient Buildings by the Thermal Method, Journal of Cultural Heritage, v.3, p.21-29

Grinzato, E., Vavilov, V., Kauppinen, T. 1998. Quantitative Infrared Thermography in Buildings, Energy and Buildings, v.29, p.1-9

Halabe, U.B., Bidigalu, G.M., GangaRao, H.,V.,S., Ross, R.,J. 1997. Nondestructive Evaluation of Green Wood Using Stress Wave and Transverse Vibration Techniques, Materials and Evaluation, v.55, n.9, p.1013-1018

Halebe, U., GangaRao, H., Petro, S., Hota, V.R. 1996. Assessment of Defects and Mechanical Properties of Wood Members Using Ultrasonic Frequency Analysis, Materials Evaluation

Haslett, B.R., Acoustic Emission Study of Withinring, Internal Checking in Radiata pine Wood NDT 2000, 12<sup>th</sup> International Symposium on Nondestructive Testing of Wood, NDT. Net, March 2001, v.6, n.03

Hayashi, K., Felix, B., Govic, C. 1993. Wood Viscoelastic Compliance Determination with Special Attention to Measurement Problems, Materials and Structures, v.26, p.370-376

Henric, B. 2001. Detection of Glue Deficiency in Laminated Wood with Thermography, 12.th International Symposium on Nondestructive Testing of Wood, v.6, n.03

Hodder, I. 1996. Çatalhöyük:Orta Anadolu'da 9000 Yıllık Konut ve Yerleşme. Tarihten Günümüze Anadolu'da Konut ve Yerleşme, Habitat II, 43-48

Holman, J.P. 1981. Heat Transfer. McGraw-Hill, New York

Illston, J.M., Dinwoodie, J.M., Smith, A.A. 1979. Concrete, Timber, and Metals: The Nature and Behaviour of Structural Materials. Van Nostrand Reinhold, New York

İdil, V. 1993. Ankara: The Ancient Sites and Museums. Turistik Yayınlar A.Ş., İstanbul

İmamoğlu, V. 1992. Geleneksel Kayseri Evleri. Türkiye Halk Bankası Kültür Yayınları, İstanbul.

Jensen, P. and Gregory, D.J. 2006. Selected Physical Parameters to Characterize the State of Preservation of Waterlogged Archaeological Wood: a Practical Guide for Their Determination, *Journal of Archaeological Science*, v.33, p.551-559

Jordan, R., Feeney, F., Nesbitt, N., Evertsen, J.A. 1998. Classification of Wood Species by Neural Network Analysis of Ultrasonic Signals, *Ultrasonics*, v.36, p.219-222

Kafesçiođlu, R. 1955. Kuzey Batı Anadolu'da Ahşap Ev Yapıları. Pulhan Matbaası, İstanbul

Kafesçiođlu, R. 1949. Orta Anadolu 'da Köy Evlerinin Yapısı. Matbaacılık, T.A.O., İstanbul

Kahraman, S, Söylemez, M., Fener, M. 2008. Determination of Fracture Depth of Rock Blocks from P- Wave Velocity, *Bull Eng Geol Environ*, v.67, p.11-16

Kahraman S. 2002. Estimating the Direct P-wave Velocity Value of Intact Rock from Indirect Laboratory Measurements, *International Journal of Rock Mechanics & Mining Sciences*, v.39,p.101–104

Kanda, S., Shioya, K., Yanagiya, Y., Tamura Y., Adachi, K. 1998. Ultrasonic TOF-CT System for Wooden Pillars, *Ultrasonics Symposium, Proceedings*, v.1, p.743-746,

Kandemir A. 2000. Maintenance Guidelines for the Windows in Cumalıkızık Settlement. Unpublished Master Thesis, METU Graduate Program in Restoration, Faculty of Architecture, Department of Architecture, Supervisor: Asatekin, G.

Kandemir, A., Tavukçuođlu A., Caner-Saltık, E. 2005. Non-Destructive Analysis of Historic Timber Elements to Assess their state of Preservation, '14 th International Symposium on Non Destructive Testing of Wood', University of Applied Science, Hannover-Germany, May 2-4, p.135-144

Kandemir, A., Tavukcuoglu, A., Saltik, E. N. 2007. In Situ Assessment of Structural Timber Elements of a Historic building by Infrared Thermography and Ultrasonic Velocity, *Infrared Physics & Technology*, v.49, p.243–248

Kazmaođlu, M. and Tanyeli, U. 1979. Anadolu Konut Mimarisinde Bölgesel Farklılıklar, *Yapı*, v.33, n.3, p.29-41

Kaya, Ş. 1996. Geleneksel Safranbolu Örneklerinde Strüktür. Unpublished Master Thesis, Karadeniz Teknik Üniversitesi, Supervisor: M.R. Sümerkan

- Kim, G-H. 1989. Detection of Incipient Decay and Assessment of Residual Strength of Wood Using Nondestructive Techniques. Unpublished PhD Thesis, Mississippi State University
- Klinkhachorn, P., Nomani, S., Chatwiriya, W., Halabe, U., Petro, S. 1998. Development of a Portable Ultrasonic Timber Properties Monitoring Device, System Theory, Proceedings of the thirtieth Southeastern Symposium on 8-10,
- Knut, N. 1999. The Restoration of Paintings. (Ed. C. Westphal) Slovenia, Könemann,
- Koch M., Hunsche S., Schuacher P., Nuss MC., Feldmann J., Fromm J. 1998. THz-imaging a New Method for Density mapping of Wood, Wood Science Technology, v.32, p.421-427
- Kömürcüoğlu, E. 1950. Ankara Evleri, İstanbul Teknik Üniversitesi, Mimarlık Fakültesi, Matbaacılık T.A.O, İstanbul
- Kuban, D. 1995. The Turkish Hayat House. Muhittin Salih Eren, İstanbul
- Kuban, D. 1982. Türk Ev Geleneği Üzerine Gözlemler. Türk ve İslam Sanatı Üzerine Denemeler. Arkeoloji ve Sanat Yayınları, İstanbul, p.195-209
- Kuban, D. 1966. Türkiye’de Malzeme Koşullarına Bağlı Geleneksel Konut Mimarisi Üzerine Bazı Gözlemler, Mimarlık, v.36, p.14-20
- Kuban, D. 1966. Türkiye’de Malzeme Koşullarına Bağlı Geleneksel Konut Mimarisi Üzerinde Bazı Gözlemler, Mimarlık, Ekim, 36 (10/1966), p.15-20
- Kuklic P. and Kuklikova A. 2000. Evaluation of Structural Timber by Dynamic Methods, Proceedings of the 12<sup>th</sup> International Symposium on Non Destructive testing of Wood University of Western Hungary, Sopron, 13-15 September 2000
- Kuwamoto, S. and Williams, R.S. 2002. Acoustic Emission and Acousto-Ultrasonic Techniques for Wood and Wood-Based Composites. A Review, United States Department of Agriculture
- Küçükerman, Ö. 1973. Anadolu’daki Geleneksel Türk Evinde Odalar. Türkiye Turing ve Otomobil Kurumu, İstanbul
- Lemaster, R. L., Biernacki, J. M. and Beal, F., C. 1993. The Feasibility of Using Acousto-ultrasonics to Detect Decay in Utility Poles, in 9th International Symposium on Nondestructive Testing of Wood, 84-91

Lindstrom, R. and Stockbridge, J. 1988. Evaluating Structural Capacity in Wood Buildings, APT Bulletin, v.20, n.3, p.9-11

Lukaszewicz, J.W., Niemcewicz P. (Eds.). 2008. Proceedings of 11th International Congress on Deterioration and Conservation of Stone, September 15-20, Torun, Poland. V.1, Poland, Nicolaus Copernicus University Press, p.529-538

Machek, L., Militz, H., Sierra Alvarez, R. 2001. The Use of Acoustic Technique to Assess Wood Decay in Laboratory Soil-bed Tests, Wood Science and Technology, v.34, p.476-472

Madran, E. 1994. Vakfiyeler’de Sivil Mimarlık Örneklerine İlişkin Bilgiler. Kent, Planlama, Politika, Sanat. v.2, p.423-435

Maldague, X, Galmiche, F., Ziadi, A. 2002. Advances in Pulsed Phase Thermography, Infrared Physics&Technology, v.43, p.175-181

Maldague, X.Y., Largouët, J. P. Couturier. 1998. A study of defect depth using neural networks in pulsed phase thermography: modeling, noise, experiments. Rev. Gén. Therm., Elsevier, Paris, v.37, p.704-717

Maldague, X. 1994. Advances in Signal Processing for Nondestructive Evaluation of Materials. NATO ASI Series, v. 262

Masuda M. and Takahashi S. 2000. Thermographical Detection of Defects of Lumber and Glued Joints, 12<sup>th</sup> Symposium NDT of Wood, University of Western Hungary, Sopron, p.421-430

Mattone, M. 1999. Analyse de l’etat de Conservation des Structures en Bois au Travers d’essais non destructifs, French Journal of Timber Engineering, Annales GC Bois, v. 4, p.9-16

Maunus, A.R. 1993. Rheological Behaviour of Wood in Directions Perpendicular to the Grain, Materials and Structures, 26, p.362-369

McCuen, R.H. 1988. Spacing for Accuracy in Ultrasonic Testing of Bridge Timber Piles, Journal of Structural Engineering, v.114, n.12, 2652-2668

Meola, C, Maio,R. D., Roberti, N., Carlomagno, G. M. 2005. Application of Infrared Thermography and Geophysical Methods for Defect Detection in Architectural Structures, Engineering Failure Analysis, v.12, p.875-892

Meola C., Carlomagno G. M., Giorleo, L. 2004. The Use of Infrared Thermography for Materials Characterization, *Journal of Materials Processing Technology*, v.155–156, p.1132–1137

Meraki, Ş. 1999. Karabük İli Safranbolu İlçesi Yörük Köyü Kaynakçioğlu(Kaymakçığıl) Konağı Restorasyon Önerisi. Unpublished Master, Thesis Gazi Üniversitesi, , Supervisor: Hersek, C.M.

Minamisawa, A., Ozawa, A., Sakai, H, Takagi, K. 1990. Moisture Effects on the Ultrasonic Velocities in Woods, *Ultrasonics Symposium, Proceedings*, v.2, p.1105-1108

Mouzuras, R. 1989. Nondestructive Evaluation of Hull and Stored Timbers from the Tudor Ship Mary Rose, *Studies in Conservation*, v.35, p.173-188

Murato K. and Sadoh T. 1994. Heat Absorption and Transfer in Softwoods and Their Knot Surfaces, *Mokuzai Gakkaishi*, v.40, p.1180-1184

Naito S., Fujii Y., Sawada Y., Okumura S. 2000. Thermographic Measurement of Slope of Grain Using the Thermal Anisotropy of Wood, *Makuzai Gakkaishi*, v.46, p.182-190

Naito S., Fujii Y., Sawada Y., Okumura S. 1998. Thermography of Wood Specimens in Static Bending Test, *Kyoto Daigaku Nogaku Bu Enshurin Hokoku*, v.69, p.104-113

Neve, P. 1996. Hitit Krallığının Başkenti Hattuşaş'da Konut. Tarihten Günümüze Anadolu'da Konut ve Yerleşme. Habitat II, Sey, Y. (Ed), *Türkiye Ekonomik ve Toplumsal Tarih Vakfı, İstanbul*, p.99-115

Olivito, R.,S. 1993. Ultrasonic Measurements in Wood, *Materials Evaluations*, v.34, n.4

Okumura, S., Suzuki R., Fujii Y. 1996. Preliminary Study on Thermography of Wood Under Compression Load, *Kyoto Daigaku, Nogaku Bu Enshurin Hokoku*, v.68, p.161-169

Ortadoğu Teknik Üniversitesi. 1991. Ulus Samanpazarı Keklik Sokak ve Çevresi Koruma Geliştirme Projesi Ön Raporu, Ankara

Öney, G. 1994. Ankara'da Selcuklu ve Beylikler Devri Ahsap Malzemeli Camii ve Mescitleri, Ankara Ankara. Yapi Kredi Yayinlari, İstanbul, p.73-86

Öney, G. 1990. Ankara Aslanhane Camii. Kültür Bakanlığı Yayınları, Ankara

- Öney, G. 1978. Anadolu Selçuklu Mimarisinde Süsleme ve El Sanatları. Ajans-Türk Matbaacılık Sanayii, Ankara
- Öney, G. 1971. Ankara'da Türk Devri Dini ve Sosyal Yapıları. Ankara Üniversitesi Dil Tarih ve Coğrafya Fakültesi Yayınları, Ankara
- Öney, G. 1970. Anadolu'da Selçuklu ve Beylikler Devri Ahsap Teknikleri. Sanat Tarihi Yıllığı. İstanbul Üniversitesi Edebiyat Fakültesi Sanat Tarihi Enstitüsü, III. P.135-149
- Pizzo, B., Rizzo, G., Lavisci, P., Megna, B., Berti, S. 2002. Comparison of Thermal Expansion of Wood and Epoxy Adhesives. Holz als Roh-und Werkstoff, v.60, p.285-290
- Ridout, B. 2001. Timber Decay in Buildings, The Conservation Approach to Treatment. Spon Press, London and Newyork
- Robbins, W.P., Mueller, R.K., Schaal, T., Ebeling, T. 1991. Characteristics of Acoustic Emission Signals Generated by Termite Activity in Wood, Ultrasonics Symposium, Proceedings, v.2, p.1047-1051
- Ronca, P. and Gubana, A. 1998. Mechanical Characterisation of Wooden Structures by means of an in situ Penetration Test, Construction and Building Materials, v.12, p.233-243
- Ross, R. and Pellerin, R.F. 1988. NDE of Wood- Based Composites with Longitudinal Stress Waves, Forest Products Journal, v.38, n.5
- Ross, R. and Pellerin, R.F., 1993. Non-destructive Evaluation of Timber, Structural Engineering Natural Hazards Mitigation, Proceedings of Papers presented at the Structures Congress'93, Edited by Ang, A., Villaverde, Vol.2, The American Society of Civil Engineering
- Rug W. and Seemann A. 1991. NDT Strength of Old Timber, Test Cores from 50-400 Years Old Timber Indicates Strength of Old Timbers Corresponds to that of New, Building Research and Information, v.19, n.1, p.31-37
- Sakai, H., Minamisawa, A., Takagi, K. 1990. Effect of Moisture Content on Ultrasonic Velocity and Attenuation in Woods, Ultrasonics, v.28, n.6
- Sandoz, J.L. 2005. Personal Communication with him during the '14 th International Symposium on Non Destructive Testing of Wood', University of Applied Science, Hannover-Germany

Sandoz, J.L. 1996. Ultrasonic Solid Wood Evaluation in Industrial Applications, December 1996, v.1, n.12

Sasaki, Y. and Hasegawa, M. 2000. Ultrasonic Measurement of Applied Stresses in Wood by Acoustoelastic Birefringent Method, Proceedings of the 12<sup>th</sup> International Symposium on Non Destructive testing of Wood University of Western Hungary, Sopron, 13-15 September 2000, March 2001, v.6, n.03

Sasse, H.R. and Snethlage, R. 1997. Methods for the Evaluation of Stone Conservation Treatments, Saving our Architectural Heritage. Edited by Baer, N., S., Snethlage, R.

Schafer M.E. 2000. Ultrasound for Detection and Grading in Wood and Lumber, Ultrasonics Symposium, 20-25 October, 2000, v.1, p.771-778

Sinclair, A.N. and Farshad, M. 1987. A Comparison of Three Methods for Determining Elastic Constants of Wood, Journal of Testing and Evaluation, 15, 77-86

Sönmezer, İ. 1999. Geleneksel Türk Evinde Ahşap ve Mekan İlişkisi. Unpublished Master Thesis, Dokuz Eylül Üniversitesi, Supervisor: Levi, E.A.

Sözen, M. and Erüzün, C. 1992. Anadolu'da Ev ve İnsan. Emlak Bankası, İstanbul

Sözen, M. 1979. Konya Evleri, Odtü Mimarlık Fakültesi Dergisi, v.1, n.1

Spencer, M., Nychka J., Penn L., Boyer L., Everdale L., Liebertz J. 2008. Applying Infrared Thermography for the Purpose of Identifying Concealed Wood Framing Member Type and Subsurface Anomalies with Intended Application Towards Historic Structures, University of Kentucky, College of Design, Department of Historic Preservation.

Stamm, A. 1970. Wood Deterioration and its Preservation, Newyork Confrence on Conservation of Stone and Wooden Objects, The International Institute for Conservation of Historic and Artistic Works, London, v.1, p.1-11

Steele P.H., Patton M. D., Cooper E. 2000. Factor Influencing Differential Thermal Response of Knots and Clear Wood, 12<sup>th</sup> Symposium NDT of Wood, University of Western, Sopron, p.403-412

Sümerkan, R. 1990. Biçimlendiren Etkenler Açısından Doğu Karadeniz Kırsal Kesiminde Geleneksel Evlerin Yapı Özellikleri. Unpublished PHD Thesis, Karadeniz Teknik Üniversitesi, Supervisor: Ertürk, Z.

Şahin, N. 1995. A Study on Conservation and Rehabilitation Problems of historic Timber Houses in Ankara. Unpublished PhD Thesis, METU, Faculty of Architecture, Ankara, Supervisor: Bakırer Ö.

Şahin, N. 2002. Türkiye’de Geleneksel Ahşap Karkas Konut Onarımının Teknik Sorunları, 1. Ulusal Yapı Malzemesi Kongresi ve Sergisi, Kongre Bildirileri-II, p.627-638

Tayla, H. 2007. Geleneksel Türk Mimarisinde Yapı Sistem ve Elemanları. Türkiye Anıt Çevre Turizm Değerlerini Koruma Vakfı, İstanbul

Tomsu, L. 1950. Bursa Evleri. İstanbul Teknik Üniversitesi, Mimarlık Fakültesi, Matbaacılık, TAO, İstanbul

Tanaka, T. and Divos F. 2000, Wood Inspection by Thermography, Proceedings of the 12<sup>th</sup> International Symposium on Non Destructive testing of Wood, University of Western Hungary, Sopron, 13-15 September, v.6, n. 03

Tanaka, T. 1994. Thermographic Detection of Deteriorated Locations and Non-destructive Evaluation of Strength of the Biodeteriorated Wood, 9<sup>th</sup> International Symposium on NDT of Wood, Washington State University, Pullman, p.78-83

Tanyeli, U. 1996. Anadolu’da Bizans, Osmanlı Öncesi ve Osmanlı Dönemlerinde Yerleşme ve Barınma Düzeni. Tarihten Günümüze Anadolu’da Konut ve Yerleşme. Habitat II, Sey, Y. (Ed), Türkiye Ekonomik ve Toplumsal Tarih Vakfı, İstanbul, p.405-471

Tanyeli, U. 1996. Klasik Dönem Osmanlı Metropolünde Konutun ‘Reel’ Tarihi: Bir Standart Saptama Denemesi. Prof. Doğan Kuban’a Armağan. Ahunbay, Z., Mazlum D., Eyüggiller K. (Eds.), Eren Yayıncılık, İstanbul, 57-71

Tavukçuoğlu, A. 2001. A Study on the Maintenance of stone Monuments in Relation to Dampness Problems. Unpublished PHD Thesis, METU, faculty of Architecture, Supervisor: Saltık, E.C.

Tavukçuoğlu, A. 2003. The Assessment of Surface Water Drainage Problems in Historical Buildings by IR Thermography and Leveling Survey, Water Supply and Drainage for Buildings

Tavukcuoglu A., Düzgünes A. , Caner-Saltık, E.N., Demirci, S. 2005. Use of IR Thermography for the Assessment of Surface-Water Drainage Problems in a Historical Building, Ağzıkarahan (Aksaray), Turkey, NDT&E International, 38, p.402–410

Tavukcuoglu A. and Grinzato E. 2006. Determination of critical moisture content in porous materials by IR thermography, Quantitative Infrared Thermography Journal, v.3, n.2, p.231-245

Tavukcuoglu, A. and Grinzato, E. 2006. Determination of Critical Moisture Content in Porous Materials by IR Thermography, QIRT Journal, v.3, n.2, p.231-245

Tavukcuoglu, A., Duzgunes, A., Demirci, S., Caner-Saltık, E., N. 2007. The Assessment of a Roof Drainage System for an Historical Building, Building and Environment, v.42, p.2699–2709

Tavukcuoglu, A., Cicek, P., Grinzato E. 2008. Thermal Analysis of an Historical Turkish Bath by Quantitative IR Thermography, QIRT Journal. V.5, n. 2, p.151-173

Timber Construction Manual; a Manual for Architects, Engineers, Contractors, Laminators and Fabricators Concerned with Engineered Timber Buildings and Other Structures. 1966. American Institute of Timber Construction, Wiley, New York

Titman, D.J. 2001. Application of Thermography in Nondestructive Testing of Structures, NDT&E International, v.34, p.149-154

Tsoumis, G.T. 1991. Science and Wood Technology of Wood, Structure, Properties, Utilization, Van Nostrand Reinhold, New York

Tokay, H. 2002. Barınaktan Konuta Yöresel Malzeme ve Yapım Tekniğine Bölgesel Bir Örnek: Çukurova’da Geleneksel Konut Mimarisi ve Günümüze Yansıması ‘Huğ Evi’. 1. Ulusal Yapı Malzemesi Kongresi ve Sergisi, Kongre Bildirileri-II, TMMOB, İstanbul, 679-688

Türkmen, S. 1995. Rize Yöresi Kırsal Kesiminde Geleneksel Sivil Mimaride Kullanılan Ahşap Bağlantı Tipleri. Unpublished Master Thesis, Karadeniz Teknik Üniversitesi, Supervisor: Erten, E.

Valentin, G. and Morlier, P. 1999. L’endommagement du Bois., Synthese du Workshop 1999 de Cost E8, French Journal of Timber Engineering, Annales GC Bois, v. 4, p.49-60

Valluzzi, M.R. 2002. Structural Investigations and Analyses for the Conservation of the ‘Arsenale’ of Venice, Journal of Cultural Heritage, v.3, p.65-67

Yürekli H. 1979. Türk Evi Karakteristiklerinin dış Gözlem ile Saptanması için Bir Yöntem, ODTÜ Mimarlık Fakültesi Dergisi, v.5, n.1, p.5-14

- Wheeler A.S. 1998. Hutchinson A., R., Resin Repairs to Timber Structures, International Journal of Adhesion and Adhesives, v.18, p.1-13
- Wilcox, W.W. 1988. detection of Early Stages of Wood Decay with Ultrasonic Pulse Velocity, Forest Products, v.38, n.5, p.68-73
- Wu, D. and Busse, G. 1998. Lock-in Thermography for Non-destructive Evaluation of Materials, Rev. Gen. Therm, Elsevier, Paris, v.37, p.693-703
- Wu, D. and Busse, G. 1995. Remote Inspection of Wood with Lock-in Thermography, Proceedings of 1995 European Plastic Laminates Forum, "The leading Edge" Heidelberg, p.27-29
- Wyckhuysse, A. and Maldague, X, 2002. Wood Inspection by Infrared Thermography, Proc. of IVth. IWASPNDE, Maldague X. ed., TONES (ASNT pub.), v.6, p.201-206
- Yavuz, A.T. 2000. 19. Yüzyıl Ankara'sında Kaleiçi, Tarih İçinde Ankara: Eylül 1981, Seminer Bildirileri, Akgün, S. (Eds.), T.B.M.M. Basımevi, Ankara, p.153-195
- Yavuz, Y. 1973. Cumhuriyet Dönemi Ankara'sında Mimari Biçim Endişesi, Mimarlık, v.10, n.26-44, p.121-122
- Yavuz, Y. 1976. İkinci Meşrutiyet Döneminde Ulusal Mimari Üzerindeki Batı Etkileri (1908-1918), ODTÜ Mimarlık Fakültesi Dergisi, 2(1), p.9-34

## APPENDIX

### TECHNICAL SPECIFICATION OF INSTRUMENTS USED IN THE STUDY

#### A.1 AGEMA 550 Camera - Radiometric Handheld Infrared Camera

##### Imaging and Measurement Capabilities

System Type	Focal plane array infrared camera
Spectral Range	3.6 – 5.0 microns
Detector	PtSi, 320 x 240
Temperature Measurement Accuracy	± 2% of range or 2°
Temperature Measurement Range	–20°C to +2000°C (–4°F to +3600°F)
Field of View	20°x15°
Cooling	> 10,000 hour MTBF Stirling cooler
Spatial Resolution	76,800 pixels
Minimum Discernable Temperature	0.1°C at 30°C
Image Update Rate	30/25 Hz NTSE/PAL and 60 Hz Digital
Infrared Dynamic Range	12 bits
Image Optimization	Continuous automatic or manual
Emissivity Setting	Yes
Color/Grey Levels	256
Palettes	Multiple color or monochrome, user selectable

Display	Type Built-in, high-resolution color LCD viewfinder
Image Storage Capacity	1000 images (12 bit) on 170 MByte PC Card disk
<b>Additional Specifications</b>	
Interfaces	RS-232 interface for remote camera control; Voice annotation – headset connection; PC Card - type II or III
Video Outputs	RS 170 EIA/NTSC or CCIR/PAL, composite or S-video
Power	NiMH battery, 6 hours continuous Operation
Operating Temperature	-15°C to +50°C (5°F to +120°F)
Camera Weight (w/lens & viewfinder)	2 kg (4.4 lbs)
Camera Size	220 x 132 x 140mm (8.7 x 5.2 x 5.5 inches)
Enclosure	IP54 rated (NEMA 13), completely water- and dust-proof

**Optional Image Analysis Features Include:**

Auto hot spot; continuous image storage; automatic temperature difference readout between target and reference temperatures; automatic display of minimum, maximum and average value in defined AOI.

**Accessories**

Standard: 20° lens, AC power supply, operating manual and shipping case, multiple language support.

Optional: Software: IRwin Report for image analysis and reporting. Optics: additional lenses, filters. Video & Recording Accessories: recorders, printers, visual light cameras, 30sec. digital voice annotation per image with on-screen prompts, high-resolution 4” LCD display. Power Accessories: batteries, chargers, DC to DC adapter. Other: desktop/ laptop PCs, additional PC Cards, tripod.

## A.2 FLIR ThermaCAM E65 Infrared Camera

### Imaging Performance

Field of view/min focus distance	Interchangeable; 25° x 19° / 0.3 m, 12° x 9°/1.2m or 45° x 36° / 0.1m
Thermal sensitivity	0.10° C at 30° C
Detector type	Focal plane array (FPA) uncooled vanadium oxide microbolometer, 160x120 pixels, 50/60 Hz
Spectral range	7.5 to 13µm

### Image Presentation

Display	2.5" color LCD, 320 x 240 pixels in IR image
Image Controls	Palettes (Iron, Rainbow, B/W, B/W inv), Level, Span, Auto adjust (continuous/manual)

### Measurement

Temperature ranges	-20°C to +250°C (-4°F to +482°F) (standard)
Accuracy (optional)	+250°C to +900°C (+482°F to +1,652°F) ± 2°C or ± 2% of absolute temperature in °C
Measurement modes	3 movable spots, area max, area min, area average, temp difference, color alarm above or below
Set-up controls	Date/time, Temperature units °C/°F, Language (English, Spanish), Scale, Info field, LCD intensity (high/normal/low)
Measurement corrections	Reflected ambient. Automatic, based on user-input

### Image Storage

Digital storage functions	Freeze, Standard Calibrated JPEG images, Delete all images, Delete image, Open
---------------------------	--

Image storage capacity	Approx. 200 Calibrated JPEG Images with image gallery
Text annotation of images	Predefined text selected and stored together with image
<b>Laser LocatIR™</b>	
Classification	Class 2
Type	Semiconductor AlGaInP Diode Laser: 1mW/635 nm (red)
<b>Power Source</b>	
Battery type	Li-Ion; rechargeable, field replaceable
Battery operating time	2 hours. Display shows battery status
Battery charging	In camera (AC adapter or 12V from car) or 2 bay intelligent charger
AC operation	In camera, AC adapter or 12V from car with optional 12V cable. 2 bay intelligent charger included.
Voltage	11-16VDC
Power saving	Automatic shutdown and sleep mode (user-selectable)
<b>Environmental</b>	
Operating temperature range	-15°C to +45°C (+5°F to 113°F)
Storage temperature range	-40°C to +70°C (-40°F to 158°F)
Humidity	Operating and storage 20% to 80%, non-condensing, IEC 359
Water and dust resistant (encapsulation)	IP 54, IEC 359
Shock	25G, IEC 68-2-29
Vibration	2G, IEC 68-2-6
<b>Physical Characteristics</b>	
Weight (with standard lens)	< 1.5 lbs. (0.7 kg) including battery
Size (L x W x H)	265mm x 80mm x 105mm (10.4"x3.2"x4.1")

Color	Titanium grey
Tripod mounting	Standard, 1/4" - 20
Cover case	Plastic and rubber

**Camera includes**

IR camera, ruggedized transport case, power supply and cord, hand strap, lens cap, ThermaCAMR QuickView™ software, USB cable, video-out cable, user manual, battery (2), 2-bay battery charger, training CD.

**Interchangeable lenses (optional)**

2X Telescope (12° X 9°/1.2m)

0.5X Wide angle (45° X 34°/0.1m)

**Interfaces**

IrDA Two-way data transfer from laptop, PDA

### A.3 FLIR ThermoCAM SC640 Infrared Camera

#### Imaging Performance

Thermal:

Field of view/min focus distance	24°x18° /0.3 m
Spatial resolution (IFOV)	0.65 mrad
Thermal sensitivity	60mK at 30°C
Image frequency	30 Hz non-interlaced
Focus	Automatic or manual
Electronic zoom / pan function	1 - 8 x continuous, including pan function
Detector type	Focal Plane Array (FPA), uncooled microbolometer 640 x 480 pixels
Spectral range	7.5 to 13µm
Digital image enhancement	Normal and enhanced
Visual:	
Built-in digital video	1.3 Mpixel, full color / built-in Target Illuminator / exchangeable lens
Standard lens performance	f=8 mm / FOV 32°

#### Image Presentation

Video output	RS170 EIA/NTSC or CCIR/PAL composite video, IEEE-1394 FireWire, USB
Viewfinder	Built-in, tiltable, high-resolution color viewfinder (800 x 480 pixels)
External display	Built-in 5.6" LCD (1024 x 600 pixels)

#### Measurement

Temperature range	-40°C to +1,500°C, in 3 ranges; up to + 2000°C, optional
-------------------	--

Accuracy	$\pm 2^{\circ}\text{C}$ , $\pm 2\%$ of reading
Measurement mode	Spots/Areas (Boxes, Circles), Isotherms (above, below, interval), Delta T
Menu controls	Palettes , load custom palletes, auto adjust (manual/continuous/based on histogram equilazation), on screen live and reference image (PoP), image gallery, sequence storage, programmable storage
Alarm Functions	Automatic alarm on any selected measurement function, audible/visible alarm above/below,
Set-up controls	Date/time, Temperature $^{\circ}\text{C}/^{\circ}\text{F}$ , language
Atmospheric transmission correction	Automatic, based on inputs for distance, atmospheric temperature and relative humidity
Optics transmission correction	Automatic, based on signals from internal sensors
Emissivity correction	Variable from 0.01 to 1.0 or select from listings in pre-defined materials list
Reflected ambient temperature correction	Automatic, based on input of reflected temperature
External optics/window correction	Automatic, based on input of optics/window transmission and temperature
<b>Image Storage</b>	
Type	Removable SD-card (1 GB) Built-in RAM memory for radiometric real-time sequence storage
File formats - Thermal	Standard JPEG, 14 bit measurement data included
File formats - Visual	Standard JPEG, automatically associated with corresponding thermal image / possibility for visual marker
Voice annotation of images	30 sec. of digital voice “clip” stored together with the image wired headset;

Text annotation of images	Predefined text selected and stored together with the image
<b>Video Storage</b>	
Type	Recording of fully radiometric IR-video clips in camera, transferable to SD-card Recording of MPEG-4 non-radiometric video to SD-card
<b>Video Streaming</b>	
Type	Fully radiometric real-time 14-bit digital IR-video using FireWire, MPEG-4, IP-link using FireWire or USB
<b>Lenses (Optional)</b>	
Field of view/min focus distance	12° x 9° / 0.9m telelens 45° x 34° / 0.1m wide angle lens Close-up 50µm 32 mm x 24 mm / 75 mm
Lens identification	Automatic
<b>Laser Pointer</b>	
Classification	Class 2
Type Semiconductor	AlGaInP Diode Laser: 1mW/635 nm red
<b>Battery System</b>	
Type	Li-Ion, rechargeable, field replaceable
Operating time	3 hours continuous operation
Charging system	in camera (AC adapter or 12 V from car) or 2 bay intelligent charger
External power operation	AC adapter 110/220 V AC, 50/60 Hz or 12 V from car (cable with Std plug: optional)
Power saving	Automatic shutdown and sleep mode (user selectable)
<b>Environmental Specification</b>	
Operating temperature range	-15°C to +50°C
Storage temperature range	-40°C to +70°C
Humidity	Operating and storage 10% to 95%, non-condensing
Encapsulation	IP 54 IEC 529
Shock	Operational: 25G, IEC 68-2-29

Vibration Operational: 2G, IEC 68-2-6

**Physical Characteristics**

Weight 1.7 kg incl. battery

Size 120 mm x 145 mm x 220 mm

Tripod mounting 1/4" - 20

**Interfaces**

FireWire IEEE-1394 FireWire output (real-time radiometric or non-radiometric video / filetransfer to PC)

USB Image (thermal and visual), measurement, voice and text transfer to PC

IrDA Wireless communication

SD-card (2) I/O slot; storage slot

## A.4 HOBO WarePRO Temperature/Relative Humidity/Light/External Data Loggers

Data Storage Capacity	43.000 12-bit Samples/Readings
Sampling Rate	1 Second to 18 Hours
Measurement Range Temperature:	-20°C to 70°C (-4°C to 158°F)
Humidity:	5% to 95% RH
Light Intensity:	1 to 3000 foot-candles (lumens/ft <sup>2</sup> )
External Input Channel:	0 to 2.5 Volts DC
Accuracy	Temperature: $\pm 0.35^{\circ}\text{C}$ from $0^{\circ}\text{C}$ to $50^{\circ}\text{C}$ Humidity: $\pm 2.5\%$ RH from 10% to 90% ( $10^{\circ}\text{C}$ to $50^{\circ}\text{C}$ ) Light Intensity: Indoor Measurement of Relative Light Levels External Inputs: $\pm 2$ mV, $\pm 2.5\%$ of Absolute Reading
Resolution	Temperature: $0.03^{\circ}\text{C}$ at $25^{\circ}\text{C}$ ( $0.05^{\circ}\text{F}$ at $77^{\circ}\text{F}$ ) Humidity: 0.03% RH
Drift	Temperature: $0.01^{\circ}\text{C}/\text{year}$ ( $0.02^{\circ}\text{F}/\text{year}$ ) Humidity: $<1\%$ RH per year; RH Hysteresis 1%
Response Time (airflow: 1m/s)	Temperature: 6 Minutes, typical to 90% Humidity: 1 Minute, typical to 90%
Time Accuracy	$\pm 1$ Minute per Month at $25^{\circ}\text{C}$ ( $77^{\circ}\text{F}$ )
Operating Temperature	Logging: $-20^{\circ}\text{C}$ to $70^{\circ}\text{C}$ ( $-4^{\circ}\text{F}$ to $158^{\circ}\text{F}$ ) Launch/Readout: $0^{\circ}\text{C}$ to $50^{\circ}\text{C}$ ( $32^{\circ}\text{F}$ to $122^{\circ}\text{F}$ )
Battery Life	Typically 1 Year
Battery	3-Volt CR-2032 Lithium Battery (User Replaceable)

Standards Compliance	CE
Weight	46 g (1.6 oz)
Dimensions	58mm x 74mm x 22mm (2.3" x 2.9" x 0.9")

#### **A.5 PUNDIT PLUS PC1006 CNS FARNELL**

Modes of pulse generation	Continuous, delayed or one-shot
Operating voltages	250V, 500V and 1200V
Display options	Transit time, path length, velocity, limits and elastic modulus
Measurement units	Metric or imperial
Memory logging facility	With continuous and manual modes to store up to 112 readings
Button on receiving transducer	Facilitates Pundit Plus to be controlled by external systems
Downloaded function	Enables stored readings to be transferred to a PC

## CURRICULUM VITAE

### PERSONAL INFORMATION

Surname, Name: Kandemir, Ayşenur

Nationality: Turkish (TC)

Date and Place of Birth: 1 December 1973, Ankara

email: [aysenur2000@hotmail.com](mailto:aysenur2000@hotmail.com)

### EDUCATION

MS, METU, Faculty of Architecture, Program in Restoration, 2000

B.Arch, Gazi University Faculty of Engineering and Architecture, Dep. of Architecture, 1994

High School, Bahçelievler Deneme Lisesi, Ankara, 1990

### WORK EXPERIENCE

- Instructor; Dumlupınar Üniversitesi Meslek Yüksek Okulu, Department of Restoration, Kütahya; Duties performed: Measured drawings of historical buildings and Construction Materials; 2001
- Culture and Tourism Expert; Ministry of Culture and Tourism, Duties performed: Restoration and conservation of historical buildings, historical sites; 2004-

### FOREIGN LANGUAGES

Advanced English

### PUBLICATIONS

- **Kandemir-Yucel A.**, 2005. Tavukçuoğlu A., Caner-Saltık, E., Non-Destructive Analysis of Historic Timber Elements to Assess their state of Preservation, '14 th International Symposium on Non Destructive Testing of Wood', University of Applied Science, Hannover-Germany, 2005, May 2-4: 135-144.
- **Kandemir Yucel, A.**, Tavukcuoglu, A., Saltik, E. N. , 2007. In Situ Assessment of Structural Timber Elements of a Historic building by Infrared Thermography and Ultrasonic Velocity. *Infrared Physics & Technology*, 49, 243–248